



# LUND UNIVERSITY

## Models of Neuroimaging, Biomarkers, and Cognitive in Alzheimer's Disease. Implications for Clinical Trial Design.

Insel, Philip

2021

*Document Version:*

Publisher's PDF, also known as Version of record

[Link to publication](#)

*Citation for published version (APA):*

Insel, P. (2021). *Models of Neuroimaging, Biomarkers, and Cognitive in Alzheimer's Disease. Implications for Clinical Trial Design*. [Doctoral Thesis (compilation), Department of Clinical Sciences, Malmö]. Lund University, Faculty of Medicine.

*Total number of authors:*

1

### General rights

Unless other specific re-use rights are stated the following general rights apply:

Copyright and moral rights for the publications made accessible in the public portal are retained by the authors and/or other copyright owners and it is a condition of accessing publications that users recognise and abide by the legal requirements associated with these rights.

- Users may download and print one copy of any publication from the public portal for the purpose of private study or research.
- You may not further distribute the material or use it for any profit-making activity or commercial gain
- You may freely distribute the URL identifying the publication in the public portal

Read more about Creative commons licenses: <https://creativecommons.org/licenses/>

### Take down policy

If you believe that this document breaches copyright please contact us providing details, and we will remove access to the work immediately and investigate your claim.

LUND UNIVERSITY

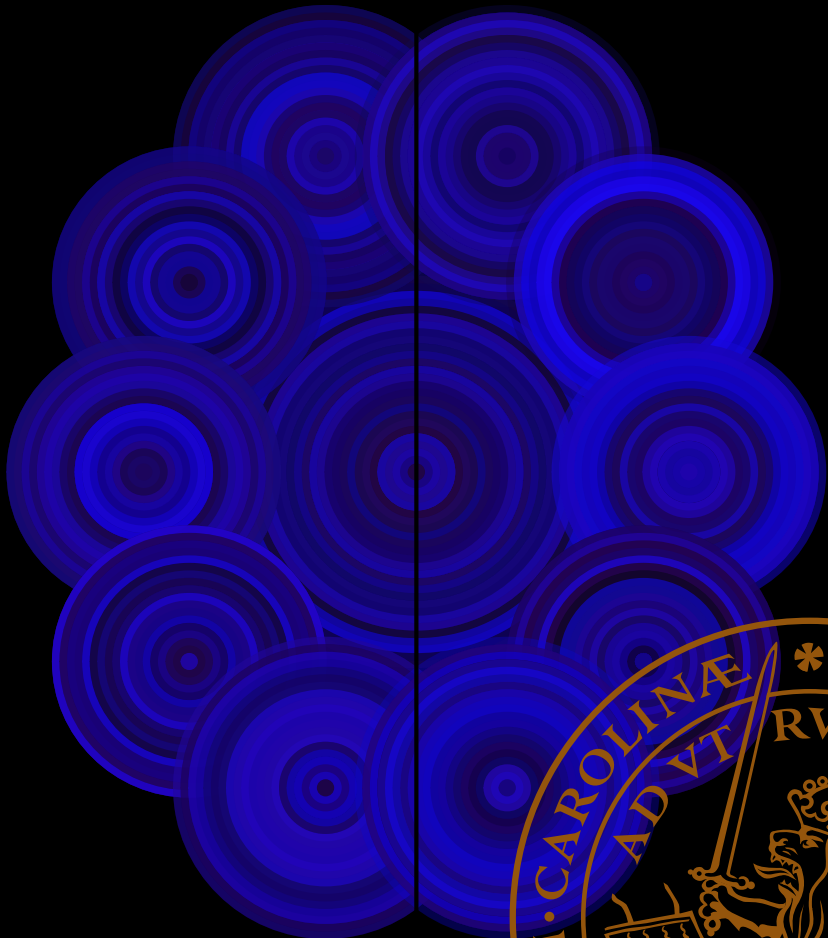
PO Box 117  
221 00 Lund  
+46 46-222 00 00

# Models of Neuroimaging, Biomarkers, and Cognitive Change in Alzheimer's Disease

## Implications for Clinical Trial Design

PHILIP S. INSEL

DEPARTMENT OF CLINICAL SCIENCES, MALMÖ | LUND UNIVERSITY





# Models of Neuroimaging, Biomarkers, and Cognitive Change in Alzheimer's Disease

Implications for Clinical Trial Design

by Philip S. Insel



**LUND**  
UNIVERSITY

DOCTORAL DISSERTATION

by due permission of the Faculty of Medicine, Lund University, Sweden.  
To be defended at Segerfalksalen, on 21 May 2021 at 13:00.

*Faculty opponent*  
Michael Egan

Organization LUND UNIVERSITY Department of Clinical Sciences, Lund University, Sölvegatan 19 – BMC F12, 221 84 Lund Author Philip S. Insel	Document name DOCTORAL DISSERTATION Date of issue 2021-05-21 Sponsoring organization	
Title and subtitle Models of Neuroimaging, Biomarkers and Cognitive Change in Alzheimer's Disease Implications for Clinical Trial Design		
Abstract Objectives: Identify a window for early treatment by estimating the time course of early pathophysiological changes in Alzheimer's disease, clarify the relationship between emerging pathology and symptom onset as well as estimate the time to clinically meaningful decline in order to inform clinical trial design. Methods: The participants included in the analyses of the five papers were drawn from four cohorts: ADNI, AIBL, BioFINDER, A4. Repeated measures of longitudinal MRI, PET, CSF and cognitive responses were modeled using (1) mixed-effects regression with a random intercept and slope or (2) generalized least squares. Nonlinearity in longitudinal responses was captured using restricted cubic splines. Clinical trial scenarios were simulated to estimate the power to detect assumed drug effects. Results: Clinical trials in preclinical AD are generally underpowered to detect a plausible treatment effect. Optimal composites to capture decline in the observed preclinical AD population were equal weight composites across all available cognitive and functional measures. Estimates of several major milestone events of AD progression include changes in CSF A $\beta$ 24 29 years before A $\beta$ -positivity, an increase in regional A $\beta$ PET deposition 15 years before, increases in tau pathology 7–8 years before, and signs of cognitive dysfunction 4–6 years before A $\beta$ -positivity. Cognitively unimpaired A $\beta$ + participants approach early MCI cognitive performance levels on general cognition six years after baseline. To achieve 80% power to detect a 25% treatment effect, 2,000 participants/group for a 4-year trial and 600 participants/group for a 6-year trial are required. Discussion: Including a large number of components in a cognitive/functional composite endpoint may smooth over aberrations in scores in a particular assessment from visit to visit within a subject, thus lowering the within-subject variance and improving signal to noise. In later stage preclinical AD, suitable power for a phase III trial can be achieved with considerably lower sample sizes while capturing both cognitive and functional change to demonstrate a clinically meaningful drug effect—both while initiating treatment in subjects who are still cognitively unimpaired. Small but meaningful increases in levels of CSF tau and temporoparietal tau are observed years before the current threshold for A $\beta$ -positivity. In the context of secondary prevention trials, tau levels in these participants would already have been increasing for several years, likely more. These data support the use of primary prevention trials against A $\beta$ where treatment is initiated years before the current threshold for A $\beta$ -positivity. The separation between cognitively unimpaired participants and early MCI was just over one SD on the PACC, suggesting that one point of additional decline in A $\beta$ + participants compared to A $\beta$ - participants could be taken as an approximate benchmark for clinically meaningful decline. Based on the PACC estimates, a treatment effect of 40%–50% would be required to delay the cognitive decline of a group of A $\beta$ + participants from reaching the one SD milestone by three years.		
Key words		
Classification system and/or index terms (if any)		
Supplementary bibliographical information	Language English	
ISSN and key title 1652-8220 Doctoral Dissertation Series 2021:50 (Lund University Faculty of Medicine)	ISBN 978-91-8021-056-0	
Recipient's notes	Number of pages	Price
	Security classification	

I, the undersigned, being the copyright owner of the abstract of the above-mentioned dissertation, hereby grant to all reference sources permission to publish and disseminate the abstract of the above-mentioned dissertation.

Signature



Date 2021-0415

# Models of Neuroimaging, Biomarkers, and Cognitive Change in Alzheimer's Disease

Implications for Clinical Trial Design

by Philip S. Insel



**LUND**  
UNIVERSITY

Copyright pp 1-62 Philip S. Insel (2021)

Paper 1 © Elsevier

Paper 2 © Elsevier

Paper 3 © Wolters Kluwer

Paper 4 © John Wiley & Sons

Paper 5 © American Medical Association

Faculty of Medicine, Department of Clinical Sciences

ISBN 978-91-8021-056-0 Doctoral Dissertation Series 2021:50


ISSN 1652-8220

Printed in Sweden by Media-Tryck, Lund University

Lund 2021



Media-Tryck is a Nordic Swan Ecolabel certified provider of printed material. Read more about our environmental work at [www.mediatryck.lu.se](http://www.mediatryck.lu.se)

**MADE IN SWEDEN** 

*M'darlings Pap, Sallytoe, Claw —*

*95, 1062, 2700, 789...time of my life.*



# Table of Contents

Abbreviations	8
List of publications	10
Abstract	11
<b>Background</b>	<b>13</b>
<b>Introduction</b>	<b>14</b>
Paper #1:	14
Paper #2:	16
Paper #3:	17
Paper #4:	17
Paper #5:	18
<b>Aims</b>	<b>19</b>
<b>Methods</b>	<b>21</b>
Participants	21
Cerebrospinal Fluid	22
A $\beta$ Positron Emission Tomography	22
Tau Positron Emission Tomography	23
Magnetic Resonance Imaging	24
Cognitive and Functional Measures	24
Statistical Methods	25
<b>Results</b>	<b>28</b>
Paper #1:	28
Paper #2:	31
Paper #3:	36
Paper #4:	39
Paper #5:	41

Discussion	44
Conclusion	50
Acknowledgements	51
References	54

# Abbreviations

A4	Anti-Amyloid Treatment in Asymptomatic Alzheimer's (study)
ADAS13	Alzheimer's Disease Assessment Scale—Cognitive Subscale, 13 item
AIBL	Australian Imaging, Biomarkers & Lifestyle (study)
AD	Alzheimer's Disease
ADNI	Alzheimer's Disease Neuroimaging Initiative
AIC	Akaike Information Criterion
<i>APOE</i>	Apolipoprotein E
A $\beta$	Amyloid $\beta$
AVLT	Auditory Verbal Learning Test
BioFINDER	Biomarkers for Identifying Neurodegenerative Disorders Early and Reliably (study)
cCN	Cognitively Normal Converter
CDR-SB	Clinical Dementia Rating—Sum of Boxes
CI	Confidence interval
CSF	Cerebrospinal fluid
CU	Cognitively Unimpaired
ERC	Entorhinal Cortex
FAQ	Functional Activities Questionnaire
FCSRT	Free and Cued Selective Reminding Test
LASSO	Least Absolute Shrinkage and Selection Operator
LPL	Lateral Parietal Lobe
LTL	Lateral Temporal Lobe
MMRM	Mixed-Model Repeated Measures
MMSE	Mini-Mental State Examination
MPL	Medial Parietal Lobe
MRI	Magnetic Resonance Imaging

MTL	Medial Temporal Lobe
ng/L	Nanograms per Liter
OR	Odds Ratio
PACC	Preclinical Alzheimer's Cognitive Composite
pcCN	Predicted Cognitively Normal Converter
PET	Positron Emission Tomography
P-tau	Phosphorylated Tau
ROI	Region of Interest
sCN	Stable Cognitively Normal
SD	Standard Deviation
SE	Standard Error
SUVR	Standardized Uptake Value Ratio
TFA $\beta$ +	Time from amyloid $\beta$ positivity
T-tau	Total Tau

## List of publications

- I. Cognitive and functional changes associated with A $\beta$  pathology and the progression to mild cognitive impairment  
Insel, Philip S., Michael C. Donohue, R. Scott Mackin, Paul S. Aisen, Oskar Hansson, Michael W. Weiner, Niklas Mattsson. *Neurobiology of aging* 48 (2016): 172-181.
- II. Time between milestone events in the Alzheimer's disease amyloid cascade  
Insel, Philip S., Michael C. Donohue, David Berron, Oskar Hansson, and Niklas Mattsson-Carlgen. *NeuroImage* (2020): 117676.
- III. Determining clinically meaningful decline in preclinical Alzheimer disease  
Insel, Philip S., Michael Weiner, R. Scott Mackin, Elizabeth Mormino, Yen Ying Lim, Erik Stomrud, Sebastian Palmqvist, Masters, Colin L., Maruff, Paul.T., Hansson, Oskar. and Mattsson, Niklas. *Neurology* 93, no. 4 (2019): e322-e333.
- IV. Predicting diagnosis and cognition with <sup>18</sup>F-AV-1451 tau PET and structural MRI in Alzheimer's disease  
Mattsson, Niklas, Philip S. Insel, Michael Donohue, Jonas Jögi, Rik Ossenkoppele, Tomas Olsson, Michael Schöll, Ruben Smith, and Oskar Hansson. *Alzheimer's & Dementia* 15, no. 4 (2019): 570-580.
- V. Association between apolipoprotein E  $\epsilon$ 2 vs  $\epsilon$ 4, age, and  $\beta$ -amyloid in adults without cognitive impairment  
Insel, Philip S., Oskar Hansson, and Niklas Mattsson-Carlgen. *JAMA Neurology* (2020).

# Abstract

**Objectives:** Identify a window for early treatment by estimating the time course of early pathophysiological changes in Alzheimer's disease, clarify the relationship between emerging pathology and symptom onset as well as estimate the time to clinically meaningful decline in order to inform clinical trial design.

**Methods:** The participants included in the analyses of the five papers were drawn from four cohorts: ADNI, AIBL, BioFINDER, A4. Repeated measures of longitudinal MRI, PET, CSF and cognitive responses were modeled using (1) mixed-effects regression with a random intercept and slope or (2) generalized least squares. Nonlinearity in longitudinal responses was captured using restricted cubic splines. Clinical trial scenarios were simulated to estimate the power to detect assumed drug effects.

**Results:** Clinical trials in preclinical AD are generally underpowered to detect a plausible treatment effect. Optimal composites to capture decline in the observed preclinical AD population were equal weight composites across all available cognitive and functional measures.

Estimates of several major milestone events of AD progression include changes in CSF A $\beta$ 42 29 years before A $\beta$ -positivity, an increase in regional A $\beta$  PET deposition 15 years before, increases in tau pathology 7–8 years before, and signs of cognitive dysfunction 4–6 years before A $\beta$ -positivity.

Cognitively unimpaired A $\beta$ + participants approach early MCI cognitive performance levels on general cognition six years after baseline. To achieve 80% power to detect a 25% treatment effect, 2,000 participants/group for a 4-year trial and 600 participants/group for a 6-year trial are required.

**Discussion:** Including a large number of components in a cognitive/functional composite endpoint may smooth over aberrations in scores in a particular assessment from visit to visit within a subject, thus lowering the within-subject variance and improving signal to noise. In later stage preclinical AD, suitable power for a phase III trial can be achieved with considerably lower sample sizes while capturing both cognitive and functional change to demonstrate a clinically meaningful drug effect—both while initiating treatment in subjects who are still cognitively unimpaired.

Small but meaningful increases in levels of CSF tau and temporoparietal tau are observed years before the current threshold for A $\beta$ -positivity. In the context of secondary prevention trials, tau levels in these participants would already have been increasing for several years, likely more. These data support the use of primary prevention trials against A $\beta$  where treatment is initiated years before the current threshold for A $\beta$ -positivity.

The separation between cognitively unimpaired participants and early MCI was just over one SD on the PACC, suggesting that one point of additional decline in A $\beta$ + participants compared to A $\beta$ - participants could be taken as an approximate benchmark for clinically meaningful decline. Based on the PACC estimates, a treatment effect of 40%–50% would be required to delay the cognitive decline of a group of A $\beta$ + participants from reaching the one SD milestone by three years.

# Background

The focus of this thesis is the improved design of clinical trials in early Alzheimer's Disease (AD). There is no disease-modifying treatment for AD, although at the time of this writing (March 2021), for the first time, there is one phase III anti-A $\beta$  therapy (Sevigny et al., 2016), under review for approval by the FDA.

A series of failed attempts to treat AD dementia patients with A $\beta$ -modifying therapies led some in the field to question the amyloid cascade hypothesis and the A $\beta$  pathway as a target for treatment. Despite significant treatment effects on biomarkers including A $\beta$  and tau, treatments in phase III trials have failed to show significant effects on primary clinical outcomes (Doody et al., 2014; Salloway et al., 2014). These failures led to a shift toward earlier treatment in hopes of an improved likelihood of success. Attempts at earlier treatment, especially in those without cognitive impairment, poses complications in terms of trial design. Participants without symptoms of cognitive dysfunction are unlikely to decline reliably in the way that AD dementia patients would, raising questions about the trial length, sample size and outcome measurements required to detect a treatment effect. Without clinical symptoms, participants would need to be recruited based on biomarker inclusion criteria, leading to questions about the time course of the disease in terms of the relationship between accumulating A $\beta$  and tau pathology and emerging cognitive decline.

This thesis concentrates primarily on identifying a window for early treatment by estimating the time course of early pathophysiological changes in AD, its relationship to symptom onset, and the implications for trial design features including outcome measure sensitivity, trial length and clinically meaningful decline, as well as the power to detect meaningful treatment effects.



# Introduction

The papers in this thesis attempt to answer questions regarding the optimization of clinical trial design in Alzheimer's disease — what populations should be recruited to test potential treatments, what measures should be used to evaluate change over time and test treatment effects, what is the window for treatment that may optimize the likelihood of successful treatment and what is the expected time frame for cognitive decline in relation to biomarker and imaging changes?

Paper #1 dealt primarily with which population should be recruited, and which instruments should be used to measure clinical decline over time. Directly linked to who should be recruited is when should therapeutic interventions occur — the primary aim of paper #2 was to estimate the time course of disease, especially the initial changes, and identify an optimal window for early treatment while maintaining trial feasibility and efficiency. Paper #3 also focused on the time frame of decline and characterizing the time required to reach a clinically meaningful threshold for early cognitive dysfunction. Paper #4 evaluated the relationship between several imaging measures closely associated with clinical outcomes — imaging measures that may be essential secondary or concurrent outcomes in AD clinical trials. Finally, in a slight departure, paper #5 demonstrated the potential for a drug that might mimic the biochemical properties of the APOE2 allele — a potential early treatment option for populations at high risk for AD.

The overarching theme of these papers is the estimation of the changes that occur throughout the lifespan of AD in order to identify individuals at high risk for future cognitive decline based on the earliest signals in biomarker and imaging measures. Early identification and sensitive measures of biomarker, imaging and clinical changes are essential to facilitate and optimize clinical trials in AD.

## Paper #1:

Cognitive and functional changes associated with A $\beta$  pathology and the progression to mild cognitive impairment

In 2015, at the time this paper was being developed, the Food and Drug Administration (FDA) had recently offered draft guidance to update their recommendations on primary endpoint selection in clinical trials for early-stage AD (Food and Drug Administration, 2013). With the focus of recent clinical trials on treatment in these earlier stages of AD, including prodromal AD and preclinical AD, the FDA recognized the difficulty in demonstrating drug efficacy using prior guidelines developed for trials with subjects in the dementia stage of AD (Kozauer and Katz, 2013; Mckhann et al., 2011). Trial design in later stages of AD has typically included a coprimary endpoint to demonstrate efficacy on both a cognitive and a functional assessment. However, the assessment tools used in these trials have not been validated in earlier stage subjects (Snyder et al., 2014), leading the FDA to consider the use of a single primary composite endpoint that captures both cognitive and functional decline, in trials of prodromal AD subjects. Preclinical AD subjects are, by definition, cognitively unimpaired and should not have any functional impairment due to cognitive dysfunction. We hypothesize that as the target population progresses on the continuum of decline, assessing functional changes may take a more central role in demonstrating a drug effect to be clinically meaningful. However, the feasibility and value of assessing functional decline as part of a trial endpoint in a preclinical population are unknown.

Since the FDA guidance, several cognitive composites have been developed to capture the decline specific to subjects with preclinical AD, but no attempts have been made to develop combined cognitive and functional composites. The Alzheimer's Prevention Initiative (API) has developed cognitive composites using Presenilin 1 E280A mutation carriers (Ayutyanont et al., 2014) and also cognitively unimpaired elders who progressed to MCI or AD (Langbaum et al., 2014). A third cognitive composite, to be used as the primary endpoint in the A4 trial (Sperling et al., 2014), was developed to capture decline in  $A\beta+$  cognitively unimpaired elders (Donohue et al., 2014).

The analyses in paper #1 sought to characterize and compare the cognitive and functional decline in (1) cognitively unimpaired individuals who progress to mild cognitive impairment (MCI) and (2) cognitively unimpaired  $A\beta+$  individuals. Identifying the cognitive and functional assessments and their weighted combinations that maximize the longitudinal decline specific to these groups may facilitate optimizing the clinical endpoints used in clinical trials of early AD and evaluate the potential role of functional assessments in cognitively unimpaired populations.

## Paper #2:

Time between milestone events in the Alzheimer's disease amyloid cascade

Previous neuropathological and biomarker data suggest that the overall time-course of AD is several decades (Li et al., 2017; Villemagne et al., 2013). In autosomal dominant AD, the estimated years to clinical onset has been used to estimate the time-course of various biomarkers in AD (Bateman et al., 2012). However, the time-course of the spread of A $\beta$  and tau and the onset of clinical symptoms in sporadic AD is unknown.

With repeated measures of A $\beta$  over time, the level and rate of change with respect to the key initiating AD pathology may offer a measure of disease progression in sporadic AD. The duration of amyloid positivity (chronicity) has been shown to be associated with increased tau pathology and faster cognitive decline and valuable in explaining heterogeneity in early disease progression (Koscik et al., 2020). With level and change information, the time from the threshold for significant A $\beta$  pathology can be estimated within individuals, providing the temporal disease progression information important for evaluating biomarker trajectories. By incorporating this longitudinal information, disease progression with respect to A $\beta$  pathology can be represented to reflect its continuous nature, resulting in a more powerful way to model the relationship between A $\beta$  and downstream processes.

Paper #2 Sought to demonstrate the utility and predictive ability of the time-from-A $\beta$ -positivity (TFA $\beta$ +) formulation and to evaluate the relationships between TFA $\beta$ + and downstream biomarker and cognitive responses in order to estimate the time of the earliest signs of progression in sporadic AD. Using serial <sup>18</sup>F-florbetapir (A $\beta$ ) PET measurements, rates of change of A $\beta$  were estimated and used to calculate the time-from-threshold for each participant. These subject-specific estimates of the proximity to the threshold for A $\beta$ -positivity (A $\beta$ +) were then used to model the trajectories and temporal ordering of other key markers in AD including CSF A $\beta$ 42, regional A $\beta$  PET, several measures of tau including CSF phosphorylated (P-tau) and total tau (T-tau), regional <sup>18</sup>F-flortaucipir (AV-1451) tau PET, and cognition. Estimates of the time and ordering of these pathophysiological changes may facilitate the design of future prevention trials and identify a window for early treatment.

## Paper #3:

### Determining clinically meaningful decline in preclinical Alzheimer disease

Demonstrating that treatments are effective during the preclinical stage will require understanding the magnitude of early A $\beta$ -related cognitive decline in cognitively unimpaired adults (Sperling et al., 2014). Defining meaningful decline will help determine the time frame for subtle cognitive changes to progress to incipient functional decline and to identify an optimal treatment window.

The association between A $\beta$  status and cognition in preclinical AD varies widely across studies (Baker et al., 2017; Hedden et al., 2013; Insel et al., 2018; Mormino et al., 2017; Vemuri et al., 2015; Vos et al., 2014; Wirth et al., 2013), highlighting an inconsistent picture of early cognitive decline and uncertain implications for powering a trial in early AD. Understanding how sampling variation and study design features influence estimates of cognitive decline will improve the design of trials in preclinical AD.

Paper #3 Sought to harmonize several large studies in order to (1) determine the time required for a preclinical AD population to decline in a clinically meaningful way, (2) characterize how decline differs by cognitive domain, (3) update previous study design assumptions regarding sample size, power, and the required treatment effect, and (4) identify factors that modify A $\beta$ -related decline.

## Paper #4:

### Predicting diagnosis and cognition with <sup>18</sup>F-AV-1451 tau PET and structural MRI in Alzheimer's disease

The accumulation of A $\beta$  is assumed to lead to tau aggregation, brain atrophy, and cognitive decline (Mattsson et al., 2015; Tosun et al., 2017). However, A $\beta$  has limited toxicity and does not typically colocalize with changes in brain structure or function. In contrast, tau spreads within and beyond regions that show atrophy in AD and correlates with cognitive decline (Villemagne et al., 2015). Tau is therefore suspected to be essential for the development of atrophy and cognitive decline in AD. This study sought to clarify the degree to which tau aggregation and atrophy are independent processes and in which brain regions tau and atrophy are most critical for development of various clinical symptoms.

Paper #4 attempted to identify brain regions where tau pathology and brain structure are most strongly associated with cognitive features of AD and as well as test for overlapping and complementary effects of tau and brain structure. We hypothesized

that an optimized measure of tau would be superior to brain structure to identify AD and cognitive impairment. However, because atrophy and cognition may also be affected by other processes than tau pathology, including Lewy body pathology, vascular pathology, and TDP-43 pathology, we hypothesized that brain structure would provide some complementary information about cognition.

## Paper #5:

Association Between Apolipoprotein E  $\epsilon 2$  vs  $\epsilon 4$ , Age, and  $\beta$ -Amyloid in Adults Without Cognitive Impairment

Increasing evidence suggests that the *APOE* genotype and its corresponding protein (apoE) affect the pathogenesis of Alzheimer's disease (AD) through multiple biological pathways, including the differential regulation of A $\beta$  aggregation and clearance (Liu et al., 2013; Suidan and Ramaswamy, 2019). Although the most common recent approach in AD drug discovery is to directly target the A $\beta$  pathway, the high prevalence of *APOE*  $\epsilon 4$  in AD and the ease of identifying  $\epsilon 4$  carriers at any age make *APOE* pathways appealing therapeutic targets to slow A $\beta$  accumulation (Suidan and Ramaswamy, 2019).

By mimicking the biochemical properties associated with the apoE2 isoform, it may be possible to increase the A $\beta$  clearance that is reduced with apoE4. However, a central question is whether apoE2 remains protective in the presence of apoE4. This question has been difficult to answer, in large part because the simultaneous carriage of both the  $\epsilon 2$  and  $\epsilon 4$  alleles is rare—approximately 2% of the population has the  $\epsilon 24$  genotype (Mahley, 1988).

Paper #5 sought to determine whether apoE2 remains protective in the presence of apoE4 and to evaluate how the principal risk factors for AD (age and *APOE* genotype) are associated with early A $\beta$  accumulation, measured by fluroine 18–labeled ( $^{18}\text{F}$ )-florbetapir positron emission tomography (PET).

# Aims

Paper #1: Cognitive and functional changes associated with A $\beta$  pathology and the progression to mild cognitive impairment

- (1) Characterize cognitive and functional decline in
  - a. cognitively unimpaired participants who progress to mild cognitive impairment
  - b. cognitively unimpaired A $\beta$ + participants
- (2) Identify and compare the cognitive and functional assessments and their weighted combinations that maximize the longitudinal decline in these groups
- (3) Evaluate the potential role of functional assessments in studies of early AD.

Paper #2: Time between milestone events in the Alzheimer's disease amyloid cascade

- (1) Demonstrate the utility and predictive ability of the time-from-A $\beta$ -positivity (TFA $\beta$ +) formulation
- (2) Evaluate the relationships between TFA $\beta$ + and downstream biomarker and cognitive responses to estimate the time of the earliest signs of progression in sporadic AD.
- (3) Identify a window for early treatment using estimates of the time and ordering of pathophysiological changes.

Paper #3: Determining clinically meaningful decline in preclinical Alzheimer disease

- (1) Determine the time required for a preclinical AD population to decline in a clinically meaningful way
- (2) Characterize how decline differs by cognitive domain
- (3) Update previous study design assumptions regarding sample size, power, and the required treatment effect
- (4) Identify factors that modify A $\beta$ -related decline.

Paper #4: Predicting diagnosis and cognition with  $^{18}\text{F}$ -AV-1451 tau PET and structural MRI in Alzheimer's disease

- (1) Identify regions where tau pathology and brain structure are most strongly associated with cognitive features of AD
- (2) Test for overlapping and complementary effects of tau and brain structure

Paper #5: Association Between Apolipoprotein E  $\epsilon 2$  vs  $\epsilon 4$ , Age, and  $\beta$ -Amyloid in Adults Without Cognitive Impairment

- (1) Determine whether apoE2 remains protective in the presence of apoE4
- (2) Evaluate how the principal risk factors for AD (age and *APOE* genotype) are associated with  $\text{A}\beta$  accumulation

# Methods

## Participants

The participants included in the analyses of the five papers were drawn from four cohorts:

- (1) The Alzheimer's Disease Neuroimaging Initiative (ADNI) (Mueller et al., 2005)
- (2) The Swedish Biomarkers for Identifying Neurodegenerative Disorders Early and Reliably Study (BioFINDER) (Palmqvist et al., 2014)
- (3) The Australian Imaging, Biomarkers & Lifestyle (AIBL) Study (Ellis, 2009)
- (4) The Anti-Amyloid Treatment in Asymptomatic Alzheimer Disease Study (The A4 Study) (Sperling et al., 2020)

ADNI participants were recruited from over 50 sites across the United States and Canada (see [www.adni-info.org](http://www.adni-info.org)). Participants were enrolled during multiple phases of ADNI: ADNI-1, ADNI-Go, and ADNI-2 across the spectrum of cognitive classifications including cognitively unimpaired, subjective memory complaint, mild cognitive impairment (MCI) and Alzheimer's disease dementia. ADNI participants were included in papers #1-3.

BioFINDER participants were enrolled consecutively at three memory outpatient clinics in Sweden. BioFINDER participants were cognitively unimpaired, had mild cognitive impairment or Alzheimer's disease dementia. BioFINDER participants were included in papers #3-4.

AIBL participants were assessed at three sites in Australia. All AIBL participants included were enrolled into the cognitively unimpaired group and were included in paper #4.

A4 participants were enrolled at 67 clinical trial sites in the US, Canada, Australia, and Japan. All A4 participants were assessed to be cognitively unimpaired and were included in paper #5.



Participants for all studies were required to have A $\beta$  information, whether from CSF or PET, as well as completed a neuropsychological test battery. Participants were excluded if they had a major neurologic or psychiatric illness or substance abuse. ADNI participants were excluded if the screening MRI showed evidence of infection, infarction or other focal lesion. Informed written consent was obtained from all participants at each site.

## Cerebrospinal Fluid

ADNI CSF samples were collected by lumbar puncture and shipped on dry ice to the ADNI Biomarker Core laboratory at the University of Pennsylvania Medical Center for long-term storage at 80 C. CSF A $\beta$ 42 was measured using the multiplex xMAP Luminex platform (Luminex Corp, Austin, TX, USA) with the research use only INNOBIA AlzBio3 kit (Fujirebio/Innogenetics, Ghent, Belgium) (Olsson et al., 2005; Shaw et al., 2009). CSF A $\beta$ + was defined as CSF A $\beta$ 42 < 192.

BioFINDER CSF samples were analyzed for CSF A $\beta$ 42 and A $\beta$ 40 using ELISA assays (ADx/EUROIMMUN AG, Lübeck, Germany). CSF A $\beta$ + was defined as CSF A $\beta$ 42/ A $\beta$ 40 < 0.1 (Janelidze et al., 2016).

## A $\beta$ Positron Emission Tomography

ADNI <sup>18</sup>F-florbetapir PET image data were acquired 50–70 min postinjection, and images were averaged, spatially aligned, interpolated to a standard voxel size, and smoothed to a common resolution of 8 mm full width at half maximum. Methods to acquire and process ADNI <sup>18</sup>F-florbetapir PET image data are described in (Landau et al., 2012). Full details of acquisition and analysis can be found at <http://adni.loni.usc.edu/methods/>. We used an a priori defined threshold for A $\beta$ -positivity (SUVR = 1.1) (ADNI, 2012; Joshi et al., 2012) applied to the ratio of the average of the four target regions (temporal, cingulate, frontal, and parietal lobes) and the cerebellum. A $\beta$  PET ROI outcomes were also considered (Landau and Jagust, 2015; Mormino et al., 2009), (1) the temporal lobe (middle and superior temporal lobe), (2) the parietal lobe (precuneus, supramarginal, inferior and superior parietal lobe), (3) the cingulate gyrus (isthmus, posterior, caudal and rostral anterior cingulate), (4) the frontal lobe (pars opercularis, pars triangularis, pars orbitalis, caudal/rostral middle frontal, medial/lateral orbitofrontal, frontal pole, and superior frontal lobe), and (5) a composite of regions thought to be early in accumulating A $\beta$  (precuneus and

posterior cingulate) (Palmqvist et al., 2017). These ROIs comprise the regions included in the global composite, grouped into individual lobes plus an additional early ROI.  $^{18}\text{F}$ -florbetapir ROIs were expressed as SUVRs with a cerebellar reference region.

A $\beta$  PET imaging in the A4 Study was done using  $^{18}\text{F}$ -florbetapir data, which was acquired 50 to 70 minutes postinjection. Images were realigned and averaged and then spatially aligned to a standard space template.  $^{18}\text{F}$ -florbetapir, sampled in a global neocortical region for A $\beta$ , was expressed as a standardized uptake value ratio (SUVR) with a cerebellar reference region (Johnson et al., 2018).  $\beta$ -Amyloid positivity was defined as participants with an  $^{18}\text{F}$ -florbetapir PET SUVR greater than or equal to 1.10 (Clark et al., 2012; Joshi et al., 2012).

A $\beta$  PET was used in AIBL to define A $\beta$ -positivity. A $\beta$ -positivity was defined as  $^{18}\text{F}$ -florbetapir PET SUVR >1.1 (n = 72), 11C-PiB PET SUVR >1.5 (n = 201), or  $^{18}\text{F}$ -flutemetamol SUVR >0.62 (n = 75) (Villemagne et al., 2014).

## Tau Positron Emission Tomography

Methods to acquire and process tau ( $^{18}\text{F}$ -flortaucipir) PET image data in ADNI were described in (Maass et al., 2017). Six tau ROI outcomes, corrected for partial-volume, were considered: (1) the medial temporal lobe (MTL) (amygdala, entorhinal and parahippocampal cortex; from Braak stage I and III), (2) the lateral temporal lobe (LTL) (inferior/middle/superior temporal lobe, banks of the superior temporal sulcus, transverse temporal lobe, temporal pole; from Braak stage IV and V), (3) the medial parietal lobe (MPL) (isthmus cingulate, precuneus; from Braak stage IV and V), (4) the lateral parietal lobe (LPL) (inferior/superior parietal lobe, supramarginal; from Braak stage V), (5) frontal lobe (pars, orbitofrontal and middle/superior frontal lobe; from Braak stage V), and (6) the occipital lobe (cuneus, lingual, pericalcarine, and lateral occipital lobe; from Braak stage III, V, and VI).  $^{18}\text{F}$ -flortaucipir ROIs were expressed as SUVRs with an inferior cerebellar gray matter reference region. Scanner type and site were evaluated for their association with PET outcomes through covariate adjustment. Full details of PET acquisition and analysis can be found at <http://adni.loni.usc.edu/methods/>.

Tau PET imaging in BioFINDER was done with procedures described in Smith et al., 2016.  $^{18}\text{F}$ -AV-1451 was synthesized at Skåne University Hospital, Lund (Hahn et al., 2017), and PET scans were performed on a GE Discovery 690 PET scanner (General Electric Medical Systems). Partial volume error correction was performed using the Geometric Transfer Method (Rousset et al., 1998) and combined with a region-based voxelwise approach (Thomas et al., 2011). FreeSurfer parcellation in MR

space of the anatomical scan was applied to processed, coregistered, and time averaged PET images to extract regional uptake values.  $^{18}\text{F}$ -AV-1451 standardized uptake value ratio images were based on mean uptake over 80-100 min postinjection normalized to uptake in a gray matter masked cerebellum reference region. The same FreeSurfer regions as for MRI were included for  $^{18}\text{F}$ -AV-1451. Besides hippocampus and amygdala, all non-neocortical structures were removed because of susceptibility to off-target binding (Smith et al., 2016). Hippocampus may also be susceptible to off-target binding because of its proximity to the choroid plexus (Lowe et al., 2016). However, we chose to include it because it is a recognized key region for structural brain changes and to facilitate comparisons between  $^{18}\text{F}$ -AV-1451 PET and MRI data.

## Magnetic Resonance Imaging

In BioFINDER, T1-weighted MRI was performed on 3T MR scanners (Siemens Tim Trio 3T and Siemens Skyra; Siemens Medical Solutions, Erlangen, Germany), producing a high-resolution anatomical MP-RAGE image (TR5 1950 ms, TE53.4 ms, 1 mm isotropic voxels, and 178 slices). Cortical reconstruction and volumetric segmentation were performed with the FreeSurfer (v5.3) image analysis pipelines (MP-RAGE images underwent correction for intensity homogeneity (Sled et al., 1998), removal of nonbrain tissue, and segmentation into gray matter and white matter with intensity gradient and connectivity among voxels (Dale et al., 1999; Fischl et al., 2002; Fischl and Dale, 2000). Cortical thickness was measured as the distance from the gray matter/white matter boundary to the corresponding pial surface (Fischl and Dale, 2000). Reconstructed data sets were visually inspected for accuracy, and segmentation errors were corrected. Bilaterally averaged thickness measures of all available neocortical areas, plus volumes of hippocampus and amygdala, were included.

## Cognitive and Functional Measures

Cognitive measures assessed in ADNI were the Mini Mental State Examination (MMSE), Alzheimer's Disease Assessment Scale cognitive subscale, 13-item version (ADAS13), immediate and delayed memory recall from the Wechsler Memory Scale immediate and delayed Rey Auditory Verbal Learning Test, Trail Making Test parts A and B (Trails A & B), Boston Naming Test, and Category Fluency. The Clinical Dementia Rating Sum of Boxes (CDR-SB) was also assessed, which includes both cognitive and functional items, and finally the Functional Assessment Questionnaire

(FAQ), which is purely a functional assessment (Morris, 1993; Pfeffer et al., 1982; Reitan, 1958; Rey, 1958; Rosen et al., 1984; Wechsler, 1987).

Cognitive and functional measures in BioFINDER included the MMSE, immediate and delayed word list recall tests from the Alzheimer's Disease Assessment Scale–cognitive subscale, Trail Making Test part A & B, and category (animal) fluency.

Measures assessed for AIBL participants included the MMSE, Logical Memory Delayed Recall, Digit Symbol Substitution Test, the Delayed Recall from the California Verbal Learning Test, and the CDR-SB.

A4 participants completed a neuropsychological test battery including the Preclinical Alzheimer's Cognitive Composite (PACC) (Donohue et al., 2017, 2014) comprising the MMSE, Logical Memory Delayed Recall, Free and Cued Selective Reminding Test (FCSRT96), and the Digit Symbol Substitution Test. To calculate the PACC, the individual components were centered on their means and scaled to their standard deviations and summed, calculated using all participants. This sum was then centered on the mean and standard deviation of the sum, calculated using only the A $\beta$ -negative group. We evaluated the FCSRT96 formulation of the FCSRT as well as the Free Recall portion of the FCRST because of evidence of their sensitivity to early A $\beta$ -related cognitive changes. (Donohue et al., 2014; Mormino et al., 2017; Papp et al., 2017, 2015).

Modified versions of the PACC were calculated for ADNI, BioFINDER and AIBL. For ADNI, the modified PACC comprised the MMSE, Logical Memory Delayed Recall, Trail-Making Test B (Trails B), and the Delayed Word Recall from the Alzheimer's Disease Assessment Scale–Cognitive Subscale. For AIBL, the PACC was constructed using the MMSE, Logical Memory Delayed Recall, Digit Symbol Substitution Test, and the Delayed Recall from the California Verbal Learning Test. For BioFINDER, the PACC consisted of the MMSE, Delayed Word Recall from the Alzheimer's Disease Assessment Scale–Cognitive Subscale and Trails B.

## Statistical Methods

Repeated measures of longitudinal imaging, biofluid and cognitive responses were modeled using (1) mixed-effects regression with a random intercept and slope or (2) generalized least squares. For development of composite cognitive and functional endpoints, numerical optimization via bound constrained optimization (Byrd et al., 1995) was used. Nonlinearity in longitudinal responses was captured using restricted cubic splines. Differences in group trajectories (frequently A $\beta$ - vs A $\beta$ +) over time were tested using likelihood ratio tests. P-values from multiple comparisons over many

cognitive domains or imaging ROIs were adjusted using a Hochberg correction (Hochberg, 1988). Cross-validation was used to protect against overfitting. Clinical trial scenarios were simulated and the power to detect assumed drug effects were estimated using mixed model repeated measures (MMRM) change and variance estimates.

Several analyses, especially in paper #2, focused on estimating the time course of imaging, biomarker and cognitive changes over the lifetime of AD. Each of these analyses were done in two steps. Step one involved estimating a time-from-threshold measure to place individuals on a pathological timeline. This measure used time from significant A $\beta$  deposition (TFA $\beta$ +) as the anchoring event. TFA $\beta$ + was estimated based on the longitudinal measures of global A $\beta$  PET SUVR. In step two, TFA $\beta$ + estimates were used to predict cross-sectional measures of regional tau and A $\beta$  PET, CSF and cognitive outcomes. To demonstrate the value of the TFA $\beta$ + measure, we did head-to-head comparisons of (i) TFA $\beta$ + vs (ii) intercepts and slopes of longitudinal A $\beta$  PET, modeled separately, to predict the outcomes.

Because TFA $\beta$ + was not directly observed, in step one, linear mixed-effects models were fit to all available longitudinal global A $\beta$  PET SUVR data to estimate subject-specific intercepts and slopes of A $\beta$  pathology. Because A $\beta$  slopes are unlikely to remain constant over long periods of time as subjects move toward and away from the A $\beta$  threshold, natural splines (Hastie and Tibshirani, 1990) were used to estimate the nonlinear shape of the slopes with respect to baseline A $\beta$ , using quantile regression (Koenker and D'Orey, 1987). Rather than modeling the mean A $\beta$  slope with respect to baseline A $\beta$ , quantile regression provides a separate curve for each quantile, allowing the relationship between slope and intercept to differ depending on the location in the distribution of A $\beta$  slope. For each subject, TFA $\beta$ + was estimated by integrating over each subject's quantile curve from the subject's intercept to the threshold for A $\beta$ -positivity (PET SUVR = 1.1). For example, for a subject with a baseline SUVR of 1.2 and a slope in the 0.6 quantile, TFA $\beta$ + was taken to be the time it would take to go from SUVR = 1.1 to 1.2, using the slope estimates from the quantile curve. For incremental changes on the x-axis (baseline SUVR), the time required to travel the incremental distance is equal to distance/rate. Using the trapezoid rule (Atkinson, 1989), TFA $\beta$ + is the sum of these incremental times spanning SUVR = 1.1–1.2. Sensitivity analyses were done to determine the effect of varying the threshold for A $\beta$ +. We repeated the estimation of TFA $\beta$ + using an early threshold (SUVR 1.07) and a late threshold (SUVR 1.13).

Methods for paper #5 included estimating the individual and joint ability of <sup>18</sup>F-AV-1451 and MRI to predict diagnosis and cognition and was done in two steps. Step one: <sup>18</sup>F-AV-1451 and MRI composite scores. All cognitive responses (or diagnosis) were

regressed on  $^{18}\text{F-AV-1451}$  and MRI, separately. For the analyses on cognition, A $\beta$ -negative controls were removed, to evaluate cognition through the continuum of AD (preclinical, prodromal, and dementia stages). Each response was regressed on all included regions with  $^{18}\text{F-AV-1451}$  retention levels or cortical thickness (or volume for hippocampus and amygdala), adjusting for demographics (age, sex, and years of education). The least absolute shrinkage and selection operator (LASSO) (Tibshirani, 1996) was used for model selection and to estimate regional weights to be used to form  $^{18}\text{F-AV-1451}$  and MRI composites. The LASSO selects important predictors by shrinking the individual coefficients toward zero. The coefficients of covariates that do not provide additional predictive information are shrunk to zero, resulting in parsimonious and interpretable models. The LASSO is well suited to handle large numbers of highly correlated variables such as imaging regions of interest. Ten-fold cross-validation was used to tune the amount of shrinkage. Models were subsequently fit on all data using the cross-validated penalty parameter. Step two: Predictive value of  $^{18}\text{F-AV-1451}$  and MRI composite scores. All responses were regressed on the composites developed in step one. The models were summarized with regression coefficients, standard errors, Wald test p-values, and the Akaike Information Criterion (AIC) (Akaike, 1974). The predictive ability of each imaging modality was summarized with classification accuracy for diagnosis and  $R^2$  for cognitive responses. Ninety-five percent confidence intervals were estimated using jackknife estimated standard errors. Finally, all responses were regressed on both  $^{18}\text{F-AV-1451}$  and MRI composites simultaneously to estimate the joint predictive ability of both modalities, as well as the adjusted regression coefficients, standard errors, and p-values. The reduction of the regression coefficients after adjustment was reported along with 95% confidence intervals. For prediction of diagnosis, we also present (for comparison) the accuracy of a priori selected individual regions (inferior temporal lobe for  $^{18}\text{F-AV-1451}$  and hippocampal volume for MRI).

# Results

## Paper #1:

Cognitive and functional changes associated with A $\beta$  pathology and the progression to mild cognitive impairment

### *Cohort Characteristics*

In the ADNI data set, 68 subjects converted to MCI (cCN) during 7 years of follow-up while 70 subjects remained cognitively normal (sCN) throughout the same period. cCN subjects were older and had more *APOE*  $\epsilon 4$  carriers compared to sCN. There were no significant differences in gender or education. We also identified a group of cognitively unimpaired subjects who were predicted to convert to MCI (pcCN, only including A $\beta$ + subjects).

One hundred thirty-seven A $\beta$ + subjects and 210 A $\beta$ - subjects were included in the analysis. A $\beta$ + subjects were older, less educated, and had more *APOE*  $\epsilon 4$  carriers. There was no difference in gender.

Of the 68 cCN participants, 56 had A $\beta$  information: 31 (55.4%) were A $\beta$ + and 25 (44.6%) were A $\beta$ -. Of the 70 sCN participants, 57 had A $\beta$  information: 18 (31.6%) were A $\beta$ + and 39 (68.4%) were A $\beta$ -.

### *Baseline cognitive/functional differences*

When baseline cognitive/functional measures were compared in cCN versus sCN, cCN subjects performed worse on all 12 outcomes. There were fewer differences on baseline cognitive/functional measures in A $\beta$ + versus A $\beta$ - participants.

### *Longitudinal change*

cCN subjects worsened significantly faster on 10 of the 12 cognitive and functional outcomes compared to sCN subjects, with the exception of the Boston Naming Test and Trails A over 7 years of follow-up. The largest effect size was in the CDR-SB, and the largest effect sizes among measures without functional items were in the immediate AVLT and the ADAS13.

A $\beta$ <sup>+</sup> subjects worsened significantly faster on 6 of the 12 outcomes compared to A $\beta$ <sup>-</sup> subjects. The largest effect size was in the ADAS13. cCN subjects were more likely than sCN subjects to be missing data during the course of the 7 years of follow-up (log OR = 0.82, standard error = 0.15,  $p < 0.001$ ). However, sCN subjects were selected to have a minimum follow-up time of 7 years. A $\beta$ -positivity was not associated with increased missingness (log OR = -0.04, standard error = 0.27,  $p = 0.87$ ).

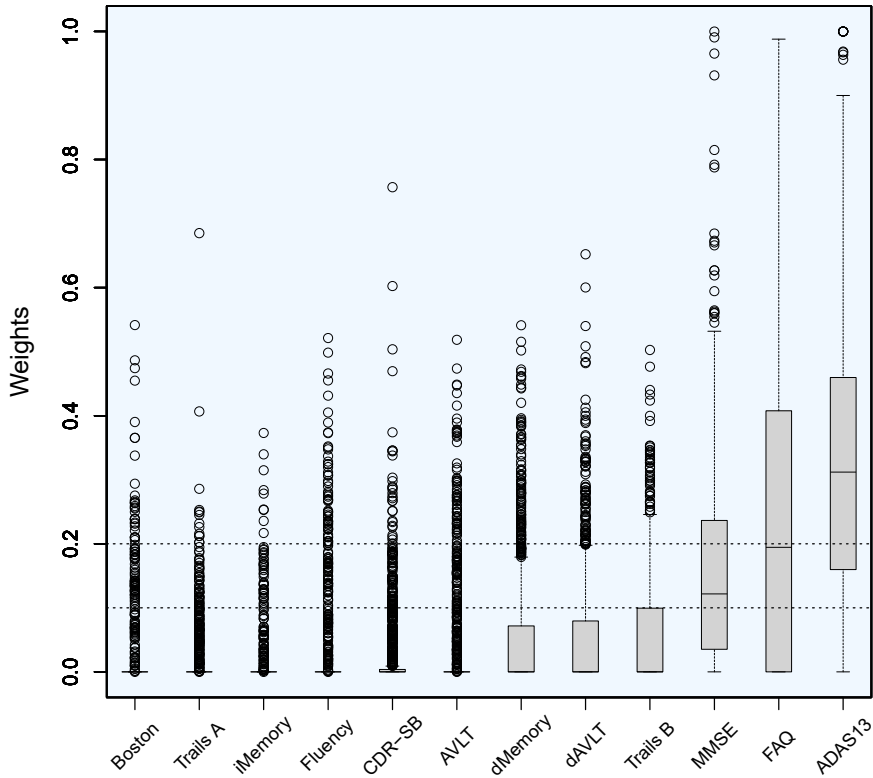
### *Composite weight distributions*

The distributions of the composite weights were estimated from 1000 bootstrap samples. Composite weights were estimated separately for the 3 groups (cCN, pcCN, and A $\beta$ <sup>+</sup>). The largest contributing outcomes in the composite for cCN versus sCN were the 2 delayed memory recall measures (delayed Logical Memory, delayed AVLT), CDR-SB, and the MMSE. Outcomes with smaller, although nonzero, positive median weights, included Category Fluency, immediate Logical Memory, Trails A, and the Boston Naming Test. When the functional measures were excluded, the delayed memory recall measures and MMSE remained the largest weighted outcomes and ADAS13 became more heavily weighted. Composite weights that maximized the separation of pcCN and sCN subjects were also estimated. Similar to the cCN composite, the main outcomes for the pcCN composite were delayed Logical Memory, CDR-SB, and MMSE, but in contrast, included the Boston Naming Test. When functional measures were excluded, the ADAS13 carried more weight.

The composites for A $\beta$ <sup>+</sup> versus A $\beta$ <sup>-</sup> were heavily weighted by ADAS13, FAQ, and MMSE, as seen below.



## A $\beta$ +: Cognition/Function



When functional measures were excluded, ADAS13 and MMSE dominated the composites.

### *Best subset components*

The best subset results were similar to the continuous optimization results. For the cCN versus sCN comparison, 5 components provided the optimal cross-validated composite, with the MMSE, delayed Logical Memory, delayed AVLT, CDR-SB, and Category Fluency selected in nearly all cross-validation folds. For the pcCN versus sCN comparison, 7 components were selected, including the MMSE, delayed Logical Memory, delayed AVLT, CDR-SB, Category Fluency, and immediate Logical Memory in nearly all folds and occasionally either ADAS13 or Trails A.

For the A $\beta$ <sup>+</sup> versus A $\beta$ <sup>-</sup> comparison, 3 components were selected — the MMSE, ADAS13, and FAQ.

### *Power*

We estimated the power to detect a 30% slowing of decline using the average out-of-sample estimates of change and variance for each composite and group, over a range of sample sizes. The composite with flat weights across all measures was the best performing composite, attaining 80% power with 375 completers/arm in a hypothetical 30-month trial. Eighty percent power was attained with 450 completers per arm using the optimized cognitive/functional composite in a hypothetical 30-month clinical trial. Sixty-five percent of power was obtained with 500 completers per arm over a 30-month trial, using a composite with cognition only. We also compared flat weight and optimized cognitive/functional composites in 48-month trials for A $\beta$ + pcCN subjects. They performed similarly.

With similar sample sizes as the comparisons mentioned previously, power estimates for A $\beta$ + subjects never exceeded 40% with any type of composite.

## Paper #2:

Time between milestone events in the Alzheimer's disease amyloid cascade

### *Cohort Characteristics*

Two-hundred and twenty-seven CU (127 A $\beta$ - and 100 A $\beta$ +), 70 A $\beta$ + MCI and 38 A $\beta$ + AD participants were included in the analysis. The diagnostic groups varied by mean age, sex, years of education, and proportion of *APOE*  $\epsilon$ 4+. The CU- group was significantly younger than all other diagnostic groups ( $p \leq 0.04$ ). The MCI group had a significantly smaller proportion of females than both the CU- group ( $p = 0.02$ ) and the CU+ group ( $p = 0.05$ ). The MCI group had significantly lower mean years of education compared to the CU- group ( $p = 0.04$ ) and the CU+ group ( $p = 0.02$ ). The AD group also had significantly lower mean years of education compared to the CU- group ( $p = 0.01$ ) and the CU+ group ( $p = 0.005$ ). The CU- group had a significantly smaller proportion of *APOE*  $\epsilon$ 4 carriers than all other diagnostic groups ( $p < 0.003$ ).

### *A $\beta$ PET and estimation of TFA $\beta$ +*

TFA $\beta$ + was estimated with a median of 3 (range: 1 to 5) A $\beta$  PET scans per participant. The average time between first and last scan was 3.3 years (SD = 2.9) and the average time between scans was 2.2 years (SD = 0.8). The correlation between subject-specific random intercepts and slopes was 0.32 (0.06 to 0.55). Across diagnoses, TFA $\beta$ + ranged from - 29 to 46 years, where higher (positive) TFA $\beta$ + values indicate more time spent

with a significant A $\beta$  burden. The CU- group had a significantly lower mean TFA $\beta$ + compared to all other diagnostic groups ( $p < 0.001$ ). The CU+ group had a significantly lower mean TFA $\beta$ + compared to the MCI group ( $p < 0.001$ ) and the AD group ( $p < 0.001$ ), and the MCI was significantly lower than the AD group ( $p = 0.02$ ).

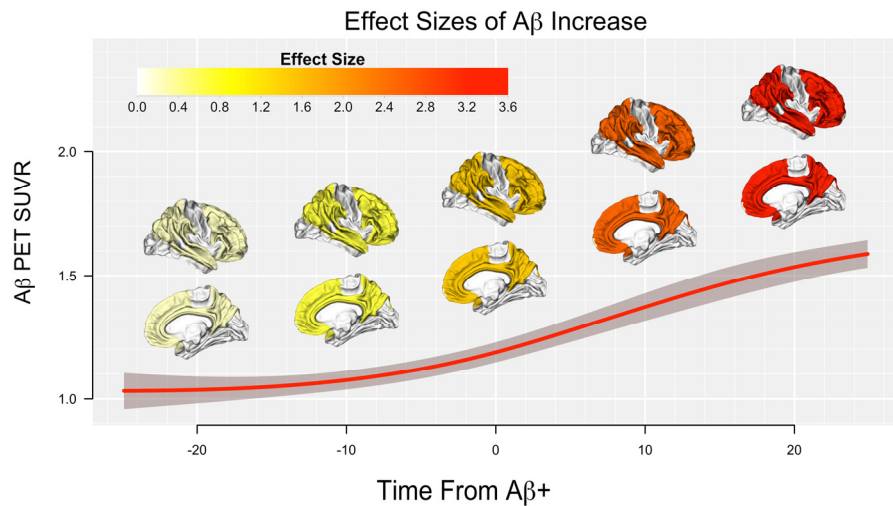
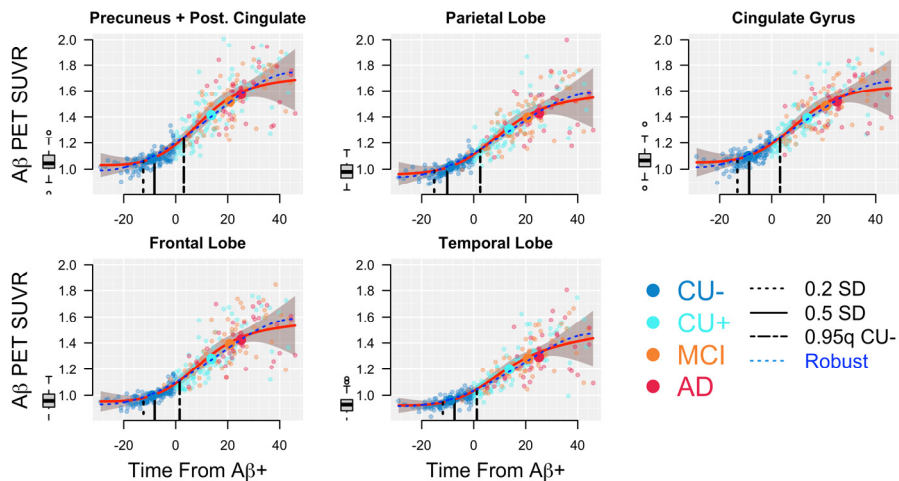
TFA $\beta$ + estimates were not sensitive to alternative thresholds for A $\beta$ + beyond a shift reflecting an earlier or later threshold. When the earlier threshold (SUVR 1.07) was used rather than SUVR 1.10, TFA $\beta$ + estimates were shifted a median of 3.2 years earlier but remained almost perfectly correlated with TFA $\beta$ + using the SUVR 1.10 threshold ( $\rho = 0.996$ ). Similarly, when the late threshold was used (SUVR 1.13), TFA $\beta$ + estimates shifted a median of 3.1 years later, but also remained almost perfectly correlated with TFA $\beta$ + using the SUVR 1.10 threshold ( $\rho = 0.997$ ).

### *TFA $\beta$ + Performance*

TFA $\beta$ + was highly correlated with observed time of A $\beta$ + ( $\rho = 0.93$ , 95% CI: 0.87 to 0.97,  $p < 0.001$ ). When also including the seven participants with a subsequent negative scan after their initial positive scan, the correlation between TFA $\beta$ + and the observed time of A $\beta$ + was 0.89, 95% CI: 0.80 to 0.94,  $p < 0.001$ . When comparing the performance of TFA $\beta$ + versus using A $\beta$  intercepts and slopes as separate predictors, TFA $\beta$ + significantly outperformed separate intercepts and slopes most, but not all of the time. TFA $\beta$ + significantly outperformed covariate only models for all outcomes. Using TFA $\beta$ + resulted in significantly better prediction of MTL tau ( $AIC_{TFA\beta+} = 345.1$ ,  $AIC_{IntSlope} = 360.2$ ,  $AIC_{cov} = 484.8$ ), MPL tau ( $AIC_{TFA\beta+} = 467.9$ ,  $AIC_{IntSlope} = 472.4$ ,  $AIC_{cov} = 532.9$ ), occipital lobe tau ( $AIC_{TFA\beta+} = 272.1$ ,  $AIC_{IntSlope} = 274.2$ ,  $AIC_{cov} = 325.8$ ), CSF A $\beta$  ( $AIC_{TFA\beta+} = 1825.1$ ,  $AIC_{IntSlope} = 1827.4$ ,  $AIC_{cov} = 1962.1$ ), CSF T-tau ( $AIC_{TFA\beta+} = 1854.4$ ,  $AIC_{IntSlope} = 1863.4$ ,  $AIC_{cov} = 1902.9$ ), MMSE ( $AIC_{TFA\beta+} = 1534.8$ ,  $AIC_{IntSlope} = 1549.4$ ,  $AIC_{cov} = 1600.4$ ), and the PACC ( $AIC_{TFA\beta+} = 1251.2$ ,  $AIC_{IntSlope} = 1261.8$ ,  $AIC_{cov} = 1347.4$ ). There was no difference between TFA $\beta$ + and separate intercepts and slopes for LTL tau ( $AIC_{TFA\beta+} = 398.6$ ,  $AIC_{IntSlope} = 399.5$ ,  $AIC_{cov} = 471.5$ ) and CSF P-tau ( $AIC_{TFA\beta+} = 1711.3$ ,  $AIC_{IntSlope} = 1709.6$ ,  $AIC_{cov} = 1748.3$ ) and separate intercepts and slopes was significantly better than TFA $\beta$ + in predicting frontal lobe tau ( $AIC_{TFA\beta+} = 194.2$ ,  $AIC_{IntSlope} = 188.4$ ,  $AIC_{cov} = 245.9$ ) and LPL tau ( $AIC_{TFA\beta+} = 444.9$ ,  $AIC_{IntSlope} = 441.9$ ,  $AIC_{cov} = 512.3$ ).

### Regional A $\beta$ PET

Five regional ROIs (precuneus + posterior cingulate, frontal lobe, cingulate gyrus, temporal and parietal lobes) were estimated to reach a small, but meaningful (0.2 SD) increase in SUVR between 12 and 15 years before A $\beta$ -positivity, i.e. TFA $\beta$ + = 0, as seen in the figure below.



At  $TFA\beta_+ = 0$ , all regions showed large, significant increases in SUVR ( $\Delta SUVR \geq 0.11$ ,  $p \leq 0.01$ ) with the precuneus + posterior cingulate composite showing the largest increase ( $\Delta SUVR = 0.16$ ,  $p < 0.01$ ) and the temporal lobe showing the smallest ( $\Delta SUVR = 0.11$ ,  $p < 0.01$ ). Effect sizes for all regions were large ( $\geq 1$ ) by the time of  $A\beta_+$ . Analyses of regional  $A\beta$  PET outcomes were repeated using robust regression with robust standard errors. The robust curves are similar to the unweighted regression curves with some mild flattening in the  $TFA\beta_+ = 5$  to 25 year range. The 0.2 SD change point estimates for the increase in SUVR ranged from 18 to 20 years before  $A\beta$ -positivity (compared to 12–15 years before  $A\beta$ -positivity in the main analyses). Similar to the unweighted analyses, all regions showed significance of  $A\beta$  at  $TFA\beta_+ = 0$  ( $p < 0.01$ ).

### *Cerebrospinal Fluid*

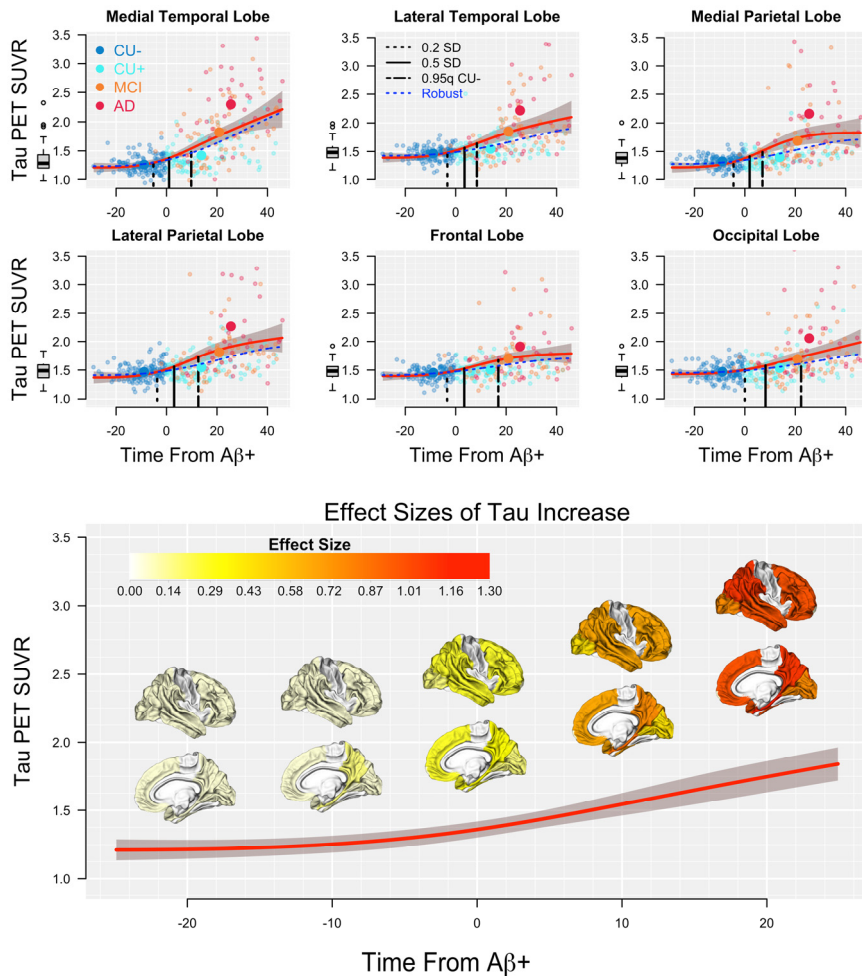
A 0.2 SD drop in CSF  $A\beta_{42}$  was estimated to occur 29 years before  $A\beta$ -positivity ( $TFA\beta_+ = -29$ ). At  $TFA\beta_+ = 0$ , CSF  $A\beta_{42}$  showed a very large effect size ( $\Delta A\beta_{42} = -68$  ng/L,  $p < 0.01$ , effect size =  $-1.99$ ). At  $TFA\beta_+ = -2$ , or two years before  $A\beta$ -positivity, the population curve passes through a previously published CSF  $A\beta_{42}$  threshold for  $A\beta$ -positivity (192 ng/L) (Shaw et al., 2009).

A 0.2 SD increase in CSF T-tau and P-tau was estimated to occur 7–8 years before the time of  $A\beta$ -positivity ( $TFA\beta_+ = -7$  and  $-8$ , respectively). At  $TFA\beta_+ = 0$ , significant increases of medium effect size of T-tau ( $\Delta T\text{-tau} = 19$  ng/L,  $p = 0.04$ , effect size = 0.46) and P-tau ( $\Delta P\text{-tau} = 12$  ng/L,  $p = 0.04$ , effect size = 0.47) were observed.

For the robust regression models, the change point estimate was 26 years before  $A\beta$ -positivity for the decrease in CSF  $A\beta$ , 13 years before  $A\beta$ -positivity for CSF P-tau, and 8 years before  $A\beta$ -positivity for CSF T-tau. A more substantial flattening of the curves can be seen in both CSF P-tau and T-tau for  $TFA\beta_+ > 0$ . The effect size for CSF T-tau at  $TFA\beta_+ = 0$  remained almost identical (0.47,  $p = 0.03$ ) and the effect size for CSF P-tau increased moderately to 0.56 ( $p = 0.01$ ). The effect size for CSF  $A\beta_{42}$  increased to  $-2.52$  at  $TFA\beta_+ = 0$  and remained significant ( $p < 0.01$ ).

### *Tau PET*

Six regional ROIs (MTL, LTL, MPL, LPL, frontal and occipital lobes) were evaluated, show in the figure below.



Five of the six regions were estimated to reach a 0.2 SD increase in SUVR 3–5 years before Aβ- positivity, with the occipital lobe reaching a 0.2 SD increase at the time of Aβ-positivity. At TFAβ+ = 0, four regions (MTL, LTL, MPL, LPL) showed significant increases in SUVR ( $\Delta\text{SUVR} \geq 0.14$ ,  $p \leq 0.03$ ) with the MTL showing the largest effect size (0.36). The frontal and occipital lobes did not increase significantly by TFAβ+ = 0 ( $\Delta\text{SUVR} = 0.09$ ,  $p = 0.06$  and  $\Delta\text{SUVR} = 0.07$ ,  $p = 0.13$ , respectively).

The robust curves show substantial flattening for TFAβ+ > 0. The robust 0.2 SD change point estimates for the increase in SUVR for the tau PET ROIs ranged from 6 to 9 years before Aβ-positivity. The significance of changes in tau PET at TFAβ+ = 0

were similar to the unweighted analyses with the exception of the frontal lobe, which increased in effect size and became statistically significant (0.44,  $p = 0.02$ ).

### *Cognition*

The MMSE showed a 0.2 SD drop six years before A $\beta$ -positivity, followed by the PACC four years before A $\beta$ -positivity. Neither measure decreased significantly by the time of A $\beta$ -positivity ( $\Delta$ MMSE = -0.71,  $p = 0.13$ , effect size = -0.30;  $\Delta$ PACC = -0.50,  $p = 0.10$ , effect size = -0.32).

The robust curves show mild flattening for TFA $\beta$ + > 0, compared to the unweighted analyses. The change point estimates for the decrease in cognitive scores was two years before A $\beta$ -positivity for MMSE and four years before A $\beta$ -positivity for the PACC. The robust estimate for the effect size of decrease in MMSE scores was reduced to -0.23 but became statistically significant ( $p = 0.03$ ). The robust estimate for the effect size of decrease in PACC scores was similar (-0.30), and also became statistically significant ( $p = 0.03$ ).

Summary curves and 0.2 SD change points for some of the earliest changing measures of each outcome type include CSF A $\beta$  and P-tau, precuneus + posterior cingulate A $\beta$  PET, MTL tau PET and the PACC.

## Paper #3:

Determining clinically meaningful decline in preclinical Alzheimer disease

### *Cohort characteristics*

A total of 443 cognitively healthy controls from ADNI, 348 from AIBL, and 329 from BioFINDER were included in the study. A $\beta$ + groups were older, had a higher frequency of APOE e4 positivity, and performed significantly worse on several cognitive tests at baseline, compared to A $\beta$ - groups, in all cohorts.

### *Cognitive changes*

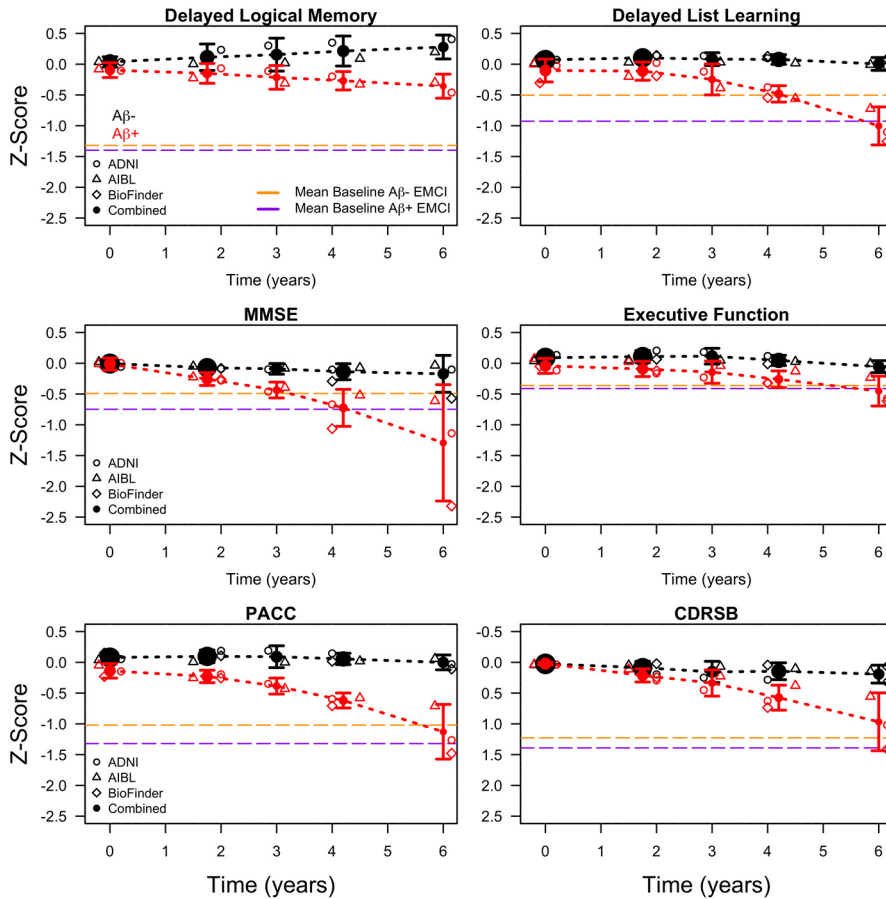
A $\beta$ + participants declined significantly more on the PACC and all individual components of the PACC compared to A $\beta$ - participants, in all 3 cohorts, with the exception of Trails B in BioFINDER ( $p = 0.08$ ).

At year 4, the A $\beta$ + groups declined by -0.45 points on the PACC (ADNI), -0.48 points (BioFINDER), and -0.53 points (at 4.5 years, AIBL). At year 4, the A $\beta$ - group improved 0.09 points on the PACC in ADNI and declined by -0.14 points in BioFINDER and -0.02 points in AIBL.

### *Clinical significance*

To evaluate decline and to characterize what might be considered a clinically significant change, we compared the scores of the cognitively unimpaired participants to the baseline scores of the early MCI participants in ADNI. The mean PACC score in A $\beta$ - and A $\beta$ + early MCI participants at baseline was -1.01 and -1.30, respectively. Six years after baseline, the estimated PACC score combined across cohorts of the preclinical AD groups was midway between the A $\beta$ - and A $\beta$ + early MCI performance, seen in the figure below.





Similarly, the early MCI Aβ<sup>-</sup> and Aβ<sup>+</sup> scores at baseline on the CDRSB were 1.22 and 1.38, respectively, whereas the preclinical AD groups averaged about 1.0 at 6 years.

On each of the MMSE, delayed list learning, and executive function, the cognitively normal Aβ<sup>+</sup> groups averaged worse scores than both MCI groups by 6 years after baseline. The cognitively normal Aβ<sup>+</sup> groups did not approach the MCI groups' delayed logical memory scores by 6 years after baseline. Note that delayed logical memory was not available in BioFINDER.

### Power

Using estimates of change and variance, we calculated the power for hypothetical 4- and 6-year clinical trials for each cohort, assuming a 30% dropout rate, and various sample sizes and drug effects. In 4-year trials, assuming a 25% drug effect, i.e. a 25% slowing of cognitive decline in the treatment group, the required sample size to reach

80% power was 2,000 per group for the estimate combining all cohorts. Assuming a larger effect size of 35%, the required sample size to reach 80% power was 1,000 per group on average. In 6-year trials, assuming a 25% drug effect, the required sample size to reach 80% power was about 600 per group for the estimate combining all cohorts. Assuming a 35% effect size, the required sample size to reach 80% power was 300 per group on average.

## Paper #4:

Predicting diagnosis and cognition with  $^{18}\text{F}$ -AV-1451 tau PET and structural MRI in Alzheimer's disease

### *Cohort Characteristics*

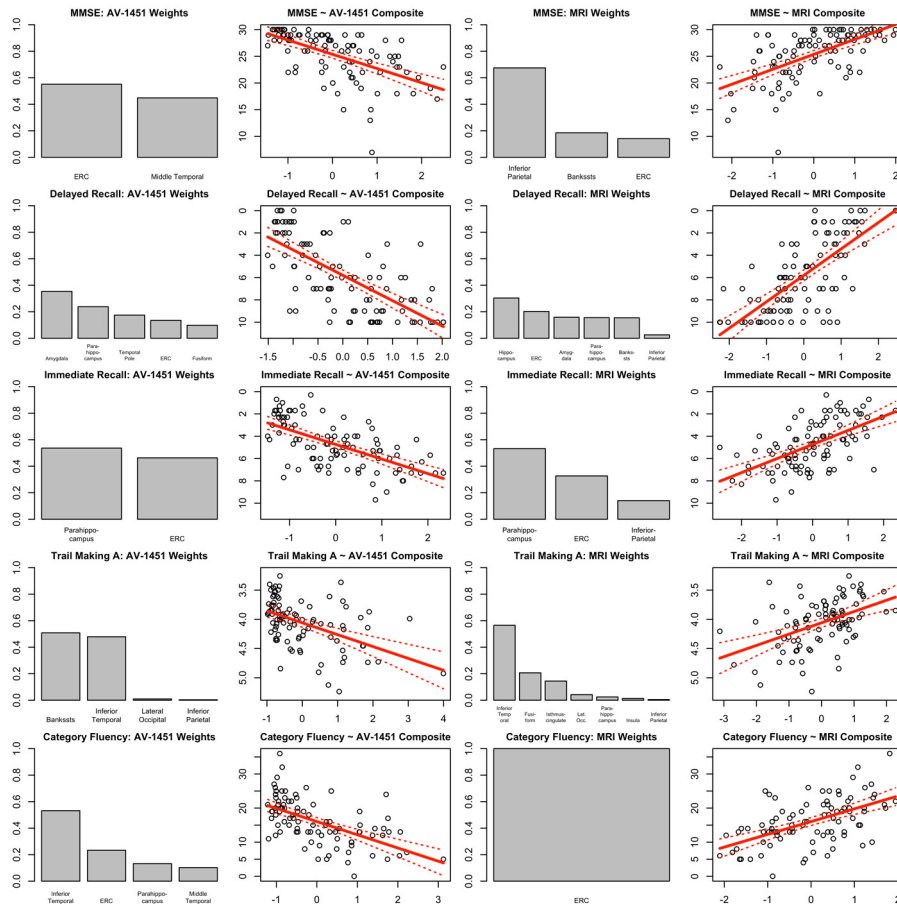
One hundred twenty-seven participants including 56 CU controls, 32 patients with prodromal AD, and 39 patients with AD dementia were examined. All prodromal AD and AD dementia participants and 27 controls (preclinical AD) were  $\text{A}\beta+$ . For models of diagnosis, we compared all CU with the combined group of prodromal AD and AD dementia patients. The prodromal/dementia AD patients were younger on average than the CU (72.5 years vs. 74.7 years,  $p = 0.04$ ) and had a higher proportion of apolipoprotein E (*APOE*)  $\epsilon 4$  positivity (defined as the presence of one or two *APOE*  $\epsilon 4$  alleles; 79% vs. 43%,  $p < 0.01$ ). There was no difference in education (11.9 years vs. 12.2 years,  $p = 0.76$ ) and a borderline significant difference in sex (63% vs. 46% male,  $p = 0.07$ ). For models of cognition, we included all preclinical AD, prodromal AD, and AD dementia participants (98 persons, with 54 males, average age 73.0 years, average education 11.9 years, 75% *APOE*  $\epsilon 4$  positivity).

### *$^{18}\text{F}$ -AV-1451 tau PET*

The  $^{18}\text{F}$ -AV-1451 signal was increased in prodromal AD and AD dementia in several regions throughout the temporal, parietal, frontal, and occipital lobes. The optimal  $^{18}\text{F}$ -AV-1451 classifier was 93% accurate in classifying AD (prodromal AD and AD dementia) versus CU (95% CI: 89% to 97%). The regions selected for classification were the amygdala, the parahippocampal gyrus, the entorhinal cortex (ERC), the fusiform cortex, and the inferior parietal lobule. The *a priori* selected individual region inferior temporal cortex had 89% accuracy (95% CI: 80% to 98%).

Within  $\text{A}\beta+$  participants with preclinical or clinical AD,  $^{18}\text{F}$ -AV-1451 was strongly associated with all cognitive responses ( $p < 0.001$  for all responses). LASSO selected

different regions for each cognitive test. The ERC and middle temporal gyrus were selected for MMSE, shown in the figure below.



The parahippocampal gyrus and the ERC were selected for immediate recall. The amygdala, parahippocampal gyrus, temporal pole, ERC, and fusiform cortex were selected for delayed recall. The banks of the superior temporal sulcus, inferior temporal gyrus, lateral occipital cortex, and inferior parietal lobule were selected for Trail Making A. The inferior temporal gyrus, ERC, parahippocampal gyrus, and middle temporal gyrus were selected for category fluency.

### *Magnetic resonance imaging*

Structural MRI was 83% accurate in classifying participants as AD (prodromal AD and AD dementia) versus CU (95% CI 68% to 98%). The main regions selected to classify diagnosis were the ERC, hippocampus, and fusiform gyrus. The *a priori* selected

individual region hippocampus had 76% accuracy (95% CI: 60% to 92%). Within A $\beta$ + participants, structural MRI was also strongly associated with all cognitive scores ( $P < .001$  for all responses). The LASSO selected different regions for the cognitive tests. The ERC, the banks of the superior temporal sulcus, and inferior parietal lobule were selected for MMSE. The parahippocampal gyrus, ERC, and the inferior parietal lobule were selected for immediate recall. The hippocampus, ERC, amygdala, parahippocampal gyrus, banks of the superior temporal sulcus, and the inferior parietal lobule were selected for delayed recall. Several regions were selected for Trail Making A, with the inferior temporal gyrus, fusiform gyrus, and isthmus cingulate being the most influential regions. The ERC was selected for category fluency.

#### *Competing and complementary predictive information: MRI and $^{18}\text{F-AV-1451}$*

$^{18}\text{F-AV-1451}$  showed strongest associations with delayed recall ( $R^2 = 0.48$ ), followed by immediate recall ( $R^2 = 0.41$ ), MMSE ( $R^2 = 0.36$ ), category fluency ( $R^2 = 0.33$ ), and Trail Making A ( $R^2 = 0.23$ ). MRI had similar strength of associations with delayed recall ( $R^2 = 0.48$ ), MMSE ( $R^2 = 0.35$ ), immediate recall ( $R^2 = 0.34$ ), category fluency ( $R^2 = 0.29$ ), and Trail Making A ( $R^2 = 0.22$ ). The estimates for  $^{18}\text{F-AV-1451}$  were reduced between -2% (for diagnosis) and 43% (for MMSE) when adjusting for MRI. Reduction of MRI estimates ranged from 35% (for diagnosis) to 49% (for immediate recall) when adjusting for tau. AIC selected the models ( $\Delta\text{AIC}$  when comparing two models  $> 2$  favors the model with smallest AIC) with both  $^{18}\text{F-AV-1451}$  and MRI to predict diagnosis and all cognitive responses.

## Paper #5:

Association Between Apolipoprotein E  $\epsilon 2$  vs  $\epsilon 4$ , Age, and  $\beta$ -Amyloid in Adults Without Cognitive Impairment

Of the 6943 participants who were part of the multicenter clinical trial screening visit, 4432 adults without cognitive impairment were included (2634 women [59.4%] and 1798 men [40.6%]; mean [SD] age, 71.3 [4.7] years). Individuals had mean (SD) of 16.6 (2.8) years of education, and 1512 had a positive A $\beta$  level (34.1%).

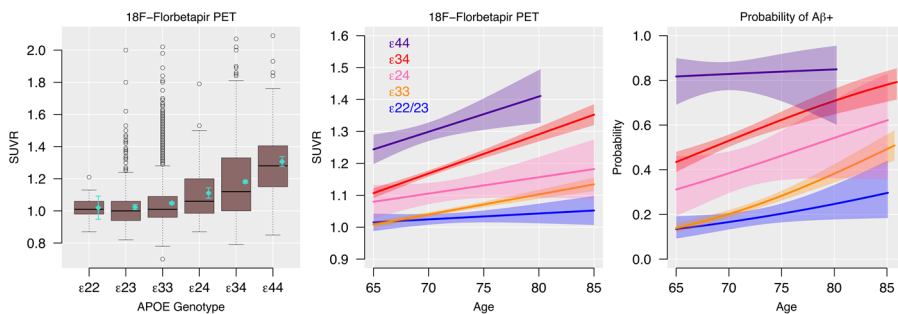
#### *APOE and $^{18}\text{F-Florbetapir SUVR}$*

*APOE* genotype was significantly associated with  $^{18}\text{F-florbetapir SUVR}$  ( $\chi^2 = 708.93$ ;  $p < 0.001$ ). Every *APOE* allele combination was significantly different from all other combinations with the exception of  $\epsilon 22$  vs  $\epsilon 23$  (1.02 vs 1.02;  $p = 0.91$ ) and  $\epsilon 22$  vs  $\epsilon 33$  (1.02 vs 1.05;  $p = 0.43$ ); note the small sample size of the  $\epsilon 22$  group ( $n = 25$ ). A sample

size of 272 for the  $\epsilon 22$  group was required to detect the observed difference from the  $\epsilon 33$  group with 80% power. Notably, the  $\epsilon 23$  group had a significantly lower mean  $^{18}\text{F}$ -florbetapir SUVR compared with the  $\epsilon 33$  group (1.02 vs 1.05;  $p = 0.01$ ), and the  $\epsilon 24$  group had a significantly lower mean  $^{18}\text{F}$ -florbetapir SUVR compared with the  $\epsilon 34$  group (1.11 vs 1.18;  $p < 0.001$ ). Adjusting for cardiovascular risk score did not affect the APOE genotype estimates and was not associated with  $^{18}\text{F}$ -florbetapir SUVR ( $\beta = 0.0001$ ;  $p = 0.98$ ).

### *APOE, Age, and $^{18}\text{F}$ -Florbetapir SUVR*

There was a significant interaction between APOE genotype and age to predict  $^{18}\text{F}$ -florbetapir SUVR ( $p < 0.001$ ;  $\Delta\text{AIC} = -26.4$ ). The increase in  $^{18}\text{F}$ -florbetapir in the  $\epsilon 33$  group was 0.006 SUVR per year (for every 1-year increase in age). Comparing each APOE group to the  $\epsilon 33$  group, the  $\epsilon 22/\epsilon 23$  group (combined because of sparse data over age in the  $\epsilon 22$  group) increased significantly more slowly (0.002 SUVR per year;  $p = 0.01$ ); the  $\epsilon 24$  group increased similarly to the  $\epsilon 33$  group (0.005 SUVR per year;  $p = 0.73$ ); the  $\epsilon 34$  group had approximately twice the rate of the  $\epsilon 33$  group (0.012 SUVR per year;  $p < 0.001$ ); and the  $\epsilon 44$  group also had approximately twice the rate, although not significantly different from the  $\epsilon 33$  group (0.011 SUVR per year;  $p = 0.23$ ), shown in the figure below.



The  $\epsilon 24$  group also increased at less than half the rate of the  $\epsilon 34$  group (rate difference: 0.005 in the  $\epsilon 24$  group vs 0.012 in the  $\epsilon 34$  group;  $p = 0.04$ ). There was no significant interaction between the APOE genotype and age to predict the odds of A $\beta$  positivity ( $\chi^2 = 3.94$ ;  $p = 0.41$ ).

### *A $\beta$ , APOE, and the PACC*

The association between  $^{18}\text{F}$ -florbetapir SUVR and decreasing PACC scores did not differ by APOE genotype ( $\Delta\text{AIC} = 23.4$ ;  $p = 0.97$ ). Cardiovascular risk was associated with worse PACC scores ( $\beta = -0.06$ ;  $p < 0.001$ ) but did not affect the interaction

between age and *APOE* genotype to predict PACC scores ( $\Delta\text{AIC} = 22.9$ ;  $p = 0.96$ ). There was also no difference when comparing  $\epsilon 4$  carriers to  $\epsilon 4$  noncarriers ( $\Delta\text{AIC} = 4.4$ ;  $p = 0.67$ ).

When adjusting for age, sex, and education but not  $^{18}\text{F}$ -florbetapir SUVR, the *APOE*  $\epsilon 34$  group performed 0.08 points worse on the PACC compared with the *APOE*  $\epsilon 33$  group ( $\beta = -0.08$ ;  $p = 0.01$ ). When adjusting for cardiovascular risk, all *APOE* estimates remained similar, including the effect of *APOE*  $\epsilon 34$  ( $\beta = -0.086$ ;  $p = 0.007$ ). When also adjusting for  $^{18}\text{F}$ -florbetapir SUVR, the effect of the *APOE*  $\epsilon 34$  group was removed ( $\beta = -0.012$ ;  $p = 0.71$ ). For the  $\epsilon 4$  carriers vs noncarriers, the unadjusted difference was  $-0.084$  ( $p = 0.005$ ); after adjusting for  $^{18}\text{F}$ -florbetapir, the difference was  $-0.006$  ( $p = 0.85$ ), and after adjusting for  $^{18}\text{F}$ -florbetapir and cardiovascular scores, the difference was  $-0.009$  ( $p = 0.78$ ).

# Discussion

The overall findings of the analyses included in this thesis are

- (1) Clinical trials in preclinical AD, using conventional thresholds for significant A $\beta$  burden are generally underpowered to detect a plausible treatment effect. A $\beta$ -positive participants do show some functional decline over the course of 4 to 5 years, warranting the inclusion of functional measures to capture decline and increase power. Optimal composites to capture decline in the observed preclinical AD population were equal weight composites across all 12 cognitive and functional measures.
- (2) Based on the amyloid cascade hypothesis, a relevant overarching time scale of the disease processes could be based on the development of A $\beta$  pathology. Integrating A $\beta$  PET level and rate of change information places each individual on a pathological timeline. Estimates of several major milestone events of AD progression include changes in CSF A $\beta$ 42 29 years before A $\beta$ -positivity and an increase in regional A $\beta$  PET deposition 15 years before A $\beta$ -positivity. Using the biomarkers tested here, the first changes in CSF A $\beta$ 42 may define the onset of AD. Increases in tau pathology were estimated to occur 7–8 years before A $\beta$ -positivity, as measured by CSF and 5 years before, as measured by PET. Signs of cognitive dysfunction occurred 4–6 years before A $\beta$ -positivity. These findings provide a general time scale for initial changes in sporadic AD, which may inform clinical trials aimed at specific stages of the disease.
- (3) Cognitively unimpaired A $\beta$ + participants approach early MCI cognitive performance levels on general cognition and global outcomes, delayed list recall, and executive function by six years after baseline. To achieve 80% power to detect a 25% treatment effect, 2,000 participants/group for a 4-year trial and 600 participants/group for a 6-year trial are required, using conventional definitions of elevated levels of A $\beta$  burden.

- (4) An optimized classifier that used regional  $^{18}\text{F-AV-1451}$  had superior diagnostic accuracy for AD compared to brain MRI.  $^{18}\text{F-AV-1451}$  and MRI had overall similar strengths of associations with cognition. Both  $^{18}\text{F-AV-1451}$  and MRI contributed complementary information about cognitive impairment through the continuum from preclinical to prodromal and dementia stages of AD, with regional differences between the modalities.
- (5) In a cognitively unimpaired population, *APOE*  $\epsilon 2$  was associated with a reduction in both the overall and the age dependent level of  $\text{A}\beta$  in the presence of  $\epsilon 4$ . Large differences in levels of  $\text{A}\beta$  between *APOE* groups were already apparent at age 65 years. The association between  $\text{A}\beta$  and decreasing global cognitive scores did not differ by *APOE* genotype. The associated reduction in cognitive performance in *APOE*  $\epsilon 4$  carriers compared with noncarriers was completely mediated by  $\text{A}\beta$ .

Paper #1 demonstrates that equal weights over a fair number of cognitive and functional tests performs well in this population. The failure of the optimization to beat the equal weight composites suggests that using either continuous weights or best subset component selection results in overfitting the training sets and a subsequent reduction of test set power. Including a large number of components in a composite may smooth over aberrations in scores in a particular assessment from visit to visit within a subject, thus lowering the within-subject variance and improving signal to noise. Similarly, the equal weight composite provided the most power in  $\text{A}\beta+$  participants, although power did not approach levels suitable for a phase III trial.

As the number of components included in the composite increases, the magnitude of change over time decreases, however, both the within-subject and between-subject errors are decreasing at a rate that overcomes the decrease in the magnitude of change, resulting in an increasing effect size. The increase in effect size plateaus in the 6-10 component range for both the converter and  $\text{A}\beta+$  groups. The decrease in within-subject variance is clear in both groups.

We evaluated assessments available in the ADNI neuropsychological battery, although it is possible or likely that there are other measures more sensitive to decline in preclinical AD. We also did not consider item-level data from already formed composites, which may have affected the results due to carrying insensitive items along with more sensitive ones. We also make the assumption that a treatment will slow the progression of components selected for their fast decline. In reality, it is unknown which cognitive or functional components a treatment may affect and it is possible that an endpoint comprising slower progressing domains will yield more power.



The results suggest preclinical AD subjects with lower cognitive scores at baseline decline more reliably across both cognitive and functional measures compared to A $\beta$ + subjects without signs of subtle cognitive dysfunction. Later stage preclinical AD may represent a more feasible target population for clinical trials designed to slow cognitive decline. In this population, suitable power for a phase III trial can be achieved with considerably lower sample sizes while capturing both cognitive and functional change to demonstrate a clinically meaningful drug effect—both while initiating treatment in subjects who are still cognitively unimpaired. Multiple measures of delayed memory recall, orientation, processing speed, as well as multiple functional measures should be considered when forming a composite. Finally, when selecting measures, erring on the side of too many components may be preferable to too few.

In paper #2, small but meaningful increases in levels of CSF tau and temporoparietal tau are observed years before the current threshold for A $\beta$ -positivity. In the context of secondary prevention trials where A $\beta$ -positivity at current thresholds is required for study inclusion, tau levels in these participants would already have been increasing for several years, likely more. The spread of tau beyond the MTL to the parietal lobe and other regions may be a critical milestone in the progression of AD. Considering that a 0.2 SD increase in MPL tau can potentially be detected several years before A $\beta$ -positivity, these data support the use of primary prevention trials against A $\beta$  where treatment is initiated years before the current threshold for A $\beta$ -positivity, if treatment efficacy relies on early intervention, prior to the development of tau pathology.

These analyses lack the power and precision to place the temporal and parietal tau regions in a particular order with confidence, but instead demonstrate that widespread tau is increasing years before A $\beta$ -positivity. The ADNI CU, MCI and AD cohorts are also age matched. The AD patients, on average, have dementia by age 75, while the participants in the CU cohort who may eventually develop AD, are unlikely to do so for many years, possibly decades. By design, these cohorts with age matched groups are therefore on systematically different disease trajectories with respect to age. If earlier onset is associated with a more aggressive form of the disease, then the AD cohort may have the most aggressive form while the CU cohort, the least aggressive. If the developing A $\beta$  pathology in the ADNI CU- cohort represents a less aggressive disease process compared with a more typical AD process, the estimates reported here could be conservative and biased toward later time estimates for downstream events. The ADNI MCI cohort may represent a more typical trajectory with respect to downstream events along the A $\beta$  pathological timeline. Additionally, the change point estimates are influenced by both biological variation and measurement error, which varies from marker to marker. Change points in measures with high variability in the “normal” range and excess measurement error may require additional biological change to detect, despite an earlier, real increase in pathology.

Incorporating longitudinal information facilitates the estimation of the time-course of downstream events such as the spread of tau and the onset of subtle cognitive dysfunction. As the technology to measure AD pathology becomes more cost effective and noninvasive, such as plasma measures of A $\beta$  or tau (Janelidze et al., 2020; Mielke et al., 2018; Palmqvist et al., 2019; Schindler et al., 2019), longitudinal evaluations in the context of trial-ready cohorts may greatly improve early diagnosis and expedite the execution of clinical trials in early AD.

To benchmark the magnitude of cognitive decline to a measure of clinical meaningfulness, in paper #3 we compared the scores of the cognitively unimpaired participants to those classified as early MCI—a group with incipient functional decline. The separation between these groups was just over one SD on the PACC, suggesting that one point of additional decline in A $\beta$ + participants compared to A $\beta$ - participants could be taken as an approximate benchmark for clinically meaningful decline. Combining results across cohorts shows the average A $\beta$ + participant to have the same PACC score at six years post baseline as the average patient with early MCI had at baseline. Based on the PACC estimates, a treatment effect of 40%–50% would be required to delay the cognitive decline of a group of A $\beta$ + participants from reaching the one SD milestone by three years.

Delaying the cognitive decline equivalent to the level of the average early MCI patient by three years may be a clinically meaningful treatment effect. But 40%–50% is a large treatment effect and highlights the difficulties in preclinical AD trial design. In order to reliably achieve 80% power for a modest, real-world effect size of 20%–30%, investors in AD research for therapeutics development will have to prepare to support larger and longer trials than are currently envisaged.

These analyses show that large sample sizes and sufficiently long follow-up times result in consistent estimates of decline in preclinical AD. Despite substantial design and sampling differences, these results support the potential for internationally conducted clinical trials in preclinical AD. However, it is likely that designers of preclinical AD treatment trials will have to prepare for larger and longer trials than are currently considered.

The findings of paper #4 suggest that although tau is the more critical measure between <sup>18</sup>F-AV-1451 tau PET and structural brain MRI, both measures capture partly unique information that is relevant for the clinical deterioration in AD. The selected regions were mainly temporal lobe regions, where tau pathology presumably occurs in early stages of AD (ERC, amygdala, fusiform, and the parahippocampal gyrus), but also the inferior parietal lobule, which presumably is involved in later stages of the disease (Cho et al., 2016).

The optimal MRI-based classifier achieved lower accuracy and partly included similar regions as the <sup>18</sup>F-AV-1451 classifier (ERC, fusiform) plus the hippocampus, the

banks of the superior temporal sulcus, and the inferior parietal lobule. The classification accuracy for the model including both  $^{18}\text{F-AV-1451}$  and MRI did not improve over  $^{18}\text{F-AV-1451}$  alone, indicating that brain structure contributes little beyond tau to the identification of patients with AD.

We conclude that  $^{18}\text{F-AV-1451}$  tau PET was strongly associated with AD diagnosis, with stronger associations than structural MRI. However, both  $^{18}\text{F-AV-1451}$  and structural MRI were independently associated with cognitive impairment, across the entire disease continuum from preclinical to prodromal and dementia stages of AD.

In paper #5, the separation between the  $\epsilon 24$  and  $\epsilon 34$  groups in terms of  $\text{A}\beta$  levels becomes clear as the groups approach 70 years of age. The reduced levels of  $\text{A}\beta$  in  $\epsilon 24$  compared with  $\epsilon 34$  participants shown here may be one of the primary drivers behind the protective effect of the  $\epsilon 2$  allele against AD dementia, shown previously in a large case-control study (Reiman et al., 2020). The  $\epsilon 24$  group demonstrated an associated reduced risk of AD dementia (odds ratio, 2.68 [95%CI, 1.65-4.36]) compared with the  $\epsilon 34$  group (odds ratio, 6.13 [95% CI, 5.08-7.41]) when comparing both groups with  $\epsilon 33$  participants. However, the presence of the  $\epsilon 2$  allele does not completely protect against  $\text{A}\beta$  positivity, as 16% of  $\epsilon 2$  homozygotes in the A4 Study had positive  $\text{A}\beta$  levels, nor does it completely protect against AD dementia, as 5 of 24  $\epsilon 2$  homozygotes had a neuropathologically confirmed AD dementia diagnosis (Reiman et al., 2020). Although the *APOE* genotype is one of the strongest risk factors for AD, it does not determine  $\text{A}\beta$  accumulation or cognitive decline.

The *APOE*  $\epsilon 34$  and *APOE*  $\epsilon 44$  groups had mean SUVRs of approximately 1.10 and 1.25 at age 65, whereas the  $\epsilon 33$  and  $\epsilon 23$  groups had mean SUVRs near 1.0. *APOE*  $\epsilon 4$  carrier longitudinal rates of global  $^{18}\text{F}$ -florbetapir change have been estimated to be 0.0044 SUVR per year in  $\text{A}\beta$ -negative individuals and 0.0126 SUVR per year in  $\text{A}\beta$ -positive individuals (Lim and Mormino, 2017), suggesting that it would take decades for the *APOE*  $\epsilon 4$  carrier groups to reach the  $\text{A}\beta$  levels observed at age 65 years in this study. This coincides with the estimated prevalence of  $\text{A}\beta$  positivity in  $\epsilon 44$  individuals between 25% and 30% at age 45 years and 10% in  $\epsilon 34$  individuals at age 50 years (Jansen et al., 2018). With  $\text{A}\beta$  positivity already observable in some individuals in their 40s, the gradual accumulation likely begins much earlier. Indeed, reductions of cerebrospinal fluid  $\text{A}\beta$  have been observed in  $\epsilon 44$  carriers in their 20s (Lautner et al., 2017). A protein-modifying treatment mimicking the protective effect of the  $\epsilon 2$  allele against  $\text{A}\beta$  accumulation may be most effective before significant  $\text{A}\beta$  deposition. The age at which such a treatment should be initiated would vary greatly by *APOE* genotype and individual, but if done safely, it could be used to slow  $\text{A}\beta$  accumulation in early middle age for those at highest risk.

This study's findings suggest that the protective effect of carrying an  $\epsilon 2$  allele in the presence of an  $\epsilon 4$  allele offers potential for a treatment that attempts to mimic this protective outcome in order to facilitate  $A\beta$  clearance in  $\epsilon 4$  carriers. Such a treatment strategy is appealing, as  $\epsilon 4$  carriers make up 67% of patients with AD dementia, and it could represent an early treatment option, as many  $\epsilon 4$  carriers begin to accumulate  $A\beta$  in early middle age. If the goal is to interfere early in the disease process before activation of downstream pathways, AD prevention trials may consider targeting much younger people before the accumulation of high or even intermediate levels of  $A\beta$  develop.

# Conclusion

Results from phase III trials of potential disease-modifying treatments in AD continue to be almost strictly negative. However, clinical trials in AD look different today compared with the trials of ten years ago (Egan et al., 2019). Imaging and biomarker research over the last decade has led to substantial gains in the understanding of the progression of AD. This understanding has transformed clinical trial design. Previously, it was common for participants to be recruited into trials without inclusion criteria regarding A $\beta$  pathology. For anti-A $\beta$  treatment trials, this meant that many participants would not even harbor the pathology the treatment was targeting.

Longitudinal imaging and biomarker studies over the last decade have clarified the time course of the earliest changes in A $\beta$  and tau, further demonstrating how late the dementia stage is in the disease process and how difficult it might be to halt or reverse cognitive decline once this stage has begun. There are currently several ongoing treatment trials targeting early biomarker changes in participants without cognitive impairment, using the latest imaging and biomarker technology to monitor the progression of early AD pathology (Mintun et al., 2021).

These advances in imaging and biomarker research have facilitated clinical trials in earlier patient populations, identified a potentially optimal treatment window, and may be the key to accelerating drug discovery in AD.

# Acknowledgements

Different funding agencies supported work at Lund University (for overall study coordination, and for the BioFINDER study) and the ADNI and AIBL studies. Work at Lund University in the authors' laboratory is generously supported by The Knut and Alice Wallenberg foundation, the Medical Faculty at Lund University, Region Skåne, the European Research Council, the Swedish Research Council, the Marianne and Marcus Wallenberg foundation, the Strategic Research Area MultiPark (Multidisciplinary Research in Parkinson's disease) at Lund University, the Swedish Alzheimer Association, the Swedish Brain Foundation, the Skåne University Hospital Foundation, the Bundy Academy, and the Swedish federal government under the ALF agreement.

Data collection and sharing for the Alzheimer's Disease Neuroimaging Initiative (ADNI) (National Institutes of Health Grant U01 AG024904) is funded by the National Institute on Aging, the National Institute of Biomedical Imaging and Bioengineering, and through generous contributions from the following: Alzheimer's Association; Alzheimer's Drug Discovery Foundation; BioClinica, Inc.; Biogen Idec Inc.; Bristol-Myers Squibb Company; Eisai Inc.; Elan Pharmaceuticals, Inc.; Eli Lilly and Company; F. Hoffmann-La Roche Ltd and its affiliated company Genentech, Inc.; GE Healthcare; Innogenetics, N.V.; IXICO Ltd.; Janssen Alzheimer Immunotherapy Research & Development, LLC.; Johnson & Johnson Pharmaceutical Research & Development LLC.; Medpace, Inc.; Merck & Co., Inc.; Meso Scale Diagnostics, LLC.; NeuroRx Research; Novartis Pharmaceuticals Corporation; Pfizer Inc.; Piramal Imaging; Servier; Synarc Inc.; and Takeda Pharmaceutical Company. The Canadian Institutes of Health Research provided funds to support ADNI clinical sites in Canada. Private sector contributions were facilitated by the Foundation for the National Institutes of Health ([www.fnih.org](http://www.fnih.org)). The grantee organization is the Northern California Institute for Research and Education, and the study is coordinated by the Alzheimer's Disease Cooperative Study at the University of California, San Diego. ADNI data are disseminated by the Laboratory for NeuroImaging at the University of Southern California. A complete listing of ADNI investigators can be found at: [https://adni.loni.usc.edu/wp-content/uploads/how\\_to\\_apply/ADNI\\_Acknowledgement\\_List.pdf](https://adni.loni.usc.edu/wp-content/uploads/how_to_apply/ADNI_Acknowledgement_List.pdf).

Partial financial support of AIBL was provided by the Alzheimer's Association (US), the Alzheimer's Drug Discovery Foundation, an Anonymous foundation, the Science and Industry Endowment Fund, the Dementia Collaborative Research Centres, the McCusker Alzheimer's Research Foundation, the National Health and Medical Research Council (AUS), and the Yulgilbar Foundation, plus numerous commercial interactions supporting data collection. Details of the AIBL consortium can be found at [www.AIBL.csiro.au](http://www.AIBL.csiro.au) and a list of the researchers of AIBL is provided at <http://aibl.csiro.au/>.

The Anti-Amyloid Treatment in Asymptomatic Alzheimer Disease Study (A4 Study) is a secondary prevention trial in preclinical Alzheimer disease, aiming to slow cognitive decline associated with brain amyloid accumulation in clinically normal older individuals. The A4 Study is funded by a public-private-philanthropic partnership, including funding from the National Institutes of Health-National Institute on Aging (U19AG010483; R01AG063689), Eli Lilly and Company, Alzheimer Association, Accelerating Medicines Partnership, GHR Foundation, an anonymous foundation, and additional private donors, with in-kind support from Avid, Cogstate, Albert Einstein College of Medicine, US Against Alzheimer Disease, and Foundation for Neurologic Diseases. The companion observational Longitudinal Evaluation of Amyloid Risk and Neurodegeneration Study is funded by the Alzheimer Association and GHR Foundation. The A4 and Longitudinal Evaluation of Amyloid Risk and Neurodegeneration Studies are led by Reisa Sperling, MD, at the Brigham and Women's Hospital, Harvard Medical School and Paul Aisen, MD, at the Alzheimer Therapeutic Research Institute, University of Southern California. The A4 and Longitudinal Evaluation of Amyloid Risk and Neurodegeneration Studies are coordinated by the Alzheimer Therapeutic Research Institute at the University of Southern California, and the data are made available through the Laboratory for Neuro Imaging at the University of Southern California. The participants screening for the A4 Study provided permission to share their deidentified data in order to advance the quest to find a successful treatment for Alzheimer disease. The complete A4 Study Team list is available at [a4study.org/a4-study-team](http://a4study.org/a4-study-team). We thank all the participants, the site personnel, and all of the partnership team members who continue to make the A4 Study and Longitudinal Evaluation of Amyloid Risk and Neurodegeneration Studies possible. There was no financial compensation for these contributions.

Thank you to Niklas, without whom I would never have seen The Philadelphia Experiment, understood the practical differences between hydrofluoric and hydrochloric acid, or started or finished this thesis. Thank you to Oskar for excellent guidance and motivating the rewrite of The Final Countdown. Thank you to Mike Donohue for an endless supply of creative solutions and consistently circumnavigating the 55/55 split. Thank you to Beth Mormino for support, the box trifecta, and the

answers to past and future neuroanatomy questions. Thank you to Lon Schneider for introducing me to Alzheimer's disease research and Mike Weiner for introducing me to neuroimaging.



# References

- ADNI, 2012. ADNI Commonly Used Tables [WWW Document]. URL <https://adni.loni.usc.edu/wp-content/uploads/2012/08/instruction-about-data.pdf>
- Akaike, H., 1974. A new look at the statistical model identification. *Autom. Control. IEEE Trans.* 19, 716–723. doi:10.1007/s00198-008-0566-6
- Atkinson, K.E., 1989. *An Introduction to Numerical Analysis*, 2nd ed. John Wiley & Sons, New York.
- Ayutyanont, N., Langbaum, J.B.S., Hendrix, S.B., Chen, K., Fleisher, A.S., Friesenhahn, M., Ward, M., Aguirre, C., Acosta-Baena, N., Madrigal, L., Muñoz, C., Tirado, V., Moreno, S., Tariot, P.N., Lopera, F., Reiman, E.M., 2014. The Alzheimer’s prevention initiative composite cognitive test score: Sample size estimates for the evaluation of preclinical Alzheimer’s disease treatments in presenilin 1 E280A mutation carriers. *J. Clin. Psychiatry* 75, 652–660. doi:10.4088/JCP.13m08927
- Baker, J.E., Lim, Y.Y., Pietrzak, R.H., Hassenstab, J., Snyder, P.J., Masters, C.L., Maruff, P., 2017. Cognitive impairment and decline in cognitively normal older adults with high amyloid- $\beta$ : A meta-analysis. *Alzheimer’s Dement. Diagnosis, Assess. Dis. Monit.* 6, 108–121. doi:10.1016/j.dadm.2016.09.002
- Bateman, R.J., Xiong, C., Benzinger, T.L.S., Fagan, A.M., Goate, A., Fox, N.C., Marcus, D.S., Cairns, N.J., Xie, X., Blazey, T.M., Holtzman, D.M., Santacruz, A., Buckles, V., Oliver, A., Moulder, K., Aisen, P.S., Ghetti, B., Klunk, W.E., McDade, E., Martins, R.N., Masters, C.L., Mayeux, R., Ringman, J.M., Rossor, M.N., Schofield, P.R., Sperling, R.A., Salloway, S., Morris, J.C., 2012. Clinical and biomarker changes in dominantly inherited Alzheimer’s disease. *N. Engl. J. Med.* 367, 795–804. doi:10.1056/NEJMoal202753
- Byrd, R., Lu, P., Nocedal, J., Zhu, C., 1995. A LIMITED MEMORY ALGORITHM FOR BOUND CONSTRAINED OPTIMIZATION. *SIAM J. Sci. Comput.* 16, 1190–1208.
- Cho, H., Choi, J.Y., Hwang, M.S., Kim, Y.J., Lee, H.M., Lee, H.S., Lee, J.H., Ryu, Y.H., Lee, M.S., Lyoo, C.H., 2016. In vivo cortical spreading pattern of tau and amyloid in the Alzheimer disease spectrum. *Ann. Neurol.* 80, 247–258. doi:10.1002/ana.24711
- Clark, C.M., Pontecorvo, M.J., Beach, T.G., Bedell, B.J., Coleman, R.E., Doraiswamy, P.M., Fleisher, A.S., 2012. Cerebral PET with florbetapir compared with neuropathology at autopsy for detection of neuritic amyloid- $\beta$  plaques : a prospective cohort study. *Lancet Neurol.* 11, 669–678. doi:10.1016/S1474-4422(12)70142-4

- Dale, A.M., Fischl, B., Sereno, M.I., 1999. Cortical Surface-Based Analysis 1. Segmentation and Surface Reconstruction 194, 179–194.
- Donohue, M.C., Sperling, R.A., Petersen, R., Sun, C.-K., Weiner, M.W., Aisen, P.S., 2017. Association Between Elevated Brain Amyloid and Subsequent Cognitive Decline Among Cognitively Normal Persons. *JAMA* 317, 2305–2316. doi:10.1001/jama.2017.6669
- Donohue, M.C., Sperling, R.A., Salmon, D.P., Rentz, D.M., Raman, R., Thomas, R.G., Weiner, M., Aisen, P.S., Australian Imaging, Biomarkers, and Lifestyle Flagship Study of Ageing, Alzheimer’s Disease Neuroimaging Initiative, Alzheimer’s Disease Cooperative Study, 2014. The preclinical Alzheimer cognitive composite: measuring amyloid-related decline. *JAMA Neurol.* 71, 961–70. doi:10.1001/jamaneurol.2014.803
- Doody, R.S., Thomas, R., Farlow, M., Iwatsubo, T., Vellas, B., Joffe, S., Kieburtz, K., Raman, R., Ph, D., Sun, X., 2014. Phase 3 Trials of Solanezumab for Mild-to-Moderate Alzheimer’s Disease 311–321. doi:10.1056/NEJMoa1312889
- Egan, M.F., Kost, J., Voss, T., Mukai, Y., Aisen, P.S., Cummings, J.L., Sc, D., Tariot, P.N., Zhang, Y., Ph, D., Li, W., Ph, D., Furtek, C., Mahoney, E., Mozley, L.H., Ph, D., Mo, Y., Ph, D., Sur, C., Ph, D., Michelson, D., 2019. Randomized Trial of Verubecestat for Prodromal Alzheimer’s Disease 1408–1420. doi:10.1056/NEJMoa1812840
- Ellis, K.A., 2009. The Australian Imaging, Biomarkers and Lifestyle (AIBL) study of aging: methodology and baseline characteristics of 1112 individuals recruited for a longitudinal study of Alzheimer’s disease. *Int. Psychogeriatr.* 21, 672–687.
- Fischl, B., Dale, A.M., 2000. Measuring the thickness of the human cerebral cortex from magnetic resonance images 2000.
- Fischl, B., Salat, D.H., Busa, E., Albert, M., Dieterich, M., Haselgrove, C., van der Kouwe, A., Killiany, R., Kennedy, D., Klaveness, S., Montillo, A., Makris, N., Rosen, B., Dale, A.M., 2002. Whole Brain Segmentation: Neurotechnique Automated Labeling of Neuroanatomical Structures in the Human Brain. *Neuron* 33, 341–355. doi:10.1016/S0896-6273(02)00569-X
- Food and Drug Administration, 2013. Guidance for Industry Alzheimer’s Disease: Developing Drugs for the Treatment of Early Stage Disease.
- Hahn, A., Schain, M., Erlandsson, M., Sj, P., James, G.M., Strandberg, O.T., Douglas, H., Lanzenberger, R., Jonas, J., Olsson, T.G., Smith, R., Hansson, O., 2017. Modeling Strategies for Quantification of In Vivo Binding in Patients with Tau Pathology. *J. Nucl. Med.* 58, 623–631. doi:10.2967/jnumed.116.174508
- Hastie, T.J., Tibshirani, R.J., 1990. Generalized Additive Models. *Monogr. Stat. Appl. Probab.* doi:10.1016/j.csda.2010.05.004
- Hedden, T., Oh, H., Younger, A.P., Patel, T.A., 2013. Meta-analysis of amyloid-cognition relations in cognitively normal older adults. *Neurology* 80, 1341–1348. doi:10.1212/WNL.0b013e31828ab35d
- Hochberg, B.Y.Y., 1988. A sharper Bonferroni procedure for multiple tests of significance. *Biometrika* 75, 1986–1988.

- Insel, P.S., Hansson, O., Mackin, R.S., Weiner, M., Mattsson, N., 2018. Amyloid pathology in the progression to mild cognitive impairment. *Neurobiol. Aging* 64, 76–84. doi:10.1016/j.neurobiolaging.2017.12.018
- Janelidze, S., Mattsson, N., Palmqvist, S., Smith, R., Beach, T.G., Serrano, G.E., Chai, X., Proctor, N.K., Eichenlaub, U., Zetterberg, H., Blennow, K., Reiman, E.M., Stomrud, E., Dage, J.L., Hansson, O., 2020. Plasma P-tau181 in Alzheimer's disease: relationship to other biomarkers, differential diagnosis, and longitudinal progression to Alzheimer's dementia. *Nat. Med.* 26, 379–386. doi:10.1038/s41591-020-0755-1
- Janelidze, S., Zetterberg, H., Mattsson, N., Palmqvist, S., Vanderstichele, H., Lindberg, O., van Westen, D., Stomrud, E., Minthon, L., Blennow, K., Hansson, O., 2016. CSF A $\beta$ 42/A $\beta$ 40 and A $\beta$ 42/A $\beta$ 38 ratios: Better diagnostic markers of Alzheimer disease. *Ann. Clin. Transl. Neurol.* 3, 154–165. doi:10.1002/acn3.274
- Jansen, W.J., Ossenkoppele, R., Tijms, B.M., Fagan, A.M., Hansson, O., Klunk, W.E., Van Der Flier, W.M., Villemagne, V.L., Frisoni, G.B., Fleisher, A.S., Lleó, A., Mintun, M.A., Wallin, A., Engelborghs, S., Na, D.L., Chételat, G., Molinuevo, J.L., Landau, S.M., Mattsson, N., Kornhuber, J., Sabri, O., Rowe, C.C., Parnetti, L., Popp, J., Fladby, T., Jagust, W.J., Aalten, P., Lee, D.Y., Vandenberghe, R., De Oliveira, C.R., Kapaki, E., Froelich, L., Ivanou, A., Gabryelewicz, T., Verbeek, M.M., Sanchez-Juan, P., Hildebrandt, H., Camus, V., Zboch, M., Brooks, D.J., Drzezga, A., Rinne, J.O., Newberg, A., De Mendonça, A., Sarazin, M., Rabinovici, G.D., Madsen, K., Kramberger, M.G., Nordberg, A., Mok, V., Mroczko, B., Wolk, D.A., Meyer, P.T., Tsolaki, M., Scheltens, P., Verhey, F.R.J., Visser, P.J., Aarsland, D., Alcolea, D., Alexander, M., Almdahl, I.S., Arnold, S.E., Baldeiras, I., Barthel, H., Van Berckel, B.N.M., Blennow, K., Van Buchem, M.A., Cavedo, E., Chen, K., Chipi, E., Cohen, A.D., Förster, S., Fortea, J., Frederiksen, K.S., Freund-Levi, Y., Gkatzima, O., Gordon, M.F., Grimmer, T., Hampel, H., Hausner, L., Hellwig, S., Herukka, S.K., Johannsen, P., Klimkowicz-Mrowiec, A., Köhler, S., Koglin, N., Van Laere, K., De Leon, M., Lisetti, V., Maier, W., Marcusson, J., Meulenbroek, O., Møllergård, H.M., Morris, J.C., Nordlund, A., Novak, G.P., Paraskevas, G.P., Perera, G., Peters, O., Ramakers, I.H.G.B., Rami, L., Rodríguez-Rodríguez, E., Roe, C.M., Rot, U., Rütther, E., Santana, I., Schröder, J., Seo, S.W., Sorininen, H., Spira, L., Stomrud, E., Struyfs, H., Teunissen, C.E., Vos, S.J.B., Van Waalwijk Van Doorn, L.J.C., Waldemar, G., Wallin, Å.K., Wiltfang, J., Zetterberg, H., 2018. Association of cerebral amyloid- $\beta$  Aggregation with cognitive functioning in persons without dementia. *JAMA Psychiatry* 75, 84–95. doi:10.1001/jamapsychiatry.2017.3391
- Johnson, K.A., Schultz, A.P., Raman, R., Donohue, M.C., Sun, C.-K., Jacobs, H.I., Marek, K., Seibyl, J., Mintun, M.A., Shcherbinin, S., Pontecorvo, M.J., Mormino, B.C., Rowe, C.C., van Dyck, C.H., Salloway, S., Jack, C.R., Yaari, R., Holdridge, K.C., Aisen, P.S., Sperling, R.A., 2018. Tau Pet in A4: Preliminary Report, in: *Alzheimer's & Dementia*. Elsevier Ltd, pp. P1583–P1584. doi:10.1016/j.jalz.2018.07.144
- Joshi, A.D., Pontecorvo, M.J., Clark, C.M., Carpenter, A.P., Jennings, D.L., Mintun, M.A., Adler, L.P., Burns, J.D., Saha, K., Sadowsky, C.H., Kovnat, K.D., Lowrey, M.J., Arora,

- A., Seibyl, J.P., Skovronsky, D.M., 2012. Performance Characteristics of Amyloid PET with Florbetapir F 18 in Patients with Alzheimer's Disease and Cognitively Normal Subjects. *J. Nucl. Med.* 53, 378–384. doi:10.2967/jnumed.111.090340
- Koenker, R., D'Orey, V., 1987. Algorithm AS 229 : Computing Regression Quantiles Author ( s ): Roger W . Koenker and Vasco D ' Orey Source : Journal of the Royal Statistical Society . Series C ( Applied Statistics ), Vol . 36 , No . 3 Published by : Blackwell Publishing for the Royal S. J. R. Stat. Soc. Ser. C (Applied Stat. 36, 383–393.
- Koscik, R.L., Betthausen, T.J., Jonaitis, E.M., Allison, S.L., Clark, L.R., Hermann, B.P., Cody, K.A., Engle, J.W., Barnhart, T.E., Stone, C.K., Chin, N.A., Carlsson, C.M., Asthana, S., Christian, B.T., Johnson, S.C., 2020. Amyloid duration is associated with preclinical cognitive decline and tau PET. *Alzheimer's Dement. Diagnosis, Assess. Dis. Monit.* 12, 1–10. doi:10.1002/dad2.12007
- Kozauer, N., Katz, R., 2013. Regulatory Innovation and Drug Development for Early-Stage Alzheimer's Disease. *N. Engl. J. Med.* 368, 1169–1171. doi:10.1056/NEJMp1302513
- Landau, S., Jagust, W., 2015. Florbetapir processing methods [WWW Document]. URL [https://adni.bitbucket.io/reference/docs/UCBERKELEYAV45/ADNI\\_AV45\\_Methods\\_JagustLab\\_06.25.15.pdf](https://adni.bitbucket.io/reference/docs/UCBERKELEYAV45/ADNI_AV45_Methods_JagustLab_06.25.15.pdf)
- Landau, S.M., Mintun, M.A., Joshi, A.D., Koeppe, R.A., Petersen, R.C., Aisen, P.S., Weiner, M.W., Jagust, W.J., 2012. Amyloid deposition, hypometabolism, and longitudinal cognitive decline. *Ann. Neurol.* 72, 578–586. doi:10.1002/ana.23650
- Langbaum, J.B., Hendrix, S.B., Ayutyanont, N., Chen, K., Fleisher, A.S., Shah, R.C., Barnes, L.L., Bennett, D.A., Tariot, P.N., Reiman, E.M., 2014. An empirically derived composite cognitive test score with improved power to track and evaluate treatments for preclinical Alzheimer's disease. *Alzheimer's Dement.* 10, 666–674. doi:10.1016/j.jalz.2014.02.002
- Lautner, R., Insel, P.S., Skillbäck, T., Olsson, B., Landén, M., Frisoni, G.B., Herukka, S.K., Hampel, H., Wallin, A., Minthon, L., Hansson, O., Blennow, K., Mattsson, N., Zetterberg, H., 2017. Preclinical effects of APOE  $\epsilon$ 4 on cerebrospinal fluid A $\beta$ 42 concentrations. *Alzheimer's Res. Ther.* 9, 1–7. doi:10.1186/s13195-017-0313-3
- Li, D., Iddi, S., Thompson, W.K., Donohue, M.C., 2017. Bayesian latent time joint mixed effect models for multicohort longitudinal data. *Stat. Methods Med. Res.* 1–11. doi:10.1177/0962280217737566
- Lim, Y.Y., Mormino, E.C., 2017. APOE genotype and early  $\beta$ -amyloid accumulation in older adults without dementia. *Neurology* 89, 1028–1034. doi:10.1212/WNL.0000000000004336
- Liu, C.C., Kanekiyo, T., Xu, H., Bu, G., 2013. Apolipoprotein e and Alzheimer disease: Risk, mechanisms and therapy. *Nat. Rev. Neurol.* 9, 106–118. doi:10.1038/nrneurol.2012.263
- Lowe, V.J., Curran, G., Fang, P., Liesinger, A.M., Josephs, K.A., Parisi, J.E., Kantarci, K., Boeve, B.F., Pandey, M.K., Bruinsma, T., Knopman, D.S., Jones, D.T., Petrucelli, L.,

- Cook, C.N., Graff-radford, N.R., Dickson, D.W., Petersen, R.C., Jr, C.R.J., Murray, M.E., 2016. An autoradiographic evaluation of AV-1451 Tau PET in dementia. *Acta Neuropathol. Commun.* 1–19. doi:10.1186/s40478-016-0315-6
- Maass, A., Landau, S., Horng, A., Lockhart, S.N., Rabinovici, G.D., Jagust, W.J., Baker, S.L., La Joie, R., 2017. Comparison of multiple tau-PET measures as biomarkers in aging and Alzheimer’s disease. *Neuroimage* 157, 448–463. doi:10.1016/j.neuroimage.2017.05.058
- Mahley, R.W., 1988. Apolipoprotein E: Cholesterol transport protein with expanding role in cell biology. *Science* (80-. ). 240, 622–630. doi:10.1126/science.3283935
- Mattsson, N., Insel, P.S., Aisen, P.S., Jagust, W., Mackin, S., Weiner, M., 2015. Brain structure and function as mediators of the effects of amyloid on memory. *Neurology* 84, 1136–1144. doi:10.1212/WNL.0000000000001375
- Mckhann, G.M., Knopman, D.S., Chertkow, H., Hyman, B.T., Jack, C.R., Kawas, C.H., Klunk, W.E., Koroshetz, W.J., Manly, J.J., Mayeux, R., Mohs, R.C., Morris, J.C., Rossor, M.N., Scheltens, P., Carrillo, M.C., Thies, B., Weintraub, S., Phelps, C.H., 2011. The diagnosis of dementia due to Alzheimer ’ s disease : Recommendations from the National Institute on Aging-Alzheimer ’ s Association workgroups on diagnostic guidelines for Alzheimer ’ s disease. *Alzheimer’s Dement. J. Alzheimer’s Assoc.* 7, 263–269. doi:10.1016/j.jalz.2011.03.005
- Mielke, M.M., Hagen, C.E., Xu, J., Chai, X., Vemuri, P., Lowe, V.J., Airey, D.C., Knopman, D.S., Roberts, R.O., Machulda, M.M., Jack, C.R., Petersen, R.C., Dage, J.L., 2018. Plasma phospho-tau181 increases with Alzheimer’s disease clinical severity and is associated with tau- and amyloid-positron emission tomography. *Alzheimer’s Dement.* 14, 989–997. doi:10.1016/j.jalz.2018.02.013
- Mintun, M., Lo, A.C., Evans, C.D., Wessels, A.M., Ardayfio, P.A., Andersen, S.W., Shcherbinin, S., Sparks, J., Sims, J.R., Brys, M., Apostolova, L.G., Salloway, S., Skovronsky, D., 2021. Donanemab in Early Alzheimer’s Disease. *New Engl.* 1–14. doi:10.1056/NEJMoa2100708
- Mormino, E.C., Kluth, J.T., Madison, C.M., Rabinovici, G.D., Baker, S.L., Miller, B.L., Koeppe, R.A., Mathis, C.A., Weiner, M.W., Jagust, W.J., 2009. Episodic memory loss is related to hippocampal-mediated  $\beta$ -amyloid deposition in elderly subjects. *Brain* 132, 1310–1323. doi:10.1093/brain/awn320
- Mormino, E.C., Papp, K. V., Rentz, D.M., Donohue, M.C., Amariglio, R., Quiroz, Y.T., Chhatwal, J., Marshall, G.A., Donovan, N., Jackson, J., Gatchel, J.R., Hanseeuw, B.J., Schultz, A.P., Aisen, P.S., Johnson, K.A., Sperling, R.A., 2017. Early and late change on the preclinical Alzheimer’s cognitive composite in clinically normal older individuals with elevated amyloid  $\beta$ . *Alzheimer’s Dement.* 13, 1004–1012. doi:10.1016/j.jalz.2017.01.018
- Morris, J.C., 1993. The Clinical Dementia Rating (CDR): current version and scoring rules. *Neurology* 43, 2412–2414. doi:10.1212/WNL.43.11.2412-a

- Mueller, S.G., Weiner, M.W., Thal, L.J., Petersen, R.C., Jack, C.R., Jagust, W., Trojanowski, J.Q., Toga, A.W., Beckett, L., 2005. Ways toward an early diagnosis in Alzheimer ' s disease : The Alzheimer ' s Disease Neuroimaging Initiative ( ADNI ) 1, 55–66. doi:10.1016/j.jalz.2005.06.003
- Olsson, A., Vanderstichele, H., Andreasen, N., De Meyer, G., Wallin, A., Holmberg, B., Rosengren, L., Vanmechelen, E., Blennow, K., 2005. Simultaneous measurement of beta-amyloid(1-42), total tau, and phosphorylated tau (Thr181) in cerebrospinal fluid by the xMAP technology. *Clin Chem* 51, 336–45.
- Palmqvist, S., Janelidze, S., Stomrud, E., Zetterberg, H., Karl, J., Zink, K., Bittner, T., Mattsson, N., Eichenlaub, U., Blennow, K., Hansson, O., 2019. Performance of Fully Automated Plasma Assays as Screening Tests for Alzheimer Disease-Related  $\beta$ -Amyloid Status. *JAMA Neurol.* 76, 1060–1069. doi:10.1001/jamaneurol.2019.1632
- Palmqvist, S., Schöll, M., Strandberg, O., Mattsson, N., Stomrud, E., Zetterberg, H., Blennow, K., Landau, S., Jagust, W., Hansson, O., 2017. Earliest accumulation of  $\beta$ -amyloid occurs within the default-mode network and concurrently affects brain connectivity. *Nat. Commun.* 8. doi:10.1038/s41467-017-01150-x
- Palmqvist, S., Zetterberg, H., Blennow, K., Vestberg, S., Andreasson, U., Brooks, D.J., Owenius, R., Hägerström, D., Wollmer, P., Minthon, L., Hansson, O., 2014. Accuracy of brain amyloid detection in clinical practice using cerebrospinal fluid  $\beta$ -Amyloid 42: A cross-validation study against amyloid positron emission tomography. *JAMA Neurol.* 71, 1282–1289. doi:10.1001/jamaneurol.2014.1358
- Papp, K. V., Rentz, D.M., Mormino, E.C., Schultz, A.P., Amariglio, R.E., Quiroz, Y., Johnson, K.A., Sperling, R.A., 2017. Cued memory decline in biomarker-defined preclinical Alzheimer disease. *Neurology* 88, 1431–1438. doi:10.1212/WNL.0000000000003812
- Papp, K. V., Amariglio, R.E., Mormino, E.C., Hedden, T., Dekhytar, M., Johnson, K.A., Sperling, R.A., Rentz, D.M., 2015. Free and cued memory in relation to biomarker-defined abnormalities in clinically normal older adults and those at risk for Alzheimer ' s disease. *Neuropsychologia* 73, 169–175. doi:10.1016/j.neuropsychologia.2015.04.034
- Pfeffer, R.I., Kurosaki, T.T., Harrah, C.H., Chance, J.M., Filos, S., 1982. Measurement of functional activities in older adults in the community. *J. Gerontol.* 37, 323–329. doi:10.1093/geronj/37.3.323
- Reiman, E.M., Arboleda-Velasquez, J.F., Quiroz, Y.T., Huentelman, M.J., Beach, T.G., Caselli, R.J., Chen, Y., Su, Y., Myers, A.J., Hardy, J., Paul Vonsattel, J., Younkin, S.G., Bennett, D.A., De Jager, P.L., Larson, E.B., Crane, P.K., Keene, C.D., Kamboh, M.I., Kofler, J.K., Duque, L., Gilbert, J.R., Gwirtsman, H.E., Buxbaum, J.D., Dickson, D.W., Frosch, M.P., Ghetti, B.F., Lunetta, K.L., Wang, L.S., Hyman, B.T., Kukull, W.A., Foroud, T., Haines, J.L., Mayeux, R.P., Pericak-Vance, M.A., Schneider, J.A., Trojanowski, J.Q., Farrer, L.A., Schellenberg, G.D., Beecham, G.W., Montine, T.J., Jun, G.R., Abner, E., Adams, P.M., Albert, M.S., Albin, R.L., Apostolova, L.G., Arnold, S.E., Asthana, S., Atwood, C.S., Baldwin, C.T., Barber, R.C., Barnes, L.L.,

- Barral, S., Becker, J.T., Beekly, D., Bigio, E.H., Bird, T.D., Blacker, D., Boeve, B.F., Bowen, J.D., Boxer, A., Burke, J.R., Burns, J.M., Cairns, N.J., Cantwell, L.B., Cao, C., Carlson, C.S., Carlsson, C.M., Carney, R.M., Carrasquillo, M.M., Chui, H.C., Cribbs, D.H., Crocco, E.A., Cruchaga, C., DeCarli, C., Dick, M., Doody, R.S., Duara, R., Ertekin-Taner, N., Evans, D.A., Faber, K.M., Fairchild, T.J., Fallon, K.B., Fardo, D.W., Farlow, M.R., Ferris, S., Galasko, D.R., Gearing, M., Geschwind, D.H., Ghisays, V., Goate, A.M., Graff-Radford, N.R., Green, R.C., Growdon, J.H., Hakonarson, H., Hamilton, R.L., Hamilton-Nelson, K.L., Harrell, L.E., Honig, L.S., Huebinger, R.M., Hulette, C.M., Jarvik, G.P., Jin, L.W., Karydas, A., Katz, M.J., Kauwe, J.S.K., Kaye, J.A., Kim, R., Kowall, N.W., Kramer, J.H., Kunkle, B.W., Kuzma, A.P., LaFerla, F.M., Lah, J.J., Leung, Y.Y., Leverenz, J.B., Levey, A.I., Li, G., Lieberman, A.P., Lipton, R.B., Lopez, O.L., Lyketsos, C.G., Malamon, J., Marson, D.C., Martin, E.R., Martiniuk, F., Mash, D.C., Masliah, E., McCormick, W.C., McCurry, S.M., McDavid, A.N., McDonough, S., McKee, A.C., Mesulam, M., Miller, B.L., Miller, C.A., Miller, J.W., Morris, J.C., Mukherjee, S., Naj, A.C., O'Bryant, S., Olichney, J.M., Parisi, J.E., Paulson, H.L., Peskind, E., Petersen, R.C., Pierce, A., Poon, W.W., Potter, H., Qu, L., Quinn, J.F., Raj, A., Raskind, M., Reisberg, B., Reisch, J.S., Reitz, C., Ringman, J.M., Roberson, E.D., Rogaeva, E., Rosen, H.J., Rosenberg, R.N., Royall, D.R., Sager, M.A., Sano, M., Saykin, A.J., Schneider, L.S., Seeley, W.W., Smith, A.G., Sonnen, J.A., Spina, S., George-Hyslop, P.S., Stern, R.A., Swerdlow, R.H., Tanzi, R.E., Troncoso, J.C., Tsuang, D.W., Valladares, O., Van Deerlin, V.M., Van Eldik, L.J., Vardarajan, B.N., Vinters, H. V., Weintraub, S., Welsh-Bohmer, K.A., Wilhelmsen, K.C., Williamson, J., Wingo, T.S., Woltjer, R.L., Wright, C.B., Wu, C.K., Yu, C.E., Yu, L., Zhao, Y., 2020. Exceptionally low likelihood of Alzheimer's dementia in APOE2 homozygotes from a 5,000-person neuropathological study. *Nat. Commun.* 11. doi:10.1038/s41467-019-14279-8
- Reitan, R., 1958. Validity of the Trail Making Test as an indicator of organic brain damage. *Percept. Mot. Skills* 8, 271–276. doi:10.2466/PMS.8.7.271-276
- Rey, A., 1958. L'examen clinique en psychologie., *Lexamen clinique en psychologie.* doi:CRJ Alz lib Copy2 #618; CRJ Alz lib Copy2-Converted #618; CRJ Alz Library 2 shared lib-Converted #1017; MMM Master\_Reference\_List-Converted #21; JLW MCI-Converted #22; JLW PCA-Converted #58; JLW VBMprediction-Converted #87
- Rosen, W.G., Mohs, R.C., Davis, K.L., 1984. A new rating scale for Alzheimer's disease. *Am. J. Psychiatry.* doi:6496779
- Rousset, O.G., Ma, Y., Evans, A.C., 1998. Correction for Partial Volume Effects in PET: Principle and Validation. *J. Nucl. Med.* 39, 904–11.
- Salloway, S., Sperling, R., Fox, N.C., Blennow, K., Klunk, W., Raskind, M., Sabbagh, M., Honig, L.S., Porsteinsson, A.P., Ferris, S., Reichert, M., Ketter, N., Nejadnik, B., Guenzler, V., Miloslavsky, M., Wang, D., Lu, Y., Lull, J., Tudor, I.C., Liu, E., Grundman, M., Yuen, E., Black, R., Brashear, H.R., 2014. Two Phase 3 Trials of Bapineuzumab in Mild-to-Moderate Alzheimer's Disease. doi:10.1056/NEJMoa1304839

- Schindler, S.E., Bollinger, J.G., Ovod, V., Mawuenyega, K.G., Li, Y., Gordon, B.A., Holtzman, D.M., Morris, J.C., Benzinger, T.L.S., Xiong, C., Fagan, A.M., Bateman, R.J., 2019. High-precision plasma  $\beta$ -amyloid 42/40 predicts current and future brain amyloidosis. *Neurology* 10.1212/WNL.0000000000008081. doi:10.1212/wnl.0000000000008081
- Sevigny, J., Chiao, P., Bussière, T., Weinreb, P.H., Williams, L., Maier, M., Dunstan, R., Salloway, S., Chen, T., Ling, Y., Gorman, J.O., Qian, F., Arastu, M., Li, M., Chollate, S., Brennan, M.S., Quintero-monzon, O., Scannevin, R.H., Arnold, H.M., Engber, T., Rhodes, K., 2016. The antibody aducanumab reduces A $\beta$  plaques in Alzheimer's disease. *Nature* 537. doi:10.1038/nature19323
- Shaw, L.M., Vanderstichele, H., Knapiak-Czajka, M., Clark, C.M., Aisen, P.S., Petersen, R.C., Blennow, K., Soares, H., Simon, A., Lewczuk, P., Dean, R., Siemers, E., Potter, W., Lee, V.M.Y., Trojanowski, J.Q., 2009. Cerebrospinal fluid biomarker signature in alzheimer's disease neuroimaging initiative subjects. *Ann. Neurol.* 65, 403–413. doi:10.1002/ana.21610
- Sled, J.G., Zijdenbos, A.P., Evans, A.C., 1998. A Nonparametric Method for Automatic Correction of Intensity Nonuniformity in MRI Data. *IEEE Trans. Med. Imaging* 17, 87–97.
- Smith, R., Schain, M., Nilsson, C., Strandberg, O., Olsson, T., 2016. Increased Basal Ganglia Binding of 18 F-AV-1451 in Patients With Progressive Supranuclear Palsy 00, 1–7. doi:10.1002/mds.26813
- Snyder, P.J., Kahle-Wroblewski, K., Brannan, S., Miller, D.S., Schindler, R.J., Desanti, S., Ryan, J.M., Morrison, G., Grundman, M., Chandler, J., Caselli, R.J., Isaac, M., Bain, L., Carrillo, M.C., 2014. Assessing cognition and function in Alzheimer's disease clinical trials: Do we have the right tools? *Alzheimer's Dement.* 10, 853–860. doi:10.1016/j.jalz.2014.07.158
- Sperling, R. a, Rentz, D.M., Johnson, K. a, Karlawish, J., Donohue, M., Salmon, D.P., Aisen, P., 2014. The A4 study: stopping AD before symptoms begin? *Sci. Transl. Med.* 6, 228fs13. doi:10.1126/scitranslmed.3007941
- Sperling, R., Donohue, M., Raman, R., Sun, C.-K., Yaari, R., Holdridge, K., Siemers, E., Johnson, K., Aisen, P., 2020. Association of Factors With Elevated Amyloid Burden in Clinically Normal Older Individuals. *JAMA Neurol.* 77, 735–745. doi:10.1001/jamaneurol.2020.0387
- Suidan, G.L., Ramaswamy, G., 2019. Targeting apolipoprotein E for alzheimer's disease: An industry perspective. *Int. J. Mol. Sci.* 20. doi:10.3390/ijms20092161
- Thomas, B.A., Erlandsson, K., Modat, M., Thurfjell, L., Vandenberghe, R., Ourselin, S., Hutton, B.F., 2011. The importance of appropriate partial volume correction for PET quantification in Alzheimer ' s disease. *Eur. J. Nucl. Med. Mol. Imaging* 38, 1104–1119. doi:10.1007/s00259-011-1745-9
- Tibshirani, R., 1996. Regression Shrinkage and Selection via the Lasso 58, 267–288.



- Tosun, D., Landau, S., Aisen, P.S., Petersen, R.C., Mintun, M., 2017. Association between tau deposition and antecedent amyloid- $\beta$  accumulation rates in normal and early symptomatic individuals. *Brain* 140, 1499–1512. doi:10.1093/awx065
- Vemuri, P., Lesnick, T.G., Przybelski, S.A., Knopman, D.S., Preboske, G.M., Kantarci, K., Raman, M.R., Machulda, M.M., Mielke, M.M., Lowe, V.J., Senjem, M.L., Gunter, J.L., Rocca, W.A., Roberts, R.O., Petersen, R.C., Jack, C.R., 2015. Vascular and amyloid pathologies are independent predictors of cognitive decline in normal elderly. *Brain* 138, 761–771. doi:10.1093/brain/awu393
- Villemagne, V.L., Burnham, S., Bourgeat, P., Brown, B., Ellis, K.A., Salvado, O., Szoek, C., Macaulay, S.L., Martins, R., Maruff, P., Ames, D., Rowe, C.C., Masters, C.L., 2013. Amyloid  $\beta$  deposition, neurodegeneration, and cognitive decline in sporadic Alzheimer's disease: A prospective cohort study. *Lancet Neurol.* 12, 357–367. doi:10.1016/S1474-4422(13)70044-9
- Villemagne, V.L., Doré, V., Yates, P., Brown, B., Mulligan, R., Bourgeat, P., Veljanoski, R., Rainey-smith, S.R., Ong, K., Rembach, A., Williams, R., Burnham, S.C., Laws, S.M., Salvado, O., Taddei, K., Macaulay, S.L., Martins, R.N., Ames, D., Masters, C.L., Rowe, C.C., 2014. En Attendant Centiloid. *Adv. Res.* 2, 723–729.
- Villemagne, V.L., Fodero-tavoletti, M.T., Masters, C.L., Rowe, C.C., Health, A., 2015. Tau imaging: early progress and future directions. *Lancet Neurol.* 14, 114–124. doi:10.1016/S1474-4422(14)70252-2
- Vos, S.J.B., Xiong, C., Visser, P.J., Mateusz, S., Hassenstab, J., Grant, E.A., Cairns, N.J., Morris, J.C., Holtzman, D.M., Fagan, A.M., 2014. Preclinical Alzheimer's disease and its outcome: a longitudinal cohort study. *Lancet Neurol* 12, 957–965. doi:10.1016/S1474-4422(13)70194-7.Preclinical
- Wechsler, D., 1987. Manual for Wechsler Memory Scale - Revised, The Psychological Corporation. doi:PCA-Converted #56
- Wirth, M., Oh, H., Mormino, E.C., Markley, C., Landau, S.M., Jagust, W.J., 2013. The effect of amyloid  $\beta$  on cognitive decline is modulated by neural integrity in cognitively normal elderly. *Alzheimer's Dement.* 9, 687–698. doi:10.1016/j.jalz.2012.10.012

Paper I







## Cognitive and functional changes associated with A $\beta$ pathology and the progression to mild cognitive impairment



Philip S. Insel<sup>a,b,c,\*</sup>, Michael C. Donohue<sup>d</sup>, R. Scott Mackin<sup>b,e</sup>, Paul S. Aisen<sup>d</sup>, Oskar Hansson<sup>a,f</sup>, Michael W. Weiner<sup>b,c</sup>, Niklas Mattsson<sup>a,f,g</sup>, and the Alzheimer's Disease Neuroimaging Initiative

<sup>a</sup> Clinical Memory Research Unit, Faculty of Medicine, Lund University, Lund, Sweden

<sup>b</sup> Center for Imaging of Neurodegenerative Diseases, Department of Veterans Affairs Medical Center, San Francisco, CA, USA

<sup>c</sup> Department of Radiology and Biomedical Imaging, University of California, San Francisco, CA, USA

<sup>d</sup> Department of Neurology, Keck School of Medicine, University of Southern California, Los Angeles, CA, USA

<sup>e</sup> Department of Psychiatry, University of California, San Francisco, CA, USA

<sup>f</sup> Memory Clinic, Skåne University Hospital, Lund University, Lund, Sweden

<sup>g</sup> Department of Neurology, Skåne University Hospital, Lund University, Lund, Sweden

### ARTICLE INFO

#### Article history:

Received 5 December 2015

Received in revised form 12 August 2016

Accepted 15 August 2016

Available online 26 August 2016

#### Keywords:

$\beta$ -amyloid

Clinical trials

Cognition

Function

Composite

Mild cognitive impairment

### ABSTRACT

Cognitively-normal people with evidence of  $\beta$ -amyloid (A $\beta$ ) pathology and subtle cognitive dysfunction are believed to be at high risk for progression to mild cognitive impairment due to Alzheimer's disease (AD). Clinical trials in later stages of AD typically include a coprimary endpoint to demonstrate efficacy on both cognitive and functional assessments. Recent trials focus on cognitively-normal people, but functional decline has not been explored for trial designs in this group. The goal of this study was therefore to characterize cognitive and functional decline in (1) cognitively-normal people converting to mild cognitive impairment (MCI) and (2) cognitively-normal  $\beta$ -amyloid-positive (A $\beta$ +) people. Specifically, we sought to identify and compare the cognitive and functional assessments and their weighted combinations that maximize the longitudinal decline specific to these 2 groups. We studied 68 people who converted from normal cognition to MCI and 70 nonconverters, as well as 137 A $\beta$ + and 210  $\beta$ -amyloid-negative cognitively-normal people. We used bootstrap aggregation and cross-validated mixed-models to estimate the distribution of weights applied to cognitive and functional outcomes to form composites. We also evaluated best subset optimization. Using optimized composites, we estimated statistical power for a variety of clinical trial scenarios. Overall, 55.4% of cognitively-normal to MCI converters were A $\beta$ +. Large gains in power estimates were obtained when requiring participants to have both subtle cognitive dysfunction and A $\beta$  pathology compared with requiring A $\beta$  pathology alone. Additional power resulted when including functional as well as cognitive outcomes as part of the composite. Composites formed by applying equal weights to all measures provided the highest estimates of cross-validated power, although similar to both continuous weight optimization and best subset optimization. Using a composite to detect a 30% slowing of decline, 80% power was obtained for predicted A $\beta$ + converters with 375 completers/arm for a 30-month trial using a combination of cognitive/functional measures. In the A $\beta$ + group, power to approach levels suitable for a phase III clinical trial would require considerably larger sample sizes. Composites incorporating both cognitive and functional measures may substantially increase the power of a trial in a preclinical (A $\beta$ +) AD population with subtle evidence of cognitive dysfunction.

© 2016 Elsevier Inc. All rights reserved.

### 1. Introduction

Accumulating evidence from Alzheimer's disease (AD) biomarker studies suggests  $\beta$ -amyloid (A $\beta$ ) deposition may occur decades before the diagnosis of clinical dementia (Morris, 2005). Anti-A $\beta$  treatments are thought to have a higher likelihood of slowing progression if administered at the earliest signs of the

\* Corresponding author at: Center for Imaging of Neurodegenerative Diseases, Department of Veterans Affairs Medical Center, San Francisco, CA 94121, USA. Tel.: +1 858 652 8480; fax: 415-221-4810.

E-mail address: [philipinsel@gmail.com](mailto:philipinsel@gmail.com) (P.S. Insel).

pathological cascade, before substantial neurodegeneration and other downstream effects of A $\beta$  deposition (Sperling et al., 2011b). Classification of Alzheimer's disease into progressive stages has helped to organize the current thinking about the emergence of subtle clinical symptoms and the development of cognitive and functional impairment during the continuum of disease progression (Sperling et al., 2011a). The initial stages of preclinical AD are defined by amyloidosis and neurodegeneration. The final preclinical stage also includes some evidence of subtle cognitive dysfunction, although below levels of cognitive and functional impairment required to meet criteria for mild cognitive impairment (MCI) due to AD. As the disease progresses into MCI and dementia, cognitive and functional deficits may be observed. Identifying the biomarkers and clinical assessments that can predict and monitor the progression from the early stages of AD to more advanced disease will help to elucidate the disease process and inform clinical trial design (Insel et al., 2015). Here we sought to determine the optimal combination of cognitive and functional measures to track disease progression in cognitively-normal people progressing to MCI, and of A $\beta$ -positive (A $\beta$ +) cognitively-normal people. Composite endpoints comprising both cognitive and functional measures are currently being used in clinical trials of MCI populations (Ard et al., 2015; Raghavan et al., 2013; Wang et al., 2016). Here we consider the inclusion of functional measures in the endpoint for clinical trials in preclinical AD.

The Food and Drug Administration (FDA) recently offered draft guidance to update their recommendations on primary endpoint selection in clinical trials for early-stage AD (US Dept of Health and Human Services, 2015). With the focus of recent clinical trials on treatment in these earlier stages of AD, including prodromal AD and preclinical AD, the FDA recognized the difficulty in demonstrating drug efficacy using prior guidelines developed for trials with subjects in the dementia stage of AD (Kozauer et al., 2013; McKhann et al., 2011). Trial design in later stages of AD has typically included a coprimary endpoint to demonstrate efficacy on both a cognitive and a functional assessment. However, the assessment tools used in these trials have not been validated in earlier stage subjects (Snyder et al., 2014), leading the FDA to consider the use of a single primary composite endpoint that captures both cognitive and functional decline, in trials of prodromal AD subjects. Preclinical AD subjects are, by definition, cognitively-normal and should not have any functional impairment due to cognitive dysfunction. We hypothesize that as the target population progresses on the continuum of decline, assessing functional changes may take a more central role in demonstrating a drug effect to be clinically meaningful. However, the feasibility and value of assessing functional decline as part of a trial endpoint in a pre-clinical population are unknown.

Since the FDA guidance, several cognitive composites have been developed to capture the decline specific to subjects with preclinical AD, but no attempts have been made to develop combined cognitive and functional composites. The Alzheimer's Prevention Initiative (API) has developed cognitive composites using Presenilin 1 E280A mutation carriers (Ayutyanont et al., 2014) and also cognitively-normal elders who converted to MCI or AD (Langbaum et al., 2014). A third cognitive composite, to be used as the primary endpoint in the A4 trial (Sperling et al., 2014), was developed to capture decline in A $\beta$ +/ cognitively-normal elders (Donohue et al., 2014), and selected individual components based on a literature review. Functional assessments were not evaluated in the API or the A4 composites.

The aim of this study was to identify and compare the cognitive and/or functional assessments and their weighted combinations that maximize the longitudinal decline specific to (1) cognitively-normal to MCI converters (cCN); and (2) cognitively-normal

A $\beta$ +/ subjects. Conversion status is not known at the beginning of the study, and thus, power estimates based on subjects' true conversion status would not be useful to inform a clinical trial. Therefore, to reflect a realistic modern trial scenario, subjects who were both predicted to convert using information available at baseline and were also A $\beta$ +/ (pcCN), were used to estimate clinical trial power. Using the battery of assessments from the Alzheimer's Disease Neuroimaging Initiative (ADNI), we sought to characterize the importance of each cognitive and functional assessment in our 3 groups (cCN, pcCN, and A $\beta$ +) as well as provide cross-validated estimates of power when using the composites in clinical trial scenarios.

## 2. Material and methods

### 2.1. Participants

Data were obtained from the ADNI database ([adni.loni.usc.edu](http://adni.loni.usc.edu)). ADNI is the result of efforts of many coinvestigators, and participants have been recruited from over 50 sites across the United States and Canada (see [www.adni-info.org](http://www.adni-info.org)). The population in this study included ADNI-1 and ADNI-2 participants enrolled into the cognitively-normal or subjective memory complaint cohorts, were tested for cerebrospinal fluid (CSF) biomarkers or <sup>18</sup>F-florbetapir positron emission tomography (PET), and were followed longitudinally for neuropsychological testing.

### 2.2. Cerebrospinal fluid biomarker concentrations

Each CSF sample was collected by lumbar puncture and shipped on dry ice to the ADNI Biomarker Core laboratory at the University of Pennsylvania Medical Center for long-term storage at  $-80^{\circ}\text{C}$ . CSF A $\beta_{42}$  was measured using the multiplex xMAP Luminex platform (Luminex Corp, Austin, TX, USA) with the research use only INNOBIA AlzBio3 kit (Fujirebio/Innogenetics, Ghent, Belgium) (Olsson et al., 2005; Shaw et al., 2009).

### 2.3. Florbetapir PET

Methods to acquire and process ADNI florbetapir PET image data were described previously (Landau et al., 2012). Full details of acquisition and analysis can be found at <http://adni.loni.usc.edu/methods/>.

### 2.4. Cognitive and functional outcomes

Cognitive measures assessed were the Mini-Mental State Examination (MMSE), Alzheimer's Disease Assessment Scale—cognitive subscale, 13-item version (ADAS13), immediate and delayed memory recall from the Wechsler Memory Scale (iMemory, dMemory), immediate and delayed Rey Auditory Verbal Learning Test (iAVLT, dAVLT), Trail Making Test parts A and B (Trails A & B), Boston Naming Test, and Category Fluency. The Clinical Dementia Rating Sum of Boxes (CDR-SB) was also assessed, which includes both cognitive and functional items, and finally the Functional Assessment Questionnaire (FAQ), which is purely a functional assessment (Kaplan et al., 1982; Morris, 1993; Pfeiffer et al., 1982; Reitan, 1958; Rey, 1964; Rosen et al., 1984; Wechsler, 1987).

### 2.5. Statistical analysis

This study included 3 main sets of analyses. The first was a comparison of normal participants who converted to a diagnosis of MCI (cCN) during 7 years of follow-up versus stable cognitively-normal (sCN) participants, during the same period. Follow-up on

converters continued beyond diagnosis of MCI. The second analysis was a comparison of participants predicted to convert to MCI (pcCN, only including A $\beta$ + subjects) versus the  $\beta$ -amyloid-negative (A $\beta$ -) participants from the sCN group. The third analysis was a comparison of A $\beta$ + versus A $\beta$ - participants, irrespective of conversion information. There was considerable overlap among these groups. The cCN or sCN participants that also had A $\beta$  information ( $n = 56$  from the cCN group, and  $n = 57$  from the sCN group) were also included in either the A $\beta$ - or A $\beta$ + groups. This is described further in the results section. All pcCN participants were included in the A $\beta$ + group.

A $\beta$ + was defined as florbetapir PET SUVR  $>1.10$  at any point during follow-up (Landau et al., 2012). Subjects without florbetapir PET were considered A $\beta$ + if CSF A $\beta_{42} < 192$  ng/L (Shaw et al., 2009).

In each of the 3 groups, we compared 2 types of optimization: the first allowed continuous weights for each component while the second was more constrained, allowing only combinations of components with 0 or 1 weights (0 = exclusion, 1 = inclusion), providing the best subset of components. For the continuous weight optimization, in each group, composite weights were estimated via bootstrap resampling and cross-validation to find the set of weights that maximized the separation of the groups over the first 48 months of follow-up. Spline knots for models limited to 48-month follow-up were placed at 12, 24, and 36 months, post baseline. The median weight from this distribution for each outcome was used to form the composite to be evaluated for trial power. Details of each step are described in the following.

Longitudinal cognitive and functional measures were modeled using linear mixed-effects regression with a random intercept and slope and an unstructured covariance matrix for the random effects. Variance components were estimated conditional on converter (or amyloid) status. All models included age (years), education (years), gender, group, time since initial visit, and the interaction between group and time, as predictors. To capture departures from linearity in the trajectory of cognition and function, continuous time from the baseline test was parameterized using a 3-knot restricted cubic spline, with knots placed at 1, 3, and 5 years, post baseline. Differences in group trajectories were tested using interactions between the 2 parameters for time resulting from the spline and the group factor,  $\text{group} \times (\beta_{\text{time1}} + \beta_{\text{time2}})$ . Likelihood ratio tests were used to test the significance of the interaction for longitudinal differences and Wald tests on the main effect for group were used to test for baseline differences (Chambers and Hastie, 1992). The  $p$ -values were 2-sided and adjusted for multiplicity using a Hochberg correction (Hochberg, 1988). The  $p$ -values  $< 0.05$  were considered significant and the  $p$ -values  $< 0.10$  were considered marginally significant.

Within each analysis, we aimed to identify the composite weights that maximized the separation of the trajectories of the groups over time. We evaluated 2 types of composites: one that considered only the 10 cognitive components and another that also included the 2 measures with functional assessments. To form the composites,  $z$ -scores (mean centered and scaled to the standard deviation of all baseline and longitudinal scores) of each component were weighted and summed. For the continuous weight optimization, weights for each component could be anywhere on the interval [0, 1]. Numerical optimization was used to search the space of candidate weights to maximize the separation of the groups. Bound constrained optimization (Byrd et al., 1995) was used to maximize the likelihood ratio test for group trajectory differences.

The large number of cognitive and functional components considered and the space of possible weight combinations increases the risk of overfitting. To minimize overfitting, weights were estimated and evaluated using bootstrap aggregation and 10-

fold cross-validation (Breiman, 1996). Folds were balanced on group status and cognitive and functional measures. In each training set, 100 bootstrap samples were used to estimate a distribution of optimal composite weights. The median weight for each component from this distribution was then used to form the composite to be evaluated in the test set. The steps of the analysis are shown in a flowchart in Supplementary Fig. 1. The resulting estimates of longitudinal change and variance in the test sets were averaged and used to estimate power for hypothetical clinical trials, as described in the following. For the best subset optimization, the number of components that maximized the cross-validated likelihood ratio test was used in the final composite.

To determine the value of the composites derived by this analysis, we used the cross-validated estimates of change and variance to simulate hypothetical clinical trial scenarios with a proportional treatment effect over time in the active group. Averaging over test set estimates for change from baseline to 18, 24, 30, and 36 months and the estimates of the residual error, subject-specific intercepts and slopes, and the correlation between the intercepts and slopes, we estimated the power to detect a 30% decrease in the difference between the change in the groups. Sampling from the aforementioned estimates and assuming a range of sample sizes, we simulated 1000 longitudinal clinical trials for each sample size, composite type (cognition and function, cognition only, best subset, and for comparison, flat weights across all 12 components), and group. Power was estimated as the proportion of significant  $p$ -values for the difference in change from baseline at the final visit between the drug and placebo groups, using a mixed-model repeated-measures design (Siddiqui et al., 2009).

The pcCN subjects (restricted to A $\beta$ + subjects) were identified using baseline cognitive/functional assessments, and demographic and APOE information, with a random forest model (Breiman, 2001). Using cross-validated estimates of the probability of conversion, we repeated all steps of the analysis described previously to estimate power for a clinical trial based on participants who were both A $\beta$ + and predicted to convert (pcCN), to make our results applicable to trials requiring A $\beta$ + for inclusion. Three-fold cross-validation was used for the pcCN analysis because of the reduced sample size.

The association between groups within each cohort and missing data was modeled using generalized mixed-effects regression with a binomial indicator for a missing visit. All analyses were done in R version 3.1.1 (The R Foundation for Statistical Computing, Vienna, Austria; [www.r-project.org](http://www.r-project.org)).

### 3. Results

#### 3.1. Cohort characteristics

In the ADNI data set, 68 subjects converted to MCI during 7 years of follow-up while 70 subjects remained cognitively-normal throughout the same period. cCN subjects were older and had more APOE  $\epsilon 4$  carriers compared to sCN (Table 1). There were no significant differences in gender or education. As described in the Section 2.5, we also identified a group of cognitively-normal subjects who were predicted to convert to MCI (pcCN, only including A $\beta$ + subjects). Characteristics of the pcCN group are shown in Supplementary Table 1.

One hundred thirty-seven A $\beta$ + subjects and 210 A $\beta$ - subjects were included in the analysis. A $\beta$ + subjects were older, less educated, and had more APOE  $\epsilon 4$  carriers (Table 1). There was no difference in gender. A Kaplan-Meier plot showing the distribution of conversion times for the cCN, A $\beta$ -, and A $\beta$ + groups is shown in Supplementary Fig. 2.

**Table 1**  
Baseline characteristics

Variable	Converters (N = 68), mean (SD)	Nonconverters (N = 70), mean (SD)	p
Age	76.5 (5.55)	74.9 (4.11)	0.014
Gender, female N (%)	28 (41.2)	37 (52.9)	0.178
Education	16.0 (2.67)	16.4 (2.75)	0.255
APOE ε4 N (%)	26 (38.2)	16 (22.9)	0.064
Aβ positivity N (%) (available for 56 cCN and 57 sCN)	31 (55.4)	18 (31.6)	0.014
	Aβ+ (N = 137), mean (SD)	Aβ- (N = 210), mean (SD)	p
Age	75.6 (5.09)	73.5 (5.91)	<0.001
Gender, female N (%)	74 (54.0)	98 (46.7)	0.189
Education	16.0 (2.71)	16.6 (2.65)	0.044
APOE ε4 N (%)	51 (37.2)	40 (19.0)	<0.001

Key: Aβ+, β-amyloid-positive; Aβ-, β-amyloid-negative; SD, standard deviation.

Of the 68 cCN participants, 56 had Aβ information: 31 (55.4%) were Aβ+ and 25 (44.6%) were Aβ-. Of the 70 sCN participants, 57 had Aβ information: 18 (31.6%) were Aβ+ and 39 (68.4%) were Aβ-.

### 3.2. Baseline cognitive/functional differences

When baseline cognitive/functional measures were compared in cCN versus sCN, cCN subjects performed worse on all 12 outcomes. Results with multiple comparison corrections are shown on the top left of Table 2. There were fewer differences on baseline cognitive/functional measures in Aβ+ versus Aβ- participants (top right of Table 2).

### 3.3. Longitudinal change

cCN subjects worsened significantly faster on 10 of the 12 cognitive and functional outcomes compared to sCN subjects, with the exception of the Boston Naming Test and Trails A over 7 years of follow-up (Fig. 1, Table 2, Supplementary Fig. 3). The largest effect size was in the CDR-SB, and the largest effect sizes among measures without functional items were in the iAVLT and the ADAS13. Longitudinal trajectories of the pcCN group are shown in Supplementary Fig. 4.

Aβ+ subjects worsened significantly faster on 6 of the 12 outcomes compared to Aβ- subjects (Fig. 1, Table 2). The largest effect size was in the ADAS13.

cCN subjects were more likely than sCN subjects to be missing data during the course of the 7 years of follow-up (log OR = 0.82, standard error = 0.15,  $p < 0.001$ ). However, sCN subjects were selected to have a minimum follow-up time of 7 years. Aβ-positivity was not associated with increased missingness (log OR = -0.04, standard error = 0.27,  $p = 0.87$ ).

### 3.4. Composite weight distributions

The distributions from 1000 bootstrap samples of the composite weights that maximized the separation of the groups are shown in Supplementary Fig. 5. Composite weights were estimated separately for the 3 groups (cCN, pcCN, and Aβ+).

The largest contributing outcomes in the composite for cCN versus sCN were the 2 delayed memory recall measures (dMemory, dAVLT), CDR-SB, and the MMSE (top left of Supplementary Fig. 5). Outcomes with smaller, although nonzero, positive median weights, included Category Fluency, iMemory, Trails A, and the Boston Naming Test. When the functional measures were excluded,

**Table 2**  
Baseline and longitudinal differences

Baseline	Baseline difference, converters versus nonconverters (N = 138)		Baseline difference, Aβ+ versus Aβ- (N = 347)	
	Z <sub>converter</sub> - Z <sub>nonconverter</sub> (SE)	p	Z <sub>Aβ+</sub> - Z <sub>Aβ-</sub> (SE)	p
MMSE	-0.06 (0.13)	0.641	0.06 (0.09)	0.997
ADAS13	0.58 (0.11)	<0.001	0.02 (0.08)	0.997
dMemory	-0.44 (0.13)	0.01	-0.09 (0.09)	0.997
iMemory	-0.42 (0.13)	0.012	-0.05 (0.09)	0.997
dAVLT	-0.46 (0.14)	0.01	-0.03 (0.10)	0.997
iAVLT	-0.48 (0.12)	0.001	0.03 (0.09)	0.997
Trails A	0.37 (0.14)	0.063	0.23 (0.10)	0.298
Trails B	0.32 (0.12)	0.063	0.28 (0.10)	0.062
Boston Naming Test	-0.32 (0.13)	0.084	-0.06 (0.09)	0.997
Category Fluency	-0.30 (0.16)	0.191	0.06 (0.10)	0.997
CDR-SB	0.09 (0.06)	0.299	0.0002 (0.04)	0.997
FAQ	0.19 (0.09)	0.156	-0.06 (0.06)	0.997
Longitudinal change	Converters versus nonconverters (N = 138, N Obs = 871)		Aβ+ versus Aβ- (N = 347, N Obs = 1441)	
	χ <sup>2</sup>	p	χ <sup>2</sup>	p
MMSE	15.03	0.002	25.96	<0.001
ADAS13	29.25	<0.001	38.95	<0.001
dMemory	24.73	<0.001	11.92	0.018
iMemory	18.47	<0.001	11.99	0.018
dAVLT	26.75	<0.001	5.48	0.194
iAVLT	32.26	<0.001	9.44	0.052
Trails A	6.83	0.066	1.85	0.396
Trails B	21.55	<0.001	3.38	0.369
Boston Naming Test	3.82	0.148	9.13	0.052
Category Fluency	15.16	0.002	5.79	0.194
CDR-SB	51.61	<0.001	17.64	0.001
FAQ	51.22	<0.001	34.18	<0.001

Key: Aβ+, β-amyloid-positive; Aβ-, β-amyloid-negative; ADAS13, Alzheimer's Disease Assessment Scale—cognitive subscale, 13-item version; iAVLT, immediate Rey Auditory Verbal Learning Test; CDR-SB, Clinical Dementia Rating Sum of Boxes; dAVLT, delayed Rey Auditory Verbal Learning Test; dMemory, delayed memory recall from the Wechsler Memory Scale; FAQ, Functional Assessment Questionnaire; iMemory, immediate memory recall from the Wechsler Memory Scale; MMSE, Mini-Mental State Examination; SE, standard error.

the delayed memory recall measures and MMSE remained the largest weighted outcomes and ADAS13 became more heavily weighted.

Composite weights that maximized the separation of pcCN and sCN subjects were also estimated. Using baseline information including demographics, APOE ε4 status, and cognitive/functional variables that were not heavily weighted in the true converter composite (ADAS13, Trails A & B, FAQ, Boston Naming Test, iAVLT, and iMemory), composite weights were estimated based on 32 Aβ+ pcCN and 31 Aβ- sCN participants. In reality, these 32 pcCN participants consisted of 25 converters and 7 nonconverters, resulting in a 78% positive predicted value from the model estimates. pcCN subjects were older, less educated, had more APOE ε4 allele carriers, and had lower cognitive scores at baseline compared with sCN subjects, similar to cCN subjects (Supplementary Table 1). We then estimated composite weights for this cohort. These weights are shown in the middle row of Supplementary Fig. 5. Similar to the cCN composite, the main outcomes for the pcCN composite were dMemory, CDR-SB, and MMSE, but in contrast, included the Boston Naming Test. When functional measures were excluded, the ADAS13 carried more weight. Note that the pcCN were Aβ+ by design because we aimed to make our results applicable to a trial requiring Aβ+ for inclusion.

The composites for Aβ+ versus Aβ- were heavily weighted by ADAS13, FAQ, and MMSE (bottom left Supplementary Fig. 5). When functional measures were excluded, ADAS13 and MMSE dominated the composites.

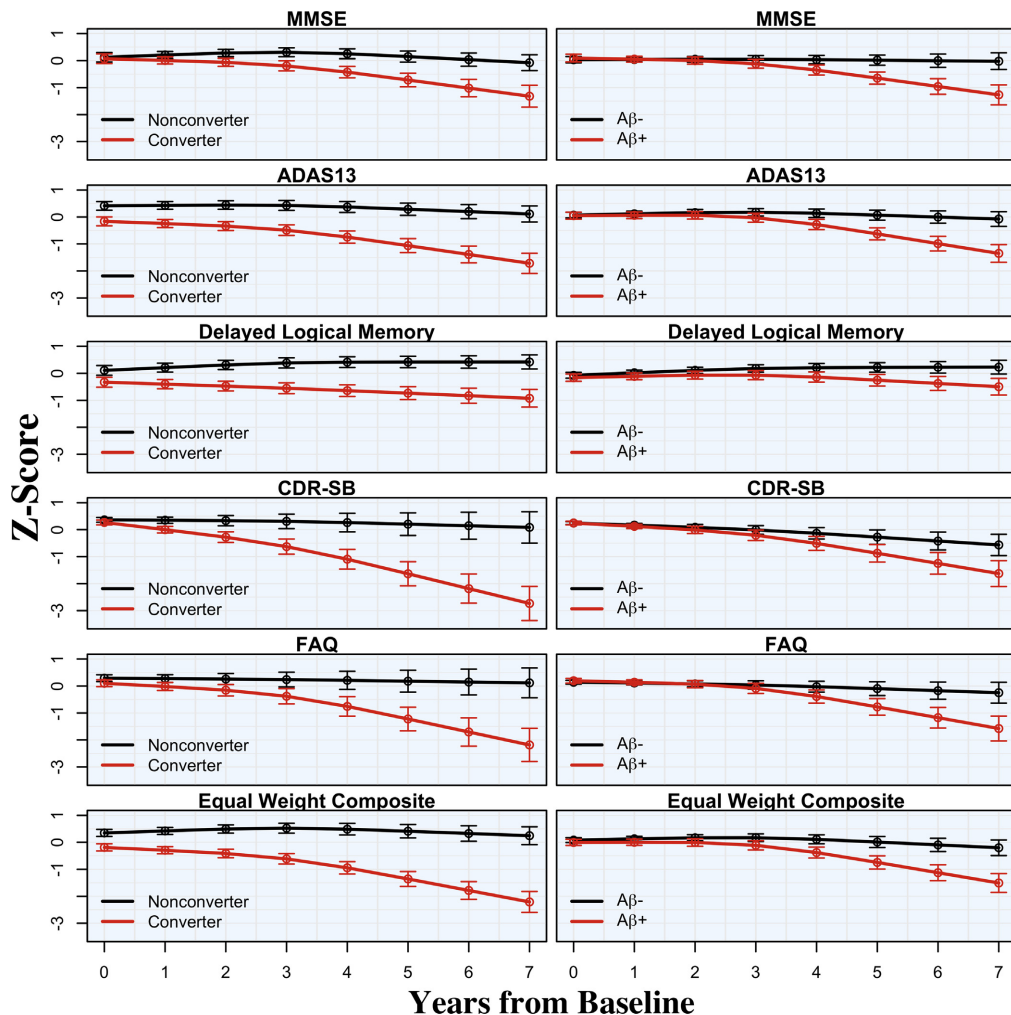


**Fig. 1.** Longitudinal plots of cognitive and functional assessments of converters versus nonconverters on the left and  $A\beta^+$  versus  $A\beta^-$  on the right. Z-scores of each assessment are plotted from baseline through 7 years of follow-up. Abbreviations:  $A\beta^+$ ,  $\beta$ -amyloid-positive;  $A\beta^-$ ,  $\beta$ -amyloid-negative; ADAS13, Alzheimer's Disease Assessment Scale—cognitive subscale, 13-item version; CDR-SB, Clinical Dementia Rating Sum of Boxes; FAQ, Functional Assessment Questionnaire; MMSE, Mini-Mental State Examination.

### 3.5. Best subset components

The best subset results were similar to the continuous optimization results. For the cCN versus sCN comparison, 5 components provided the optimal cross-validated composite, with the MMSE, dMemory, dAVLT, CDR-SB, and Category Fluency selected in nearly all cross-validation folds. For the pcCN versus sCN comparison, 7 components were selected, including the MMSE, dMemory, dAVLT, CDR-SB, Category Fluency, and iMemory in nearly all folds and occasionally either ADAS13 or Trails A. For the  $A\beta^+$  versus  $A\beta^-$  comparison, 3 components were selected—the MMSE, ADAS13, and FAQ. The power for these composites is described in the following.

### 3.6. Power

We estimated the power to detect a 30% slowing of decline using the average out-of-sample estimates of change and variance for each composite and group, over a range of sample sizes. The composite with flat weights across all measures was the best performing composite, attaining 80% power with 375 completers/arm in a hypothetical 30-month trial. Eighty percent power was attained with 450 completers per arm using the optimized cognitive/functional composite in a hypothetical 30-month clinical trial. Sixty-five percent of power was obtained with 500 completers per arm over a 30-month trial, using a



composite with cognition only. We also compared flat weight and optimized cognitive/functional composites in 48-month trials for Aβ+ pcCN subjects. They performed similarly (Supplementary Fig. 6).

The power estimates for the Aβ+ subjects are shown in the lower portion of Fig. 2. With similar sample sizes as the comparisons mentioned previously, power estimates never exceeded 40% with any type of composite.

### 3.7. Effect sizes and variance components

In Fig. 3, the magnitude of change, the within- and between-subject standard deviations, and effect sizes are plotted against the number of components included in the best subset composites, for cCN versus sCN and Aβ+ versus Aβ-. For both groups, the magnitude of change and both types of SD decrease with an increasing number of components included in the composites.

## 4. Discussion

The main findings of this study were as follows: (1) including participants with Aβ pathology as well as subtle cognitive dysfunction, predictive of progression to MCI, resulted in large gains in power estimates compared to participants with Aβ pathology alone; (2) further gains in power were obtained by including measures with functional items in the composite; (3) composites formed by applying equal weights to all 12 measures provided the highest estimates of cross-validated power, although similar to continuous weight optimization and best subset optimization; (4) as the number of components in the composite increased, the magnitude of change decreased, but both the within-subject and between-subject variance decreased, leading to an increase in effect size; (5) in cCN and pcCN participants, the composite measures selected via optimization were both delayed memory recall assessments, CDR-SB, MMSE, Category Fluency, and immediate memory recall; in Aβ+ participants, ADAS13, MMSE, and FAQ were

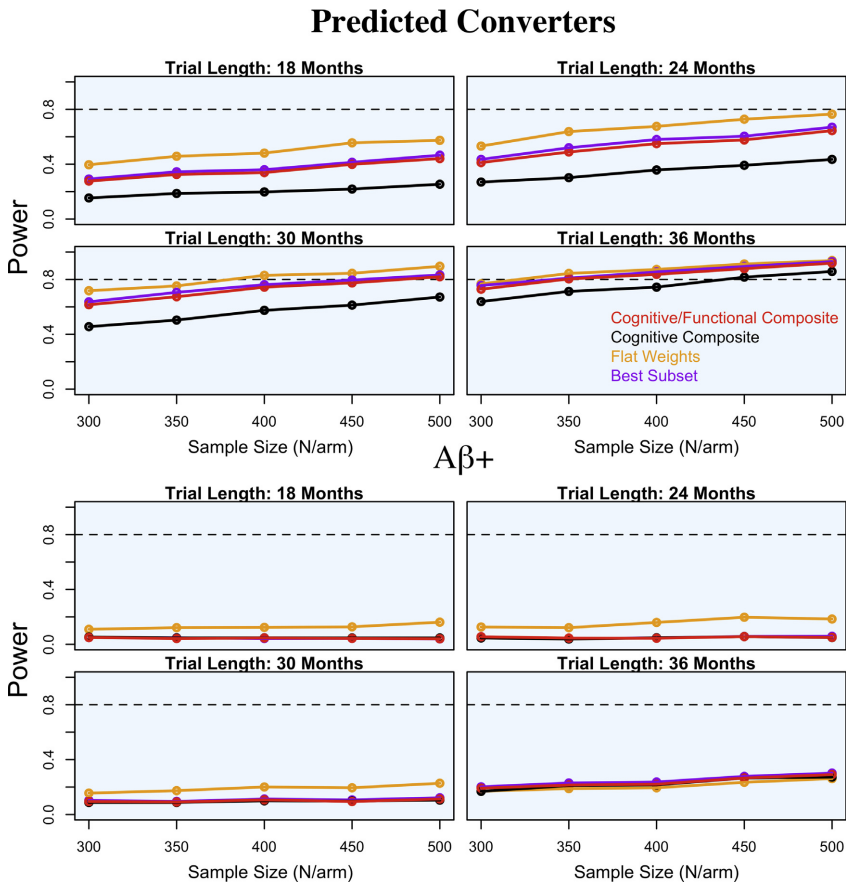
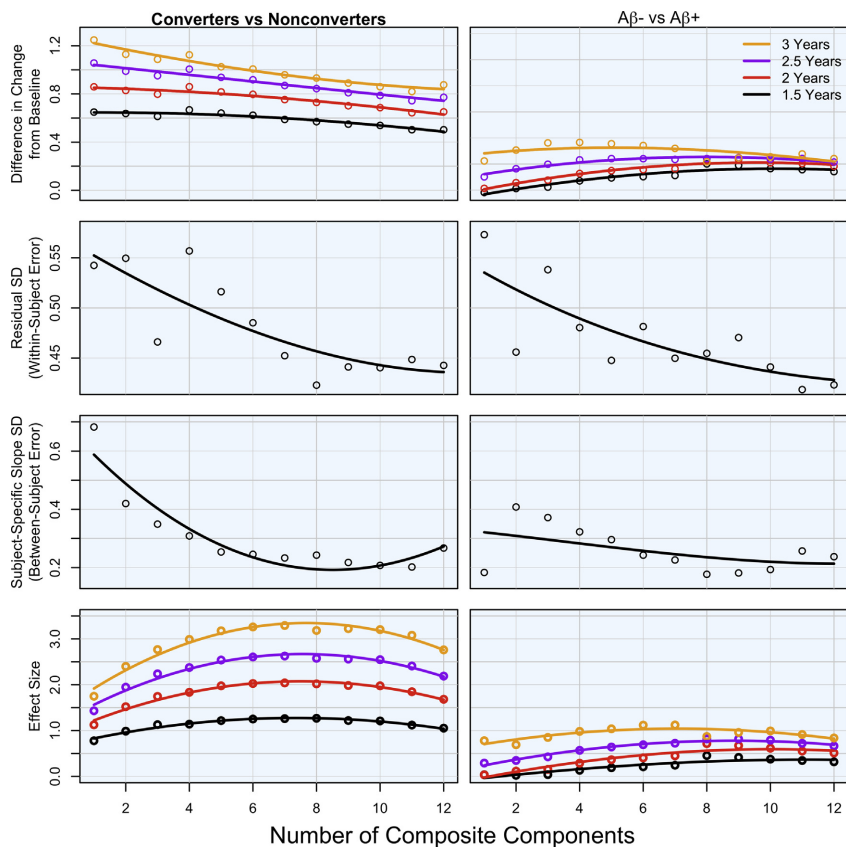


Fig. 2. Plots of power estimates at different sample sizes of completers per arm. The top 2 rows show power estimates for the predicted converters for trials ranging from 18 to 36 months with 300–500 subjects per arm for the 4 types of endpoints. The bottom 2 rows show power estimates for Aβ+ subjects over the same length trials and sample sizes for the 4 types of composites. Abbreviation: Aβ+, β-amyloid-positive.



**Fig. 3.** Differences in the magnitude of change between groups are plotted against the number of components included in the composite, in the top row. The best single component is furthest left on the x-axis, followed by best 2-component combination, all with equal weights. The second and third rows show how the within- and between-subject variance changes as the number of components increases for each analysis group. The bottom rows show how the effect size changes with increasing number of components. Abbreviations: A $\beta$ +,  $\beta$ -amyloid-positive; A $\beta$ -,  $\beta$ -amyloid-negative; SD, standard deviation.

selected, however, these composites did not outperform the equal weight composites when cross-validated in either group; and (6) only 55.4% of cCN subjects were A $\beta$ +, which explains part of the difference between our analysis of cCN and A $\beta$  subjects, and points to the importance of non-A $\beta$ -mediated processes to explain development of cognitive and functional decline.

#### 4.1. Power increase with predicted converters

Substantial increases in power estimates result when including pcCN subjects compared to A $\beta$  subjects, in all clinical trial simulations (Fig. 2). This might be expected when considering Fig. 1 and Table 2, where decline is limited both in magnitude and number of outcomes in the A $\beta$  subjects compared to cCN subjects, especially over the first 36 months. In contrast, the cCN subjects have already diverged from sCN subjects on several measures at baseline and continue to separate on delayed memory recall, global cognitive, and functional outcomes. Lower cognitive scores and continued decline in both the pcCN and cCN groups indicate that these

participants are likely already in a later stage of disease at baseline compared with A $\beta$  participants. The lower power estimates using ADNI A $\beta$  subjects are consistent with estimates reported in the analysis of 2 A $\beta$  cohorts for the A4 composite (Donohue et al., 2014). Substantially shallower decline was observed in the cognitively-normal ADNI A $\beta$  subjects compared to the cognitively-normal A $\beta$  subjects from the Australian Imaging, Biomarkers & Lifestyle Flagship Study of Ageing (AIBL, Ellis et al., 2009; Donohue et al., 2014). The sharper decline seen in the A $\beta$  subjects in the AIBL cohort may be due to subtle cognitive dysfunction at baseline including a 0.4 point lower average MMSE score, 0.5 point lower delayed memory delayed recall score, as well as a 20% increase in APOE  $\epsilon$ 4 allele carriers, compared with the ADNI A $\beta$  subjects. These subtle differences in baseline cognition and the increased proportion of APOE  $\epsilon$ 4 carriers may account for the differences in power estimates, which are closer to the estimates of the pcCN cohort observed in this analysis. Taken together, these results point to the importance of assessing other baseline characteristics besides A $\beta$  status when selecting preclinical populations

for trial enrichment. This should come as no surprise given the vast literature on the variability of the clinical impact of A $\beta$  pathology in elderly people, where a similar degree of A $\beta$  pathology may be seen in people who are cognitively normal, slightly impaired or fully demented. This variability likely stems from individual differences in cognitive and brain reserve mechanisms, differences in the presence and spread of important copathologies (including tau pathology), and differences in the time that the individual has been exposed to A $\beta$  pathology before testing. Additional sources of variation regarding the effect of A $\beta$  pathology on cognition in cognitively-normal cohorts include biomarker modality (PET vs. CSF) and also choice of threshold for A $\beta$ -positivity (Insel et al., 2014; Mattsson et al., 2014, 2015). The impact of this on the power of clinical trials, as found in our results, is in agreement with a previously proposed staging of preclinical AD (Spertling et al., 2011b), where subjects with a combination of positive AD biomarkers (including A $\beta$  biomarkers) and subtle cognitive dysfunction are thought to be at much higher risk for future clinical deterioration compared to subjects with positive A $\beta$  biomarkers alone (Vos et al., 2013).

#### 4.2. Additional power increase with functional components

Including the CDR-SB and FAQ in either the optimized composite or the equal weight composite resulted in an additional increase in power over the cognitive composite in the pcCN subjects, reaching 80% power with 375 completers per arm for a 30-month trial (Fig. 2). Including measures with functional items provided moderate improvements in power for the composites in A $\beta$ + subjects for trials less than 36 months, although power remained low. To convert from normal cognition to MCI, a subject must demonstrate a clinically meaningful level of functional decline. Steep decline is observed on both the CDR-SB (Fig. 1) and on the FAQ immediately after baseline in cCN subjects. Thus, it follows that including measures with functional assessments in a composite results in a more sensitive instrument, in a population of converters. However, because conversion status is not known at baseline, the inclusion of functional assessments in a prospective study will only improve sensitivity if information available at baseline can successfully identify subjects who are on the verge of functional decline. When functional measures are excluded, the weights for both the ADAS13 and the MMSE increase. This may reflect that poor scores on a global cognitive test are likely more correlated with functional decline compared to single domain measures. A $\beta$ + subjects do not show substantial decline on either CDR-SB or FAQ before month 48.

#### 4.3. Functional and cognitive outcome selection

Delayed memory recall, the MMSE, and the CDR-SB were selected via optimization for both the cCN and the pcCN composites. However, even the top-weighted measures had relatively low median weights, with 10 of the 12 measures having positive weights for cCN subjects, and 6 of 12 having positive weights for pcCN subjects (Supplementary Fig. 5). The spread of the weights suggests that many domains are declining early in the conversion process. Thus, it follows that the equal weight composites performed well. The failure of the optimization to beat the equal weight composites suggests that using either continuous weights or best subset component selection results in overfitting the training sets and a subsequent reduction of test set power. Including a large number of components in a composite may smooth over aberrations in scores in a particular assessment from visit to visit within a subject, thus lowering the within-subject variance and improving signal to noise. Similarly, the equal weight composite provided the most power in A $\beta$ + participants,

although power did not approach levels suitable for a phase III trial (Fig. 2).

#### 4.4. Equal weight composite: effect size, magnitude of change, and variance

Reasons for slight increases in power with the equal weight composite become clear from inspection of Fig. 3. As the number of components included in the composite increases, the magnitude of change decreases. This would result in a decrease in effect size (if the variance is held constant) and subsequently, a decrease in power. If we start with the best single component and continue by adding additional components, the magnitude of change may become diluted as less-sensitive components are included in the composite. We might expect the effect size to drop with each additional component; however, both the within-subject and between-subject errors are decreasing at a rate that overcomes the decrease in the magnitude of change, resulting in an increasing effect size, as seen at the bottom of Fig. 3. The increase in effect size plateaus in the 6–10 component range for both the converter and A $\beta$ + groups. The decrease in within-subject variance is clear in both groups; however, the drop in between-subject variance is steeper for converters, likely due to more consistent decline across all components. Or alternatively, the converters' scores are more variable, with more room for a reduction in within-subject variance when the number of composite components increases.

#### 4.5. Outcome selection in other studies

The outcomes selected via optimization are consistent with the measures found to capture decline in other cohorts. The API composite in Presenilin 1 E280A mutation carriers includes the Word List Recall (CERAD), MMSE (orientation to time), and also Constructional Praxis and Raven's Progressive Matrices (Ayutyanont et al., 2014). The API composite developed from normal to MCI or AD converters includes Category Fluency, Logical Memory II (dMemory), MMSE (orientation to time), and also Ravens Progressive Matrices Subset, and Symbol Digit Modalities (Langbaum et al., 2014). The A4 composite for A $\beta$ -positivity includes the Total Recall score from the Free and Cued Selective Reminding Test, Logical Memory II (dMemory), MMSE, and the Digit Symbol Substitution Test (Donohue et al., 2014). Delayed memory recall, orientation, and processing speed are consistently selected domains.

A variety of approaches can be used to develop composites that are sensitive to change over time (Ard et al., 2015). The development of composite measures may require the comparison of a large number of combinations of items, especially if weights are considered, leading to an increased risk of overfitting and an inflated estimate of the sensitivity and statistical power of the constructed composite. A validation procedure in a sample outside that used to identify the items and weights will be critical to accurately assess the composite's performance (Hendrix, 2012). As seen in our analysis, both types of optimization resulted in reduced power compared with the equal weight composites, likely due at least in part by overfitting the training sets. Importantly, the composites developed in this study and for the A4 study were evaluated out of sample. Neither study was able to reliably improve on equal weights.

#### 4.6. Limitations

This study has several limitations. We evaluated assessments available in the ADNI neuropsychological battery, although it is possible or likely that there are other measures more sensitive to

decline in preclinical AD. We also did not consider item-level data from already formed composites, such as the orientation to time component of the MMSE (Langbaum et al., 2014), which may have affected the results due to carrying insensitive items along with more sensitive ones. We also make the assumption that a treatment will slow the progression of components selected for their fast decline. In reality, it is unknown which cognitive or functional components a treatment may affect and it is possible that an endpoint comprising slower progressing domains will yield more power. Additionally, we used restricted cubic splines to model the observed data and subsequently simulated clinical trials assuming an MMRM model. Maximizing the group trajectory differences assuming a spline model averages change over all time points to estimate the group curves, whereas the MMRM model allows change at each time point to be estimated more independently. Assuming an MMRM model for both steps of the analysis and allowing the weights to be differentially optimized according to trial length may yield different results. The ADNI cohort, with high levels of education possibly contributing to increased cognitive reserve, and also limited cognitive decline observed in the A $\beta$ + subjects compared with other cohorts, is potentially different from a population recruited for a clinical trial. The pCN cohort is also considerably smaller with only 32 participants, reducing the stability of the estimates compared with the other cohorts. We used some of the same measures to predict conversion at screening and also track decline in the reference (equal weight) composite. It's possible that a regression to the mean effect could result in a reduction of power. However, the equal weight composite remained the most reliably performing composite with considerable power.

## 5. Conclusion

Our results suggest preclinical AD subjects with lower cognitive scores at baseline decline more reliably across both cognitive and functional measures compared to A $\beta$ + subjects without signs of subtle cognitive dysfunction. This provides a challenge to designers of preclinical AD trials to identify the level of cognitive dysfunction to be required at screening that will result in further decline, allowing a treatment effect to be demonstrated. Later stage preclinical AD may represent a more feasible target population for clinical trials designed to slow cognitive decline. In this population, suitable power for a phase III trial can be achieved with considerably lower sample sizes while capturing both cognitive and functional change to demonstrate a clinically meaningful drug effect—both while initiating treatment in subjects who are still cognitively normal. Multiple measures of delayed memory recall, orientation, processing speed, as well as multiple functional measures should be considered when forming a composite. Finally, when selecting measures, erring on the side of too many components may be preferable to too few.

## Disclosure statement

Mr. Insel, Dr. Mattsson, Dr. Hansson, and Dr. Mackin report no disclosures. Dr. Donohue was a consultant for Bristol-Myers Squibb. Dr. Aisen serves on a scientific advisory board for NeuroPhage; has served as a consultant to Elan, Wyeth, Eisai, Schering-Plough, Bristol-Myers Squibb, Eli Lilly and Company, NeuroPhage, Merck, Roche, Amgen, Genentech, Abbott, Pfizer, Novartis, Bayer, Astellas, Dainippon, Biomarin, Solvay, Otsuka, Daiichi, AstraZeneca, Janssen, Medivation, Ichor, Toyama, Lundbeck, Biogen Idec, iPerian, Probiobio, Somaxon, Biotie, Cardeus, Anavex, Kyowa Hakko Kirin Pharma, and Medtronic; and receives research support from Eli Lilly and Baxter and the NIH (NIA U01-AG10483 [PI], NIA U01-AG024904

[Coordinating Center Director], NIA R01-AG030048 [PI], and R01-AG16381 [Co-I]). Dr. Weiner has been on scientific advisory boards for Pfizer and BOLT International; has been consultant for Pfizer Inc, Janssen, KJ Associates, Easton Associates, Harvard University, inThought, INC Research, Inc, University of California, Los Angeles, Alzheimer's Drug Discovery Foundation, and Sanofi-Aventis Groupe; has received funding for travel from Pfizer, ADPD meeting, Paul Sabatier University, Novartis, Tohoku University, MCI Group, France, Travel eDreams, Inc, Neuroscience School of Advanced Studies (NSAS), Danone Trading, BV, CTAD ANT Congres; serves as an associated editor of Alzheimer's & Dementia; has received honoraria from Pfizer, Tohoku University, and Danone Trading BV; has research support from Merck, Avid, DOD, and VA; and has stock options in Synarc and Elan.

## Acknowledgements

Data collection and sharing for this project was funded by the Alzheimer's Disease Neuroimaging Initiative (ADNI) (National Institutes of Health grant U01 AG024904). ADNI is funded by the National Institute on Aging, the National Institute of Biomedical Imaging and Bioengineering (P30 AG010129 and K01 AG030514), and through generous contributions from the following: Alzheimer's Association; Alzheimer's Drug Discovery Foundation; BioClinica, Inc; Biogen Idec Inc; Bristol-Myers Squibb Company; Eisai Inc; Elan Pharmaceuticals, Inc; Eli Lilly and Company; F. Hoffmann-La Roche Ltd and its affiliated company Genentech, Inc; GE Healthcare; Innogenetics, N.V.; IXICO Ltd; Janssen Alzheimer Immunotherapy Research & Development, LLC; Johnson & Johnson Pharmaceutical Research & Development LLC; Medpace, Inc.; Merck & Co, Inc; Meso Scale Diagnostics, LLC; NeuroRx Research; Novartis Pharmaceuticals Corporation; Pfizer Inc; Piramal Imaging; Servier; Synarc Inc; and Takeda Pharmaceutical Company. The Canadian Institutes of Health Research is providing funds to support ADNI clinical sites in Canada. Private sector contributions are facilitated by the Foundation for the National Institutes of Health ([www.fnih.org](http://www.fnih.org)). This research was also supported by The Strategic Research Area MultiPark at Lund University. The grantee organization is the Northern California Institute for Research and Education, and the study is coordinated by the Alzheimer's Disease Cooperative Study at the University of California, San Diego. ADNI data are disseminated by the Laboratory for Neuro Imaging at the University of Southern California. This research was also supported by National Institutes of Health (NIH) grants P30 AG010129 and K01 AG030514. Data used in preparation of this article were obtained from the Alzheimer's Disease Neuroimaging Initiative (ADNI) database ([adni.loni.usc.edu](http://adni.loni.usc.edu)). As such, the investigators within the ADNI contributed to the design and implementation of ADNI and/or provided data but did not participate in analysis or writing of this report. A complete listing of ADNI investigators can be found at: [http://adni.loni.usc.edu/wp-content/uploads/how\\_to\\_apply/ADNI\\_Acknowledgement\\_List.pdf](http://adni.loni.usc.edu/wp-content/uploads/how_to_apply/ADNI_Acknowledgement_List.pdf).

## Appendix A. Supplementary data

Supplementary data related to this article can be found at <http://dx.doi.org/10.1016/j.neurobiolaging.2016.08.017>.

## References

- Ard, M.C., Raghavan, N., Edland, S.D., 2015. Optimal composite scores for longitudinal clinical trials under the linear mixed effects model. *Pharm. Stat.* 14, 418–426.
- Ayutyanont, N., Langbaum, J.B., Hendrix, S.B., Chen, K., Fleisher, A.S., Friesenahn, M., 2014. The Alzheimer's prevention initiative composite cognitive test score: sample size estimates for the evaluation of preclinical

- Alzheimer's disease treatments in presenilin 1 E280A mutation carriers. *J. Clin. Psychiatry* 75, 652–660.
- Breiman, L., 1996. Bagging predictors. *Machine Learn.* 24, 123–140.
- Breiman, L., 2001. Random forests. *Machine Learn.* 45, 5–32.
- Byrd, R.H., Lu, P., Nocedal, J., Zhu, C., 1995. A limited memory algorithm for bound constrained optimization. *SIAM J. Scientific Comput.* 16, 1190–1208.
- Chambers, J.M., Hastie, T.J., 1992. *Statistical Models in S*. Wadsworth & Brooks/Cole.
- Donohue, M.C., Sperling, R.A., Salmon, D.P., Rentz, D.M., Raman, R., Thomas, R.G., Weiner, M., Aisen, P.S., 2014. The preclinical Alzheimer cognitive composite: measuring amyloid-related decline. *JAMA Neurol.* 71, 961–970.
- Ellis, K.A., Bush, A.I., Darby, D., De Fazio, D., Foster, J., Hudson, P., Lautenschlager, N.T., Lenzo, N., Martins, R.N., Maruff, P., Masters, C., 2009. The Australian Imaging, Biomarkers and Lifestyle (AIBL) study of aging: methodology and baseline characteristics of 1112 individuals recruited for a longitudinal study of Alzheimer's disease. *Int. Psychogeriatrics* 21, 672–687.
- Hendrix, S.B., 2012. Measuring clinical progression in MCI and pre-MCI populations: enrichment and optimizing clinical outcomes over time. *Alzheimers Res. Ther.* 4, 24.
- Hochberg, Y., 1988. A sharper Bonferroni procedure for multiple tests of significance. *Biometrika* 75, 800–802.
- Insel, P., Mattsson, N., Donohue, M.C., Mackin, S., Aisen, P., Jack, C., Shaw, L.M., Trojanowski, J.Q., Weiner, M.W., 2014. The transitional association between beta-amyloid pathology and regional brain atrophy. *Alzheimers Dement.* 10, P837–P838.
- Insel, P.S., Mattsson, N., Mackin, R.S., Kornak, J., Nosheny, R., Tosun-Turgut, D., Donohue, M.C., Aisen, P.S., Weiner, M.W., 2015. Biomarkers and cognitive endpoints to optimize trials in Alzheimer's disease. *Ann. Clin. Transl. Neurol.* 2, 534–547.
- Kaplan, E.F., Goodglass, H., Weintraub, S., 1982. *The Boston Naming Test*, second ed. Lea & Febiger, Philadelphia.
- Kozauer, N., Katz, R., 2013. Regulatory innovation and drug development for early-stage Alzheimer's disease. *N. Engl. J. Med.* 368, 1169–1171.
- Landau, S.M., Mintun, M.A., Joshi, A.D., Koeppe, R.A., Petersen, R.C., Aisen, P.S., Weiner, M.W., Jagust, W.J., 2012. Amyloid deposition, hypometabolism, and longitudinal cognitive decline. *Ann. Neurol.* 72, 578–586.
- Langbaum, J.B., Hendrix, S.B., Ayutyanont, N., Chen, K., Fleisher, A.S., Shah, R.C., Barnes, L.L., Bennett, D.A., Tariot, P.N., Reiman, E.M., 2014. An empirically derived composite cognitive test score with improved power to track and evaluate treatments for preclinical Alzheimer's disease. *Alzheimers Dement.* 10, 666–674.
- Mattsson, N., Insel, P.S., Donohue, M., Landau, S., Jagust, W.J., Shaw, L.M., Trojanowski, J.Q., Zetterberg, H., Blennow, K., Weiner, M.W., 2015. Independent information from cerebrospinal fluid amyloid- $\beta$  and florbetapir imaging in Alzheimer's disease. *Brain* 138, 772–783.
- Mattsson, N., Insel, P.S., Nosheny, R., Tosun, D., Trojanowski, J.Q., Shaw, L.M., Jack, C.R., Donohue, M.C., Weiner, M.W., 2014. Emerging  $\beta$ -amyloid pathology and accelerated cortical atrophy. *JAMA Neurol.* 71, 725–734.
- McKhann, G.M., Knopman, D.S., Chertkow, H., Hyman, B.T., Jack, C.R., Kawas, C.H., Klunk, W.E., Koroshetz, W.J., Manly, J.J., Mayeux, R., Mohs, R.C., 2011. The diagnosis of dementia due to Alzheimer's disease: recommendations from the National Institute on Aging-Alzheimer's Association workgroups on diagnostic guidelines for Alzheimer's disease. *Alzheimers Dement.* 7, 263–269.
- Morris, J.C., 1993. The clinical dementia rating (CDR): current version and scoring rules. *Neurology* 43, 2412–2414.
- Morris, J.C., 2005. Early-stage and preclinical Alzheimer disease. *Alzheimer Dis. Assoc. Disord.* 19, 163–165.
- Olsson, A., Vanderstichele, H., Andreassen, N., De Meyer, G., Wallin, A., Holmberg, B., Rosengren, L., VanMechele, E., Blennow, K., 2005. Simultaneous measurement of beta-amyloid(1–42), total tau, and phosphorylated tau (Thr181) in cerebrospinal fluid by the xMAP technology. *Clin. Chem.* 51, 336–345.
- Pfeffer, R.I., Kurosaki, T.T., Harrah Jr., C.H., Chance, J.M., Filos, S., 1982. Measurement of functional activities in older adults in the community. *J. Gerontol.* 37, 323–329.
- Raghavan, N., Samtani, M.N., Farnum, M., Yang, E., Novak, G., Grundman, M., Narayan, V., DiBernardo, A., 2013. The ADAS-Cog revisited: novel composite scales based on ADAS-Cog to improve efficiency in MCI and early AD trials. *Alzheimers Dement.* 9, S21–S31.
- Reitan, R.M., 1958. Validity of the trail making test as an indicator of organic brain damage. *Perceptual Mot. Skills* 8, 271–276.
- Rey, A., 1964. *L'examen clinique en psychologie*. Presses Universitaires De France, Paris.
- Rosen, W.G., Mohs, R.C., Davis, K.L., 1984. A new rating scale for Alzheimer's disease. *Am. J. Psychiatry* 141, 1356–1364.
- Shaw, L.M., Vanderstichele, H., Knopik-Czajka, M., Clark, C.M., Aisen, P.S., Petersen, R.C., Blennow, K., Soares, H., Simon, A., Lewczuk, P., Dean, R., 2009. Cerebrospinal fluid biomarker signature in Alzheimer's Disease Neuroimaging Initiative subjects. *Ann. Neurol.* 65, 403–413.
- Siddiqui, O., Hung, H.J., O'Neill, R., 2009. MMRM vs. LOCF: a comprehensive comparison based on simulation study and 25 NDA datasets. *J. Biopharm. Stat.* 19, 227–246.
- Snyder, P.J., Kahle-Wroblewski, K., Brannan, S., Miller, D.S., Schindler, R.J., DeSanti, S., Ryan, J.M., Morrison, G., Grundman, M., Chandler, J., Caselli, R.J., 2014. Assessing cognition and function in Alzheimer's disease clinical trials: do we have the right tools? *Alzheimers Dement.* 10, 853–860.
- Sperling, R.A., Aisen, P.S., Beckett, L.A., Bennett, D.A., Craft, S., Fagan, A.M., Iwatsubo, T., Jack, C.R., Kaye, J., Montine, T.J., Park, D.C., 2011a. Toward defining the preclinical stages of Alzheimer's disease: recommendations from the national institute on aging-Alzheimer's association workgroups on diagnostic guidelines for Alzheimer's disease. *Alzheimers Dement.* 7, 280–292.
- Sperling, R.A., Jack Jr., C.R., Aisen, P.S., 2011b. Testing the right target and right drug at the right stage. *Sci. Transl. Med.* 3, 111cm33.
- Sperling, R.A., Rentz, D.M., Johnson, K.A., Karlawish, J., Donohue, M., Salmon, D.P., Aisen, P., 2014. The A4 study: stopping AD before symptoms begin? *Sci. Transl. Med.* 6, 228fs13.
- US Dept of Health and Human Services; US Food and Drug Administration; Center for Drug Evaluation and Research. *Guidance for industry: Alzheimer's disease: developing drugs for the treatment of early stage disease (draft guidance)*. Available at: <http://www.fda.gov/downloads/Drugs/GuidanceComplianceRegulatoryInformation/Guidances/UCM338287.pdf>. Accessed August 8, 2015.
- Vos, S.J., Xiong, C., Visser, P.J., Jasielec, M.S., Hassenstab, J., Grant, E.A., Cairns, N.J., Morris, J.C., Holtzman, D.M., Fagan, A.M., 2013. Preclinical Alzheimer's disease and its outcome: a longitudinal cohort study. *Lancet Neurol.* 12, 957–965.
- Wang, J., Logovinsky, V., Hendrix, S.B., Stanworth, S.H., Perdomo, C., Xu, L., Dhadda, S., Do, I., Rabe, M., Luthman, J., Cummings, J., 2016. ADCOMS: a composite clinical outcome for prodromal Alzheimer's disease trials. *J. Neurol. Neurosurg. Psychiatry* 87, 993–999.
- Wechsler, D.A., 1987. *Wechsler Adult Intelligence Scale—Revised*. Psychological Corporation, New York.

Paper II







## Time between milestone events in the Alzheimer's disease amyloid cascade

Philip S. Insel<sup>a,b,\*</sup>, Michael C. Donohue<sup>c</sup>, David Berron<sup>a</sup>, Oskar Hansson<sup>a,d</sup>,  
Niklas Mattsson-Carlgren<sup>a,e,f,\*</sup>

<sup>a</sup> Clinical Memory Research Unit, Department of Clinical Sciences Malmö, Lund University, Sweden

<sup>b</sup> Department of Psychiatry and Behavioral Sciences, University of California, San Francisco, CA, United States

<sup>c</sup> Alzheimer's Therapeutic Research Institute, Keck School of Medicine, University of Southern California, San Diego, CA, United States

<sup>d</sup> Memory Clinic, Skåne University Hospital, Malmö, Sweden

<sup>e</sup> Department of Neurology, Skåne University Hospital, Lund, Sweden

<sup>f</sup> Wallenberg Center for Molecular Medicine, Lund University, Lund, Sweden

### ARTICLE INFO

**Keywords:**  
Alzheimer's disease  
 $\beta$ -amyloid  
Tau PET  
Cognition

### ABSTRACT

**Objective:** Estimate the time-course of the spread of key pathological markers and the onset of cognitive dysfunction in Alzheimer's disease.

**Methods:** In a cohort of 335 older adults, ranging in cognitive functioning, we estimated the time of initial changes of  $A\beta$ , tau, and decreases in cognition with respect to the time of  $A\beta$ -positivity.

**Results:** Small effect sizes of change in CSF  $A\beta$ 42 and regional  $A\beta$  PET were estimated to occur several decades before  $A\beta$ -positivity. Increases in CSF tau occurred 7–8 years before  $A\beta$ -positivity. Temporoparietal tau PET showed increases 4–5 years before  $A\beta$ -positivity. Subtle cognitive dysfunction was observed 4–6 years before  $A\beta$ -positivity.

**Conclusions:** Increases in tau and cognitive dysfunction occur years before commonly used thresholds for  $A\beta$ -positivity. Explicit estimates of the time for these events provide a clearer picture of the time-course of the amyloid cascade and identify potential windows for specific treatments.

### Introduction

Disconcerting clinical trial results for the treatment of Alzheimer's disease (AD) have led to a shift toward earlier intervention, focusing on the early clinical or presymptomatic phases, when biomarkers are needed to identify the disease. The amyloid cascade (Hardy and Selkoe, 2002) is thought to start with elevated levels of two key amyloids in the brain,  $\beta$ -amyloid ( $A\beta$ ) and tau, and end with severe cognitive and functional impairment (Jack et al., 2010). Growing evidence suggests that an early sign that the cascade has begun is change in cerebrospinal fluid (CSF)  $A\beta$ , potentially detectable prior to significant  $A\beta$  deposition in the brain as measured by positron emission tomography (PET) (Palmqvist et al., 2016). This accumulation of  $A\beta$  has been suggested to be followed by increases in CSF tau and the spread of tau pathology beyond the temporal lobe (Braak and Braak, 1991; Schöll et al., 2016). The build-up and spread of these two brain pathologies is paralleled by gradual cognitive and functional decline (Zetterberg and Mattsson, 2014).

Previous neuropathological and biomarker data suggest that the overall time-course of AD is several decades (Li et al., 2017; Villemagne et al., 2013). In autosomal dominant AD, the estimated

years to clinical onset has been used to estimate the time-course of different biomarkers in AD (Bateman et al., 2012). However, the time-course of the spread of  $A\beta$  and tau and the onset of clinical symptoms in sporadic AD is unknown. With repeated measures of  $A\beta$  over time, the level and rate of change with respect to the key initiating AD pathology may offer a measure of disease progression in sporadic AD. The duration of amyloid positivity (chronicity) has been shown to be associated with increased tau pathology and faster cognitive decline and valuable in explaining heterogeneity in early disease progression (Koscik et al., 2020). With level and change information, the time from the threshold for significant  $A\beta$  pathology can be estimated within individuals, providing the temporal disease progression information important for evaluating biomarker trajectories. Without longitudinal information, cross-sectional studies frequently categorize subjects into two groups – those below a threshold for significant pathology and those above, where subjects just below the threshold who will cross over within months are considered pathologically equivalent to subjects who will not cross over for decades. By incorporating longitudinal information, disease progression with respect to  $A\beta$  pathology can be represented to reflect its continuous nature, resulting in a more

\* Corresponding authors at: Clinical Memory Research Unit, Department of Clinical Sciences Malmö, Lund University, Sweden.  
E-mail addresses: [philip.insel@med.lu.se](mailto:philip.insel@med.lu.se) (P.S. Insel), [niklas.mattsson-carlgren@med.lu.se](mailto:niklas.mattsson-carlgren@med.lu.se) (N. Mattsson-Carlgren).

<https://doi.org/10.1016/j.neuroimage.2020.117676>

Received 28 July 2020; Received in revised form 29 October 2020; Accepted 15 December 2020

Available online 24 December 2020

1053-8119/© 2020 The Authors. Published by Elsevier Inc. This is an open access article under the CC BY license (<http://creativecommons.org/licenses/by/4.0/>)



powerful way to model the relationship between  $A\beta$  and downstream processes.

The aims of this study were to demonstrate the utility and predictive ability of the time-from- $A\beta$ -positivity (TFA $\beta$ +) formulation and to evaluate the relationships between TFA $\beta$  and downstream biomarker and cognitive responses in order to estimate the time of the earliest signs of progression in sporadic AD. Using serial  $^{18}\text{F}$ -florbetapir ( $A\beta$ ) PET measurements, rates of change of  $A\beta$  were estimated and used to calculate the time-from-threshold for each subject. These subject-specific estimates of the proximity to the threshold for  $A\beta$ -positivity ( $A\beta$ +) were then used to model the trajectories and temporal ordering of other key markers in AD including CSF  $A\beta$ 42, regional  $A\beta$  PET, several measures of tau including CSF phosphorylated (P-tau) and total tau (T-tau), regional  $^{18}\text{F}$ -flortaucipir (AV-1451) tau PET, and cognition. Estimates of the time and ordering of these pathophysiological changes may facilitate the design of future prevention trials and identify a window for early treatment.

## Materials and methods

### Standard protocol approvals, registrations, and patient consents

This study was approved by the Institutional Review Boards of all of the participating institutions. Informed written consent was obtained from all participants at each site.

### Data availability

All data is publicly available (<http://adni.loni.usc.edu/>). R code is available on Github.

### Participants

Data were obtained from the Alzheimer's Disease Neuroimaging Initiative (ADNI) database (<http://adni.loni.usc.edu/>, [www.adni-info.org](http://www.adni-info.org)) on 1/21/2020. An initial analysis was done on ADNI participants with available  $A\beta$  PET data (in  $N = 962$   $A\beta$ -cognitively unimpaired (CU-),  $A\beta$ + cognitively unimpaired (CU+),  $A\beta$ + MCI and  $A\beta$ + AD), to facilitate the estimation of TFA $\beta$ +, though not all 962 were included in the analysis of the main outcomes. Participants were classified as cognitively unimpaired if they had an MMSE score of 24–30, CDR score of 0, no memory complaint, and a Logical Memory II subscale of the Wechsler Memory Scale-Revised score  $\geq 9$  for 16 years of education,  $\geq 5$  for 8–15 years of education, and  $\geq 3$  for 0–7 years of education. Participants were classified as MCI if they had an MMSE score of 24–30, a CDR score of 0.5 as well as a memory box score of 0.5, and a Logical Memory II score  $\leq 8$  for 16 years of education,  $\leq 4$  for 8–15 years of education, and  $\leq 2$  for 0–7 years of education. Subjects were classified as having AD dementia if they had a memory complaint, met the same criteria for Logical Memory as the MCI group, had a CDR score of 0.5 or 1, and met the National Institute of Neurological and Communicative Disorders and Stroke–Alzheimer's Disease and Related Disorders Association criteria for probable AD. The population in the primary analyses of PET and cognitive outcomes only included ADNI participants with available measurements of  $A\beta$  and tau PET and cognition. Of these, all cognitively unimpaired (CU- and CU+), prodromal AD ( $A\beta$ + MCI) and  $A\beta$ + AD dementia participants were included in the analysis, where  $A\beta$ -positivity was defined using a previously established threshold (Standardized Uptake Value Ratio, SUVR = 1.10) (Joshi et al., 2012).  $A\beta$ - MCI ( $N = 224$ , including  $A\beta$ - CU to MCI progressors) and  $A\beta$ - "AD dementia" subjects ( $N = 51$ , including  $A\beta$ - MCI to AD dementia progressors; we consider these to be misdiagnosed, because we assume AD requires  $A\beta$ +) were not included in the main analysis given our aim to model head to head comparisons of initial biomarker and cognitive changes of individuals on the AD continuum and not other diseases. In order to estimate the time of emerging cognitive decline associated with increasing  $A\beta$ , those

with cognitive impairment, but low levels of  $A\beta$  were excluded. MCI and AD participants were considered  $A\beta$ - if their SUVR remained below the threshold at all scans during follow-up. Visualizations of their biomarker data are included for comparison in Figs. 2–4 (see Figure legends). Additional description is included in the statistical analysis section.

### Cerebrospinal fluid biomarker concentrations

Cerebrospinal fluid (CSF) samples were collected at baseline by lumbar puncture in a subsample ( $N = 185$ ). CSF  $A\beta$ 42, total tau (T-tau) and phosphorylated tau (P-tau) were measured by an xMAP assay (IN-NOBIA AlzBio3, Ghent, Belgium, Fujirebio), as described previously (Olsson et al., 2005; Shaw et al., 2009).

### PET imaging

Methods to acquire and process  $A\beta$  ( $^{18}\text{F}$ -florbetapir) PET image data were described previously (Jagust et al., 2015; Landau et al., 2012). Briefly, florbetapir image data were acquired 50–70 min postinjection, and images were averaged, spatially aligned, interpolated to a standard voxel size, and smoothed to a common resolution of 8 mm full width at half maximum. We used an a priori defined threshold for  $A\beta$ -positivity (SUVR=1.1) (ADNI, 2012; Joshi et al., 2012) applied to the ratio of the average of the four target regions (temporal, cingulate, frontal, and parietal lobes) and the cerebellum, in the estimation of time-from- $A\beta$ -positivity, described in detail below. In a second part of the analysis, five  $A\beta$  PET ROI outcomes were considered (Landau and Jagust, 2015; Mormino et al., 2009), (1) the temporal lobe (middle and superior temporal lobe), (2) the parietal lobe (precuneus, supramarginal, inferior and superior parietal lobe), (3) the cingulate gyrus (isthmus, posterior, caudal and rostral anterior cingulate), (4) the frontal lobe (pars opercularis, pars triangularis, pars orbitalis, caudal/rostral middle frontal, medial/lateral orbitofrontal, frontal pole, and superior frontal lobe), and (5) a composite of regions thought to be early in accumulating  $A\beta$  (precuneus and posterior cingulate) (Palmqvist et al., 2017). These ROIs comprise the regions included in the global composite, grouped into individual lobes plus an additional early ROI.  $^{18}\text{F}$ -florbetapir ROIs were expressed as SUVRs with a cerebellar reference region.

Methods to acquire and process tau ( $^{18}\text{F}$ -flortaucipir) PET image data were described previously (Maass et al., 2017). Six tau ROI outcomes, corrected for partial-volume, were considered: (1) the medial temporal lobe (MTL) (amygdala, entorhinal and parahippocampal cortex; from Braak stage I and III), (2) the lateral temporal lobe (LTL) (inferior/middle/superior temporal lobe, banks of the superior temporal sulcus, transverse temporal lobe, temporal pole; from Braak stage IV and V), (3) the medial parietal lobe (MPL) (isthmus cingulate, precuneus; from Braak stage IV and V), (4) the lateral parietal lobe (LPL) (inferior/superior parietal lobe, supramarginal; from Braak stage V), (5) frontal lobe (pars, orbitofrontal and middle/superior frontal lobe; from Braak stage V), and (6) the occipital lobe (cuneus, lingual, pericalcarine, and lateral occipital lobe; from Braak stage III, V, and VI).  $^{18}\text{F}$ -flortaucipir ROIs were expressed as SUVRs with an inferior cerebellar gray matter reference region. Scanner type and site were evaluated for their association with PET outcomes through covariate adjustment. Full details of PET acquisition and analysis can be found at <http://adni.loni.usc.edu/methods/>.

### Cognition

Cognitive measures assessed included the Mini-Mental State Examination (MMSE) as a measure of global cognition, and the Preclinical Alzheimer's Cognitive Composite (PACC), as a measure of early AD-related cognitive changes. The PACC comprised the MMSE, the Logical Memory Delayed Word Recall from the Wechsler Memory Scale, the Alzheimer's Disease Assessment Scale—Cognitive Subscale Delayed Word Recall, and the Trail Making Test part B (reversed such

that high scores indicated better performance and log transformed) (Donohue et al., 2017, 2014). The PACC was constructed from available data in the sample. Components were z-transformed, summed and scaled to the baseline scores of the A $\beta$ - CU.

### Statistical analysis

The aims of these analyses were to (1) demonstrate the utility and predictive ability of the TFA $\beta$ + formulation of A $\beta$  information and (2) evaluate the relationship between TFA $\beta$ + and CSF, PET, and cognitive responses in order to estimate the time of the earliest signs of progression. The overall analysis consisted of two steps. Step one was estimating TFA $\beta$ + based on the longitudinal measures of global A $\beta$  PET SUVR. In step two, TFA $\beta$ + estimates were used to predict cross-sectional measures of regional tau and A $\beta$  PET, CSF and cognitive outcomes. To demonstrate the value of the TFA $\beta$ + measure, we did head-to-head comparisons of (i) TFA $\beta$ + vs (ii) intercepts and slopes of longitudinal A $\beta$  PET, modeled separately, to predict the outcomes. These comparisons are described in detail below.

Because TFA $\beta$ + was not directly observed, in step one, linear mixed-effects models were fit to all available longitudinal global A $\beta$  PET SUVR data to estimate subject-specific intercepts and slopes of A $\beta$  pathology.

For the  $i^{\text{th}}$  individual at the  $j^{\text{th}}$  measurement time,

$$y_{ij} = \beta_0 + \beta_1 t_{ij} + b_{0i} + b_{1i} t_{ij} + e_{ij}, j = 1, \dots, n_i,$$

where  $y_i$  is A $\beta$  SUVR,  $\beta_0$  and  $\beta_1$  are the fixed intercept and slope over time,  $t_{ij}$  is time (years from baseline),  $b_{0i}$  and  $b_{1i}$  are the random intercept and slope over time, and  $e_{ij}$  is a Gaussian-distributed error term.

Because A $\beta$  slopes are unlikely to remain constant over long periods of time as subjects move toward and away from the A $\beta$  threshold, natural splines (Hastie and Tibshirani, 1990) were used to estimate the nonlinear shape of the slopes with respect to baseline A $\beta$ , using quantile regression (Koenker and D'Orey, 1987). Rather than modeling the mean A $\beta$  slope with respect to baseline A $\beta$ , quantile regression provides a separate curve for each quantile, allowing the relationship between slope and intercept to differ depending on the location in the distribution of A $\beta$  slope.

For a random variable  $X_i$  with distribution function  $F$ , the  $r$ th quantile of  $X$  is defined as,  $Q_X(\tau) = F^{-1}_X(\tau)$ . Taking the sum of the random and fixed slope,  $S_i = \beta_1 + b_{1i}$ , gives subject-specific estimates of the slope over time of A $\beta$  SUVR. Similarly, taking the sum,  $I_i = \beta_0 + b_{0i}$ , gives subject-specific estimates of the intercept of A $\beta$  SUVR. Quantile curves were estimated by regressing  $S$  on  $I$  for  $\tau \in (0, 1)$ ,

$$Q_{S_i}(\tau) = \alpha_0(\tau) + \alpha_1(\tau)X_{i1} + \dots + \alpha_k(\tau)X_{ik} + e_i,$$

where  $x_{i1}, \dots, x_{ik}$  is the  $k$ -dimensional natural spline basis for  $I_i$ . The dimension  $k$ , was selected by AIC.

For each subject, TFA $\beta$ + was estimated by integrating over each subject's quantile curve from the subject's intercept to the threshold for A $\beta$ -positivity (PET SUVR = 1.1). For example, for a subject with a baseline SUVR of 1.2 and a slope in the 0.6 quantile, TFA $\beta$ + was taken to be the time it would take to go from SUVR = 1.1 to 1.2, using the slope estimates from the quantile curve. For incremental changes on the x-axis (baseline SUVR), the time required to travel the incremental distance is equal to distance/rate. Using the trapezoid rule (Atkinson, 1989), TFA $\beta$ + is the sum of these incremental times spanning SUVR = 1.1–1.2. An example of calculating TFA $\beta$ + is given in the top left panel of Fig. 1. Sensitivity analyses were done to determine the effect of varying the threshold for A $\beta$ +. We repeated the estimation of TFA $\beta$ + using an early threshold (SUVR 1.07) and a late threshold (SUVR 1.13).

To evaluate the accuracy of the TFA $\beta$ + estimates, we compared the observed times of A $\beta$ + to the estimated times of A $\beta$ + values in participants who were A $\beta$ - at baseline and became A $\beta$ + during follow-up. Observed time of A $\beta$ + occurred in the interval between the last A $\beta$ - scan and the first A $\beta$ + scan. The observed time was calculated as a weighted average of the two scan times, weighted proportionally toward the scan

where the participant was closest to hitting the threshold. Observed and estimated values were compared in  $N = 37$  participants who crossed the threshold for A $\beta$ + and remained A $\beta$ + throughout follow-up. We also compared observed and estimated values in 44 participants including the original 37 plus seven additional subjects who crossed the threshold but had a subsequent negative scan.

Our analyses aim to model participants who are ostensibly on the AD trajectory and had calculable TFA $\beta$ +, i.e., they must be A $\beta$  accumulators (positive rates of accumulation). Therefore, of the 982 participants with A $\beta$  PET, we excluded  $N = 20$  participants with negative A $\beta$  accumulation rates (negative rates were largely driven by one early high A $\beta$  PET measure), we also excluded  $N = 6$  participants with low levels of A $\beta$  and accumulation rates such that they were predicted to become A $\beta$ + later than 120 years of age (biomarker data from these subjects are included for visual comparisons in Figs. 3–5, see Figure legends). Fig. 1 shows the flow of participant inclusion. We included subjects where the TFA $\beta$ + metric indicated very early accumulation of A $\beta$ , but for participants estimated to have become A $\beta$ + before age 40 ( $N = 25$ , median estimated age at A $\beta$ + = 30, IQR: 27 to 34), we truncated TFA $\beta$ + to age 40, based on previously described rates of A $\beta$ -positivity in middle age (Jansen et al., 2015). These were mostly MCI and AD participants, APOE  $\epsilon 4$  carriers, in their mid 60 s to late 70 s.

In the second step, the relationship between TFA $\beta$ + and the responses was modeled using monotone penalized regression splines. The model takes the form,

$$y_i = f(\text{TFA}\beta+) + e_i = a_1(\text{TFA}\beta+)\beta_1 + \dots + a_q(\text{TFA}\beta+)\beta_q + e_i,$$

where  $y_i$  is the one of the PET, CSF, or cognitive responses, measured cross-sectionally, and  $f$  is a smooth monotone function, represented by  $a_1, \dots, a_q$  basis functions. Generalized cross-validation was used to control the basis dimension  $q$  and the degree of smoothing (Wood, 1994). Cognitive responses were covaried for age, gender and education; CSF A $\beta$ 42, T-tau, P-tau and PET measures were covaried for age and gender.

Because the variance of the outcomes increases with advancing pathology and several outcomes contained clusters of extreme values, resulting in large residuals, we repeated step two of the analyses using M-estimation to provide robust estimates with robust standard errors (Huber and Ronchetti, 1981). This model takes the same form as described above, but is fit using iteratively reweighted least squares in order to downweight large residuals.

In order to account for the variance across steps 1 and 2, the entire process was repeated in 500 bootstrap samples to estimate 95% confidence intervals for the association between TFA $\beta$ + and the responses.

To assess the predictive ability of TFA $\beta$ +, we compared (i) models using TFA $\beta$ + vs (ii) models using both the subject-specific intercepts and slopes of longitudinal A $\beta$ , to predict the responses. Two models for each response were compared. In model 1, responses were regressed on TFA $\beta$ + using penalized regression splines as described above, adjusting for covariates. In model 2, responses were regressed on both A $\beta$  intercepts and slopes using penalized regression splines, adjusting for covariates. Model 1 and 2 were compared using the Akaike Information Criterion (AIC) (Akaike, 1974).

Meaningful effect sizes of change of increase in pathology or decrease in cognition with respect to TFA $\beta$ + were estimated as part of step two of the analysis. A Cohen's  $d$  effect size of 0.2 SD was considered small, 0.5 SD was considered medium, and a 0.8 SD effect was considered large (Cohen, 1988). A 0.2 standard deviation (SD) change from the mean response at the longest times (least pathological) from A $\beta$ -positivity was taken to be the initial point of meaningful change. A 0.5 SD change was also shown as a more substantial effect size of change. For example, if the estimated mean PACC score at the lowest level of A $\beta$  was 0 and the estimated mean PACC score at the time of A $\beta$ -positivity was  $-0.5$  and the residual SD of the PACC was 1.5, then the effect size at the time of A $\beta$ -positivity =  $(-0.5 - 0)/1.5 = -0.33$ . A drop of 0.33 points on the PACC would be considered between a small (0.2) and medium (0.5) effect size, according to Cohen's guidelines for interpreting the magnitude of

Fig. 1. Participant inclusion/exclusion.

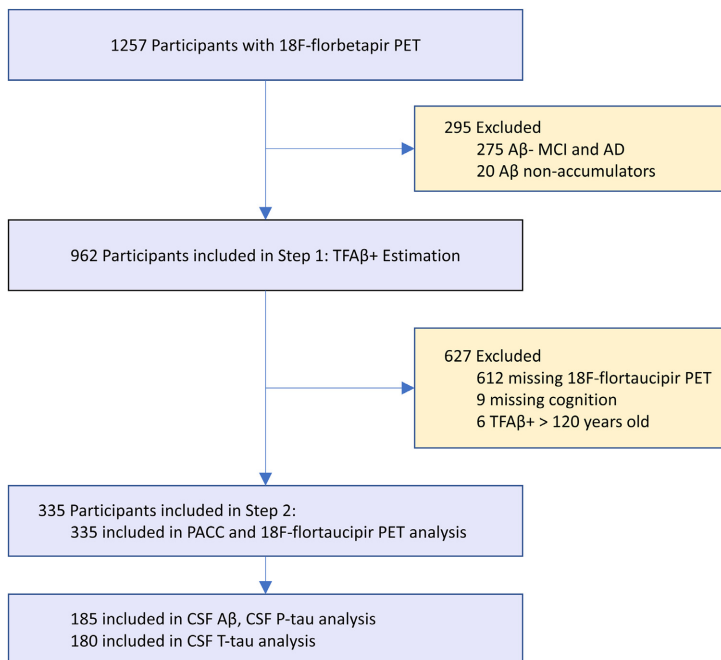


Table 1  
Cohort Characteristics.

	CU- (N = 127)	CU+ (N = 100)	MCI (N = 70)	AD (N = 38)	p
Age, mean (SD), y	70.1 (5.8)	72.9 (6.6)	72.0 (6.9)	74.5 (7.2)	<0.001
Sex, No. F (%)	76 (59.8)	58 (58.0)	29 (41.4)	18 (47.4)	0.06
Education, mean (SD), y	16.7 (2.4)	16.9 (2.3)	16.0 (2.7)	15.6 (2.5)	0.01
APOE ε4, No. carriers (%)	31 (25.6)	47 (50.5)	39 (60.9)	19 (54.3)	<0.001
TFAβ+, mean (SD), y	-8.9 (6.4)	13.8 (11.0)	20.9 (11.5)	25.5 (10.8)	<0.001

effect sizes. We also estimated change, 95% confidence intervals with bootstrap-estimated 2.5 and 97.5 quantiles, and statistical significance of change for each response at TFAβ+ = 0, the time of Aβ-positivity, with bootstrap-estimated standard errors.

Associations between missing data (CSF subsample vs full cohort) and demographics and TFAβ+ were evaluated using logistic regression with a binomial indicator for missing data. Baseline associations between demographics and TFAβ+ were assessed using Pearson correlation for age and years of education and a t-test for gender. Associations between diagnosis and demographics were assessed using F and t-tests for continuous variables and χ<sup>2</sup> tests for categorical variables. P-values were 2-sided and considered significant for p < 0.05. A drop of 2 or more in AIC was considered meaningful model improvement. All analyses were done in R v4.0.0 ([www.r-project.org](http://www.r-project.org)).

Results

Cohort characteristics

Two-hundred and twenty-seven CU (127 Aβ- and 100 Aβ+), 70 Aβ+ MCI and 38 Aβ+ AD participants were included in the analysis. The diagnostic groups varied by mean age, sex, years of education, and pro-

portion of APOE ε4+ (Table 1). The CU- group was significantly younger than all other diagnostic groups (p ≤ 0.04). The MCI group had a significantly smaller proportion of females than both the CU- group (p = 0.02) and the CU+ group (p = 0.05). The MCI group had significantly lower mean years of education compared to the CU- group (p = 0.04) and the CU+ group (p = 0.02). The AD group also had significantly lower mean years of education compared to the CU- group (p = 0.01) and the CU+ group (p = 0.005). The CU- group had a significantly smaller proportion of APOE ε4 carriers than all other diagnostic groups (p < 0.003).

Aβ PET and estimation of TFAβ+

TFAβ+ was estimated with a median of 3 (range: 1 to 5) Aβ PET scans per participant. The average time between first and last scan was 3.3 years (SD=2.9) and the average time between scans was 2.2 years (SD=0.8). PET data came from 17 types of scanners across 58 sites. Neither site nor scanner type were associated with any Aβ PET outcome (ΔAIC > 12) or tau PET outcomes (ΔAIC > 19) and were not included in subsequent models. The correlation between subject-specific random intercepts and slopes was 0.32 (0.06 to 0.55). Residuals from the mixed model of repeated global Aβ PET SUVrs appeared approximately normal and with constant variance over time.

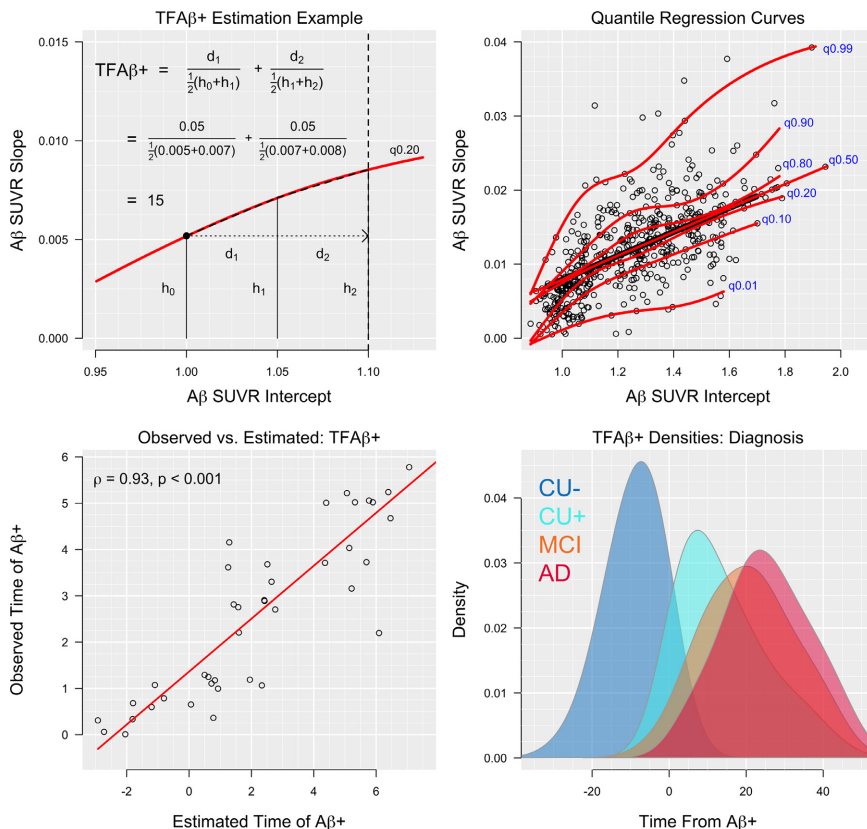


**Fig. 2.** Observed vs. estimated TFAβ+, quantile regression curves and TFAβ+ densities. Top left panel: an example of how TFAβ+ is estimated. Here we have a participant with an estimated intercept of SUVR = 1.00 and an accumulation rate (slope) of 0.005 SUVR/year. We want to calculate how long it will take for them to reach the 1.10 threshold. A slope of 0.005 SUVR/year puts this participant on the 0.20 quantile (20% percentile) curve. We know this participant must accumulate 0.10 SUVR to reach the threshold and we will assume they will continue to have an accumulation rate in the 0.20 quantile. Partitioning the curve into segments from SUVR = 1.00–1.10 and using the formula time = distance/rate, the time to cross each segment is calculated and summed. In the figure, only two segments are shown, but in the actual calculation, the curve is partitioned into a large number of segments. Assuming a linear rate increase within each segment (shown in the dashed black line along the red quantile curve), the time to travel the distance in the 1st segment, from SUVR 1.00 to 1.05 is given by, time<sub>1</sub> = d<sub>1</sub> /rate<sub>1</sub>, where d<sub>1</sub> is 0.05 and rate<sub>1</sub> is the average rate in segment 1, which is 1/2(h<sub>0</sub>+h<sub>1</sub>), as shown in the panel. A similar calculation is done for segment 2 and the results are summed to give TFAβ+ = 15. Top right panel: quantile regression curves of Aβ PET slopes plotted against intercepts in all 962 participants with Aβ PET data. Curves for several selected quantiles (0.01, 0.10, ..., 0.99) are shown in red. Bottom left panel: observed time of Aβ+ plotted against estimated time of Aβ+ in the 37 participants who became and remained Aβ+ during follow-up. Bottom right panel: distributions of TFAβ+ for each group, 127 Aβ- CU (CU-), 100 Aβ+ CU (CU+), 70 Aβ+ MCI, and 38 Aβ+ AD are shown.

Across diagnoses, TFAβ+ ranged from -29 to 46 years, where higher (positive) TFAβ+ values indicate more time spent with a significant Aβ burden. The CU- group had a significantly lower mean TFAβ+ compared to all other diagnostic groups (p<0.001). The CU+ group had a significantly lower mean TFAβ+ compared to the MCI group (p<0.001) and the AD group (p<0.001), and the MCI was significantly lower than the AD group (p = 0.02).

Higher TFAβ+ was significantly associated with older age (ρ=0.28, 95% CI: 0.17 to 0.37, p<0.001), lower education (ρ=-0.15, 95% CI: -0.25 to -0.04, p = 0.01) and APOE ε4-positivity (mean TFAβ+ in APOE ε4 = 3.3 (SD=16.1) years and mean TFAβ+ in APOE ε4+ = 13.6 (SD=15.8) years, p<0.001). TFAβ+ was not associated with sex (mean

TFAβ+ = 9.4 (SD=17.1) and 6.8 (SD=16.4) in males and females, respectively, p = 0.16). Within-diagnosis TFAβ+ distributions are shown on the bottom right panel of Fig. 2. Quantile curves of the relationship between Aβ intercepts and slopes are also shown in the top right panel of Fig. 2, displaying the variation of acceleration of Aβ deposition over different levels of baseline Aβ.

TFAβ+ estimates were not sensitive to alternative thresholds for Aβ+ beyond a shift reflecting an earlier or later threshold. When the earlier threshold (SUVR 1.07) was used rather than SUVR 1.10, TFAβ+ estimates were shifted a median of 3.2 years earlier, but remained almost perfectly correlated with TFAB+ using the SUVR 1.10 threshold (ρ=0.996). Similarly, when the late threshold was used (SUVR 1.13),

TFA $\beta$ + estimates shifter a median of 3.1 years later, but also remained almost perfectly correlated with TFAB+ using the SUVR 1.10 threshold ( $\rho=0.997$ ).

#### TFA $\beta$ + performance

TFA $\beta$ + was highly correlated with observed time of A $\beta$ + ( $\rho=0.93$ , 95% CI: 0.87 to 0.97,  $p<0.001$ , bottom left panel of Fig. 2). When also including the seven participants with a subsequent negative scan after their initial positive scan, the correlation between TFA $\beta$ + and the observed time of A $\beta$ + was 0.89, 95% CI: 0.80 to 0.94,  $p<0.001$ .

When comparing the performance of TFA $\beta$ + versus using A $\beta$  intercepts and slopes as separate predictors, TFA $\beta$ + significantly outperformed separate intercepts and slopes most, but not all of the time. TFA $\beta$ + significantly outperformed covariate only models for all outcomes. Using TFA $\beta$ + resulted in significantly better prediction of MTL tau (AIC<sub>TFA $\beta$ +</sub>=345.1, AIC<sub>IntSlope</sub>=360.2, AIC<sub>Cov</sub>=484.8), MPL tau (AIC<sub>TFA $\beta$ +</sub>=467.9, AIC<sub>IntSlope</sub>=472.4, AIC<sub>Cov</sub>=532.9), occipital lobe tau (AIC<sub>TFA $\beta$ +</sub>=272.1, AIC<sub>IntSlope</sub>=274.2, AIC<sub>Cov</sub>=325.8), CSF A $\beta$  (AIC<sub>TFA $\beta$ +</sub>=1825.1, AIC<sub>IntSlope</sub>=1827.4, AIC<sub>Cov</sub>=1962.1), CSF T-tau (AIC<sub>TFA $\beta$ +</sub>=1854.4, AIC<sub>IntSlope</sub>=1863.4, AIC<sub>Cov</sub>=1902.9), MMSE (AIC<sub>TFA $\beta$ +</sub>=1534.8, AIC<sub>IntSlope</sub>=1549.4, AIC<sub>Cov</sub>=1600.4), and the PACC (AIC<sub>TFA $\beta$ +</sub>=1251.2, AIC<sub>IntSlope</sub>=1261.8, AIC<sub>Cov</sub>=1347.4). There was no difference between TFA $\beta$ + and separate intercepts and slopes for LTL tau (AIC<sub>TFA $\beta$ +</sub>=398.6, AIC<sub>IntSlope</sub>=399.5, AIC<sub>Cov</sub>=471.5) and CSF P-tau (AIC<sub>TFA $\beta$ +</sub>=1711.3, AIC<sub>IntSlope</sub>=1709.6, AIC<sub>Cov</sub>=1748.3) and separate intercepts and slopes was significantly better than TFA $\beta$ + in predicting frontal lobe tau (AIC<sub>TFA $\beta$ +</sub>=194.2, AIC<sub>IntSlope</sub>=188.4, AIC<sub>Cov</sub>=245.9) and LPL tau (AIC<sub>TFA $\beta$ +</sub>=444.9, AIC<sub>IntSlope</sub>=441.9, AIC<sub>Cov</sub>=512.3).

#### Regional A $\beta$ PET

Five regional ROIs (precuneus + posterior cingulate, frontal lobe, cingulate gyrus, temporal and parietal lobes) are shown plotted against TFA $\beta$ + in Fig. 3. All 5 regions were estimated to reach a small, but meaningful (0.2 SD) increase in SUVR between 12 and 15 years before A $\beta$ -positivity, i.e. TFA $\beta$ + = 0. Effect sizes over the span of TFA $\beta$ + are shown in Fig. 3. At TFA $\beta$ + = 0, all regions showed large, significant increases in SUVR ( $\Delta$ SUVR  $\geq 0.11$ ,  $p \leq 0.01$ ) with the precuneus + posterior cingulate composite showing the largest increase ( $\Delta$ SUVR = 0.16,  $p < 0.01$ ) and the temporal lobe showing the smallest ( $\Delta$ SUVR = 0.11,  $p < 0.01$ ). Effect sizes for all regions were large ( $\geq 1$ ) by the time of A $\beta$ +. Table 2 summarizes the values of the outcomes at the longest times before A $\beta$ +, i.e. the least pathological TFA $\beta$ +. Table 2 also shows the value and change of each outcome at the time of A $\beta$ -positivity (TFA $\beta$ + = 0),  $p$ -value, the effect size of change of each outcome, the 0.2 SD change point with respect to TFA $\beta$ +, and corresponding 95% confidence intervals.

Analyses of regional A $\beta$  PET outcomes were repeated using robust regression with robust standard errors. The dashed blue curves in Fig. 3 depict the robust fit. The robust curves are similar to the unweighted regression curves with some mild flattening in the TFA $\beta$ + = 5 to 25 year range. The 0.2 SD change point estimates for the increase in SUVR ranged from 18 to 20 years before A $\beta$ -positivity (compared to 12–15 years before A $\beta$ -positivity in the main analyses). Similar to the unweighted analyses, all regions showed significance of A $\beta$  at TFA $\beta$ + = 0 ( $p < 0.01$ ).

#### CSF

CSF responses are plotted against TFA $\beta$ + in Fig. 4. A 0.2 SD drop in CSF A $\beta$ 42 was estimated to occur 29 years before A $\beta$ -positivity (TFA $\beta$ + = -29). At TFA $\beta$ + = 0, CSF A $\beta$ 42 showed a very large effect size ( $\Delta$ A $\beta$ 42 = -68 ng/L,  $p < 0.01$ , effect size = -1.99). At TFA $\beta$ + = -2, or two years before A $\beta$ -positivity, the population curve passes through a previously published CSF A $\beta$ 42 threshold for A $\beta$ -positivity (192 ng/L) (Shaw et al., 2009).

A 0.2 SD increase in CSF T-tau and P-tau was estimated to occur 7–8 years before the time of A $\beta$ -positivity (TFA $\beta$ + = -7 and -8, respectively). At TFA $\beta$ + = 0, significant increases of medium effect size of T-tau ( $\Delta$ T-tau = 19 ng/L,  $p = 0.04$ , effect size = 0.46) and P-tau ( $\Delta$ P-tau = 12 ng/L,  $p = 0.04$ , effect size = 0.47) were observed.

Robust curves are shown in dashed blue in Fig. 4. The change point estimate was 26 years before A $\beta$ -positivity for the decrease in CSF A $\beta$ , 13 years before A $\beta$ -positivity for CSF P-tau, and 8 years before A $\beta$ -positivity for CSF T-tau. A more substantial flattening of the curves can be seen in both CSF P-tau and T-tau for TFA $\beta$ + > 0. The effect size for CSF T-tau at TFA $\beta$ + = 0 remained almost identical (0.47,  $p = 0.03$ ) and the effect size for CSF P-tau increased moderately to 0.56 ( $p = 0.01$ ). The effect size for CSF A $\beta$ 42 increased to -2.52 at TFA $\beta$ + = 0 and remained significant ( $p < 0.01$ ).

In comparing the CSF subsample ( $N = 185$ ) to the full cohort, missing CSF A $\beta$ 42 (or P-tau) was not associated with age (OR=0.996,  $p = 0.42$ ), sex (OR=1.08,  $p = 0.15$ ), or TFA $\beta$ + (OR=1.00,  $p = 0.96$ ). Missing CSF T-tau was not associated with age (OR=0.996,  $p = 0.32$ ), sex (OR=1.07,  $p = 0.22$ ), or TFA $\beta$ + (OR=1.00,  $p = 0.72$ ).

#### Tau PET

Six regional ROIs (MTL, LTL, MPL, LPL, frontal and occipital lobes) are shown plotted against TFA $\beta$ + in Fig. 5. Five of the six regions were estimated to reach a 0.2 SD increase in SUVR 3–5 years before A $\beta$ -positivity, with the occipital lobe reaching a 0.2 SD increase at the time of A $\beta$ -positivity. Effect sizes over the span of TFA $\beta$ + are shown in Fig. 5. At TFA $\beta$ + = 0, four regions (MTL, LTL, MPL, LPL) showed significant increases in SUVR ( $\Delta$ SUVR  $\geq 0.14$ ,  $p \leq 0.03$ ) with the MTL showing the largest effect size (0.36). The frontal and occipital lobes did not increase significantly by TFA $\beta$ + = 0 ( $\Delta$ SUVR = 0.09 ( $p = 0.06$ ) and 0.07 ( $p = 0.13$ ), respectively). Estimates are summarized in Table 2.

Robust curves are shown in dashed blue in Fig. 5. The robust curves show substantial flattening for TFA $\beta$ + > 0. The robust 0.2 SD change point estimates for the increase in SUVR for the tau PET ROIs ranged from 6 to 9 years before A $\beta$ -positivity. The significance of changes in tau PET at TFA $\beta$ + = 0 were similar to the unweighted analyses with the exception of the frontal lobe, which increased in effect size and became statistically significant (0.44,  $p = 0.02$ ).

#### Cognition

Cognitive measures are shown in Fig. 6. The MMSE showed a 0.2 SD drop six years before A $\beta$ -positivity, followed by the PACC four years before A $\beta$ -positivity. Neither measure decreased significantly by the time of A $\beta$ -positivity ( $\Delta$ MMSE = -0.71,  $p = 0.13$ , effect size=-0.30;  $\Delta$ PACC = -0.50,  $p = 0.10$ , effect size=-0.32).

Robust curves are shown in dashed blue in Fig. 6 and show mild flattening for TFA $\beta$ + > 0, compared to the unweighted analyses. The change point estimates for the decrease in cognitive scores was two years before A $\beta$ -positivity for MMSE and four years before A $\beta$ -positivity for the PACC. The robust estimate for the effect size of decrease in MMSE scores was reduced to -0.23 but became statistically significant ( $p = 0.03$ ). The robust estimate for the effect size of decrease in PACC scores was similar (-0.30), and also became statistically significant ( $p = 0.03$ ).

Summary curves and 0.2 SD change points for some of the earliest changing measures of each outcome type (CSF A $\beta$  and P-tau, precuneus + posterior cingulate A $\beta$  PET, MTL tau PET and the PACC) are shown in Fig. 7.

#### Discussion

Several biological processes develop over time in sporadic AD, including accumulation of A $\beta$  and tau across wide areas of the brain, as well as cognitive decline. Based on the amyloid cascade hypothesis, a relevant overarching time scale of the disease processes could be based

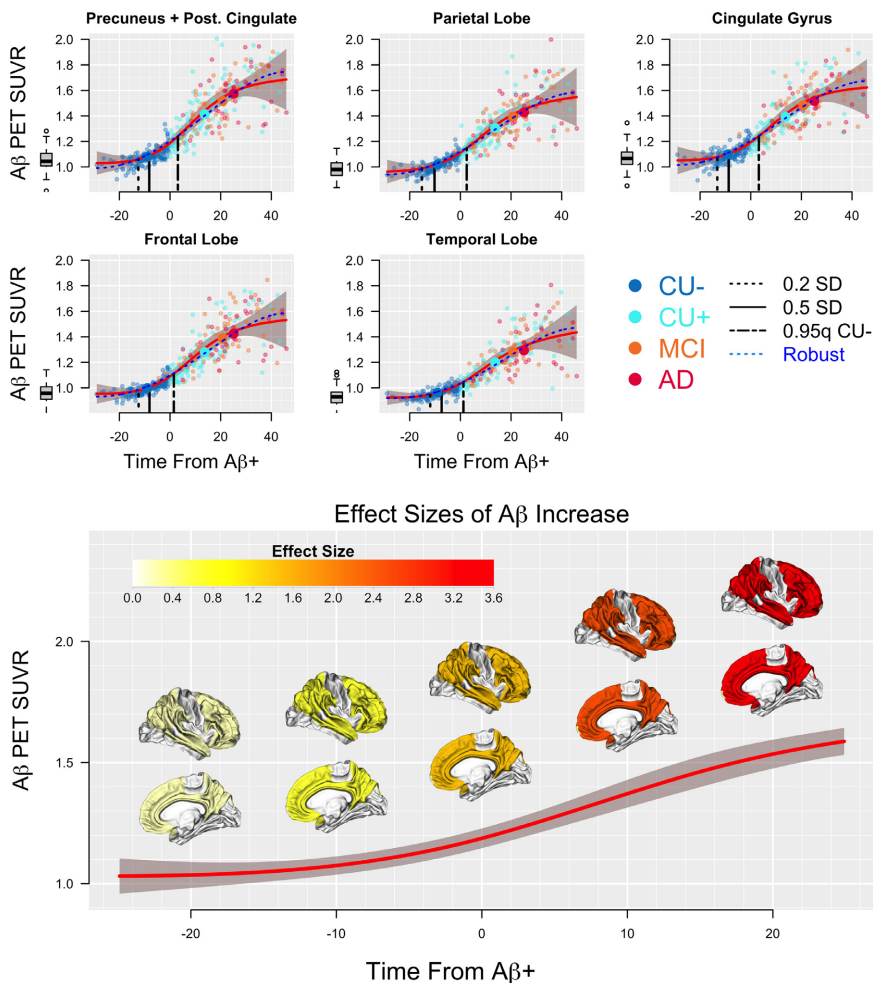


Fig. 3. Regional Aβ PET.

Aβ PET ROIs are plotted against TFAβ+. Effect sizes, depicting change points are shown as vertical dashed (0.2 SD, initial change) and solid (0.5 SD) lines. Unweighted regression curves (red) and corresponding 95% CIs (shaded gray) are shown. Robust curves are shown in dashed blue. Mean values of the response are plotted against mean TFAβ+ for each of the four diagnosis groups (large symbols). The 0.95 quantile (approximately 1.65 SD if normally distributed) of the response for the CU- group is also shown (short/long dashed line). The 0.95 quantile (or 0.05 quantile for responses where low values are worse) of the biomarkers in CU-, provided for all responses to facilitate comparisons of when (in terms of TFAβ+) the average level of each response is no longer in the normal range. The boxplots to the left of each figure show the biomarker distribution in subjects that were determined to not be on the AD trajectory (including subjects where the model estimated them to become Aβ+ at over 120 years of age). Effect sizes of Aβ increase are shown in the bottom panel at TFAβ+ = -20, -10, 0, 10, and 20 years.

on the development of Aβ pathology (Koscik et al., 2020). Integrating Aβ PET level and rate of change information places each individual on a pathological timeline. While this timeline, represented in these analyses by TFAβ+, was more closely associated with tau PET, CSF and measures of cognition in most measures, compared with intercept and slope information modeled separately, the main advantage is that it is parameterized to directly estimate the time of downstream events in the amyloid cascade. We estimated several major milestone events of AD progression including a small drop in CSF Aβ42 29 years before Aβ-

positivity and a small increase in regional Aβ PET deposition 15 years before Aβ-positivity. Using the biomarkers tested here, the first changes in CSF Aβ42 may define the onset of AD. Small increases in tau pathology were estimated to occur 7–8 years before Aβ-positivity, as measured by CSF and 5 years before, as measured by PET. More substantial and statistically significant increases in CSF as well as temporoparietal tau PET were detected by the time of Aβ-positivity. Small effects of cognitive dysfunction occurred 4–6 years before Aβ-positivity, coinciding with previous reports (Insel et al., 2017). These findings provide a

**Table 2**  
Initial values, effect sizes and change points.

	Initial value* (SD)	Value** at TFAβ+ = 0	Difference at TFAβ+ = 0 (p-value)	95% CI	Effect size (difference at TFAβ+ = 0)	95% CI	TFAβ+ Change Point (0.2 SD)	95% CI
<i>Aβ</i> PET (N = 335)								
Precuneus+PC	1.03 (0.14)	1.19	0.16 (<0.01)	0.06 to 0.25	1.10	0.43 to 1.79	-13	-21 to -5
Parietal Lobe	0.96 (0.12)	1.11	0.15 (<0.01)	0.06 to 0.24	1.20	0.50 to 2.00	-15	-23 to -8
Cingulate Gyrus	1.05 (0.13)	1.19	0.14 (0.01)	0.04 to 0.25	1.11	0.31 to 1.92	-13	-21 to -6
Frontal Lobe	0.95 (0.13)	1.09	0.14 (<0.01)	0.05 to 0.22	1.08	0.38 to 1.69	-12	-21 to -4
Temporal Lobe	0.92 (0.11)	1.03	0.11 (<0.01)	0.04 to 0.18	0.98	0.36 to 1.64	-12	-21 to -3
CSF								
<i>Aβ</i> (N = 185)								
T-tau (N = 180)	255 (34)	186	-68 (<0.01)	-109 to -28	-1.99	-3.18 to -0.81	-29	-38 to -20
P-tau (N = 185)	50 (42)	69	19 (0.04)	1 to 38	0.46	0.03 to 0.89	-7	-20 to 6
Tau PET (N = 335)	27 (25)	38	12 (0.04)	1 to 22	0.47	0.03 to 0.90	-8	-22 to 5
MPL								
MTL	1.21 (0.41)	1.36	0.15 (0.01)	0.04 to 0.26	0.36	0.10 to 0.63	-5	-14 to 4
MPL	1.22 (0.49)	1.38	0.16 (0.01)	0.04 to 0.29	0.34	0.08 to 0.59	-5	-14 to 4
LTL	1.39 (0.44)	1.52	0.13 (0.03)	0.02 to 0.24	0.29	0.05 to 0.55	-3	-12 to 6
LPL	1.37 (0.47)	1.51	0.14 (0.03)	0.01 to 0.27	0.30	0.02 to 0.57	-4	-13 to 6
Frontal Lobe	1.39 (0.32)	1.49	0.09 (0.06)	0.00 to 0.19	0.29	0.00 to 0.59	-3	-15 to 8
Occipital Lobe	1.43 (0.36)	1.50	0.07 (0.13)	-0.02 to 0.16	0.20	-0.06 to 0.44	0	-11 to 11
Cognition (N = 335)								
MMSE	29.3 (2.38)	28.6	-0.71 (0.13)	-1.62 to 0.21	-0.30	-0.68 to 0.09	-6	-23 to 11
PACC	0.04 (1.57)	-0.46	-0.50 (0.10)	-1.08 to 0.09	-0.32	-0.69 to 0.06	-4	-16 to 8

\* Initial Value indicates the estimated mean of the outcome at the minimum TFAβ+ value.  
\*\* Value at TFAβ+ = 0 is the model-estimated outcome value of the population curve at TFAβ+ = 0.

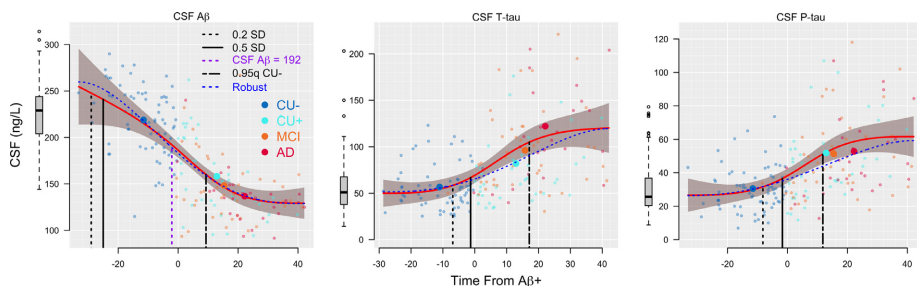


**Fig. 4.** CSF biomarkers.

CSF biomarker responses are plotted against TFAβ+. Effect sizes, depicting change points are shown as vertical dashed (0.2 SD, initial change) and solid (0.5 SD) lines. Un weighted regression curves (red) and corresponding 95% CIs (shaded gray) are shown. Robust curves are shown in dashed blue. Mean values of the response are plotted against mean TFAβ+ for each of the four diagnosis groups (large symbols). The 0.95 quantile (approximately 1.65 SD if normally distributed) of the response for the CU- group is also shown (short/long dashed line). The dashed purple line indicates a previously identified threshold for Aβ-positivity based on CSF Aβ. Note that this line occurs close to the TFAβ+ threshold for Aβ-positivity. The boxplots to the left of each figure show the biomarker distribution in subjects that were determined not to be on the AD trajectory (including subjects where the model estimated them to become Aβ+ over 120 years of age).

general time scale for initial changes in sporadic AD, which may inform clinical trials aimed at specific stages of the disease.

Once beyond the threshold for Aβ-positivity, there is a substantial increase in the variance of the tau and cognitive responses. A handful of participants show large increases, especially in tau PET, and large decreases in cognition, resulting in clusters of outliers. These outliers appear to have marked influence on both the shape of the curves and the estimates of the variance, as shown by the difference between the un-weighted and the robust analyses. The robust curves are generally flatter beyond the threshold for Aβ-positivity, less influenced by extreme values. The curves are reasonably similar prior to Aβ-positivity, although the overall variance estimates are smaller, resulting in earlier estimates of change points for several of the outcomes and more significant differences at the threshold for Aβ-positivity. In both sets of analyses, significant increases in both CSF tau and tau PET are observed to occur by the time of Aβ-positivity.

A 0.2 SD difference, a small, but meaningful increase in levels of CSF tau and temporoparietal lobe tau are observed years before the current threshold for Aβ-positivity. In the context of secondary prevention trials

where Aβ-positivity at current thresholds is required for study inclusion, tau levels in these participants would already have been increasing for several years, likely more. The finding that temporoparietal tau starts to increase prior to other regions is in accordance with 18F-flortaucipir studies on other populations. Cross-sectional studies showed early tau deposition in cognitively healthy elderly (with or without significant Aβ pathology) in temporal and medial parietal regions, most dominant in entorhinal and parahippocampal cortex, the amygdala and inferior temporal cortex. Longitudinal studies further suggest that cognitively healthy elderly accumulate tau in the medial temporal and medial parietal lobe, while (Aβ positive) AD dementia patients increased in tau primarily in the frontal lobe (Harrison et al., 2018). The spread of tau beyond the MTL to the parietal lobe and other regions may be a critical milestone in the progression of AD. The early changes observed in the MPL in this study coincide with a recent report of the earliest tau deposition found in medial parietal regions (precuneus and isthmus cingulate) in autosomal dominant AD (Gordon et al., 2019). Considering that a 0.2 SD increase in MPL tau can potentially be detected several years before Aβ-positivity (Fig. 5), these data support the use of primary

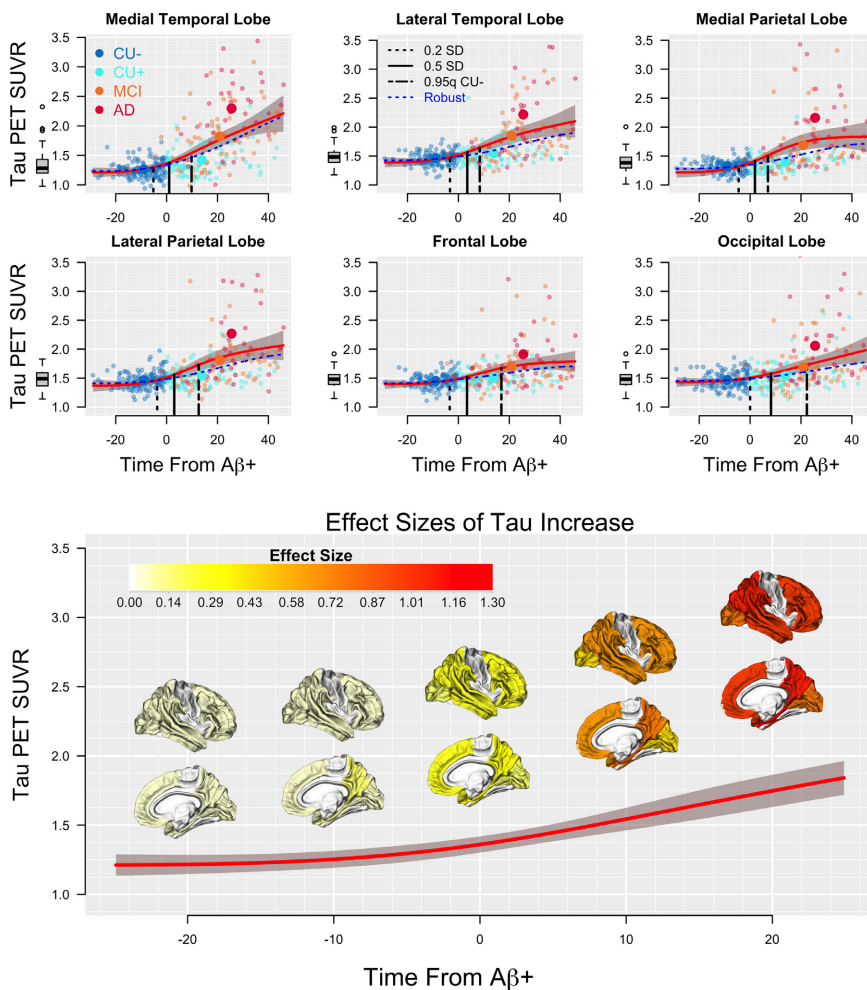


**Fig. 5.** Regional Tau PET. Tau PET ROIs are plotted against TFAβ+. Effect sizes, depicting change points are shown as vertical dashed (0.2 SD, initial change) and solid (0.5 SD) lines. Unweighted regression curves (red) and corresponding 95% CIs (shaded gray) are shown. Robust curves are shown in dashed blue. Mean values of the response are plotted against mean TFAβ+ for each of the four diagnosis groups (large symbols). The 0.95 quantile (approximately 1.65 SD if normally distributed) of the response for the CU-group is also shown (short/long dashed line). The boxplots to the left of each figure show the biomarker distribution in subjects that was determined to not be on the AD trajectory (including subjects where the model estimated them to become Aβ+ at over 120 years of age). Effect sizes of tau increase are shown in the bottom panel at TFAβ+ = -20, -10, 0, 10, and 20 years.

prevention trials against Aβ where treatment is initiated years before the current threshold for Aβ-positivity, if treatment efficacy relies on early intervention, prior to the development of tau pathology.

The initial descent in cognitive performance is estimated to occur 4–6 years before becoming Aβ-positivity (Fig. 6). Reduced cognitive performance has repeatedly been shown to be associated with elevated levels of Aβ (Baker et al., 2017; Donohue et al., 2017; Insel et al., 2017, 2016), even within the subthreshold range (Landau et al., 2018), in cognitively unimpaired individuals. The result that CSF tau measures started to change between regional Aβ and cognition in this study is in ac-

cordance with the theory that cognitive impairment in AD is caused primarily by tau pathology. This is also in line with other recent studies which show that cognitive impairment is more strongly related to accumulation of tau than to Aβ (Ossenkoppe et al., 2019), and that both tau and Aβ appear necessary for cognitive decline (Sperling et al., 2019). The ordering of the responses coincides with the magnitude of the effect sizes at the time of Aβ-positivity (Table 1), suggesting that initial changes in the responses continue to change in parallel through to the time of Aβ-positivity, without any major differences in acceleration.



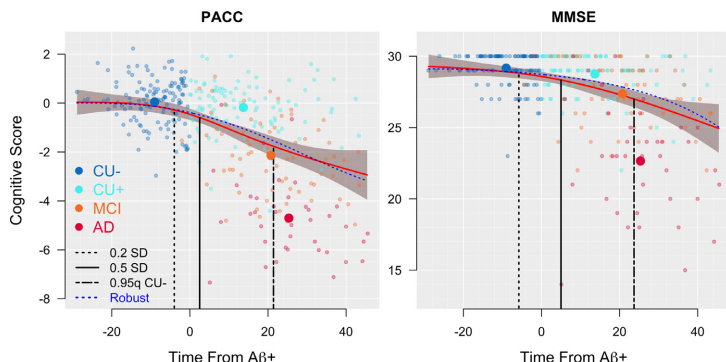


**Fig. 6.** Cognition. MMSE and PACC scores are plotted against TFAβ+. Effect sizes, depicting change points are shown as vertical dashed (0.2 SD, initial change) and solid (0.5 SD) lines. Unweighted regression curves (red) and corresponding 95% CIs (shaded gray) are shown. Robust curves are shown in dashed blue. Mean values of the response are plotted against mean TFAβ+ for each of the four diagnosis groups (large symbols). The 0.05 quantile (approximately -1.65 SD if normally distributed) of the response for the CU- group is also shown (short/long dashed line). The overall PACC mean is -1.02 (SD=1.97).

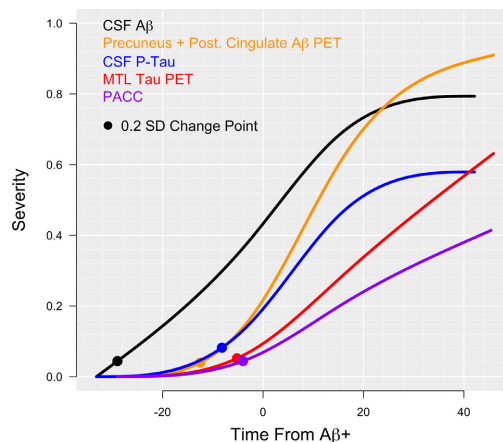


**Fig. 7.** Summary curves. Summary curves are shown for all modalities on a scale from zero to one. Responses are scaled such that zero is the least pathological point for each response and one is the mean response in the AD participants. The initial effect, defined by 0.2 SD change points are plotted.

In their 2018 draft guidance, the FDA indicated that because it is highly desirable to intervene as early as possible in AD, it follows that patients with characteristic pathophysiological changes of AD but no subjective complaint, functional impairment, or detectable abnormalities on sensitive neuropsychological measures are an important target for clinical trials (Food and Drug Administration, 2018). If the spread of tau to the lateral temporal and parietal lobes becomes a defining characteristic of pathophysiological change in AD, the window to intervene as early as possible may shift to years before the current threshold for Aβ-positivity. It is possible that early accelerations of tau may have contributed to recent failures of anti-Aβ treatments in phase III clinical trials on Aβ-positive patients (Egan et al., 2018; Honig et al., 2018). Although selecting subjects that are Aβ-positive ensures that only AD patients are included in trials, the use of conservative thresholds to define Aβ-positivity may bias trial populations toward individuals where tau pathology has already accumulated, causing downstream injuries independent of Aβ, reducing the efficacy of anti-Aβ treatments.

This study has several limitations. Tau PET data were available for only a subsample of the data, limiting comparisons to a small cross-section of the full ADNI data set. More data, especially longitudinal data in participants in the earliest stages of Aβ changes, will be required for more precise estimates of TFAβ+ as well as more precise change point estimates. Additional longitudinal Aβ information over longer periods of time will also be required to evaluate to what degree a participant may drift from their assumed quantile of accumulation. These analyses lack the power and precision to place the temporal and parietal tau regions in a particular order with confidence, but instead demonstrate that widespread tau is increasing years before Aβ-positivity. The ADNI CU, MCI and AD cohorts are also age matched. The AD patients, on average, have dementia by age 75, while the participants in the CU cohort who may eventually develop AD, are unlikely to do so for many years, possibly decades. By design, these cohorts with age matched groups are therefore on systematically different disease trajectories with respect to age. If earlier onset is associated with a more aggressive form of the disease, then the AD cohort may have the most aggressive form while the CU cohort, the least aggressive. If the developing Aβ pathology in the ADNI CU- cohort represents a less aggressive disease process compared with a more typical AD process, the estimates reported here could be conservative and biased toward later time estimates for downstream events. The ADNI MCI cohort may represent a more typical trajectory with respect to downstream events along the Aβ pathological timeline. These differences in disease trajectories are apparent from the cohort estimates in Figs. 2-5. Additionally, the change point estimates are influenced by both biological variation and measurement error, which varies from marker to marker. Change points in measures with high variability in the “normal” range and excess measurement error may require additional biological change to detect, despite an earlier, real increase in pathology. ADNI participants are highly educated on average, reducing generalizability to some degree. The associations between increasing Aβ pathology and downstream changes, including increased tau pathology reported here do not imply causality. It remains unknown whether and to what degree downstream pathological changes can be directly attributed to the accumulation of Aβ. Only studies with experimental interventions against Aβ-pathology, with clear verification of target engagement, can be used to show causal relationships between Aβ-deposition and putative downstream events. While TFAβ+ appears reasonably predictive, especially in proximity to the threshold for Aβ-positivity, longer follow-up is needed to validate its accuracy at very early and late-stage Aβ accumulation.

Longitudinal information is required to evaluate how quickly an individual’s pathophysiological changes are occurring and to accurately characterize their disease trajectory. Analyses limited to a cross-sectional evaluation of Aβ status are naïve to the time spent with a

significant  $A\beta$  burden. Incorporating longitudinal information facilitates the estimation of the time-course of downstream events such as the spread of tau and the onset of subtle cognitive dysfunction. As the technology to measure AD pathology becomes more cost effective and non-invasive, such as plasma measures of  $A\beta$  or tau (Janelidze et al., 2020; Mielke et al., 2018; Palmqvist et al., 2019; Schindler et al., 2019), longitudinal evaluations in the context of trial-ready cohorts may greatly improve early diagnosis and expedite the execution of clinical trials in early AD.

#### Data availability

All data is publicly available (<http://adni.loni.usc.edu/>). R code will be made available on Github.

#### Declaration of Competing Interest

Mr. Insel, Dr. Berron and Dr. Donohue report no competing interests. Dr. Mattsson-Carlgrén has been a consultant for ADNI.

Dr. Hansson has acquired research support (for the institution) from Roche, GE Healthcare, Biogen, AVID Radiopharmaceuticals and Euroimmun. In the past 2 years, he has received consultancy/speaker fees (paid to the institution) from Biogen and Roche.

#### Credit authorship contribution statement

**Philip S. Insel:** Conceptualization, Methodology, Software, Formal analysis, Writing - original draft, Writing - review & editing. **Michael C. Donohue:** Methodology, Writing - review & editing. **David Berron:** Methodology, Writing - review & editing. **Oskar Hansson:** Writing - review & editing, Funding acquisition. **Niklas Mattsson-Carlgrén:** Methodology, Writing - review & editing, Funding acquisition.

#### Acknowledgments

Data collection and sharing for this project was funded by the Alzheimer's Disease Neuroimaging Initiative (ADNI) (National Institutes of Health Grant U01 AG024904). ADNI is funded by the National Institute on Aging, the National Institute of Biomedical Imaging and Bioengineering, and through generous contributions from the following: Alzheimer's Association; Alzheimer's Drug Discovery Foundation; BioClinica, Inc.; Biogen Idec Inc.; Bristol-Myers Squibb Company; Eisai Inc.; Elan Pharmaceuticals, Inc.; Eli Lilly and Company; F. Hoffmann-La Roche Ltd and its affiliated company Genentech, Inc.; GE Healthcare; Innogenetics, N.V.; IXICO Ltd.; Janssen Alzheimer Immunotherapy Research & Development, LLC.; Johnson & Johnson Pharmaceutical Research & Development LLC.; Medpace, Inc.; Merck & Co., Inc.; Meso Scale Diagnostics, LLC.; NeuroRx Research; Novartis Pharmaceuticals Corporation; Pfizer Inc.; Piramal Imaging; Servier; Synarc Inc.; and Takeda Pharmaceutical Company. The Canadian Institutes of Health Research is providing funds to support ADNI clinical sites in Canada. Private sector contributions are facilitated by the Foundation for the National Institutes of Health ([www.fnih.org](http://www.fnih.org)). The grantee organization is the Northern California Institute for Research and Education, and the study is coordinated by the Alzheimer's Therapeutic Research Institute at the University of Southern California, San Diego. ADNI data are disseminated by the Laboratory for Neuro Imaging at the University of Southern California. Data used in preparation of this article were obtained from the Alzheimer's Disease Neuroimaging Initiative (ADNI) database ([adni.loni.usc.edu](http://adni.loni.usc.edu)). As such, the investigators within the ADNI contributed to the design and implementation of ADNI and/or provided data but did not participate in analysis or writing of this report. A complete listing of ADNI investigators can be found at: [http://adni.loni.usc.edu/wp-content/uploads/how\\_to\\_apply/ADNI\\_Acknowledgement\\_List.pdf](http://adni.loni.usc.edu/wp-content/uploads/how_to_apply/ADNI_Acknowledgement_List.pdf).

This research was also supported by The Wallenberg Center for Molecular Medicine at Lund University, the Knut and Alice Wallenberg foundation, The Medical Faculty at Lund University, Region Skåne, the Skåne University Hospital Foundation, the Swedish Research Council, the Swedish Alzheimer Foundation, the Swedish Brain Foundation, the Swedish Medical Association, the Konung Gustaf V:s och Drottning Victorias Frimurarestiftelse, the Greta and Johan Kock Foundation, the Thelma Zoega Foundation, the Gyllenstiernska Krapprupsstiftelsen, the Magnus Bergwall Foundation, the Bundy Academy, the Marianne and Marcus Wallenberg foundation, and the Strategic Research Area MultiPark (Multidisciplinary Research in Parkinson's disease) at Lund University. The funding sources had no role in the design and conduct of the study, in the collection, analysis, interpretation of the data or in the preparation, review or approval of the manuscript.

#### References

- ADNI, 2012. ADNI Commonly Used Tables [WWW Document]. URL <https://adni.loni.usc.edu/wp-content/uploads/2012/08/instruction-about-data.pdf>
- Akaïke, H., 1974. A new look at the statistical model identification. *Autom. Control. IEEE Trans.* 19, 716–723. doi:10.1007/s00198-008-0566-6.
- Atkinson, K.E., 1989. *An Introduction to Numerical Analysis*, 2nd ed. John Wiley & Sons, New York.
- Baker, J.E., Lim, Y.Y., Pietrzak, R.H., Hassenstab, J., Snyder, P.J., Masters, C.L., Maruff, P., 2017. Cognitive impairment and decline in cognitively normal older adults with high amyloid- $\beta$ : a meta-analysis. *Alzheimer's Dement. Diagnosis, Assess. Dis. Monit.* 6, 108–121. doi:10.1016/j.dadm.2016.09.002.
- Bateman, R.J., Xiong, C., Benzinger, T.L.S., Fagan, A.M., Goate, A., Fox, N.C., Marcus, D.S., Cairns, N.J., Xie, X., Blazey, T.M., Holtzman, D.M., Santacruz, A., Buckles, V., Oliver, A., Moulder, K., Aisen, P.S., Ghetti, B., Klunk, W.E., McDade, E., Martins, R.N., Masters, C.L., Mayeux, R., Ringman, J.M., Rossor, M.N., Schofield, P.R., Sperling, R.A., Salloway, S., Morris, J.C., 2012. Clinical and biomarker changes in dominantly inherited Alzheimer's disease. *N. Engl. J. Med.* 367, 795–804. doi:10.1056/NEJMoa1202753.
- Braak, H., Braak, E., 1991. Acta H ' pathologica Neuropathological staging of Alzheimer-related changes. *Acta Neuropathol.* 82, 239–259. doi:10.1007/BF00308809.
- Cohen, J., 1988. *Statistical Power Analysis for the Behavioral Sciences*, 2nd ed. Lawrence Erlbaum Associates, New York.
- Donohue, M.C., Sperling, R.A., Petersen, R., Sun, C.-K., Weiner, M.W., Aisen, P.S., 2017. Association between elevated brain amyloid and subsequent cognitive decline among cognitively normal persons. *JAMA* 317, 2305–2316. doi:10.1001/jama.2017.6669.
- Donohue, M.C., Sperling, R.A., Salmon, D.P., Rentz, D.M., Raman, R., Thomas, R.G., Weiner, M., Aisen, P.S. Australian Imaging, Biomarkers, and Lifestyle Flagship Study of Ageing, Alzheimer's Disease Neuroimaging Initiative, Alzheimer's Disease Cooperative Study, 2014. The preclinical Alzheimer cognitive composite: measuring amyloid-related decline. *JAMA Neurol.* 71, 961–970. doi:10.1001/jamaneuro.2014.803.
- Egan, M.F., Kost, J., Tariot, P.N., Aisen, P.S., Cummings, J.L., Vellas, B., Furtek, C., Harper Mozley, L., Mahoney, E., Vandenberghe, R., Mukai, Y., Voss, T., Mo, Y., Sur, C., Michelson, D., 2018. Randomized Trial of Verubecestat for Mild-to-Moderate Alzheimer's Disease. *N. Engl. J. Med.* 378, 1691–1703. doi:10.1056/nejmoa1706441.
- Food and Drug Administration, 2018. *Early Alzheimer's Disease: Developing Drugs for Treatment Guidance for Industry*.
- Gordon, B.A., Blazey, T.M., Christensen, J., Dincer, A., Flores, S., Keefe, S., Chen, C., Su, Y., McDade, E.M., Wang, G., Li, Y., Hassenstab, J., Aschenbrenner, A., Hornbeck, R., Jack, C.R., Ances, B.M., Berman, S.B., Brosch, J.R., Galasko, D., Gauthier, S., Lah, J.J., Masellis, M., Dyck, C.H., Van, Mintun, M.A., Klein, G., Ristic, S., Cairns, N.J., Marcus, D.S., Xiong, C., Holtzman, D.M., Raichle, M.E., Morris, J.C., Bateman, R.J., Benzinger, T.L.S., 2019. Tau PET in autosomal dominant Alzheimer's disease: relationship with cognition, dementia and other biomarkers. *Brain J. Neurol.* 142, 1063–1076. doi:10.1093/brain/awz019 BRAIN.
- Hardy, J., Selkoe, D.J., 2002. The amyloid hypothesis of Alzheimer's disease: progress and problems on the road to therapeutics. *Science* 297, 353–356. doi:10.1126/science.1072994.
- Harrison, T.M., La Joie, R., Maass, A., Baker, S.L., Swinnerton, K., Fenton, L., Mellinger, T.J., Edwards, L., Pham, J., Miller, B.L., Rabinovici, G.D., Jagust, W.J., 2018. Longitudinal tau accumulation and atrophy in aging and Alzheimer disease. *Ann. Neurol.* 85, 229–240. doi:10.1002/ana.25406.
- Hastie, T.J., Tibshirani, R.J., 1990. Generalized additive models. *Monogr. Stat. Appl. Probab.* doi:10.1016/j.csda.2010.05.004.
- Honig, L.S., Vellas, B., Woodward, M., Boada, M., Bullock, R., Borrie, M., Hager, K., Andreason, N., Scarpini, E., Liu-Seifert, H., Case, M., Dean, R.A., Hake, A., Sundell, K., Poole Hoffmann, V., Carlson, C., Khanna, R., Mintun, M., DeMattos, R., Selzler, K.J., Siemers, E., 2018. Trial of solanezumab for mild dementia due to Alzheimer's disease. *N. Engl. J. Med.* 378, 321–330. doi:10.1056/NEJMoa1705971.
- Huber, P.J., Ronchetti, E.M., 1981. *Robust Statistics*. John Wiley & Sons, New York.
- Insel, P.S., Donohue, M.C., Mackin, R.S., Aisen, P.S., Hansson, O., Weiner, M.W., Mattsson, N., 2016. Cognitive and functional changes associated with  $A\beta$  pathology and the progression to mild cognitive impairment. *Neurobiol. Aging* 48, 172–181. doi:10.1016/j.neurobiolaging.2016.08.017.

- Insel, P.S., Ossenkoppele, R., Gessert, D., Jagust, W., Landau, S., Hansson, O., Weiner, M.W., Mattsson, N., 2017. Time to amyloid positivity and preclinical changes in brain metabolism, atrophy, and cognition: evidence for emerging amyloid pathology in Alzheimer's disease. *Front. Neurosci.* 11, 1–9. doi:10.3389/fnins.2017.00281.
- Jack, C.R., Knopman, D.S., Jagust, W.J., Shaw, L.M., Aisen, P.S., Weiner, M.W., Petersen, R.C., Trojanowski, J.Q., 2010. Hypothetical model of dynamic biomarkers of the Alzheimer's pathological cascade. *Lancet Neurol.* 9, 119–128. doi:10.1016/S1474-4422(09)70299-6.
- Jagust, W.J., Landau, S.M., Koeppe, R.A., Reiman, E.M., Chen, K., Mathis, C.A., Price, J.C., Foster, N.L., Wang, A.Y., 2015. The Alzheimer's Disease Neuroimaging Initiative 2 PET Core: 2015. *Alzheimer's Dement.* 11, 757–771. doi:10.1016/j.jalz.2015.05.001.
- Janelidze, S., Mattsson, N., Palmqvist, S., Smith, R., Beach, T.G., Serrano, G.E., Chai, X., Proctor, N.K., Eichenlaub, U., Zetterberg, H., Blennow, K., Reiman, E.M., Stomrud, E., Dage, J.L., Hansson, O., 2020. The Alzheimer's Disease Neuroimaging Initiative 2 relationship to other biomarkers, differential diagnosis, and longitudinal progression to Alzheimer's disease. *Nat. Med.* 26, 379–386. doi:10.1038/s41591-020-0755-1.
- Jansen, W.J., Ossenkoppele, R., Knol, D.L., Tijms, B.M., Scheltens, P., Verhey, F.R.J., Visser, P.J., Aalten, P., Aarsland, D., Alcolea, D., Alexander, M., Almdahl, I.S., Arnold, S.E., Baldeiras, I., Barthel, H., van Berckel, B.N.M., Bibeau, K., Blennow, K., Brooks, D.J., van Buchem, M.A., Camus, V., Cavedo, E., Chen, K., Chetelat, G., Cohen, A.D., Drzezga, A., Engelborghs, S., Fagan, A.M., Fladby, T., Fleisher, A.S., van der Flier, W.M., Ford, L., Förster, S., Fortea, J., Foksett, N., Frederiksen, K.S., Freund-Levi, Y., Frisoni, G.B., Froelich, L., Gabryelewicz, T., Gill, K.D., Gkatzima, O., Gómez-Tortosa, E., Gordon, M.F., Grimmer, T., Hampel, H., Hausner, L., Hellwig, S., Herukka, S.-K., Hildebrandt, H., Ishihara, L., Ivanou, A., Jagust, W.J., Johansson, P., Kandimala, R., Kapaki, E., Klimkiewicz-Mrowiec, A., Klunk, W.E., Köhler, S., Koglin, N., Kornhuber, J., Kramberger, M.G., Van Laere, K., Landau, S.M., Lee, D.Y., de Leon, M., Lisetti, V., Lleó, A., Madsen, J., Maier, W., Marcussen, J., Mattsson, N., de Mendonça, A., Meulenbroek, O., Meyer, P.T., Mintun, M.A., Mok, V., Molinuevo, J.L., Møllergård, H.M., Morris, J.C., Mroczko, B., Van der Mussele, S., Na, D.L., Newberg, A., Nordberg, A., Nordlund, A., Novak, G.P., Parakevas, G.P., Parnetti, L., Perera, G., Peters, O., Popp, J., Prabhakar, S., Rabinovici, G.D., Ramakers, I.H.G.B., Rami, L., Resende de Oliveira, C., Rinne, J.O., Rodrigue, K.M., Rodríguez-Rodríguez, E., Roe, C.M., Rot, U., Rowe, C.C., Rütger, E., Sabri, O., Sanchez-Juan, P., Santana, I., Sarazin, M., Schröder, J., Schütte, C., Seo, S.W., Soetewy, F., Soinen, H., Spuru, L., Struyfs, H., Teunissen, C.E., Tzolaki, M., Vandenbergh, R., Verbeek, M.M., Villemeagne, V.L., Vos, S.J.B., van Waalwijk van Doorn, L.J.C., Waldermar, G., Wallin, A., Wallin, Å.K., Wiltfang, J., Wolk, D.A., Zboch, M., Zetterberg, H., 2015. Prevalence of cerebral amyloid pathology in persons without dementia: a meta-analysis. *Jama* 313, 1924–1938. doi:10.1001/jama.2015.4668.
- Joshi, A.D., Pontecorvo, M.J., Clark, C.M., Carpenter, A.P., Jennings, D.L., Mintun, M.A., Adler, L.P., Burns, J.D., Saha, K., Sadovskiy, C.H., Kovnat, K.D., Lowrey, M.J., Arora, A., Seibyl, J.P., Skovronsky, D.M., 2012. Performance characteristics of amyloid PET with florbetapir F 18 in patients with Alzheimer's disease and cognitively normal subjects. *J. Nucl. Med.* 53, 378–384. doi:10.2967/jnumed.111.090340.
- Koenker, R., D'Orey, V., 1987. Algorithm AS 229: computing regression quantiles author (s): roger W. Koenker and Vasco D. Orey Source: J. R. Stat. Soc. Ser. C (Appl. Stat.) 36 (3), 383–393 Published by: Blackwell Publishing for the Royal S. J. R. Stat. Soc. Ser. C (Applied Stat. 36).
- Koscik, R.L., Betthausen, T.J., Jonaitis, E.M., Allison, S.L., Clark, L.R., Hermann, B.P., Cody, K.A., Engle, J.W., Barnhart, T.E., Stone, C.K., Chin, N.A., Carlsson, C.M., Asthana, S., Christian, B.T., Johnson, S.C., 2020. Amyloid duration is associated with preclinical cognitive decline and tau PET. *Alzheimer's Dement. Diagnosis, Assess. Dis. Monit.* 12, 1–10. doi:10.1002/dad2.12007.
- Landau, S., Jagust, W., 2015. Florbetapir Processing Methods [WWW Document]. URL [https://adni.bidsbucket.io/reference/does/UCBERKELEYAV45/ADNI\\_AV45\\_Methods\\_JagustLab\\_06.25.15.pdf](https://adni.bidsbucket.io/reference/does/UCBERKELEYAV45/ADNI_AV45_Methods_JagustLab_06.25.15.pdf)
- Landau, S.M., Horg, A., Jagust, W.J., 2018. Memory decline accompanies subthreshold amyloid accumulation. *Neurology* doi:10.1212/WNL.0000000000005354.
- Landau, S.M., Mintun, M.A., Joshi, A.D., Koeppe, R.A., Petersen, R.C., Aisen, P.S., Weiner, M.W., Jagust, W.J., 2012. Amyloid deposition, hypometabolism, and longitudinal cognitive decline. *Ann. Neurol.* 72, 578–586. doi:10.1002/ana.23650.
- Li, D., Iddi, S., Thompson, W.K., Donohue, M.C., 2017. Bayesian latent time joint mixed effect models for multicohort longitudinal data. *Stat. Methods Med. Res.* 1–11. doi:10.1177/0962280217737566.
- Maass, A., Landau, S., Horg, A., Lockhart, S.N., Rabinovici, G.D., Jagust, W.J., Baker, S.L., La Joie, R., 2017. Comparison of multiple tau-PET measures as biomarkers in aging and Alzheimer's disease. *Neuroimage* 157, 448–463. doi:10.1016/j.neuroimage.2017.05.058.
- Mielke, M.M., Hagen, C.E., Xu, J., Chai, X., Vemuri, P., Lowe, V.J., Airey, D.C., Knopman, D.S., Roberts, R.O., Machulda, M.M., Jack, C.R., Petersen, R.C., Dage, J.L., 2018. Plasma phospho-tau181 increases with Alzheimer's disease clinical severity and is associated with tau- and amyloid-positron emission tomography. *Alzheimer's Dement.* 14, 989–997. doi:10.1016/j.jalz.2018.02.013.
- Mormino, E.C., Kluth, J.T., Madison, C.M., Rabinovici, G.D., Baker, S.L., Miller, B.L., Koeppe, R.A., Mathis, C.A., Weiner, M.W., Jagust, W.J., 2009. Episodic memory loss is related to hippocampal-mediated  $\beta$ -amyloid deposition in elderly subjects. *Brain* 132, 1310–1323. doi:10.1093/brain/awn320.
- Olsson, A., Vanderstichele, H., Andreasen, N., De Meyer, G., Wallin, A., Holmberg, B., Rosengren, L., Vanmechelen, E., Blennow, K., 2005. Simultaneous measurement of  $\beta$ -amyloid(1–42), total Tau, and phosphorylated Tau (Thr181) in cerebrospinal fluid by the xMAP technology. *Clin. Chem.* 51, 336–345. doi:10.1373/clinchem.2004.039347.
- Ossenkoppele, R., Smith, R., Ohlsson, T., Strandberg, O., Mattsson, N., Insel, P.S., Palmqvist, S., Hansson, O., 2019. Associations between tau, A $\beta$ , and cortical thickness with cognition in Alzheimer disease. *Neurology* 92, e601–e612. doi:10.1212/wnl.0000000000006875.
- Palmqvist, S., Janelidze, S., Stomrud, E., Zetterberg, H., Karl, J., Zink, K., Bittner, T., Mattsson, N., Eichenlaub, U., Blennow, K., Hansson, O., 2019. Performance of fully automated plasma assays as screening tests for Alzheimer disease-related  $\beta$ -amyloid status. *JAMA Neurol.* 76, 1060–1069. doi:10.1001/jamaneurol.2019.1632.
- Palmqvist, S., Mattsson, N., Hansson, O., 2016. Cerebrospinal fluid analysis detects cerebral amyloid- $\beta$  accumulation earlier than positron emission tomography. *Brain* 139, 1226–1236. doi:10.1093/brain/aww015.
- Palmqvist, S., Schöll, M., Strandberg, O., Mattsson, N., Stomrud, E., Zetterberg, H., Blennow, K., Landau, S., Jagust, W., Hansson, O., 2017. Earliest accumulation of  $\beta$ -amyloid occurs within the default-mode network and concurrently affects brain connectivity. *Nat. Commun.* 8. doi:10.1038/s41467-017-01150-x.
- Schindler, S.E., Bollinger, J.G., Ovod, V., Mawuenyega, K.G., Li, Y., Gordon, B.A., Holtzman, D.M., Morris, J.C., Benzinger, T.L.S., Xiong, C., Fagan, A.M., Bateman, R.J., 2019. High-precision plasma  $\beta$ -amyloid at 40 predicts current and future brain amyloidosis. *Neurology* doi:10.1212/wnl.0000000000008081.
- Schöll, M., Lockhart, S.N., Schonhaut, D.R., O'Neil, J.P., Janabi, M., Ossenkoppele, R., Baker, S.L., Vogel, J.W., Faria, J., Schwimmer, H.D., Rabinovici, G.D., Jagust, W.J., 2016. PET imaging of tau deposition in the aging human brain. *Neuron* 89, 971–982. doi:10.1016/j.neuron.2016.01.028.
- Shaw, L.M., Vanderstichele, H., Knopik-Czajka, M., Clark, C.M., Aisen, P.S., Petersen, R.C., Blennow, K., Soares, H., Simon, A., Lewczuk, P., Dean, R., Siemers, E., Potter, W., Lee, V.M., Trojanowski, J.Q., 2009. Cerebrospinal fluid biomarker signature in Alzheimer's disease neuroimaging initiative subjects. *Ann. Neurol.* 65, 403–413. doi:10.1002/ana.21610.
- Sperling, R.A., Mormino, E.C., Schultz, A.P., Betensky, R.A., Papp, K.V., Amariglio, R.E., Hanseuew, B.J., Buckley, R., Chhatwal, J., Hedden, T., Marshall, G.A., Quiroz, Y.T., Donovan, N.J., Jackson, J., Gatchel, J.R., Rabin, J.S., Jacobs, H., Yang, H.S., Proczki, M., Kim, D.R., Rentz, D.M., Johnson, K.A., 2019. The impact of amyloid-beta and tau on prospective cognitive decline in older individuals. *Ann. Neurol.* 85, 181–193. doi:10.1002/ana.25395.
- Villemeagne, V.L., Burnham, S., Bourgeat, P., Brown, B., Ellis, K.A., Salvado, O., Szeoke, C., Macaulay, S.L., Martins, R., Maruff, P., Ames, D., Rowe, C.C., Masters, C.L., 2013. Amyloid  $\beta$  deposition, neurodegeneration, and cognitive decline in sporadic Alzheimer's disease: a prospective cohort study. *Lancet Neurol.* 12, 357–367. doi:10.1016/S1474-4422(13)70044-9.
- Wood, S.N., 1994. Monotonic smoothing splines fitted by cross validation. *SIAM* 15, 1126–1133. doi:10.1137/0915069.
- Zetterberg, H., Mattsson, N., 2014. Understanding the cause of sporadic Alzheimer's disease. *Expert Rev. Neurother.* 14, 621–630. doi:10.1586/14737175.2014.915740.

# Paper III





# Determining clinically meaningful decline in preclinical Alzheimer disease

Philip S. Insel, MS, Michael Weiner, MD, R. Scott Mackin, PhD, Elizabeth Mormino, PhD, Yen Ying Lim, PhD, Erik Stomrud, MD, PhD, Sebastian Palmqvist, MD, PhD, Colin L. Masters, MD, Paul T. Maruff, PhD, Oskar Hansson, MD, PhD, and Niklas Mattsson, MD, PhD

*Neurology*® 2019;93:e1-e12. doi:10.1212/WNL.0000000000007831

## Correspondence

Mr. Insel  
philipinsel@gmail.com

## Abstract

### Objective

To determine the time required for a preclinical Alzheimer disease population to decline in a meaningful way, use estimates of decline to update previous clinical trial design assumptions, and identify factors that modify  $\beta$ -amyloid ( $A\beta$ )-related decline.

### Methods

In 1,120 cognitively unimpaired individuals from 3 international cohorts, we estimated the relationship between  $A\beta$  status and longitudinal changes across multiple cognitive domains and assessed interactions between  $A\beta$  and baseline factors. Power analyses were performed to explore sample size as a function of treatment effect.

### Results

Cognitively unimpaired  $A\beta$ + participants approach mild cognitive impairment (MCI) levels of performance 6 years after baseline, on average. Achieving 80% power in a simulated 4-year treatment trial, assuming a 25% treatment effect, required 2,000 participants/group. Multiple factors interacted with  $A\beta$  to predict cognitive decline; however, these findings were all cohort-specific. Despite design differences across the cohorts, with large sample sizes and sufficient follow-up time, the  $A\beta$ + groups declined consistently on cognitive composite measures.

### Conclusions

A preclinical AD population declines to the cognitive performance of an early MCI population in 6 years. Slowing this rate of decline by 40%–50% delays clinically relevant impairment by 3 years—a potentially meaningful treatment effect. However, assuming a 40%–50% drug effect highlights the difficulties in preclinical AD trial design, as a more commonly assumed treatment effect of 25% results in a required sample size of 2,000/group. Designers of preclinical AD treatment trials need to prepare for larger and longer trials than are currently being considered. Interactions with  $A\beta$  status were inconsistent and not readily generalizable.

## RELATED ARTICLE

### Editorial

The search for meaning in preclinical Alzheimer disease clinical trials

Page 139

## MORE ONLINE

### Podcast

Dr. Gregory Day talks with Dr. Philip Insel about his paper on determining clinically meaningful decline in preclinical Alzheimer disease.

[NPub.org/d7tb1d](https://www.ncbi.nlm.nih.gov/podcasts/npub/0000000000007831)

From the Center for Imaging of Neurodegenerative Diseases (M.W., R.S.M.), Department of Veterans Affairs Medical Center; Departments of Radiology and Biomedical Imaging (P.S.I., M.W.) and Psychiatry (P.S.I., R.S.M.), University of California, San Francisco; Clinical Memory Research Unit, Faculty of Medicine (P.S.I., E.S., S.P., O.H., N.M.), Memory Clinic (E.S., S.P., O.H.) and Department of Neurology (N.M.), Skåne University Hospital, and Wallenberg Center for Molecular Medicine (N.M.), Lund University, Sweden; Department of Neurology and Neurological Sciences (E.M.), Stanford University, CA; The Florey Institute (Y.Y.L., C.L.M., P.T.M.), The University of Melbourne; and CogState (P.T.M.), Melbourne, Australia.

Go to [Neurology.org/N](https://www.neurology.org/N) for full disclosures. Funding information and disclosures deemed relevant by the authors, if any, are provided at the end of the article. The Article Processing Charge was funded by Swedish Research Council.

This is an open access article distributed under the terms of the Creative Commons Attribution License 4.0 (CC BY), which permits unrestricted use, distribution, and reproduction in any medium, provided the original work is properly cited.

## Glossary

**A $\beta$**  =  $\beta$ -amyloid; **AD** = Alzheimer disease; **ADNI** = Alzheimer's Disease Neuroimaging Initiative; **AIBL** = Australian Imaging, Biomarkers & Lifestyle; **AIC** = Akaike information criterion; **BioFINDER** = Biomarkers for Identifying Neurodegenerative Disorders Early and Reliably; **CDR** = Clinical Dementia Rating; **CDR-SB** = CDR sum of boxes; **dADASc** = Delayed Word Recall from the Alzheimer's Disease Assessment Scale–Cognitive Subscale; **dMemory** = Logical Memory Delayed Recall; **MCI** = mild cognitive impairment; **MMSE** = Mini-Mental State Examination; **OR** = odds ratio; **PACC** = Preclinical Alzheimer's Cognitive Composite; **PiB** = Pittsburgh compound B; **SUVr** = standardized uptake value ratio; **Trails B** = Trail-Making Test B.

To effectively alter the course of Alzheimer disease (AD), interventions may need to occur during the preclinical stage of the disease, before the onset of clinical symptoms.<sup>1</sup> Demonstrating that treatments are effective during the preclinical stage will require understanding the magnitude of early  $\beta$ -amyloid (A $\beta$ )–related cognitive decline in cognitively unimpaired adults.<sup>2</sup> Defining meaningful decline will help determine the time frame for subtle cognitive changes to progress to incipient functional decline and to identify an optimal treatment window.

The association between A $\beta$  status and cognition in preclinical AD varies widely.<sup>3–9</sup> The design of the A4 study,<sup>10</sup> the first clinical trial in preclinical AD, was based on early estimates of A $\beta$ -related decline using the Alzheimer's Disease Neuroimaging Initiative (ADNI)<sup>11</sup> and the Australian Imaging, Biomarkers & Lifestyle (AIBL) Study.<sup>12</sup> The effect of A $\beta$  on cognitive decline in AIBL was 4-fold the magnitude of the effect in ADNI, highlighting an inconsistent picture of early cognitive decline and uncertain implications for powering a trial in early AD. Understanding how sampling variation and study design features influence estimates of cognitive decline will optimize the design of trials in preclinical AD.

The aims of this study were to harmonize several large studies in order to (1) determine the time required for a preclinical AD population to decline in a clinically meaningful way, (2) characterize how decline differs by cognitive domain, (3) update previous study design assumptions regarding sample size, power, and the required treatment effect, and (4) identify factors that modify A $\beta$ -related decline.

## Methods

### Standard protocol approvals, registrations, and patient consents

This study was approved by the institutional review boards of all of the participating institutions. Informed written consent was obtained from all participants at each site.

### Participants

Participants from each of the cohorts ADNI, AIBL, and the Swedish Biomarkers for Identifying Neurodegenerative Disorders Early and Reliably (BioFINDER) study<sup>13</sup> were included if they were classified as cognitively normal at baseline, were tested for A $\beta$  biomarkers (using either CSF or PET), and

were followed longitudinally with neuropsychological examinations.<sup>11–13</sup> Participants were excluded from any of the 3 studies if they had a major neurologic or psychiatric illness or a history of substance abuse. In addition, ADNI participants were excluded if the screening MRI showed evidence of infection, infarction, or other focal lesions, including multiple lacunes or lacunes in a critical memory structure. MRI results were not part of the exclusionary criteria for AIBL or BioFINDER, but BioFINDER participants were excluded if they refused MRI or lumbar puncture. Detailed exclusionary criteria for ADNI can be found at [adni.loni.usc.edu/wp-content/uploads/2008/07/adni2-procedures-manual.pdf](http://adni.loni.usc.edu/wp-content/uploads/2008/07/adni2-procedures-manual.pdf) and for BioFINDER at [biofinder.se/biofinder\\_cohorts/cognitively-healthy-elderly/](http://biofinder.se/biofinder_cohorts/cognitively-healthy-elderly/). We also included 305 participants enrolled into the early mild cognitive impairment (MCI) cohort in ADNI (defined by a subjective memory complaint and a delayed logical memory score of 9–11 for those with 16 or more years of education, 5–9 for 8–15 years of education, or 3–6 for 0–7 years of education, where possible scores range from 0 to 25)<sup>14</sup> for a comparative analysis. The extensions of ADNI introduced the distinction of MCI into early and late MCI in the attempt to define an earlier point in time for disease detection. Late MCI refers to the original definition of MCI (performance for 1.5 SD below the normative mean), whereas in early MCI, impairment is defined as performance between 1.0 SD and 1.5 SD below the normative mean on a standard test. Because of recent evidence of an artificially low reversion rate from MCI to control in ADNI,<sup>15</sup> we excluded 7 early MCI participants who consistently had a global Clinical Dementia Rating (CDR) score of zero after screening in a sensitivity analysis.

Data on memory complaints in the controls were available in AIBL and ADNI. In AIBL, participants with a memory complaint were identified by the response to the question, “Do you have difficulties with your memory?” In ADNI, the participant was required to have a significant memory concern as reported by the participant, study partner, or clinician and a score >16 on the first 12 items of the Cognitive Change Index.

### A $\beta$ biomarkers

A $\beta$  status was defined by PET imaging if available (all AIBL and a majority of ADNI participants), and otherwise by CSF biomarkers (all BioFINDER and a small proportion of ADNI participants). PET imaging was done using <sup>18</sup>F-florbetapir PET in ADNI and using <sup>18</sup>F-florbetapir, <sup>11</sup>C–Pittsburgh

compound B (PiB), or  $^{18}\text{F}$ -flutemetamol PET in AIBL. Methods to acquire and process imaging data were described previously.<sup>16–18</sup> CSF samples were collected at baseline by lumbar puncture. CSF methods have been described previously.<sup>19–21</sup> In short, ADNI CSF samples were analyzed for CSF A $\beta$ 42 using the AlzBio3 assay (Fujirebio, Ghent, Belgium) on the xMAP Luminex platform. BioFINDER CSF samples were analyzed for CSF A $\beta$ 42 and A $\beta$ 40 using ELISA assays (ADx/EUROIMMUN AG, Lübeck, Germany). For ADNI participants, A $\beta$ + was defined as  $^{18}\text{F}$ -florbetapir PET standardized uptakevalue ratio (SUVR) >1.1 (n = 381)<sup>22</sup> or CSF A $\beta$ 42 <192 ng/L (n = 62).<sup>19</sup> For AIBL, A $\beta$ + was defined as  $^{18}\text{F}$ -florbetapir PET SUVR >1.1 (n = 72),  $^{11}\text{C}$ -PiB PET SUVR >1.5 (n = 201), or  $^{18}\text{F}$ -flutemetamol SUVR >0.62 (n = 75).<sup>23</sup> In BioFINDER, A $\beta$ + was defined as CSF A $\beta$ 42/A $\beta$ 40 <0.1.<sup>24</sup>

### Cognitive testing

Participants were followed for up to 6 years for neuropsychological testing. In ADNI, tests were administered annually with an additional test at month 6 for most measures. In AIBL, tests were administered every 18 months. In BioFINDER, tests were administered every 2 years. The Preclinical Alzheimer's Cognitive Composite (PACC)<sup>25</sup> and its individual components were the primary outcomes compared in the 3 cohorts. This composite was developed specifically to be sensitive to early cognitive changes in AD and is being incorporated in clinical trials of disease-modifying treatments.<sup>10</sup> Substitutions representing the same cognitive domain were made in the case where the original PACC components were not available or had limited follow-up in a cohort's neuropsychological battery, following previous procedures.<sup>10,25</sup> Visits where all components or substitutions were available were included. For ADNI, the modified PACC comprised the Mini-Mental State Examination (MMSE), Logical Memory Delayed Recall (dMemory), Trail-Making Test B (Trails B), and the Delayed Word Recall from the Alzheimer's Disease Assessment Scale–Cognitive Subscale (dADASc). For AIBL, the PACC was constructed using the MMSE, dMemory, Digit Symbol Substitution Test, and the Delayed Recall from the California Verbal Learning Test (dCVLT). For BioFINDER, the PACC consisted of the MMSE, dADASc, and Trails B. To calculate the composite, z scores of the individual components were taken over all time points and then summed. This sum was then standardized to the mean and SD of the baseline score of the sum.

The PACC includes 2 measures of delayed memory recall; however, because only one delayed memory measure was available in BioFINDER, dADASc was given twice the weight in BioFINDER to reflect the contribution of delayed memory recall in the composite. Immediate recall (logical memory for ADNI and AIBL, Alzheimer's Disease Assessment Scale–Cognitive Subscale word recall for BioFINDER) was evaluated as a measure of baseline memory ability to predict changes in the PACC. The CDR sum of

boxes (CDR-SB) was also evaluated as an outcome measure.

### Statistical analysis

Longitudinal measures were modeled using generalized least squares regression assuming a compound symmetric covariance structure.<sup>26</sup> To capture departures from linearity in the trajectory of the neuropsychological measures, continuous time from baseline test was parameterized using restricted cubic splines.<sup>27</sup> Cubic splines are functions of polynomials allowing flexibility in the estimation of trajectories over time. Time was modeled with 3 spline knots, 2 at the boundaries and 1 at median follow-up. Differences in trajectories between A $\beta$ + and A $\beta$ - groups were tested using interactions between the 2 measures for time and the group factor using likelihood ratio tests and change in the Akaike information criterion (AIC), a model selection tool.<sup>28</sup> A lower value of AIC indicates a better fitting model. Baseline age was also modeled using restricted cubic splines to capture its nonlinear effect on cognition. Models included the 2 spline-estimated measures for baseline age; sex; years of education, where education was categorized as 0–12 years, 13–15 years, and 16 or more years; the interaction between A $\beta$  status and the 2 measures for time; and the main effects for A $\beta$  status and time.

We also evaluated interactions between A $\beta$  status and demographics (baseline age, sex, education), *APOE* (presence of at least one  $\epsilon 4$  allele), memory complaint, and baseline memory, and their effect on changes in the PACC. These models included all the terms described above as well as the 3-way interaction between time, A $\beta$  status, and the demographic term. The interaction with age was evaluated using the 2 spline-estimated measures.

To estimate power for hypothetical clinical trials, mixed models of repeated measures<sup>29</sup> were used to estimate the variance components of the change from baseline in the PACC for the A $\beta$ + subjects in each cohort. To mirror current preclinical trial design,<sup>10</sup> A $\beta$ + subjects with very high cognitive scores (dMemory >15 for ADNI [n = 32] and AIBL [n = 12] and dADASc >8 in BioFINDER [n = 29]) were excluded in order to remove “supernormals.” This was done to mitigate the inclusion of participants with little or no sign of near-term decline in order to increase the likelihood of decline in the placebo group and improve power. Model estimates were then used to calculate the power for 4- and 6-year clinical trials, assuming a range of sample sizes and drug effects, a 6-month visit interval, and a 30% dropout rate. Individual cohort estimates of change from baseline and variance were then meta-analyzed to get combined estimates of change over time.<sup>30</sup>

In order to provide a context for meaningful clinical decline in the cognitively normal participants, we compared the baseline PACC scores in the normal participants to the PACC scores in the ADNI early MCI participants (stratified by A $\beta$  status). We then evaluated the mean time for the average preclinical



AD participant to reach the mean baseline PACC score in the early MCI groups.

Baseline associations between demographics and A $\beta$  positivity were assessed using the Wilcoxon rank-sum test for continuous variables and a  $\chi^2$  test for categorical variables. Reductions of AIC >2 and *p* values <0.05 were considered significant. All analyses were done in R v3.4.3 (r-project.org). GLS models were fit using the *gls* function from the *nlme* package.

### Data availability

Data from the ADNI and AIBL cohorts are publicly available. Data from BioFINDER may be requested.

## Results

### Cohort characteristics

A total of 443 cognitively healthy controls from ADNI, 348 from AIBL, and 329 from BioFINDER were included in the study. A $\beta$ + groups were older, had a higher frequency of APOE  $\epsilon$ 4 positivity, and performed significantly worse on several cognitive tests at baseline, compared to A $\beta$ - groups, in all cohorts (table 1). The proportion of APOE  $\epsilon$ 4 positivity in the A $\beta$ + group was similar in BioFINDER (55%) and AIBL (53%) and lower in ADNI (44%). Education and sex were not associated with A $\beta$  positivity in AIBL or BioFINDER; however, A $\beta$ + ADNI participants were more likely to be female and have less education compared to A $\beta$ - ADNI participants. The majority of ADNI participants had 16 or more years of education, whereas the majority of both AIBL and BioFINDER participants had fewer than 16 years of education. There was no association between subjective memory complaint and A $\beta$  status in either ADNI or AIBL (subjective memory complaint data were not available in BioFINDER).

There was considerable variability in attrition rates across the 3 cohorts. At 4 years of follow-up, ADNI retained 46% of its participants; however, dropout was not associated with age, sex, education, A $\beta$  status, or baseline memory performance (*p* > 0.13). At 4 years, BioFINDER retained 69% of its participants. Women were less likely to drop out (odds ratio [OR] = 0.78, *p* = 0.01), participants with more education were more likely to drop out (OR = 1.35, *p* = 0.04), and older age was associated with increased drop out (OR = 1.28 for 1 SD increase in age, *p* < 0.001). AIBL retained 90% of its participants, but older age was associated with increased drop out (OR = 1.26 for 1 SD increase in age, *p* = 0.01).

### Cognitive changes

A $\beta$ + participants declined significantly more on the PACC and all individual components of the PACC compared to A $\beta$ - participants, in all 3 cohorts, with the exception of Trails B in BioFINDER (*p* = 0.08). Estimates and longitudinal plots of cognition are shown in figure 1. Estimates of the change from baseline, confidence intervals, and the residual SD for each visit and group are shown in table 2.

At year 4, the A $\beta$ + groups declined by -0.45 points on the PACC (ADNI), -0.48 points (BioFINDER), and -0.53 points (at 4½ years, AIBL) (table 2). At year 4, the A $\beta$ - group improved 0.09 points on the PACC in ADNI and declined by -0.14 points in BioFINDER and -0.02 points in AIBL.

### Clinical significance

To evaluate decline and to characterize what might be considered a clinically significant change, we compared the scores of the cognitively normal participants to the baseline scores of the early MCI participants in ADNI. The mean PACC score in A $\beta$ - and A $\beta$ + early MCI participants at baseline was -1.01 and -1.30, respectively (figure 2). Six years after baseline, the estimated PACC score combined across cohorts of the preclinical AD groups was midway between the A $\beta$ - and A $\beta$ + early MCI performance. Similarly, the early MCI A $\beta$ - and A $\beta$ + scores at baseline on the CDRSB were 1.22 and 1.38, respectively, whereas the preclinical AD groups averaged about 1.0 at 6 years.

On each of the MMSE, delayed list learning, and executive function, the cognitively normal A $\beta$ + groups averaged worse scores than both MCI groups by 6 years after baseline. The cognitively normal A $\beta$ + groups did not approach the MCI groups' delayed logical memory scores by 6 years after baseline. Note that delayed logical memory was not available in BioFINDER.

In a sensitivity analysis, 7 early MCI participants who consistently had a global CDR of zero after screening were excluded. The reduced sample scores were slightly worse than the full MCI sample with A $\beta$ - and A $\beta$ + PACC scores of -1.02 and -1.33, respectively, and CDR-SB scores of 1.23 and 1.39.

### Power

Using estimates of change and variance, we calculated the power for hypothetical 4- and 6-year clinical trials for each cohort, assuming a 30% dropout rate, and various sample sizes and drug effects (figure 3). In 4-year trials, assuming a 25% drug effect, i.e., a 25% slowing of cognitive decline in the treatment group, the required sample size to reach 80% power was 2,000 per group for the estimate combining all cohorts. Assuming a larger effect size of 35%, the required sample size to reach 80% power was 1,000 per group on average.

In 6-year trials, assuming a 25% drug effect, the required sample size to reach 80% power was about 600 per group for the estimate combining all cohorts. Assuming a 35% effect size, the required sample size to reach 80% power was 300 per group on average.

### A $\beta$ interactions

The interactions between A $\beta$  status and baseline factors to predict cognitive decline on the PACC were also assessed. Plots of the amyloid groups at different levels of the significant interacting factors, *p* values, and the change in AIC are shown in figure 4. In AIBL, there were significant interactions between

**Table 1** Baseline characteristics

Characteristic	A $\beta$ +	A $\beta$ -	<i>p</i> Value
<b>ADNI</b>	N = 165	N = 278	
Years of follow-up	4.1 (2.8)	4.3 (2.9)	0.28
Age	75.1 (5.5)	73.3 (5.9)	0.001
Female, n (%)	99 (60)	132 (47.5)	0.01
Education, y			0.002
0-12	18 (10.9)	25 (9.0)	
13-15	46 (27.9)	42 (15.1)	
16+	101 (61.2)	211 (75.9)	
Memory complaint, n (%)	42 (25.5)	64 (23)	0.64
APOE $\epsilon$ 4+, n (%)	73 (44.2)	53 (19.1)	<0.001
MMSE	29.1 (1.1)	29.0 (1.2)	0.68
dMemory	12.8 (3.4)	13.4 (3.2)	0.05
dADASc	7.0 (1.8)	7.2 (1.8)	0.33
Trails B	93.8 (44.4)	79.7 (39.4)	<0.001
<b>BioFINDER</b>	N = 85	N = 244	
Years of follow-up	3.6 (1.8)	3.6 (1.7)	0.55
Age	74.7 (5.0)	73.3 (5.0)	0.02
Female, n (%)	56 (65.9)	142 (58.2)	0.26
Education, y			0.99
0-12	51 (60.0)	146 (59.8)	
13-15	20 (23.5)	58 (23.8)	
16+	14 (16.5)	40 (16.4)	
Memory complaint, n (%)	—	—	—
APOE $\epsilon$ 4+, n (%)	46 (54.8)	46 (19)	<0.001
MMSE	29.0 (0.9)	29.1 (1.0)	0.24
dMemory	—	—	—
dADASc	7.4 (2.2)	8.2 (1.8)	0.001
Trails B	111.8 (48.7)	102.4 (50.8)	0.04
<b>AIBL</b>	N = 100	N = 248	
Years of follow-up	4.9 (1.9)	5.9 (2.9)	<0.001
Age	73.5 (7.3)	69.1 (6.0)	<0.001
Female, n (%)	49 (49)	136 (54.8)	0.39
Education, y			0.77
0-12	40 (40.4)	104 (41.9)	
13-15	23 (23.2)	42 (16.9)	
16+	36 (36.4)	102 (41.1)	
Memory complaint, n (%)	58 (58.6)	132 (53.4)	0.45
APOE $\epsilon$ 4+, n (%)	53 (53)	58 (23.4)	<0.001

**Table 1** Baseline characteristics (continued)

Characteristic	A $\beta$ +	A $\beta$ -	<i>p</i> Value
<b>MMSE</b>	28.7 (1.2)	29.0 (1.2)	0.04
<b>dMemory</b>	11.1 (4.11)	12.1 (4.0)	0.04
<b>dCVLT</b>	11.5 (3.4)	12.2 (2.9)	0.10
<b>Digit symbol</b>	57.9 (12.9)	61.3 (13.7)	0.05

Abbreviations: A $\beta$  =  $\beta$ -amyloid; ADNI = Alzheimer's Disease Neuroimaging Initiative; AIBL = Australian Imaging, Biomarkers & Lifestyle; BioFINDER = Biomarkers for Identifying Neurodegenerative Disorders Early and Reliably; dADASc = Delayed Word Recall from the Alzheimer's Disease Assessment Scale-Cognitive Subscale; dCVLT = Delayed Recall from the California Verbal Learning Test; dMemory = Logical Memory Delayed Recall; MMSE = Mini-Mental State Examination; Trails B = Trail-Making Test B.

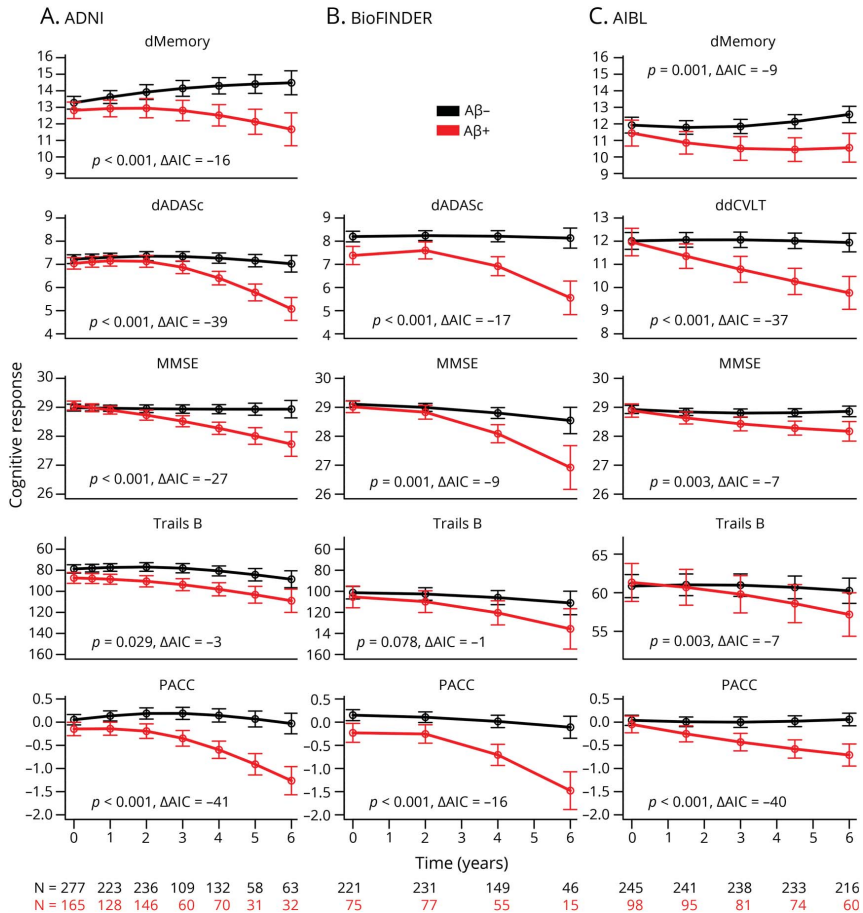
A $\beta$  and education, APOE  $\epsilon$ 4 positivity, and baseline memory. The only significant interaction in ADNI was between A $\beta$  and sex, and the only significant interaction in BioFINDER was between A $\beta$  and age. There were no significant interactions between A $\beta$  and subjective memory complaint (ADNI:  $p$  = 0.56, AIBL:  $p$  = 0.87, not available for BioFINDER).

## Discussion

The main findings of this study are (1) cognitively unimpaired A $\beta$  participants approach early MCI cognitive performance levels on general cognition and global outcomes, delayed list recall, and executive function by 6 years after baseline; (2) to achieve 80% power in a simulated treatment trial assuming a 25% treatment effect, 2,000 participants/group for a 4-year trial and 600 participants/group for a 6-year trial are required; (3) several baseline factors interacted with A $\beta$  status to predict decline on the PACC including APOE  $\epsilon$ 4 positivity, memory, and education in AIBL; age in BioFINDER; and sex in ADNI, although these findings were all cohort-specific; (4) despite considerable design differences across the cohorts, with large sample sizes and sufficient follow-up time, the cognitively unimpaired A $\beta$  groups declined consistently on cognitive composites; (5) A $\beta$  groups declined significantly faster on all cognitive tests in all cohorts, with the exception of Trails B in BioFINDER, where the A $\beta$  group declined marginally faster ( $p$  = 0.08), compared to the A $\beta$ - group.

A key question for preclinical AD trials is how to define meaningful outcomes that will support use of therapeutic interventions in people who may remain asymptomatic for many years even without treatment. Traditional AD dementia trials are frequently powered to detect a several-point difference on a global cognitive score (e.g., Alzheimer's Disease Assessment Scale-Cognitive Subscale), as well as a global/functional co-primary outcome to establish clinical meaningfulness.<sup>31</sup> Post hoc analyses of the first large trials of solanezumab in patients with mild AD showed a 34% reduction of cognitive decline and a 17% reduction of functional

**Figure 1** Cognitive change over time



Cognitive responses are plotted over time for each  $\beta$ -amyloid ( $A\beta$ ) group, in each cohort separately: (A) Alzheimer's Disease Neuroimaging Initiative (ADNI), (B) Biomarkers for Identifying Neurodegenerative Disorders Early and Reliably (BioFINDER), and (C) Australian Imaging, Biomarkers & Lifestyle (AIBL). Individual Preclinical Alzheimer's Cognitive Composite (PACC) components are shown as well as the PACC in the bottom row. Akaike information criterion and  $p$  values are shown in each plot, testing for differences between  $A\beta$  groups over time. dMemory = Logical Memory Delayed Recall; MMSE = Mini-Mental State Examination; Trails B = Trail-Making Test B.

decline.<sup>32</sup> However, these effects were not replicated in a subsequent randomized trial, which failed to show a significant treatment effect, with only an 11% reduction of cognitive decline and 15% reduction of functional decline.<sup>33</sup> In preclinical AD, the cognitive decline observed over 3–4 years is subtle, and is typically accompanied by little or no functional decline.<sup>34</sup> However, it has not been clarified what degree of decline would warrant classification as meaningful decline. To benchmark the magnitude of cognitive decline to a measure of clinical meaningfulness, we compared the scores of the cognitively unimpaired participants to those classified as early MCI—a group with incipient functional decline. The separation between these groups was just over 1 SD on the PACC, suggesting that 1 point

of additional decline in  $A\beta+$  participants compared to  $A\beta-$  participants could be taken as an approximate benchmark for clinically meaningful decline. Combining results across cohorts shows the average  $A\beta+$  participant to have the same PACC score at 6 years post baseline as the average patient with early MCI had at baseline (figure 2).  $A\beta+$  participants also reached MCI level performance at 6 years on the other cognitive outcomes, with the exception of delayed logical memory. Possible explanations for this exception include that this measure was used as inclusion criterion for enrollment. This measure was also not available in BioFINDER, the cohort demonstrating the poorest scores on all measures by the end of follow-up. Finally, delayed logical memory demonstrated a clear practice effect in

**Table 2** PACC: Change from baseline, 95% CI, and residual SD estimates

Study	Month	A $\beta$ +		A $\beta$ -		Difference ( $\Delta_{diff}$ )	95% CI	Residual SD ( $\sigma$ )	$\Delta_{diff}/\sigma$
		N	Estimate	N	Estimate				
ADNI	12	128	0.01	223	0.08	-0.08	-0.16 to 0.01	0.89	-0.09
	24	146	-0.05	236	0.14	-0.18	-0.32 to -0.04	0.89	-0.21
	36	62	-0.20	109	0.14	-0.34	-0.50 to -0.18	0.91	-0.37
	48	70	-0.45	132	0.09	-0.54	-0.72 to -0.37	1.03	-0.53
	60	31	-0.76	58	0.02	-0.78	-1.00 to -0.56	1.15	-0.68
	72	32	-1.12	63	-0.08	-1.03	-1.35 to -0.72	1.32	-0.78
BioFINDER	24	75	-0.02	221	-0.04	0.02	-0.16 to 0.20	0.70	0.03
	48	55	-0.48	149	-0.14	-0.34	-0.56 to -0.12	0.83	-0.41
	72	15	-1.25	46	-0.26	-0.99	-1.40 to -0.57	1.29	-0.77
AIBL	18	95	-0.20	241	-0.03	-0.17	-0.29 to -0.05	0.78	-0.22
	36	81	-0.38	238	-0.04	-0.34	-0.52 to -0.17	0.83	-0.41
	54	74	-0.53	233	-0.02	-0.51	-0.69 to -0.34	1.04	-0.49
	72	60	-0.66	216	0.02	-0.68	-0.88 to -0.48	0.98	-0.70

Abbreviations: A $\beta$  =  $\beta$ -amyloid; ADNI = Alzheimer's Disease Neuroimaging Initiative; AIBL = Australian Imaging, Biomarkers & Lifestyle; BioFINDER = Biomarkers for Identifying Neurodegenerative Disorders Early and Reliably; CI = confidence interval; PACC = Preclinical Alzheimer's Cognitive Composite.

the A $\beta$ - group (figure 2), with the cognitively unimpaired participants taking this test 6 times over follow-up, compared to one time for the MCI participants.

Based on the PACC estimates, a treatment effect of 40%–50% would be required to delay the cognitive decline of a group of A $\beta$ + participants from reaching the 1 SD milestone by 3 years. Delaying the cognitive decline equivalent to the level of the average early MCI patient by 3 years may be a clinically meaningful treatment effect. But 40%–50% is a large treatment effect and highlights the difficulties in preclinical AD trial design. However, the observation that clinically meaningful decline is reached within 6 years offers strong support for the use of a cognitive composite in trials that are shorter than 6 years, since short term cognitive decline can be conceptualized as a proxy for downstream functional changes. With meaningful continuous cognitive changes occurring prior to an MCI diagnosis, these results, as well as recent reports,<sup>35</sup> argue against the use of a time-to-MCI endpoint in preclinical AD trials.

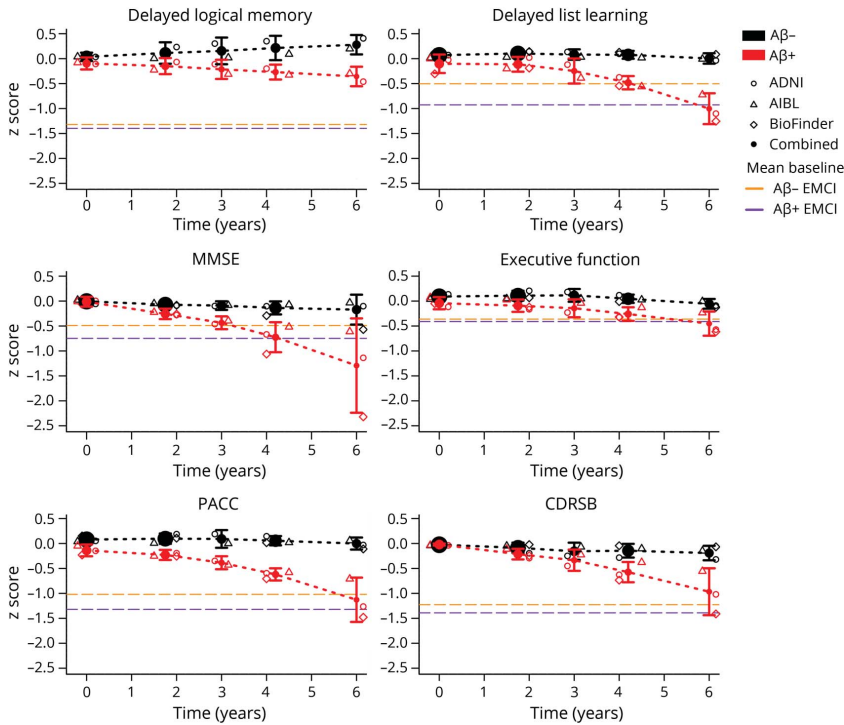
The estimated sample size or trial length requirements are sobering. Previously reported sample size and drug effect requirements of 500/group with a 30%–50% effect size in a 3-year trial were optimistic and based on approximately 20% of the data available in this study.<sup>10</sup> In order to reliably achieve 80% power for a modest, real-world effect size of 20%–30%, investors in AD research for therapeutics development will have to prepare to support larger and longer trials than are currently envisaged.

There were several significant interactions between A $\beta$  status and baseline factors. However, no interaction was observed in

more than one cohort. In AIBL, the combination of A $\beta$  status and low education, APOE  $\epsilon$ 4 positivity, or low baseline memory all led to increased rates of decline on the PACC. Decline in the A $\beta$ + groups did not depend on APOE  $\epsilon$ 4 status in ADNI or BioFINDER; however, in AIBL, little decline was observed in A $\beta$ + participants who were not also APOE  $\epsilon$ 4+ (figure 4), as was reported previously.<sup>36,37</sup> Evidence for additional risk of cognitive decline for individuals who are both A $\beta$ + and APOE  $\epsilon$ 4+ had been incorporated into the design of a phase 2b/3 trial in preclinical AD ([clinicaltrials.gov/ct2/show/NCT02569398](https://clinicaltrials.gov/ct2/show/NCT02569398)); however, this pattern was observed in only one of the 3 cohorts studied here. The additional decline observed in the A $\beta$ + participants who also had low baseline memory in AIBL is consistent with previous reports.<sup>38</sup> Still, despite wide separation at baseline, high and low baseline memory (and also high and low education) groups declined in parallel over time in both ADNI and BioFINDER. The lack of replicability of these interactions across cohorts suggests that if there are true underlying effects of these baseline factors that modify the A $\beta$ /cognition relationship, they are mild, or they depend on other/complex interactions. Another possibility is that their identification was the consequence of type I error, although the strength of the associations in AIBL (but not ADNI, reported previously<sup>39</sup> or BioFINDER) would survive a Bonferroni correction. Our findings caution against relying on interactions between A $\beta$  and demographic/clinical factors when selecting participants for preclinical AD trials.

There were considerable design differences among the 3 study cohorts including differences in geographic region, cognitive measures, visit frequency, and sampling characteristics.

**Figure 2** Meta-estimates of change



Meta-estimates of change over time are shown by  $\beta$ -amyloid ( $A\beta$ ) group. Individual cohort estimates are also shown. The mean baseline early mild cognitive impairment scores are shown in dashed purple for  $A\beta^-$  and dashed orange for  $A\beta^+$ . ADNI = Alzheimer's Disease Neuroimaging Initiative; AIBL = Australian Imaging, Biomarkers & Lifestyle; BioFINDER = Biomarkers for Identifying Neurodegenerative Disorders Early and Reliably; CDRSB = CDR sum of boxes; EMCI = early mild cognitive impairment; MMSE = Mini-Mental State Examination; PACC = Preclinical Alzheimer's Cognitive Composite.

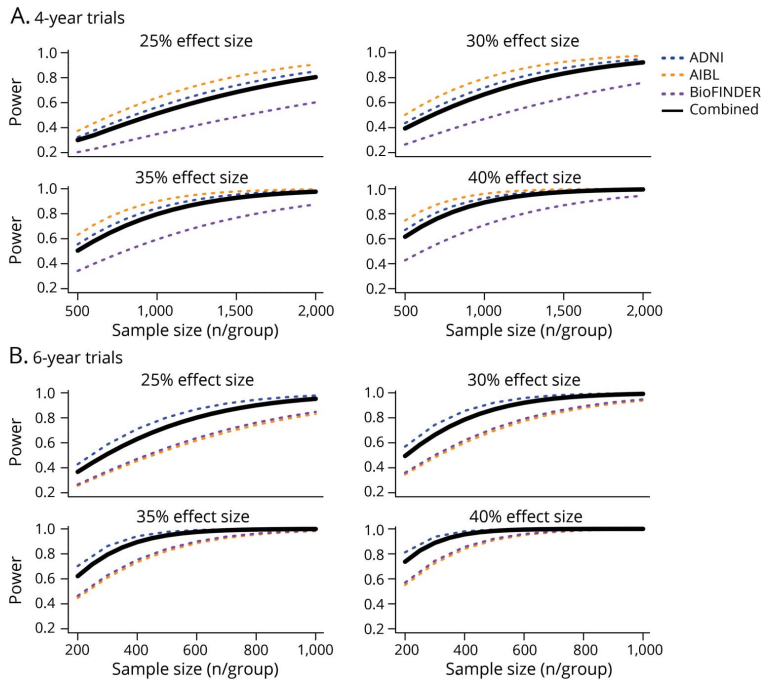
Despite these differences, the estimates of decline observed on the PACC in the  $A\beta^+$  groups at 4 years were remarkably similar:  $-0.45$  points in ADNI,  $-0.48$  in BioFINDER, and  $-0.53$  (at  $4\frac{1}{2}$  years) in AIBL (table 2). Where the cohorts differed was in the change in the  $A\beta^-$  group:  $0.09$  in ADNI,  $-0.14$  in BioFINDER, and  $-0.02$  in AIBL. The lower power estimate for BioFINDER for a clinical trial can be traced back to the additional decline observed in the  $A\beta^-$  group, which may be due in part to including participants with presence of cerebrovascular pathology such as white matter lesions (not excluded from BioFINDER, but may have been excluded from ADNI).<sup>40,41</sup> Cognitive reserve may also play a role, given the lower levels of education in BioFINDER compared to both ADNI and AIBL.

The  $A\beta$  group trajectories on the PACC were similar, though there was variation in the shape of the trajectories for some of the individual components. One design feature that may influence trajectory differences is test frequency. ADNI participants were tested every 6 months over the first year and every

year thereafter, whereas AIBL participants were tested every 18 months and BioFINDER, every 24 months. The increased test frequency and higher levels of education in ADNI may have contributed to a tendency to improve over time as seen in dMemory (figure 1). Despite this variation in dMemory slope,  $A\beta$  group separation over time was preserved in ADNI and AIBL. For delayed list learning, all  $A\beta^-$  groups remained stable, and all  $A\beta^+$  groups showed similar decline over the total follow-up time. Combining individual components into the composite seemed to mitigate individual domain trajectory differences (figure 2). Overall, the  $A\beta$  groups across all 3 cohorts started to diverge reliably around 3 years after baseline.

One of the main limitations of this study is the variation of available measures used to construct the composite cognitive scores (i.e., the PACC) in each of the cohorts. While we included the domains represented in the original PACC, it remains unclear how these substitutions may affect the estimates of  $A\beta$ -related cognitive decline. Another limitation is

**Figure 3** Power



Hypothetical clinical trial power is plotted against sample size per treatment group, for each of 4 assumed treatment effect sizes and 2 trial lengths. Individual cohort power curves and a combined estimate are shown. Sample sizes range from (A) 500 to 2,000 per group for 4-year trials and (B) 200 to 1,000 per group for 6-year trials. ADNI = Alzheimer's Disease Neuroimaging Initiative; BioFINDER = Biomarkers for Identifying Neurodegenerative Disorders Early and Reliably.

that with strict exclusionary criteria, the participants in these studies have few comorbidities, lack diversity, and do not mirror the general population. Clinical trials frequently use similar exclusionary criteria and may also lack generalizability. An additional limitation to all studies trying to inform disease-modifying AD trials is that without any information regarding potential effects of treatments, the power to detect a hypothetical effect is speculative.

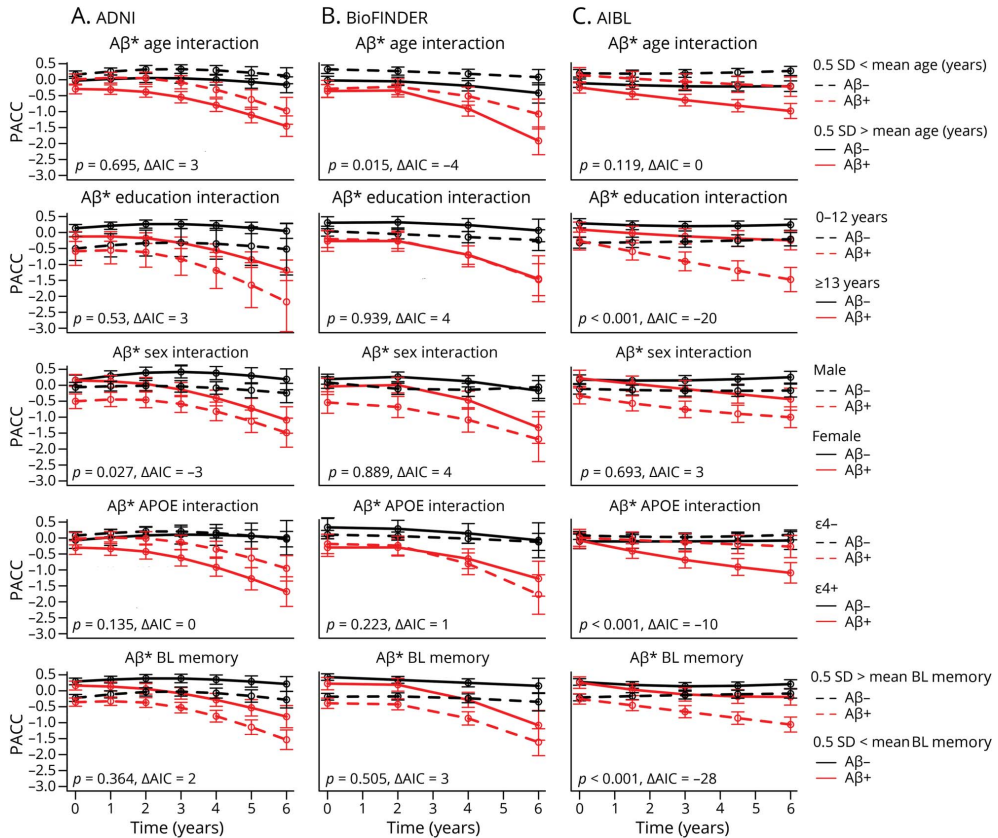
Average cognitively normal A $\beta$ + participants approach early MCI cognitive performance levels 6 years after baseline. Comparing these 3 cohorts side by side demonstrates that large sample sizes and sufficiently long follow-up times result in consistent estimates of decline in preclinical AD. Despite substantial design and sampling differences, these results support the potential for internationally conducted clinical trials in preclinical AD. However, it is likely that designers of preclinical AD treatment trials will have to prepare for larger and longer trials than are currently considered.

### Author contributions

P.S. Insel: drafting/ revising the manuscript, study concept or design, analysis or interpretation of data, accepts responsibility for conduct of research and final approval, statistical analysis, study supervision. M. Weiner: drafting/

revising the manuscript, analysis or interpretation of data, accepts responsibility for conduct of research and final approval, study supervision. R.S. Mackin: drafting/ revising the manuscript, analysis or interpretation of data, accepts responsibility for conduct of research and final approval. E. Mormino: drafting/ revising the manuscript, accepts responsibility for conduct of research and final approval. Y.Y. Lim: drafting/ revising the manuscript, analysis or interpretation of data, accepts responsibility for conduct of research and final approval, acquisition of data. E. Stomrud: data acquisition, accepts responsibility for conduct of research and final approval, acquisition of data, study supervision. S. Palmqvist: data acquisition, accepts responsibility for conduct of research and final approval, study supervision, obtaining funding. C.L. Masters: study concept or design, accepts responsibility for conduct of research and final approval, study supervision. P. Maruff: drafting/ revising the manuscript, data acquisition, study concept or design, accepts responsibility for conduct of research and final approval, study supervision, obtaining funding. O. Hansson: drafting/ revising the manuscript, data acquisition, study concept or design, accepts responsibility for conduct of research and final approval, acquisition of data, study supervision, obtaining funding. N. Mattsson: drafting/ revising the manuscript, data acquisition, study concept or design, analysis or interpretation of data,

**Figure 4**  $\beta$ -amyloid ( $A\beta$ ) interactions



Interactions between  $A\beta$  group and age, education, sex, *APOE*, and baseline memory are shown for each cohort: (A) Alzheimer's Disease Neuroimaging Initiative (ADNI), (B) Biomarkers for Identifying Neurodegenerative Disorders Early and Reliably (BioFINDER), (C) Australian Imaging, Biomarkers & Lifestyle (AIBL). Akaike information criterion (AIC) and  $p$  values are shown in each plot, testing for the significance of interactions in predicting Preclinical Alzheimer's Cognitive Composite (PACC) change over time.

accepts responsibility for conduct of research and final approval, acquisition of data, study supervision, study funding.

### Study funding

Different funding agencies supported work at Lund University (for overall study coordination, and for the BioFINDER study) and the ADNI and AIBL studies. Work at Lund University in the authors' laboratory is generously supported by The Knut and Alice Wallenberg foundation, the Medical Faculty at Lund University, Region Skåne, the European Research Council, the Swedish Research Council, the Marianne and Marcus Wallenberg foundation, the Strategic Research Area MultiPark (Multidisciplinary Research in Parkinson's disease) at Lund University, the Swedish

Alzheimer Association, the Swedish Brain Foundation, the Skåne University Hospital Foundation, the Bundy Academy, and the Swedish federal government under the ALF agreement. Data collection and sharing for the Alzheimer's Disease Neuroimaging Initiative (ADNI) (National Institutes of Health Grant U01 AG024904) is funded by the National Institute on Aging, the National Institute of Biomedical Imaging and Bioengineering, and through generous contributions from the following: Alzheimer's Association; Alzheimer's Drug Discovery Foundation; BioClinica, Inc.; Biogen Idec Inc.; Bristol-Myers Squibb Company; Eisai Inc.; Elan Pharmaceuticals, Inc.; Eli Lilly and Company; F. Hoffmann-La Roche Ltd and its affiliated company Genentech, Inc.; GE Healthcare; Innogenetics, N.V.; IXICO Ltd.; Janssen

Alzheimer Immunotherapy Research & Development, LLC.; Johnson & Johnson Pharmaceutical Research & Development LLC.; Medpace, Inc.; Merck & Co., Inc.; Meso Scale Diagnostics, LLC.; NeuroRx Research; Novartis Pharmaceuticals Corporation; Pfizer Inc.; Piramal Imaging; Servier; Synarc Inc.; and Takeda Pharmaceutical Company. The Canadian Institutes of Health Research provided funds to support ADNI clinical sites in Canada. Private sector contributions were facilitated by the Foundation for the National Institutes of Health ([www.fnih.org](http://www.fnih.org)). The grantee organization is the Northern California Institute for Research and Education, and the study is coordinated by the Alzheimer's Disease Cooperative Study at the University of California, San Diego. ADNI data are disseminated by the Laboratory for Neuro Imaging at the University of Southern California. A complete listing of ADNI investigators can be found at: [https://adni.loni.usc.edu/wp-content/uploads/how\\_to\\_apply/ADNI\\_Acknowledgement\\_List.pdf](https://adni.loni.usc.edu/wp-content/uploads/how_to_apply/ADNI_Acknowledgement_List.pdf). Partial financial support of AIBL was provided by the Alzheimer's Association (US), the Alzheimer's Drug Discovery Foundation, an Anonymous foundation, the Science and Industry Endowment Fund, the Dementia Collaborative Research Centres, the McCusker Alzheimer's Research Foundation, the National Health and Medical Research Council (AUS), and the Yuligbar Foundation, plus numerous commercial interactions supporting data collection. Details of the AIBL consortium can be found at [www.AIBL.csiro.au](http://www.AIBL.csiro.au) and a list of the researchers of AIBL is provided at <http://aibl.csiro.au/>.

## Disclosure

P. Insel reports no disclosures relevant to the manuscript. M. Weiner has served on the Scientific Advisory Boards for Pfizer, BOLT International, Neurotrope Bioscience, Eli Lilly, University of Pennsylvania's Neuroscience of Behavior Initiative, National Brain Research Centre, India, LEARN Program at University of North Carolina, and ADNI. He has provided consulting to Synarc, Pfizer, Janssen, KLJ Associates, Easton Associates, Harvard University, University of California, Los Angeles, Alzheimer's Drug Discovery Foundation, Neurotrope Bioscience, Avid Radiopharmaceuticals, Clearview Healthcare Partners, Perceptive Informatics, Smartfish AS, Decision Resources, Inc., Araclon, Merck, Defined Health, and Genentech. The following entities have provided funding for travel: Pfizer, Paul Sabatier University, MCI Group France, Travel eDreams, Inc., Neuroscience School of Advanced Studies, Danone Trading, BV, CTAD Ant Congress, Kenes, Intl, ADRC, UCLA, UCSD, Sanofi-Aventis Groupe, University Center Hospital, Toulouse, Araclon, AC Immune, Eli Lilly, New York Academy of Sciences, National Brain Research Center, India, for Johns Hopkins Medicine, Consortium for Multiple Sclerosis Centers, Northwestern University, and University of Pennsylvania. He served on the editorial boards for *Alzheimer's & Dementia* and *Magnetic Resonance Imaging*. He received honoraria from Pfizer, Tohoku University, and Danone Trading, BV. He received research support from Merck, Avid, the Veterans Administration,

and Department of Defense. R. Mackin has received research support from The National Institute of Mental Health, Johnson & Johnson, and Avid Radiopharmaceuticals, Inc. E. Mormino has served as a paid consultant for Eli Lilly and Biogen and received funding from K01AG051718. Y. Lim reports serving as a scientific consultant to CogState, Ltd., Biogen, and Lundbeck. E. Stomrud and S. Palmqvist report no disclosures relevant to the manuscript. C. Masters reports serving as an advisor to Prana Biotechnology, Ltd., and a consultant to Eli Lilly and Company. P. Maruff is an employee at Cogstate P/L. O. Hansson has served on advisory boards for Eli Lilly and received research support from GE Healthcare and Hoffmann La-Roche. N. Mattsson has been a consultant for ADNI. Go to [Neurology.org/N](http://Neurology.org/N) for full disclosures.

## Publication history

Received by *Neurology* November 30, 2018. Accepted in final form March 17, 2019.

## References

- van Dyck CH. Anti-amyloid- $\beta$  monoclonal antibodies for Alzheimer's disease. *Biol Psychiatry* 2017;83:311–319.
- Sperling RA, Rentz DM, Johnson KA, et al. The A4 study: stopping AD before symptoms begin? *Sci Transl Med* 2014;6:228f13.
- Vos SJB, Xiong C, Visser PJ, et al. Preclinical Alzheimer's disease and its outcome: a longitudinal cohort study. *Lancet Neurol* 2014;12:957–965.
- Vemuri P, Lesnick TG, Przybelski SA, et al. Vascular and amyloid pathologies are independent predictors of cognitive decline in normal elderly. *Brain* 2015;138:761–771.
- Mormino EC, Papp KV, Rentz DM, et al. Early and late change on the preclinical Alzheimer's cognitive composite in clinically normal older individuals with elevated amyloid  $\beta$ . *Alzheimers Dement* 2017;13:1004–1012.
- Wirth M, Oh H, Mormino EC, et al. The effect of amyloid  $\beta$  on cognitive decline is modulated by neural integrity in cognitively normal elderly. *Alzheimers Dement* 2013;9:687–698.
- Baker JE, Lim YY, Pietrzak RH, et al. Cognitive impairment and decline in cognitively normal older adults with high amyloid- $\beta$ : A meta-analysis. *Alzheimers Dement* 2017;6:108–121.
- Hedden T, Oh H, Younger AP, Patel TA. Meta-analysis of amyloid-cognition relations in cognitively normal older adults. *Neurology* 2013;80:1341–1348.
- Insel PS, Hansson O, Mackin RS, et al. Amyloid pathology in the progression to mild cognitive impairment. *Neurobiol Aging* 2018;64:76–84.
- Donohue MC, Sperling RA, Salmon DP, et al. The preclinical Alzheimer cognitive composite: measuring amyloid-related decline. *JAMA Neurol* 2014;71:961–970.
- Mueller SG, Weiner MW, Thal LJ, et al. Ways toward an early diagnosis in Alzheimer's disease: the Alzheimer's Disease Neuroimaging Initiative (ADNI). *Alzheimers Dement* 2005;1:55–66.
- Ellis KA, De Fazio D, Foster J, et al. The Australian Imaging, Biomarkers and Lifestyle (AIBL) study of aging: methodology and baseline characteristics of 1112 individuals recruited for a longitudinal study of Alzheimer's disease. *Int Psychogeriatr* 2009;21:672–687.
- Palmqvist S, Zetterberg H, Blennow K, et al. Accuracy of brain amyloid detection in clinical practice using cerebrospinal fluid  $\beta$ -amyloid 42: a cross-validation study against amyloid positron emission tomography. *JAMA Neurol* 2014;71:1282–1289.
- Aisen PS, Petersen RC, Donohue MC, et al. Clinical core of the Alzheimer's Disease Neuroimaging Initiative: progress and plans. *Alzheimers Dement* 2010;6:239–246.
- Thomas K, Eppig J, Weigand A, et al. Artificially low mild cognitive impairment to normal reversion rate in Alzheimer's Disease Neuroimaging Initiative. *Alzheimers Dement* 2019;15:1–9.
- Rowe CC, Ellis KA, Rimajova M, et al. Amyloid imaging results from the Australian Imaging, Biomarkers and Lifestyle (AIBL) study of aging. *Neurobiol Aging* 2010;31:1275–1283.
- Landau SM, Thomas BA, Thurfjell L, et al. Amyloid PET imaging in Alzheimer's disease: a comparison of three radiotracers. *Eur J Nucl Med Mol Imaging* 2014;41:1398–1407.
- Jagust WJ, Bandy D, Chen K, et al. The Alzheimer's Disease Neuroimaging Initiative positron emission tomography core. *Alzheimers Dement* 2010;6:221–229.
- Shaw LM, Vanderstichele H, Knopik-Czajka M, et al. Cerebrospinal fluid biomarker signature in Alzheimer's Disease Neuroimaging Initiative subjects. *Ann Neurol* 2009;65:403–413.
- Olsson A, Vanderstichele H, Andreassen N, et al. Simultaneous measurement of  $\beta$ -amyloid(1–42), total tau, and phosphorylated tau (Thr181) in cerebrospinal fluid by the xMAP technology. *Clin Chem* 2005;51:336–345.



21. Palmqvist S, Zetterberg H, Mattsson N, et al. Detailed comparison of amyloid PET and CSF biomarkers for identifying early Alzheimer disease. *Neurology* 2015;85:1240–1249.
22. Landau SM, Mintun MA, Joshi AD, et al. Amyloid deposition, hypometabolism, and longitudinal cognitive decline. *Ann Neurol* 2012;72:578–586.
23. Villemagne VL, Doré V, Yates P, et al. En attendant centiloid. *Adv Res* 2014;2:723–729.
24. Janelidze S, Zetterberg H, Mattsson N, et al. CSF A $\beta$ 42/A $\beta$ 40 and A $\beta$ 42/A $\beta$ 38 ratios: better diagnostic markers of Alzheimer disease. *Ann Clin Transl Neurol* 2016;3:154–165.
25. Donohue MC, Sperling RA, Petersen R, et al. Association between elevated brain amyloid and subsequent cognitive decline among cognitively normal persons. *JAMA* 2017;317:2305–2316.
26. Pinheiro JC, Bates DM. *Mixed-Effects Models in S and S-PLUS*. Berlin: Springer; 2000.
27. Hastie TJ, Tibshirani RJ. Generalized additive models. *Monogr Stat Appl Probab* 1990;1:352.
28. Akaike H. A new look at the statistical model identification. *Autom Control IEEE Trans* 1974;19:716–723.
29. Mallinckrodt CH, Clark WS, Stacy RD. Type I error rates from mixed-effects model repeated measures versus fixed effects analysis of variance with missing values imputed via last observation carried forward. *Drug Inform J* 2001;35:1215–1225.
30. Sidik K, Jonkman JN. A comparison of heterogeneity variance estimators in combining results of studies. *Stat Med* 2007;26:1964–1981.
31. Schneider LS, Sano M. Current Alzheimer's disease clinical trials: methods and placebo outcomes. *Alzheimers Dement* 2009;5:388–397.
32. Siemers ER, Sundell KL, Carlson C, et al. Phase 3 solanezumab trials: secondary outcomes in mild Alzheimer's disease patients. *Alzheimers Dement* 2016;12:110–120.
33. Honig LS, Vellas B, Woodward M, et al. Trial of solanezumab for mild dementia due to Alzheimer's disease. *N Engl J Med* 2018;378:321–330.
34. Kozauer N, Katz R. Regulatory innovation and drug development for early-stage Alzheimer's disease. *N Engl J Med* 2013;368:1169–1171.
35. Li D, Iddi S, Aisen P, et al. The relative efficiency of time-to-progression and continuous measures of cognition in pre-symptomatic Alzheimer's. 2019;arXiv:1902.02026 [stat.AP].
36. Mormino E, Betensky RA, Hedden T, et al. Amyloid and APOE4 interact to influence short-term decline in preclinical Alzheimer disease. *Neurology* 2014;82:1760–1767.
37. Lim YY, Kalinowski P, Pietrzak RH, et al. Association of  $\beta$ -Amyloid and apolipoprotein E  $\epsilon$ 4 with memory decline in preclinical Alzheimer disease. *JAMA Neurol* 2018;75:488–494.
38. Insel PS, Donohue MC, Mackin RS, et al. Cognitive and functional changes associated with A $\beta$  pathology and the progression to mild cognitive impairment. *Neurobiol Aging* 2016;48:172–181.
39. Buckley RF, Mormino EC, Amariglio RE, et al. Sex, amyloid, and APOE  $\epsilon$ 4 and risk of cognitive decline in preclinical Alzheimer's disease: findings from three well-characterized cohorts. *Alzheimers Dement* 2018;14:1193–1203.
40. Ramirez J, McNeely AA, Scott CJM, et al. White matter hyperintensity burden in elderly cohort studies: the Sunnybrook Dementia Study, Alzheimer's Disease Neuroimaging Initiative, and Three-City Study. *Alzheimers Dement* 2016;12:203–210.
41. Van Westen D, Lindqvist D, Blennow K, et al. Cerebral white matter lesions: associations with A $\beta$  isoforms and amyloid PET. *Sci Rep* 2016;6:1–9.

Paper IV







ELSEVIER



Alzheimer's & Dementia 15 (2019) 570-580

Alzheimer's  
&  
Dementia

Featured Article

# Predicting diagnosis and cognition with <sup>18</sup>F-AV-1451 tau PET and structural MRI in Alzheimer's disease

Niklas Mattsson<sup>a,b,c,\*</sup>, Philip S. Insel<sup>a,d,e</sup>, Michael Donohue<sup>f</sup>, Jonas Jögi<sup>g</sup>, Rik Ossenkoppele<sup>a,h</sup>, Tomas Olsson<sup>i</sup>, Michael Schöll<sup>a,j</sup>, Ruben Smith<sup>a,c</sup>, Oskar Hansson<sup>a,b</sup>

<sup>a</sup>Clinical Memory Research Unit, Faculty of Medicine, Lund University, Lund, Sweden

<sup>b</sup>Memory Clinic, Skåne University Hospital, Malmö, Sweden

<sup>c</sup>Lund University, Skåne University Hospital, Department of Clinical Sciences, Neurology, Lund, Sweden

<sup>d</sup>Center for Imaging of Neurodegenerative Diseases, Department of Veterans Affairs Medical Center, San Francisco, CA, USA

<sup>e</sup>Department of Radiology and Biomedical Imaging, University of California, San Francisco, CA, USA

<sup>f</sup>Department of Neurology, Alzheimer's Therapeutic Research Institute, University of Southern California, San Diego, CA, USA

<sup>g</sup>Department of Clinical Physiology and Nuclear Medicine, Skåne University Hospital, Lund, Sweden

<sup>h</sup>VU University Medical Center, Department of Neurology and Alzheimer Center, Amsterdam Neuroscience, Amsterdam, the Netherlands

<sup>i</sup>Department of Radiation Physics, Skåne University Hospital, Lund, Sweden

<sup>j</sup>Wallenberg Centre for Molecular and Translational Medicine and the Department of Psychiatry and Neurochemistry, University of Gothenburg, Gothenburg, Sweden

**Abstract**

**Introduction:** The relative importance of structural magnetic resonance imaging (MRI) and tau positron emission tomography (PET) to predict diagnosis and cognition in Alzheimer's disease (AD) is unclear.

**Methods:** We tested 56 cognitively unimpaired controls (including 27 preclinical AD), 32 patients with prodromal AD, and 39 patients with AD dementia. Optimal classifiers were constructed using the least absolute shrinkage and selection operator with <sup>18</sup>F-AV-1451 (tau) PET and structural MRI data (regional cortical thickness and subcortical volumes).

**Results:** <sup>18</sup>F-AV-1451 in the amygdala, entorhinal cortex, parahippocampal gyrus, fusiform, and inferior parietal lobule had 93% diagnostic accuracy for AD (prodromal or dementia). The MRI classifier involved partly the same regions plus the hippocampus, with 83% accuracy, but did not improve upon the tau classifier. <sup>18</sup>F-AV-1451 retention and MRI were independently associated with cognition.

**Discussion:** Optimized tau PET classifiers may diagnose AD with high accuracy, but both tau PET and structural brain MRI capture partly unique information relevant for the clinical deterioration in AD.

© 2018 the Alzheimer's Association. Published by Elsevier Inc. All rights reserved.

**Keywords:**

Alzheimer; Atrophy; MRI; PET; Tau

**1. Introduction**

Alzheimer's disease (AD) is characterized by β-amyloid (Aβ) and tau aggregation [1]. Aβ aggregation is assumed to lead to aggregation of tau, brain atrophy, and cognitive decline [2,3]. However, Aβ has limited toxicity and does not typically colocalize with changes in brain structure or function. In contrast, tau spreads within and beyond regions

N.M., P.S.I., M.D., J.J., R.O., T.O., M.S., and R.S. have no disclosures. O.H. has acquired research support (for the institution) from Roche, GE Healthcare, Biogen, AVID Radiopharmaceuticals, Fujirebio, and Euroimmun. In the past 2 years, he had received consultancy/speaker fees (paid to the institution) from Lilly, Roche, and Fujirebio.

\*Corresponding author. Tel: + 46 46 222 00 00; Fax: +46 46 17 79 40.

E-mail address: [niklas.mattsson@med.lu.se](mailto:niklas.mattsson@med.lu.se)

that show atrophy in AD and correlates with cognitive decline [4]. Tau is therefore suspected to be essential for the development of atrophy and cognitive decline in AD. Tau positron emission tomography (PET) has made it possible to study this by quantifying regional tau load *in vivo* [5–7]. One study on 40 patients with AD at the prodromal and dementia stages of the disease found that regional tau pathology was related to cognitive impairment and partly mediated by structural brain magnetic resonance imaging (MRI) measurements [8]. More data are needed to clarify to what degree tau aggregation and atrophy are independent processes and in which brain regions tau and atrophy are most critical for development of different symptoms. We therefore used the tau PET tracer  $^{18}\text{F}$ -AV-1451 together with structural brain MRI in healthy elderly controls and individuals with AD, including preclinical, prodromal, and dementia stage AD patients, to (1) identify brain regions where tau pathology and brain structure are most strongly associated with cognitive features of AD and (2) test for overlapping and complementary effects of tau and brain structure. We hypothesized that an optimized measure of tau would be superior over brain structure to identify AD and cognitive impairment. However, because atrophy and cognition may also be affected by other processes than tau pathology, including Lewy body pathology, vascular pathology, and TDP-43 pathology, we hypothesized that brain structure would provide some complementary information about cognition.

## 2. Methods

### 2.1. Participants

All participants were recruited from the Swedish BioFINDER (Biomarkers For Identifying Neurodegenerative Disorders Early and Reliably) study. Inclusion/exclusion criteria have been described previously [9,10]. We included 56 cognitively unimpaired (CU) individuals (including 27 A $\beta$ -positive controls, called preclinical AD), 32 prodromal AD (A $\beta$ -positive mild cognitive impairment [MCI]), and 39 AD dementia patients. All participants were assessed by physicians with expertise in dementia disorders. For CU participants, the inclusion criteria were as follows: age  $\geq 60$  years, Clinical Dementia Rating scale (CDR) 0, Mini-Mental State Examination (MMSE) 28–30, and fluency in Swedish. Exclusion criteria were as follows: refusal of lumbar puncture, presence of subjective cognitive impairment, significant neurologic or psychiatric disease, dementia or MCI, and presence of severe systemic illness. Prodromal AD cases were recruited from consecutively recruited patients with cognitive complaints at our memory clinic. The inclusion criteria were as follows: referred to the memory clinics due to cognitive complaints related to memory, executive, visuospatial, language praxis, or psychomotor function; MMSE 24–30; age 60–80 years; and fluency in Swedish. The exclusion criteria were as follows: cognitive impairment that without doubt could be explained

by another condition (other than prodromal dementia), fulfillment of criteria for dementia, severe somatic disease, and refusing lumbar puncture or neuropsychological investigation. The classification of MCI (rather than subjective cognitive impairment) was based on an extensive neuropsychological battery and the assessment of a senior neuropsychologist. Patients with a clinical syndrome of AD dementia met the DSM-IIIIR criteria for dementia [11] and the NINCDS-ADRDA criteria for AD [12].

Informed written consent was obtained from all patients. All procedures were approved by the Regional ethics committee at Lund University, the Radiation protection committee at Skåne University Hospital, and the Swedish Medical Products Agency.

### 2.2. Cognitive measures

The cognitive battery used in this study included measures representing global cognition (MMSE, measured on a scale from 0 to 30, with 30 being least impaired); episodic memory (immediate and delayed wordlist recall tests from the Alzheimer's Disease Assessment Scale–cognitive subscale [ADAS-cog], measured on scales from 0 to 10, with 0 being least impaired); processing speed/attention (Trail Making A, measured in seconds to completion of task, lower numbers indicating less impairment, natural log transformed); and semantic memory/executive function (category [animal] fluency, measured in number of items listed, greater numbers indicating less impairment).

### 2.3. CSF biomarkers

Lumbar CSF sampling was done following the Alzheimer's Association Flow Chart [13]. Samples were stored in 1-mL polypropylene tubes at  $-80^{\circ}\text{C}$  until analysis. ELISA was used for analysis of CSF A $\beta_{42}$  (INNOTEST; Fujirebio, Ghent, Belgium). A $\beta$ -positivity was defined as CSF A $\beta_{42} < 650$  ng/L [9]. All analyses were performed by board-certified laboratory technicians who were blinded for clinical data and diagnoses.

### 2.4. Magnetic resonance imaging

T1-weighted MRI was performed on 3T MR scanners (Siemens Tim Trio 3T and Siemens Skyra; Siemens Medical Solutions, Erlangen, Germany), producing a high-resolution anatomical MP-RAGE image (TR = 1950 ms, TE = 3.4 ms, 1 mm isotropic voxels, and 178 slices). Cortical reconstruction and volumetric segmentation were performed with the FreeSurfer (v5.3) image analysis pipelines (<http://surfer.nmr.mgh.harvard.edu/>). Briefly, the MP-RAGE images underwent correction for intensity homogeneity [14], removal of nonbrain tissue [15], and segmentation into gray matter and white matter with intensity gradient and connectivity among voxels [16–19]. Cortical thickness was measured as the distance from the gray matter/white matter boundary to the corresponding pial surface [17]. Reconstructed data

sets were visually inspected for accuracy, and segmentation errors were corrected. Bilaterally averaged thickness measures of all available neocortical areas, plus volumes of hippocampus and amygdala, were included (Supplementary Table).

### 2.5. $^{18}\text{F}$ -AV-1451 tau PET imaging and processing

Tau PET imaging was done with procedures described previously [20]. In brief,  $^{18}\text{F}$ -AV-1451 was synthesized at Skåne University Hospital, Lund [21], and PET scans were performed on a GE Discovery 690 PET scanner (General Electric Medical Systems). Partial volume error correction was performed using the Geometric Transfer Method [22] and combined with a region-based voxelwise approach [23]. FreeSurfer parcellation in MR space of the anatomical scan was applied to processed, coregistered, and time-averaged PET images to extract regional uptake values.  $^{18}\text{F}$ -AV-1451 standardized uptake value ratio images were based on mean uptake over 80-100 min postinjection normalized to uptake in a gray matter masked cerebellum reference region.

The same FreeSurfer regions as for MRI were included for  $^{18}\text{F}$ -AV-1451. Besides hippocampus and amygdala, all non-neocortical structures were removed because of susceptibility to off-target binding [20]. Hippocampus may also be susceptible to off-target binding because of its proximity to the choroid plexus [24]. However, we chose to include it because it is a recognized key region for structural brain changes and to facilitate comparisons between  $^{18}\text{F}$ -AV-1451 PET and MRI data.

### 2.6. Statistical analysis

The relationship between demographics and diagnosis was evaluated with Fisher's exact test for sex and Wilcoxon-Mann-Whitney rank-sum test for age and education. Estimating the individual and joint ability of  $^{18}\text{F}$ -AV-1451 and MRI to predict diagnosis and cognition was done in two steps.

Step one:  $^{18}\text{F}$ -AV-1451 and MRI composite scores. All cognitive responses (or diagnosis) were regressed on  $^{18}\text{F}$ -AV-1451 and MRI, separately. For the analyses on cognition,  $\text{A}\beta$ -negative controls were removed, to evaluate cognition through the continuum of AD (preclinical, prodromal, and dementia stages). Each response was regressed on all included regions with  $^{18}\text{F}$ -AV-1451 retention levels or cortical thickness (or volume for hippocampus and amygdala), adjusting for demographics (age, sex, and years of education). The least absolute shrinkage and selection operator (LASSO [25]) was used for model selection and to estimate regional weights to be used to form  $^{18}\text{F}$ -AV-1451 and MRI composites. The LASSO selects important predictors by shrinking the individual coefficients toward zero. The coefficients of covariates that do not provide additional predictive information are shrunk to zero, resulting in parsimonious and

interpretable models. The LASSO is well suited to handle large numbers of highly correlated variables such as imaging regions of interest. Ten-fold cross-validation was used to tune the amount of shrinkage. Models were subsequently fit on all data using the cross-validated penalty parameter.

Step two: Predictive value of  $^{18}\text{F}$ -AV-1451 and MRI composite scores. All responses were regressed on the composites developed in step one. The models were summarized with regression coefficients, standard errors, Wald test  $P$  values, and the Akaike Information Criterion (AIC) [26]. The predictive ability of each imaging modality was summarized with classification accuracy for diagnosis and  $R^2$  for cognitive responses. Ninety-five percent confidence intervals were estimated using jackknife estimated standard errors. Finally, all responses were regressed on both  $^{18}\text{F}$ -AV-1451 and MRI composites simultaneously to estimate the joint predictive ability of both modalities, as well as the adjusted regression coefficients, standard errors, and  $P$  values. The reduction of the regression coefficients after adjustment was reported along with 95% confidence intervals. For prediction of diagnosis, we also present (for comparison) the accuracy of a priori selected individual regions (inferior temporal lobe for  $^{18}\text{F}$ -AV-1451 and hippocampal volume for MRI).

All analyses were done in R v3.3.2 ([www.r-project.org](http://www.r-project.org)).

## 3. Results

One hundred twenty-seven participants including 56 CU controls, 32 patients with prodromal AD, and 39 patients with AD dementia were examined (Table 1). All prodromal AD and AD dementia participants and 27 controls (preclinical AD) were  $\text{A}\beta$ +

For models of diagnosis, we compared all CU with the combined group of prodromal AD and AD dementia patients. The prodromal/dementia AD patients were younger on average than the CU (72.5 years vs. 74.7 years,  $P = .04$ ) and had a higher proportion of apolipoprotein E (*APOE*)  $\epsilon 4$  positivity (defined as the presence of one or two *APOE*  $\epsilon 4$  alleles; 79% vs. 43%,  $P < .01$ ). There was no difference in education (11.9 years vs. 12.2 years,  $P = .76$ ) and a borderline significant difference in sex (63% vs. 46% male,  $P = .07$ ).

For models of cognition, we included all preclinical AD, prodromal AD, and AD dementia participants (98 persons, with 54 males, average age 73.0 years, average education 11.9 years, 75% *APOE*  $\epsilon 4$  positivity).

### 3.1. $^{18}\text{F}$ -AV-1451 tau PET

The  $^{18}\text{F}$ -AV-1451 signal was increased in prodromal AD and AD dementia in several regions throughout the temporal, parietal, frontal, and occipital lobes (see Fig. 1 for selected regions). The optimal  $^{18}\text{F}$ -AV-1451 classifier was 93% accurate in classifying AD (prodromal AD and AD dementia) versus CU (95% CI: 89% to 97%). The regions

Table 1  
Demographics

	A $\beta$ - CU	A $\beta$ + CU (preclinical AD)	A $\beta$ + MCI (prodromal AD)	A $\beta$ + AD dementia	<i>P</i>
N	29	27	32	39	
Age, y	75.0 (5.5)	74.4 (7.6)	72.5 (6.9)	72.6 (6.8)	.25
Male, N (%)	17 (59%)	9 (33%)	21 (66%)	24 (62%)	.063
Education, y	12.7 (3.6)	11.7 (4.2)	11.9 (3.1)	11.9 (3.8)	.66
APOE $\epsilon$ 4, -/+ (%+)	22/7 (24%)	10/17 (63%)	4/28 (88%)	10/26 (72%)	<.001
MMSE	29.0 (1.1)	29.3 (1.0)	26.5 (2.5)	21.7 (4.6)	<.001
Immediate Recall	2.6 (1.2)	2.3 (1.1)	4.9 (1.4)	6.3 (1.5)	<.001
Delayed Recall	1.9 (1.4)	2.0 (1.5)	5.8 (2.6)	8.4 (2.0)	<.001
Trail Making A	3.72 (0.31)	3.85 (0.28)	3.98 (0.36)	4.28 (0.44)	<.001
Category Fluency	24.7 (5.6)	21.6 (5.5)	16.3 (5.1)	11.1 (5.4)	<.001

Abbreviations: A $\beta$ ,  $\beta$ -amyloid; AD, Alzheimer's disease; APOE, apolipoprotein E; CU, cognitively unimpaired; MMSE, Mini-Mental Status Examination.

NOTE. Continuous data are mean (standard deviation). Trail Making A data are shown after natural log transformation. The combined CU (including both A $\beta$ - CU and preclinical AD; N = 56; 24 males) had mean age 74.7 (6.57) years, mean education 12.2 (3.9) years, mean MMSE 29.1 (1.1), mean immediate recall 2.4 (1.1), mean delayed recall 1.9 (1.5), mean Trail Making A 3.79 (0.30), and mean category fluency 23.2 (5.8). *P* values by Kruskal-Wallis test for continuous data and Fisher's exact test for categorical data.

selected for classification were the amygdala, the parahippocampal gyrus, the entorhinal cortex (ERC), the fusiform cortex, and the inferior parietal lobule (Fig. 2). The a priori selected individual region inferior temporal cortex had 89% accuracy (95% CI: 80% to 98%).

Within A $\beta$ + participants with preclinical or clinical AD, <sup>18</sup>F-AV-1451 was strongly associated with all cognitive responses (*P* < .001 for all responses). LASSO selected different regions for each cognitive test (Fig. 3). The ERC and middle temporal gyrus were selected for MMSE. The parahippocampal gyrus and the ERC were selected for immediate recall. The amygdala, parahippocampal gyrus, temporal pole, ERC, and fusiform cortex were selected for delayed recall. The banks of the superior temporal sulcus, inferior temporal gyrus, lateral occipital cortex, and inferior parietal lobule were selected for Trail Making A. The inferior temporal gyrus, ERC, parahippocampal gyrus, and middle temporal gyrus were selected for category fluency. The estimated regression coefficients from models predicting each cognitive response with weighted tau composites are shown in Table 2.

### 3.2. Magnetic resonance imaging

Structural MRI was 83% accurate in classifying participants as AD (prodromal AD and AD dementia) versus CU (95% CI 68% to 98%). The main regions selected to classify diagnosis were the ERC, hippocampus, and fusiform gyrus (Fig. 2). The a priori selected individual region hippocampus had 76% accuracy (95% CI: 60% to 92%).

Within A $\beta$ + participants, structural MRI was also strongly associated with all cognitive scores (*P* < .001 for all responses). The LASSO selected different regions for the cognitive tests (Fig. 3). The ERC, the banks of the superior temporal sulcus, and inferior parietal lobule were selected for MMSE. The parahippocampal gyrus, ERC, and the inferior parietal lobule were selected for immediate recall. The hippocampus, ERC, amygdala, parahippocampal

gyrus, banks of the superior temporal sulcus, and the inferior parietal lobule were selected for delayed recall. Several regions were selected for Trail Making A, with the inferior temporal gyrus, fusiform gyrus, and isthmus cingulate being the most influential regions. The ERC was selected for category fluency. The estimated regression coefficients from models predicting each cognitive response with weighted brain MRI composites are shown in Table 2.

### 3.3. Competing and complementary predictive information: MRI and <sup>18</sup>F-AV-1451

The effect estimates from regression models predicting diagnosis or cognition with (1) <sup>18</sup>F-AV-1451 only, (2) MRI only, and (3) <sup>18</sup>F-AV-1451 and MRI are shown in Table 2. <sup>18</sup>F-AV-1451 showed strongest associations with delayed recall (*R*<sup>2</sup> = 0.48), followed by immediate recall (*R*<sup>2</sup> = 0.41), MMSE (*R*<sup>2</sup> = 0.36), category fluency (*R*<sup>2</sup> = 0.33), and Trail Making A (*R*<sup>2</sup> = 0.23). MRI had similar strength of associations with delayed recall (*R*<sup>2</sup> = 0.48), MMSE (*R*<sup>2</sup> = 0.35), immediate recall (*R*<sup>2</sup> = 0.34), category fluency (*R*<sup>2</sup> = 0.29), and Trail Making A (*R*<sup>2</sup> = 0.22). Results from the three models show the change in the effect estimate when adjusting for the other imaging modality. The percent reduction of the regression estimate and a 95% confidence interval are shown in Table 2, as well as AIC values for each model. The estimates for <sup>18</sup>F-AV-1451 were reduced between -2% (for diagnosis) and 43% (for MMSE) when adjusting for MRI. Reduction of MRI estimates ranged from 35% (for diagnosis) to 49% (for immediate recall) when adjusting for tau. AIC selected the models ( $\Delta$ AIC) when comparing two models > 2 favors the model with smallest AIC) with both <sup>18</sup>F-AV-1451 and MRI to predict diagnosis and all cognitive responses (Table 2). Adjusted and unadjusted regression estimates and confidence intervals are shown in Fig. 4.

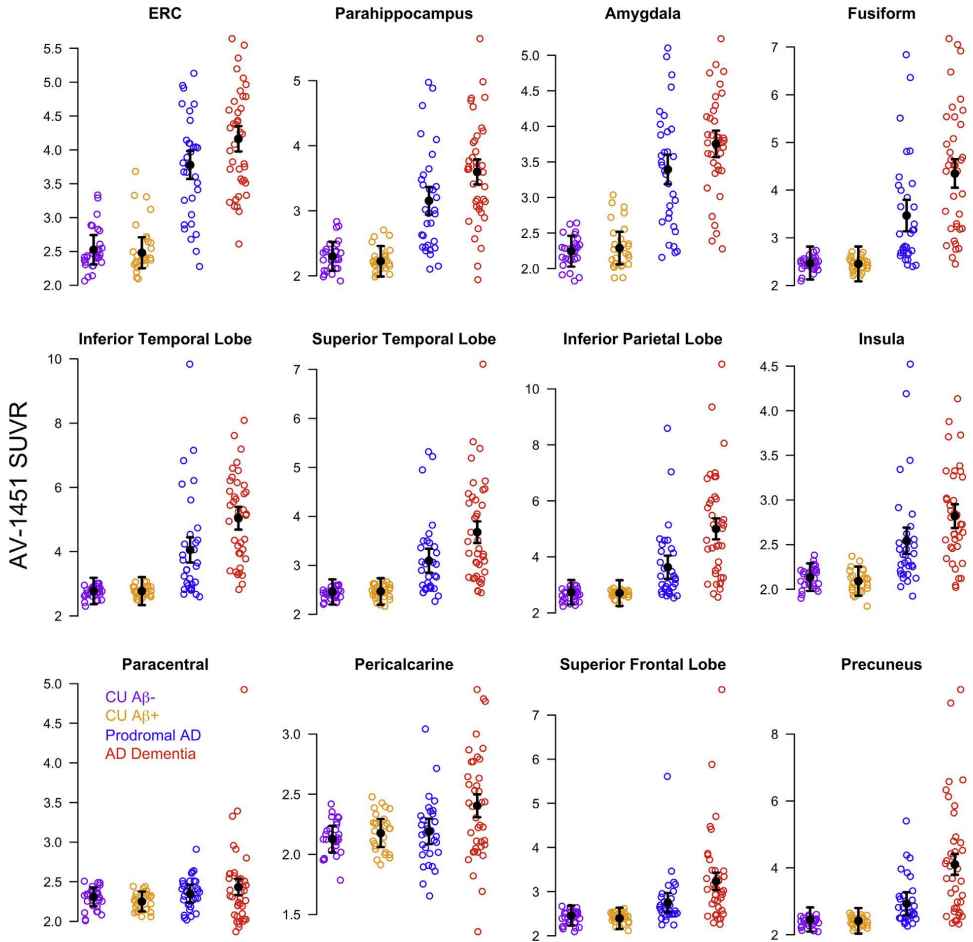


Fig. 1. <sup>18</sup>F-AV-1451 in selected regions. Selected regions in different lobes of the brain, with <sup>18</sup>F-AV-1451 SUVR on the y-axis for the different groups. Data are the sum of SUVRs from the left and right hemispheres. Abbreviations: Aβ, β-amyloid; AD, Alzheimer's disease; CU, cognitively unimpaired; ERC, entorhinal cortex; SUVR, standardized uptake value ratio.

#### 4. Discussion

We tested the predictive value of <sup>18</sup>F-AV-1451 tau PET and structural MRI to identify AD and associations with cognition. The main findings were that (1) an optimized classifier that used regional <sup>18</sup>F-AV-1451 had superior diagnostic accuracy for AD compared to brain MRI; (2) <sup>18</sup>F-AV-1451 and MRI had overall similar strengths of associations with cognition; and (3) both <sup>18</sup>F-AV-1451 and MRI contributed complementary information about cognitive impairment through the continuum from preclinical to prodromal and dementia stages of AD, with regional differences between the modalities. Several previous studies have found that

biomarkers of brain structure [27,28] and tau [5,6] are associated with clinical features of AD. However, studies directly comparing these processes and their regional effects on diagnosis and cognition in AD are rare [8]. Our novel findings suggest that although tau is the most critical of the two, both <sup>18</sup>F-AV-1451 tau PET and structural brain MRI capture partly unique information that is relevant for the clinical deterioration in AD.

With 93% accuracy, our <sup>18</sup>F-AV-1451 classifier was excellent for identification of clinical AD. The selected regions were mainly temporal lobe regions, where tau pathology presumably occurs in early stages of AD (ERC, amygdala, fusiform, and the parahippocampal gyrus), but



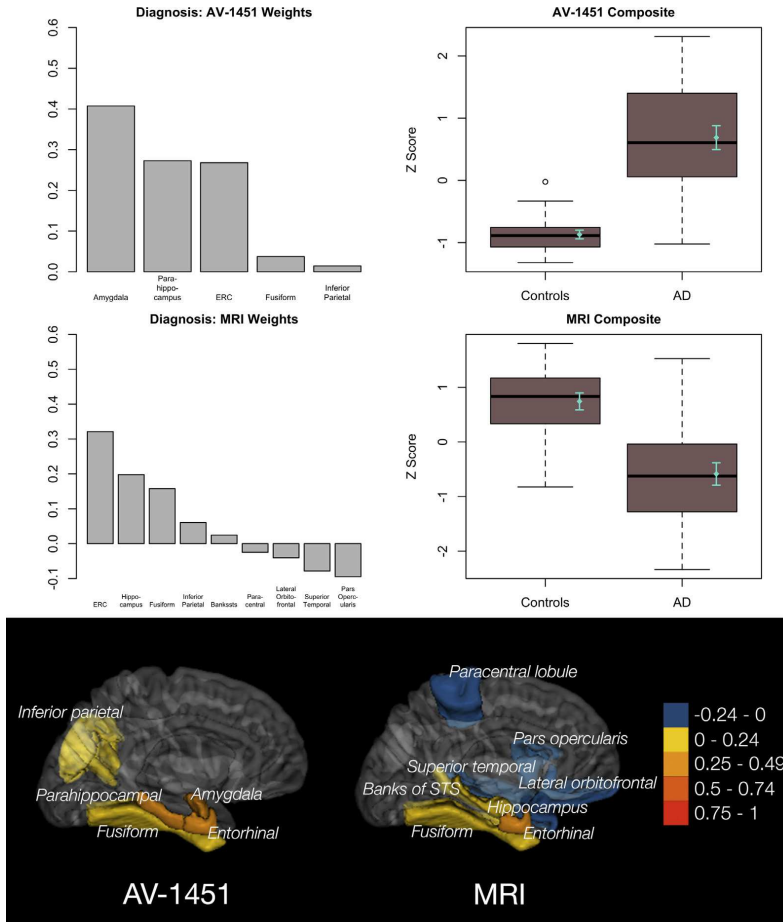


Fig. 2. <sup>18</sup>F-AV-1451 and brain MRI for diagnosis of AD. The top part shows model-estimated regional weights and boxplots of composites for both <sup>18</sup>F-AV-1451 (top row) and MRI (middle row) for the classification of diagnosis (including prodromal AD and AD dementia). The bottom part shows visualization of the model-selected regions, color-coded according to the respective model-estimated weights. Abbreviations: Aβ, β-amyloid; AD, Alzheimer's disease; ERC, entorhinal cortex; MRI, magnetic resonance imaging; STS, superior temporal sulcus; SUVR, standardized uptake value ratio.

also the inferior parietal lobule, which presumably is involved in later stages of the disease [7]. Note that these results are for a combination of patients with AD at the prodromal and dementia stages, compared with CU (which included 48% preclinical AD). This suggests that <sup>18</sup>F-AV-1451 tau PET may be used as a powerful instrument for diagnosis of AD at the clinical stage, without considering the somewhat arbitrary distinction between prodromal and dementia stages.

The optimal MRI-based classifier achieved lower accuracy (83%) and partly included similar regions as the <sup>18</sup>F-AV-1451 classifier (ERC, fusiform) plus the hippocampus, the banks of the superior temporal sulcus, and the inferior

parietal lobule. These regions are similar to but not identical with a previously proposed "temporal meta-ROI" to capture AD-related atrophy (the ERC, inferior temporal, middle temporal, and fusiform [29]). The MRI classifier also included several regions with negative coefficients (meaning that greater thickness was associated with AD diagnosis), including pars opercularis, superior temporal, paracentral, and lateral orbitofrontal cortex. One interpretation of these negative coefficients is that they control for premorbid differences in cortical thickness, but it is also possible that the negative coefficients represent variability particular to this data set. The lower accuracy of MRI compared with <sup>18</sup>F-AV-1451 may be due to the lower specificity of brain

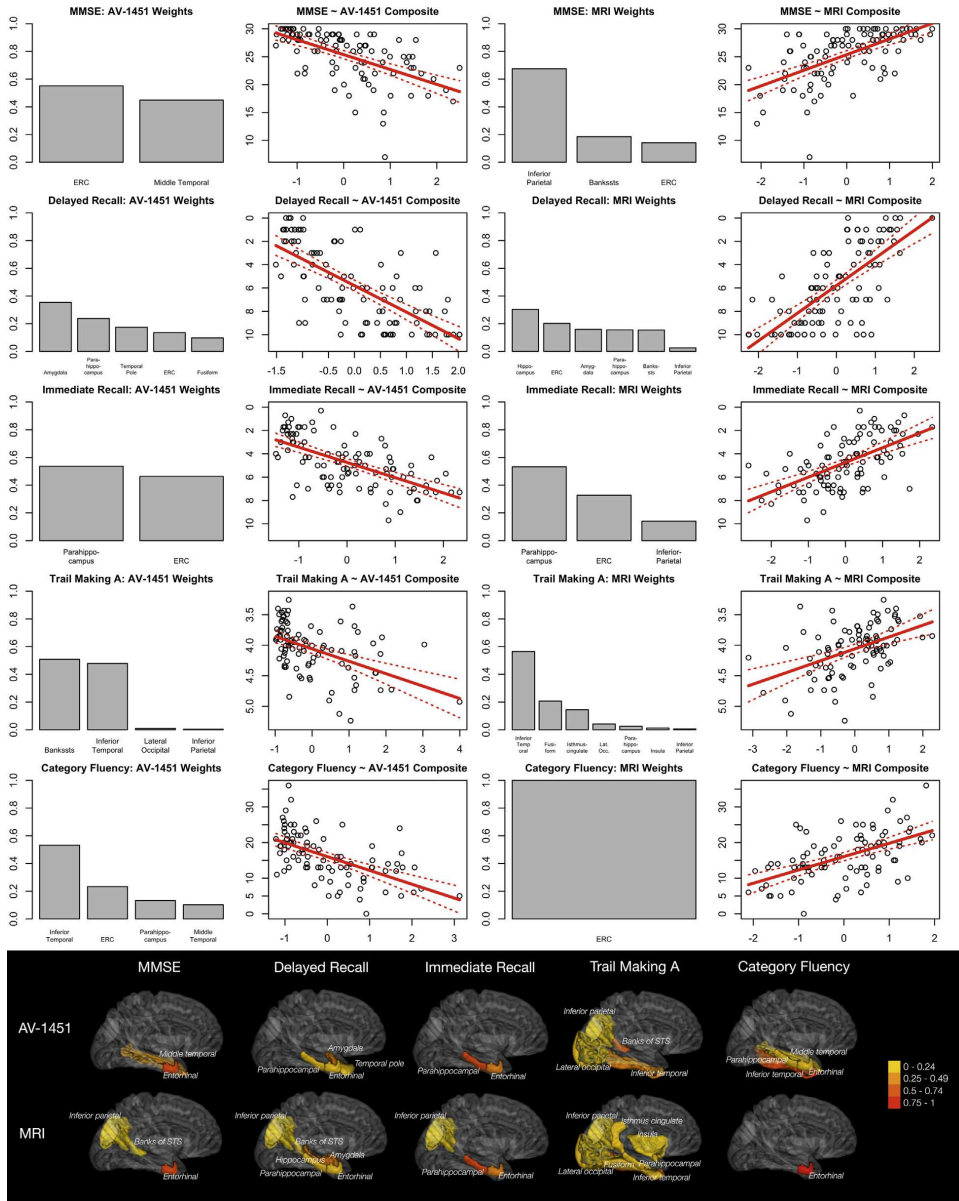


Fig. 3. <sup>18</sup>F-AV-1451, brain MRI and cognition. The top part shows model-estimated regional weights in barplots for <sup>18</sup>F-AV-1451 (left) and brain MRI (right) to predict different cognitive tests in AD (including preclinical AD, prodromal AD, and AD dementia patients). For each cognitive test and modality, cognitive scores are plotted against the composites resulting from the model-estimated weights. Regression curves and 95% confidence intervals are shown in red. The bottom part shows visualization of the model-selected regions, color-coded according to the respective model-estimated weights. Abbreviations: Aβ, β-amyloid; AD, Alzheimer's disease; ERC, entorhinal cortex; MRI, magnetic resonance imaging; STS, superior temporal sulcus; SUVR, standardized uptake value ratio.

Table 2  
Model estimates for <sup>18</sup>F-AV-1451, MRI, and combinations of <sup>18</sup>F-AV-1451 and MRI to predict diagnosis and cognition

Response	<sup>18</sup> F-AV-1451 only					MRI only					<sup>18</sup> F-AV-1451 and MRI					R <sup>2</sup>	AIC			
	B	SE	P	R <sup>2</sup>	AIC	β	SE	P	R <sup>2</sup>	AIC	β	SE	P	% Reduction (95% CI)	B			SE	P	% Reduction (95% CI)
Diagnosis	8.48	2.14	<.001	-	44.5	-2.96	0.52	<.001	-	91.9	8.61	2.64	.0011	-2 (-41 to 38)	-1.91	1.09	.081	35 (9 to 62)	-	42.1
MMSE	-2.66	0.37	<.001	0.36	534.6	2.80	0.37	<.001	0.35	531.8	-1.52	0.46	.0013	43 (16 to 69)	1.77	0.47	<.001	37 (-3 to 77)	0.49	522.7
Immediate Recall	1.31	0.16	<.001	0.41	376.9	-1.26	0.18	<.001	0.34	387.6	0.92	0.20	<.001	30 (8 to 51)	-0.64	0.22	.0039	49 (12 to 86)	0.50	370.0
Delayed Recall	2.27	0.24	<.001	0.48	450.2	-2.37	0.26	<.001	0.48	454.0	1.41	0.30	<.001	38 (19 to 57)	-1.35	0.31	<.001	43 (13 to 73)	0.61	434.3
Trail Making A	0.20	0.04	<.001	0.23	80.8	-0.19	0.04	<.001	0.22	84.9	0.14	0.05	.0024	30 (0 to 60)	-0.11	0.05	.019	42 (-8 to 93)	0.32	77.0
Category Fluency	-3.88	0.58	<.001	0.33	564.7	3.74	0.60	<.001	0.29	569.1	-2.64	0.66	<.001	32 (6 to 58)	2.23	0.67	.001	40 (-3 to 84)	0.47	555.6

Abbreviations: Aβ, β-amyloid; AD, Alzheimer's disease; AIC, Akaike Information Criterion; CU, cognitively unimpaired; LASSO, least absolute shrinkage and selection operator; MMSE, Mini-Mental Status Examination; MRI, magnetic resonance imaging.

NOTE: Results from linear regression models, adjusted for age, sex, and education. <sup>18</sup>F-AV-1451 and brain MRI measures were composites consisting of weighted regions, identified using LASSO as explained in the main text. Diagnosis is AD (prodromal/dementia) versus all CU. Trail Making A data are shown after natural log transformation. AIC can be compared for models with the same outcomes, and a smaller AIC (AIC reduction > 2) indicates a better fit corrected for the number of predictors.

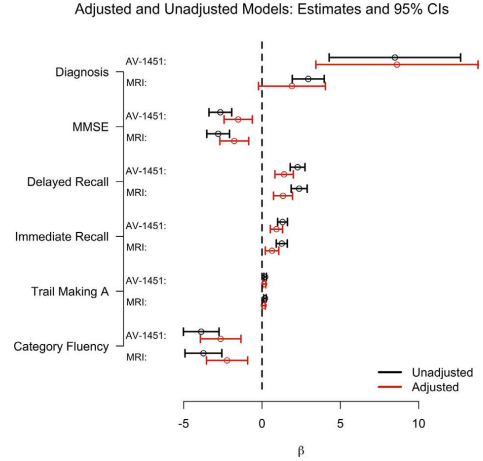


Fig. 4. Adjusted and unadjusted models for diagnosis and cognition. Regression estimates with and without adjustment for the other imaging modality are plotted with 95% confidence intervals (CIs) for each response (corresponding to Table 2). Signs for MRI estimates were inverted to facilitate comparisons with <sup>18</sup>F-AV-1451 estimates. All models were adjusted for age, sex and education. Abbreviations: MMSE, Mini-Mental Status Examination; MRI, magnetic resonance imaging.

structure because a variability in the brain structure is seen both in normal aging and due to non-AD diseases, and due to greater sensitivity of <sup>18</sup>F-AV-1451 to detect subtle AD pathology.

In addition to the higher diagnostic accuracy for <sup>18</sup>F-AV-1451, we found that when combining tau and brain structure, the association between <sup>18</sup>F-AV-1451 and AD diagnosis was minimally affected by adjusting for MRI (increased by 2%), but the association between MRI and AD was markedly reduced by adjusting for tau (reduced by 35%). The classification accuracy for the model including both <sup>18</sup>F-AV-1451 and MRI did not improve over <sup>18</sup>F-AV-1451 alone, indicating that brain structure contributes little beyond tau to the identification of patients with AD.

Hippocampus was selected for the MRI classifier but not for the <sup>18</sup>F-AV-1451 classifier. There are several possible explanations for this. First, the hippocampus may be sensitive to off-target binding for <sup>18</sup>F-AV-1451 because of its proximity to the choroid plexus, and noise from off-target binding may reduce the importance of the hippocampus for tau quantification [24] (although we used partial volume error corrected data, which reduces the influence of off-target binding, rendering estimates less sensitive to this confounding factor). Second, tau accumulation in the hippocampal structures besides CA1 may occur quite late in AD [7], and hippocampal sparing types of AD are not rare [30]. Together, these factors likely reduce the importance of hippocampal <sup>18</sup>F-AV-1451 for AD diagnosis. In contrast, hippocampal atrophy

is a key aspect of structural brain changes in AD, except for in rare variants [31].

The a priori selected regions for  $^{18}\text{F}$ -AV-1451 (inferior temporal lobe) and MRI (hippocampus) had lower accuracy than the optimal classifiers (89% vs. 93% for  $^{18}\text{F}$ -AV-1451 and 76% vs. 83% for MRI), but the differences were not statistically significant. The small increase for  $^{18}\text{F}$ -AV-1451 (4%) and the small/moderate increase for MRI (7%) may be clinically meaningful, although the power to detect those increases with the current sample was low.

Increased  $^{18}\text{F}$ -AV-1451 retention was closely related to worse cognition in AD. The strongest association was seen for delayed recall. MRI had similar associations, but when combining  $^{18}\text{F}$ -AV-1451 and MRI,  $^{18}\text{F}$ -AV-1451 was sometimes more strongly related to cognition, with greater reductions of the MRI coefficient. In particular, the effect of  $^{18}\text{F}$ -AV-1451 on immediate recall was reduced by 30% when adjusting for MRI, whereas the effect of MRI was reduced by 49% when adjusting for  $^{18}\text{F}$ -AV-1451. However, both  $^{18}\text{F}$ -AV-1451 and MRI provided partly complementary information that was not completely accounted for by the other modality, especially for general cognition (MMSE) and delayed recall. Note the difference between these associations with cognition and the associations with diagnosis described previously. When dichotomizing into diagnoses, MRI did not appear to contribute additional predictive information beyond  $^{18}\text{F}$ -AV-1451. When evaluating a continuum of cognitive scores in multiple domains throughout the course from preclinical, prodromal, and dementia stages of AD, both  $^{18}\text{F}$ -AV-1451 and MRI provided predictive information.

The partly independent effects of  $^{18}\text{F}$ -AV-1451 on cognition may suggest that tau had effects on neuronal function and integrity, with relevance for cognition before overt atrophy was seen by MRI. It has been demonstrated before that cognitive changes may occur in parallel with or even precede atrophy measures during the course of AD [32], and according to animal studies, tau may have very early effects on neuronal activity [33]. In contrast, the relationship between MRI and cognition that was partly independent of  $^{18}\text{F}$ -AV-1451 may reflect atrophy that has accelerated downstream of tau or atrophy caused by vascular disease, TDP-43 pathology, Lewy bodies, or other processes that are independent of tau [34].

The regions that were selected for cognition differed slightly from those that were selected for diagnosis and differed between  $^{18}\text{F}$ -AV-1451 and MRI. For immediate recall, the optimal tau composite was sampled from ERC and parahippocampal gyrus, and the same regions plus the inferior parietal lobule were selected for MRI. For fluency, the opposite situation was seen, with several regions selected for  $^{18}\text{F}$ -AV-1451 (inferior temporal, ERC, parahippocampal, and middle temporal cortex) but only ERC for MRI. For MMSE, both  $^{18}\text{F}$ -AV-1451 (ERC and middle temporal cortex) and MRI had unique regions (ERC, banks of the superior temporal sulcus, and inferior parietal lobule). For delayed recall, the optimal  $^{18}\text{F}$ -AV-1451 composite was

sampled from temporal regions (parahippocampal, temporal pole, amygdala, ERC, fusiform), and the optimal MRI composite included partly overlapping regions (parahippocampal, amygdala, ERC, hippocampus, inferior parietal lobule, and banks of the superior temporal sulcus). This complex regional relationship between tau, atrophy, and cognition may have implications both for future research and clinical trials. For example, if tau PET and MRI were used as trial endpoints, it may be beneficial to measure longitudinal effects in modality-dependent regions to optimize chances of detecting clinically relevant effects.

One limitation is that we only used cross-sectional biomarker data. Future use of longitudinal data may give further insights into the relationships between tau, atrophy, and cognitive decline [35,36]. Another limitation is that the relative weights in the LASSO may differ depending on slight variations in the correlations between the predictors and the response, and we therefore caution against overinterpreting the ordering of the weights. Furthermore, models with a large number of predictors may be prone to overfitting. Here, we used 10-fold cross-validation to tune the LASSO penalty parameter. By splitting the data into training and test sets, the value of the penalty parameter was selected based on subjects outside the training set. The tuning of this parameter was done to maximize parsimony and prevent overfitting.

We conclude that  $^{18}\text{F}$ -AV-1451 tau PET was strongly associated with AD diagnosis, with stronger associations than structural MRI. However, both  $^{18}\text{F}$ -AV-1451 and structural MRI were independently associated with cognitive impairment, in a cross-sectional analysis that included the entire disease continuum from preclinical to prodromal and dementia stages of AD.

## Acknowledgments

Authors' contributions: All authors contributed in drafting/ revising the manuscript for content. Study concept or design was developed by N.M., P.S.I., and O.H. Analysis or interpretation of data was done by N.M., P.S.I., and M.S. Study supervision by N.M. and O.H.

Funding: This research was supported by grants from the European Research Council, the Swedish Research Council, the Marianne and Marcus Wallenberg Foundation, the Bundy Academy, and the Strategic Research Area MultiPark (Multidisciplinary Research in Parkinson's disease) at Lund University. The funding sources had no role in the design and conduct of the study, in the collection, analysis, interpretation of the data or in the preparation, review, or approval of the manuscript. The precursor of AV-1451 was generously provided by Avid Radiopharmaceuticals.

## Supplementary data

Supplementary data to this article can be found online at <https://doi.org/10.1016/j.jalz.2018.12.001>.

## RESEARCH IN CONTEXT

1. Systematic review: We reviewed the literature using PubMed and complemented with key papers from reference lists. There are a few papers on combined brain magnetic resonance imaging and tau positron emission tomography (PET) in AD, which suggest that tau PET is more closely linked to cognition. But the results have not been conclusive, and to our knowledge, optimized classifiers for tau accumulation and brain atrophy to predict diagnosis and cognitive impairment in AD have not been tested.
2. Interpretation: In this cohort-study that included 127 participants, an optimal regional tau PET classifier had 93% diagnostic accuracy for the prodromal or dementia stages of AD, whereas an optimal brain magnetic resonance imaging classifier had 83% accuracy and did not improve upon the tau classifier. Both tau and magnetic resonance imaging were strongly (and partly independently) associated with cognitive impairment through the preclinical, prodromal, and dementia stages of AD. This supports that tau PET measures provide superior information about diagnosis and brain changes relevant for cognitive decline in AD.
3. Future directions: Studies incorporating longitudinal brain structure, tau PET, and cognition are necessary to understand the spatiotemporal dynamics of these changes in AD.

## References

- [1] Zetterberg H, Mattsson N. Understanding the cause of sporadic Alzheimer's disease. *Expert Rev Neurother* 2014;14:621–30.
- [2] Mattsson N, Insel PS, Aisen PS, Jagust W, Mackin S, Weiner M, et al. Brain structure and function as mediators of the effects of amyloid on memory. *Neurology* 2015;84:1136–44.
- [3] Tosun D, Landau S, Aisen PS, Petersen RC, Mintun M, Jagust W, et al. Association between tau deposition and antecedent amyloid- $\beta$  accumulation rates in normal and early symptomatic individuals. *Brain J Neurol* 2017;140:1499–512.
- [4] Villemagne VL, Fodero-Tavoletti MT, Masters CL, Rowe CC. Tau imaging: early progress and future directions. *Lancet Neurol* 2015;14:114–24.
- [5] Ossenkoppele R, Schonhaut DR, Schöll M, Lockhart SN, Ayakta N, Baker SL, et al. Tau PET patterns mirror clinical and neuroanatomical variability in Alzheimer's disease. *Brain J Neurol* 2016;139:1551–67.
- [6] Schöll M, Lockhart SN, Schonhaut DR, O'Neil JP, Janabi M, Ossenkoppele R, et al. PET Imaging of Tau Deposition in the Aging Human Brain. *Neuron* 2016;89:971–82.
- [7] Cho H, Choi JY, Hwang MS, Kim YJ, Lee HM, Lee HS, et al. In vivo cortical spreading pattern of tau and amyloid in the Alzheimer disease spectrum. *Ann Neurol* 2016;80:247–58.
- [8] Bejanin A, Schonhaut DR, La Joie R, Kramer JH, Baker SL, Sosa N, et al. Tau pathology and neurodegeneration contribute to cognitive impairment in Alzheimer's disease. *Brain J Neurol* 2017;140:3286–300.
- [9] Palmqvist S, Zetterberg H, Blennow K, Vestberg S, Andreasson U, Brooks DJ, et al. Accuracy of brain amyloid detection in clinical practice using cerebrospinal fluid  $\beta$ -amyloid 42: a cross-validation study against amyloid positron emission tomography. *JAMA Neurol* 2014;71:1282–9.
- [10] Palmqvist S, Zetterberg H, Mattsson N, Johansson P, Alzheimer's Disease Neuroimaging Initiative, Minthon L, et al. Detailed comparison of amyloid PET and CSF biomarkers for identifying early Alzheimer disease. *Neurology* 2015;85:1240–9.
- [11] American Psychiatric Association. In: Work Group to Revise DSM-III. Diagnostic and statistical manual of mental disorders: DSM-III-R. 3rd ed. Washington, DC: American Psychiatric Association; 1987.
- [12] McKhann G, Drachman D, Folstein M, Katzman R, Price D, Stadlan EM. Clinical diagnosis of Alzheimer's disease: report of the NINCDS-ADRDA Work Group under the auspices of Department of Health and Human Services Task Force on Alzheimer's Disease. *Neurology* 1984;34:939–44.
- [13] Blennow K, Hampel H, Weiner M, Zetterberg H. Cerebrospinal fluid and plasma biomarkers in Alzheimer disease. *Nat Rev Neurol* 2010;6:131–44.
- [14] Sled JG, Zijdenbos AP, Evans AC. A nonparametric method for automatic correction of intensity nonuniformity in MRI data. *IEEE Trans Med Imaging* 1998;17:87–97.
- [15] Ségonne F, Dale AM, Busa E, Glessner M, Salat D, Hahn HK, et al. A hybrid approach to the skull stripping problem in MRI. *NeuroImage* 2004;22:1060–75.
- [16] Dale AM, Fischl B, Sereno MI. Cortical surface-based analysis. I. Segmentation and surface reconstruction. *NeuroImage* 1999;9:179–94.
- [17] Fischl B, Dale AM. Measuring the thickness of the human cerebral cortex from magnetic resonance images. *Proc Natl Acad Sci U S A* 2000;97:11050–5.
- [18] Fischl B, Salat DH, Busa E, Albert M, Dieterich M, Haselgrove C, et al. Whole brain segmentation: automated labeling of neuroanatomical structures in the human brain. *Neuron* 2002;33:341–55.
- [19] Fischl B, Salat DH, van der Kouwe AJW, Makris N, Ségonne F, Quinn BT, et al. Sequence-independent segmentation of magnetic resonance images. *NeuroImage* 2004;23:S69–84.
- [20] Smith R, Schain M, Nilsson C, Strandberg O, Olsson T, Hägerström D, et al. Increased basal ganglia binding of (18) F-AV-1451 in patients with progressive supranuclear palsy. *Mov Disord* 2017;32:108–14.
- [21] Hahn A, Schain M, Erlandsson M, Sjölin P, James GM, Strandberg OT, et al. Modeling strategies for quantification of in vivo 18F-AV1451 binding in patients with tau pathology. *J Nucl Med* 2017;58:623–31.
- [22] Rousset OG, Ma Y, Evans AC. Correction for partial volume effects in PET: principle and validation. *J Nucl Med* 1998;39:904–11.
- [23] Thomas BA, Erlandsson K, Modat M, Thurfjell L, Vandenberghe R, Ourselin S, et al. The importance of appropriate partial volume correction for PET quantification in Alzheimer's disease. *Eur J Nucl Med Mol Imaging* 2011;38:1104–19.
- [24] Lowe VJ, Curran G, Fang P, Liesinger AM, Josephs KA, Parisi JE, et al. An autoradiographic evaluation of AV-1451 Tau PET in dementia. *Acta Neuropathol Commun* 2016;4.
- [25] Tibshirani R. Regression Shrinkage and Selection Via the Lasso. *J R Stat Soc Ser B* 1994;58:267–88.
- [26] Akaike H. A new look at the statistical model identification. *IEEE Trans Autom Control* 1974;19:716–23.
- [27] Smits LL, Tijms BM, Benedictus MR, Koedam ELGE, Koene T, Reuling IEW, et al. Regional atrophy is associated with impairment in distinct cognitive domains in Alzheimer's disease. *Alzheimers Dement* 2014;10:S299–305.
- [28] Duarte A, Hayasaka S, Du A, Schuff N, Jahng G-H, Kramer J, et al. Volumetric correlates of memory and executive function in normal elderly, mild cognitive impairment and Alzheimer's disease. *Neurosci Lett* 2006;406:60–5.

- [29] Jack CR, Wiste HJ, Weigand SD, Knopman DS, Mielke MM, Vemuri P, et al. Different definitions of neurodegeneration produce similar amyloid/neurodegeneration biomarker group findings. *Brain* 2015;138:3747-59.
- [30] Schwarz AJ, Yu P, Miller BB, Shcherbinin S, Dickson J, Navitsky M, et al. Regional profiles of the candidate tau PET ligand 18F-AV-1451 recapitulate key features of Braak histopathological stages. *Brain J Neurol* 2016;139:1539-50.
- [31] Lehmann M, Ghosh PM, Madison C, Laforce R, Corbetta-Rastelli C, Weiner MW, et al. Diverging patterns of amyloid deposition and hypometabolism in clinical variants of probable Alzheimer's disease. *Brain J Neurol* 2013;136:844-58.
- [32] Insel PS, Mattsson N, Mackinnon RS, Schöll M, Nosheny RL, Tosun D, et al. Accelerating rates of cognitive decline and imaging markers associated with  $\beta$ -amyloid pathology. *Neurology* 2016;86:1887-96.
- [33] Menkes-Caspi N, Yamin HG, Kellner V, Spiers-Jones TL, Cohen D, Stern EA. Pathological tau disrupts ongoing network activity. *Neuron* 2015;85:959-66.
- [34] Rabinovici GD, Carrillo MC, Forman M, DeSanti S, Miller DS, Kozauer N, et al. Multiple comorbid neuropathologies in the setting of Alzheimer's disease neuropathology and implications for drug development. *Alzheimers Dement* 2017;3:83-91.
- [35] Xie L, Das SR, Wisse LEM, Ittyerah R, Yushkevich PA, Wolk DA, et al. Early Tau Burden Correlates with Higher Rate of Atrophy in Transentorhinal Cortex. *J Alzheimers Dis* 2018; 62:85-92.
- [36] Das SR, Xie L, Wisse LEM, Ittyerah R, Tustison NJ, Dickerson BC, et al. Longitudinal and cross-sectional structural magnetic resonance imaging correlates of AV-1451 uptake. *Neurobiol Aging* 2018; 66:49-58.

# Did you know?

The screenshot shows the homepage of the Alzheimer's & Dementia journal website. The header includes the journal title and the Alzheimer's Association logo. A search bar is located at the top right. The main content area features a 'Current Issue' section for November 2009, Vol. 5, No. 6, with a 'Now Included on MEDLINE' badge. Below this, there are sections for 'Featured Articles' and 'Journal Access'. The 'Featured Articles' section lists several research papers, including one on cognitive performance and another on cerebral blood flow. The 'Journal Access' section provides information about full-text availability and access options. The left sidebar contains navigation links such as 'Journal Home', 'Current Issue', 'Browse All Issues', and 'Articles in Press'. The bottom of the page includes a 'STAAIT' logo and a footer with the journal's publication details.

You can  
access back  
issues of  
**Alzheimer's  
& Dementia**  
online.

[www.alzheimersanddementia.org](http://www.alzheimersanddementia.org)



Paper V







# Association Between Apolipoprotein E $\epsilon$ 2 vs $\epsilon$ 4, Age, and $\beta$ -Amyloid in Adults Without Cognitive Impairment

Philip S. Insel, MS; Oskar Hansson, MD, PhD; Niklas Mattsson-Carlgen, MD, PhD

**IMPORTANCE** Although the most common recent approach in Alzheimer disease drug discovery is to directly target the  $\beta$ -amyloid ( $A\beta$ ) pathway, the high prevalence of apolipoprotein E  $\epsilon$ 4 (*APOE*  $\epsilon$ 4) in Alzheimer disease and the ease of identifying  $\epsilon$ 4 carriers make the *APOE* genotype and its corresponding protein (apoE) an appealing therapeutic target to slow  $A\beta$  accumulation.

**OBJECTIVE** To determine whether the  $\epsilon$ 2 allele is protective against  $A\beta$  accumulation in the presence of the  $\epsilon$ 4 allele and evaluate how age and the *APOE* genotype are associated with emerging  $A\beta$  accumulation and cognitive dysfunction.

**DESIGN, SETTING, AND PARTICIPANTS** This cross-sectional study used screening data from the Anti-Amyloid Treatment in Asymptomatic Alzheimer Disease Study (A4 Study) collected from April 2014 to December 2017 and analyzed from November 2019 to July 2020. Of the 6943 participants who were a part of the multicenter clinical trial screening visit, 4432 were adults without cognitive impairment aged 65 to 85 years who completed a fluorine 18-labeled (18F)-florbetapir positron emission tomography scan, had *APOE* genotype information, and had a Clinical Dementia Rating of 0. Participants who were taking a prescription Alzheimer medication or had a current serious or unstable illness that could interfere with the study were excluded.

**MAIN OUTCOMES AND MEASURES**  $A\beta$  pathology, measured by 18F-florbetapir positron emission tomography and cognition, measured by the Preclinical Alzheimer Cognitive Composite.

**RESULTS** A total of 4432 participants were included (mean [SD] age, 71.3 [4.7] years; 2634 women [59.4%]), with a mean (SD) of 16.6 (2.8) years of education and 1512 (34.1%) with a positive  $A\beta$  level. *APOE*  $\epsilon$ 2 was associated with a reduction in both the overall (standardized uptake value ratio [SUVR],  $\epsilon$ 24, 1.11 [95% CI, 1.08-1.14];  $\epsilon$ 34, 1.18 [95% CI, 1.17-1.19]) and the age-dependent level of  $A\beta$  in the presence of  $\epsilon$ 4, with  $A\beta$  levels in the *APOE*  $\epsilon$ 24 group ( $n = 115$ ;  $\epsilon$ 24, 0.005 SUVR increase per year of age) increasing at less than half the rate with respect to increasing age compared with the *APOE*  $\epsilon$ 34 group ( $n = 1295$ ; 0.012 SUVR increase per year of age;  $P = .04$ ). The association between  $A\beta$  and decreasing Preclinical Alzheimer Cognitive Composite scores did not differ by *APOE* genotype, and the reduced performance on the Preclinical Alzheimer Cognitive Composite in *APOE*  $\epsilon$ 4 carriers compared with noncarriers was completely mediated by  $A\beta$  (unadjusted difference in composite scores between  $\epsilon$ 4 carriers and noncarriers =  $-0.084$ ,  $P = .005$ ; after adjusting for 18F-florbetapir =  $-0.006$ ,  $P = .85$ ; after adjusting for 18F-florbetapir and cardiovascular scores =  $-0.009$ ,  $P = .78$ ).

**CONCLUSIONS AND RELEVANCE** These findings suggest that the protective outcome of carrying an  $\epsilon$ 2 allele in the presence of an  $\epsilon$ 4 allele against  $A\beta$  accumulation is important for potential treatments that attempt to biochemically mimic the function of the  $\epsilon$ 2 allele in order to facilitate  $A\beta$  clearance in  $\epsilon$ 4 carriers. Such a treatment strategy is appealing, as  $\epsilon$ 4 carriers make up approximately two-thirds of patients with Alzheimer disease dementia. This strategy could represent an early treatment option, as many  $\epsilon$ 4 carriers begin to accumulate  $A\beta$  in early middle age.

JAMA Neurol. doi:10.1001/jamaneurol.2020.3780  
Published online October 12, 2020.

**Author Affiliations:** Clinical Memory Research Unit, Faculty of Medicine, Lund University, Lund, Sweden (Insel, Hansson, Mattsson-Carlgen); Department of Psychiatry and Behavioral Sciences, University of California, San Francisco (Insel); Memory Clinic, Skåne University Hospital, Lund University, Lund, Sweden (Hansson); Department of Neurology, Skåne University Hospital, Lund University, Lund, Sweden (Mattsson-Carlgen); Wallenberg Center for Molecular Medicine, Lund University, Lund, Sweden (Mattsson-Carlgen).

**Corresponding Author:** Philip S. Insel, MS, Clinical Memory Research Unit, Faculty of Medicine, Lund University, Malmö, Sweden 205 02 (philip.insel@med.lu.se).

**A**ge and the apolipoprotein E (*APOE*) genotype are among the strongest risk factors for amyloid- $\beta$  ( $A\beta$ ) accumulation. Rates of early  $A\beta$  accumulation are highest in *APOE*  $\epsilon 4$  allele carriers and lowest in  $\epsilon 2$  allele carriers compared with  $\epsilon 3$ -only carriers.<sup>1</sup> Increasing evidence suggests that the *APOE* genotype and its corresponding protein (apoE) affect the pathogenesis of Alzheimer disease (AD) through multiple biological pathways, including the differential regulation of  $A\beta$  aggregation and clearance.<sup>2,3</sup> Two-thirds of patients with AD dementia are *APOE*  $\epsilon 4$  allele carriers.<sup>4</sup> Although the most common recent approach in AD drug discovery is to directly target the  $A\beta$  pathway, the high prevalence of *APOE*  $\epsilon 4$  in AD and the ease of identifying  $\epsilon 4$  carriers at any age make *APOE* pathways an appealing therapeutic target to slow  $A\beta$  accumulation.<sup>2</sup>

Two single-nucleotide variations in *APOE* and 3 apoE isoforms (apoE2, apoE3, and apoE4) are thought to have a substantial effect on the structure and function of apoE, including  $A\beta$  binding.<sup>5</sup> From a treatment standpoint, it is unclear whether strategies that increase the “good” forms of apoE (apoE2, apoE3) or decrease the “bad” form (apoE4) would be most successful.<sup>3</sup> By mimicking the biochemical properties associated with the apoE2 isoform, it may be possible to increase the  $A\beta$  clearance that is reduced with apoE4. However, a central question is whether apoE2 remains protective in the presence of apoE4. This question has been difficult to answer, in large part because the simultaneous carriage of both the  $\epsilon 2$  and  $\epsilon 4$  alleles is rare—approximately 2% of the population has the  $\epsilon 24$  genotype.<sup>6</sup> Even in previous meta-analyses, small sample sizes of the  $\epsilon 24$  group precluded precise estimates of the effect of  $\epsilon 2$  in the presence of  $\epsilon 4$  on  $A\beta$  pathology.<sup>7</sup> Consequently, questions about the potential for therapies targeting apoE, such as synthetic peptides, to reduce  $A\beta$  pathology in the presence of apoE4 remain unanswered.

Because genetic risk factors, such as carriage of *APOE*  $\epsilon 4$ , can be determined at birth, targeting apoE4 is of particular interest as an early treatment option. Predicting when individuals may become at increased risk for abnormal rates of  $A\beta$  accumulation will help to inform the design of primary prevention. In 4432 participants without cognitive impairment who were screened for participation in the Anti-Amyloid Treatment in Asymptomatic Alzheimer Disease (A4 Study) trial,<sup>8</sup> we evaluated how the principal risk factors for AD (age and *APOE* genotype) were associated with early buildup of  $A\beta$ , measured by fluroine 18-labeled (18F)-florbetapir positron emission tomography (PET).

## Methods

In this cross-sectional study, data were collected from April 2014 to December 2017 and analyzed from November 2019 to July 2020. Participants screened for inclusion in the A4 Study<sup>8</sup> were included in this study if they completed an 18F-florbetapir PET scan, had *APOE* genotype information, completed a battery of neuropsychological testing, scored between 25 and 30 on the Mini-Mental State Examination (MMSE), had a Clinical Dementia Rating of 0, and were aged between 65 and 85 years. Exclusion criteria for the A4 study

## Key Points

**Question** Does the  $\epsilon 2$  allele remain protective against  $\beta$ -amyloid ( $A\beta$ ) accumulation in the presence of the  $\epsilon 4$  allele?

**Findings** In this cross-sectional study of 4432 older participants without cognitive impairment, apolipoprotein E  $\epsilon 2$  (*APOE*  $\epsilon 2$ ) was associated with a reduction in both the overall and age-dependent level of  $A\beta$  in the presence of  $\epsilon 4$ , with  $A\beta$  levels in the *APOE*  $\epsilon 24$  group ( $n = 115$ ) increasing at significantly less than half the rate with respect to increasing age compared with the *APOE*  $\epsilon 34$  group ( $n = 1295$ ).

**Meaning** The protective outcome of carrying an  $\epsilon 2$  allele in the presence of an  $\epsilon 4$  allele against  $A\beta$  accumulation may inform future development of disease-modifying Alzheimer disease therapies.

have been described previously.<sup>9</sup> Briefly, participants were excluded from the A4 Study if they were taking a prescription Alzheimer medication or had a current serious or unstable illness that could interfere with the study. Note that participants without evidence of brain  $A\beta$  at screening were not randomized to treatment in the A4 Study but were included in the current study regardless of their PET scan result. This study was approved by the institutional review boards of all participating institutions, and written informed consent was obtained from all participants. This study followed the Strengthening the Reporting of Observational Studies in Epidemiology (STROBE) reporting guideline.

## 18F-Florbetapir PET Imaging

$\beta$ -Amyloid PET imaging in the A4 Study was done using 18F-florbetapir data, which was acquired 50 to 70 minutes postinjection. Images were realigned and averaged and then spatially aligned to a standard space template. 18F-florbetapir, sampled in a global neocortical region for  $A\beta$ , was expressed as a standardized uptake value ratio (SUVR) with a cerebellar reference region.<sup>10</sup>  $\beta$ -Amyloid positivity was defined as participants with an 18F-florbetapir PET SUVR greater than or equal to 1.10.<sup>11,12</sup>

## Cognitive Testing

The A4 Study participants completed a neuropsychological test battery including the Preclinical Alzheimer Cognitive Composite (PACC),<sup>13,14</sup> comprising the MMSE, the Logical Memory Delayed Recall, the Free and Cued Selective Reminding Test, and the Digit Symbol Substitution Test. To calculate the PACC, individual components were  $z$ -transformed and summed. The resulting sum was then centered on the mean and SD of the  $A\beta$ -negative group.

## Cardiovascular Risk Factors

Cardiovascular risk scores were calculated based on body mass index, systolic blood pressure, smoking status, and information gathered during an initial health assessment and physical and neurologic examination. During the initial assessment, participants were asked about the chronicity and severity of underlying health conditions. Chronicity (1 = single occurrence; 2 = intermittent; and 3 = persistent) and severity

Table 1. Characteristics of the Study Cohort by *APOE* Genotype

Characteristic	<i>APOE</i>						P value
	$\epsilon 22$ (n = 25)	$\epsilon 23$ (n = 449)	$\epsilon 33$ (n = 2409)	$\epsilon 24$ (n = 115)	$\epsilon 34$ (n = 1295)	$\epsilon 44$ (n = 139)	
Age, mean (SD), y	71.1 (4.1)	71.9 (4.9)	71.5 (4.8)	71.5 (5.0)	70.7 (4.3)	69.8 (3.8)	<.001
Women, No. (%)	16 (64.0)	245 (54.6)	1455 (60.4)	66 (57.4)	771 (59.5)	81 (58.3)	.32
Race No. (%)							
White	25 (100)	395 (88.0)	2188 (90.8)	103 (89.6)	1203 (92.9)	128 (92.1)	
Black	0	31 (6.9)	71 (2.9)	9 (7.8)	41 (3.2)	7 (5.0)	
Asian	0	15 (3.3)	117 (4.9)	2 (1.7)	33 (2.6)	2 (1.4)	
American Indian	0	1 (0.2)	3 (0.1)	0	4 (0.3)	1 (0.7)	.003
Native Hawaiian	0	0	1 (0.04)	0	1 (0.08)	0	
Multiple	0	4 (0.9)	14 (0.6)	0	9 (0.7)	0	
Unknown	0	3 (0.7)	15 (0.6)	1 (0.9)	4 (0.3)	1 (0.7)	
Ethnicity, No. (%)							
Hispanic or Latino	0	8 (1.8)	89 (3.7)	6 (5.2)	29 (2.2)	6 (4.3)	
Non-Hispanic or non-Latino	25 (100)	438 (97.6)	2300 (95.5)	108 (93.9)	1255 (96.9)	133 (95.7)	.21
Unknown	0	3 (0.7)	20 (0.8)	1 (0.9)	11 (0.8)	0	
Education, mean (SD), y	17.2 (3.5)	16.5 (3.1)	16.5 (2.8)	16.6 (3.2)	16.7 (2.8)	16.5 (2.7)	.70
Cardiovascular Risk Score, mean (SD)	-0.06 (1.01)	-0.09 (0.98)	0.00 (0.99)	0.16 (0.86)	-0.03 (1.01)	-0.14 (0.96)	.08
A $\beta$ positive, No. (%)	4 (16.0)	82 (18.3)	562 (23.3)	47 (40.9)	702 (54.2)	115 (82.7)	<.001
A $\beta$ SUVR, estimated mean (95% CI)	1.02 (0.95-1.09)	1.02 (1.01-1.04)	1.05 (1.04-1.06)	1.11 (1.08-1.14)	1.18 (1.17-1.19)	1.31 (1.28-1.34)	<.001

Abbreviations: A $\beta$ ,  $\beta$ -amyloid; *APOE*, apolipoprotein E; SUVR, standardized uptake value ratio.

(1 = mild; 2 = moderate; and 3 = severe) scores were used to calculate the cardiovascular risk score, described further in the Statistical Analysis section. During the physical and neurologic examination, participants were classified as normal or abnormal with regard to cardiac health. Cardiac values (0 = normal; 1 = abnormal) were incorporated into the cardiovascular risk score.

### Statistical Analysis

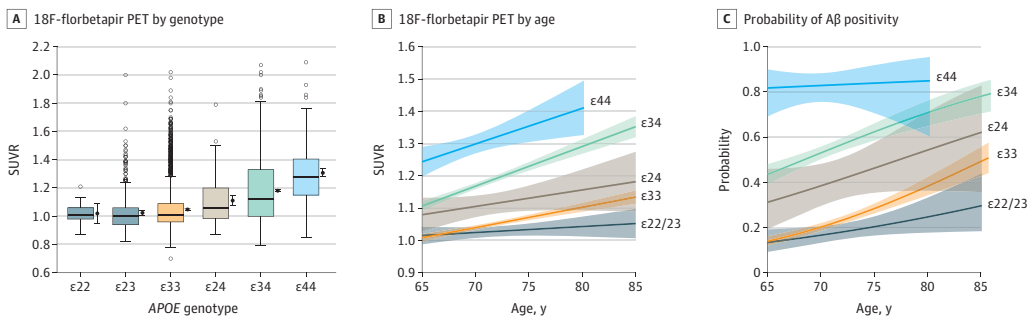
18F-Florbetapir SUVR values (both continuous and dichotomized, separately) were regressed on *APOE* genotype (all 6 genotypes), adjusting for age and sex. The interaction between *APOE* genotype and age was also assessed. Models with continuous outcomes (18F-florbetapir PET SUVRs and cognitive scores) were modeled using ordinary least-squares regression. Monotone cubic splines were used to evaluate potential nonlinearity in the associations among 18F-florbetapir PET SUVR, age, and cognition.<sup>15</sup> Models with A $\beta$  positivity as the outcome were fit with logistic regression. We also evaluated the interaction between 18F-florbetapir SUVR and *APOE* genotype to predict PACC scores, as well as the individual components of the PACC in an exploratory analysis. Statistical significance of the associations between the outcome and predictors was tested using likelihood ratio tests and the Akaike information criterion (AIC). A lower value of the AIC indicates a better-fitting model. Multiple-comparison *P* value adjustment of the PACC components was done using a Holm correction.<sup>16</sup> All models predicting 18F-florbetapir PET included age and sex. All models predicting cognition included age, sex, and years of education.

Cardiovascular risk scores were also evaluated for their association with the outcomes and the association between *APOE* genotype and the outcomes. Cardiovascular risk scores were calculated as the sum of *z*-transformed body mass index, *z*-transformed natural log systolic blood pressure, *z*-transformed product of chronicity and severity of cardiovascular symptoms from the initial health assessment, smoking status (0 = nonsmoker; 1 = smoker), and cardiac symptoms from the physical and neurologic examination (0 = normal; 1 = abnormal). The resulting sum was then *z*-transformed, providing a summary of cardiovascular risk with higher scores indicating more risk.

Associations between demographics and *APOE* genotype were assessed using a Kruskal-Wallis test for continuous variables and a  $\chi^2$  test for categorical variables. Changes in the AIC ( $\Delta$ AIC) less than -2 and 2-sided *P* < .05 were considered significant. The PACC *P* values were obtained using the Holm-Bonferroni method. All analyses were done in R software, version 3.6.0 (R Foundation).

## Results

Of the 6943 participants who were part of the multicenter clinical trial screening visit, 4432 adults without cognitive impairment were included (2634 women [59.4%] and 1798 men [40.6%]; mean [SD] age, 71.3 [4.7] years). Individuals had mean (SD) of 16.6 (2.8) years of education, and 1512 had a positive A $\beta$  level (34.1%). Cohort characteristics by *APOE* genotype are summarized in Table 1.

Figure 1. Apolipoprotein E (*APOE*), Age, and Fluorine 18-Labeled (18F)-Florbetapir Standardized Uptake Value Ratio (SUVR)

Boxplots of continuous 18F-florbetapir SUVRs are shown for each *APOE* group (A). The horizontal lines inside the boxes indicate the median; the upper and lower bounds of the boxes indicate the third and first quartiles, respectively; whiskers indicate the most extreme point no more than 1.5 times the interquartile range; and circles indicate outliers. To the right of each boxplot is the mean and 95% CI. The 18F-florbetapir SUVR is plotted by age for each *APOE*

group, separately ( $\epsilon 22$  and  $\epsilon 23$  participants were combined because of the small sample size over age for the  $\epsilon 22$  group) (B). The estimated probability of A $\beta$  positivity is plotted by age for each *APOE* group, separately (C). A $\beta$  indicates  $\beta$ -amyloid; PET, positron emission tomography. The shaded areas in B and C indicate 95% CIs.

### *APOE* and 18F-Florbetapir SUVR

*APOE* genotype was significantly associated with 18F-florbetapir SUVR ( $\chi^2 = 708.93$ ;  $P < .001$ ). Every *APOE* allele combination was significantly different from all other combinations with the exception of  $\epsilon 22$  vs  $\epsilon 23$  (1.02 vs 1.02;  $P = .91$ ) and  $\epsilon 22$  vs  $\epsilon 33$  (1.02 vs 1.05;  $P = .43$ ); note the small sample size of the  $\epsilon 22$  group ( $n = 25$ ). A sample size of 272 for the  $\epsilon 22$  group was required to detect the observed difference from the  $\epsilon 33$  group with 80% power. Mean 18F-florbetapir SUVR estimates and CIs are summarized in Table 1 and shown in Figure 1. Notably, the  $\epsilon 23$  group had a significantly lower mean 18F-florbetapir SUVR compared with the  $\epsilon 33$  group (1.02 vs 1.05;  $P = .01$ ), and the  $\epsilon 24$  group had a significantly lower mean 18F-florbetapir SUVR compared with the  $\epsilon 34$  group (1.11 vs 1.18;  $P < .001$ ). Adjusting for cardiovascular risk score did not affect the *APOE* genotype estimates and was not associated with 18F-florbetapir SUVR ( $\beta = 0.0001$ ;  $P = .98$ ).

### *APOE*, Age, and 18F-Florbetapir SUVR

There was a significant interaction between *APOE* genotype and age to predict 18F-florbetapir SUVR ( $P < .001$ ;  $\Delta AIC = -26.4$ ). The increase in 18F-florbetapir in the  $\epsilon 33$  group was 0.006 SUVR per year (for every 1-year increase in age). Comparing each *APOE* group to the  $\epsilon 33$  group, the  $\epsilon 22/\epsilon 23$  group (combined because of sparse data over age in the  $\epsilon 22$  group) increased significantly more slowly (0.002 SUVR per year;  $P = .01$ ); the  $\epsilon 24$  group increased similarly to the  $\epsilon 33$  group (0.005 SUVR per year;  $P = .73$ ); the  $\epsilon 34$  group had approximately twice the rate of the  $\epsilon 33$  group (0.012 SUVR per year;  $P < .001$ ); and the  $\epsilon 44$  group also had approximately twice the rate, although not significantly different from the  $\epsilon 33$  group (0.011 SUVR per year;  $P = .23$ ), shown in Figure 1. The  $\epsilon 24$  group also increased at less than half the rate of the  $\epsilon 34$  group (rate difference: 0.005 in the  $\epsilon 24$  group vs 0.012 in the  $\epsilon 34$  group;  $P = .04$ ). There was no significant interaction between the

*APOE* genotype and age to predict the odds of A $\beta$  positivity ( $\chi^2 = 3.94$ ;  $P = .41$ ) (Figure 1).

### A $\beta$ , *APOE*, and the PACC

The association between 18F-florbetapir SUVR and decreasing PACC scores did not differ by *APOE* genotype ( $\Delta AIC = 23.4$ ;  $P = .97$ ). Cardiovascular risk was associated with worse PACC scores ( $\beta = -0.06$ ;  $P < .001$ ) but did not affect the interaction between age and *APOE* genotype to predict PACC scores ( $\Delta AIC = 22.9$ ;  $P = .96$ ). There was also no difference when comparing  $\epsilon 4$  carriers to  $\epsilon 4$  noncarriers ( $\Delta AIC = 4.4$ ;  $P = .67$ ) (Figure 2).

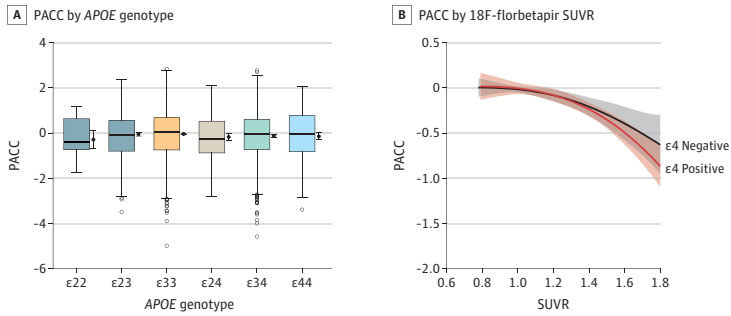
When adjusting for age, sex, and education but not 18F-florbetapir SUVR, the *APOE*  $\epsilon 34$  group performed 0.08 points worse on the PACC compared with the *APOE*  $\epsilon 33$  group ( $\beta = -0.08$ ;  $P = .01$ ). There were no other significant differences on the PACC compared with the  $\epsilon 33$  group (*APOE*  $\epsilon 22$ :  $\beta = -0.25$ ,  $P = .19$ ; *APOE*  $\epsilon 23$ :  $\beta = -0.01$ ,  $P = .89$ ; *APOE*  $\epsilon 24$ :  $\beta = -0.13$ ,  $P = .14$ ; *APOE*  $\epsilon 44$ :  $\beta = -0.11$ ;  $P = .20$ ) (Figure 2). Mean PACC scores and 95% CIs for  $\epsilon 22$ ,  $\epsilon 23$ ,  $\epsilon 33$ ,  $\epsilon 24$ ,  $\epsilon 34$ , and  $\epsilon 44$  were  $-0.29$  ( $-0.67$  to  $0.10$ );  $-0.04$  ( $-0.13$  to  $0.04$ );  $-0.04$  ( $-0.08$  to  $0.00$ );  $-0.17$  ( $-0.34$  to  $0.01$ );  $-0.12$  ( $-0.17$  to  $-0.07$ ); and  $-0.14$  ( $-0.30$  to  $0.01$ ), respectively (Table 2).

When adjusting for cardiovascular risk, all *APOE* estimates remained similar, including the effect of *APOE*  $\epsilon 34$  ( $\beta = -0.086$ ;  $P = .007$ ). When also adjusting for 18F-florbetapir SUVR, the effect of the *APOE*  $\epsilon 34$  group was removed ( $\beta = -0.012$ ;  $P = .71$ ). For the  $\epsilon 4$  carriers vs noncarriers, the unadjusted difference was  $-0.084$  ( $P = .005$ ); after adjusting for 18F-florbetapir, the difference was  $-0.006$  ( $P = .85$ ), and after adjusting for 18F-florbetapir and cardiovascular scores, the difference was  $-0.009$  ( $P = .78$ ).

### A $\beta$ , *APOE*, and the PACC Components

The association between 18F-florbetapir SUVR and decreasing PACC component scores did not differ by *APOE* genotype

Figure 2. Preclinical Alzheimer Cognitive Composite



Boxplots of the Preclinical Alzheimer Cognitive Composite (PACC) are shown by apolipoprotein E (APOE) genotype (A). The horizontal lines inside the boxes indicate the median; the upper and lower bounds of the boxes indicate the third and first quartiles, respectively; whiskers indicate the most extreme point no

more than 1.5 times the interquartile range; and circles indicate outliers. To the right of each boxplot is the mean and 95% CI. PACC scores are plotted against fluroine 18-labeled (18F)-florbetapir standardized uptake value ratios (SUVRs) for APOE ε4 carriers and noncarriers (B). The shaded areas indicate 95% CIs.

Table 2. Association of Cognition With APOE genotype

Measure	APOE, mean (95% CI)					
	ε22 (n = 25)	ε23 (n = 449)	ε33 (n = 2409)	ε24 (n = 115)	ε34 (n = 1295)	ε44 (n = 139)
PACC	-0.29 (-0.67 to 0.10)	-0.04 (-0.13 to 0.04)	-0.04 (-0.08 to 0.00)	-0.17 (-0.34 to 0.01)	-0.12 (-0.17 to -0.07)	-0.14 (-0.30 to 0.01)
FCSRT96	74.0 (71.8 to 76.3)	77.0 (76.4 to 77.5)	76.5 (76.3 to 76.7)	76.7 (75.7 to 77.7)	76.0 (75.7 to 76.3)	75.3 (74.3 to 76.2)
Logical Memory Delayed Recall	12.1 (10.8 to 13.4)	11.9 (11.6 to 12.2)	11.8 (11.6 to 11.9)	11.8 (11.2 to 12.3)	11.5 (11.4 to 11.7)	11.9 (11.4 to 12.4)
Digit Symbol Substitution	45.0 (41.5 to 48.4)	43.1 (42.3 to 43.9)	44.1 (43.8 to 44.4)	41.0 (39.5 to 42.6)	43.8 (43.3 to 44.2)	42.9 (41.5 to 44.3)
MMSE	28.3 (27.8 to 28.8)	28.8 (28.7 to 28.9)	28.8 (28.8 to 28.9)	28.8 (28.6 to 29.0)	28.8 (28.7 to 28.8)	28.8 (28.6 to 29.0)

Abbreviations: APOE, apolipoprotein E; FCSRT96, Free and Cued Selective Reminding Test; MMSE, Mini-Mental State Examination; PACC, Preclinical Alzheimer Cognitive Composite.

( $P > .87$ ;  $\Delta AIC > 20.9$  for all). When adjusting for demographics but not 18F-florbetapir SUVR or cardiovascular risk, Digit Symbol Substitution Test scores in the APOE ε24 group were reduced ( $\beta = -3.06$ ;  $P = .003$ ). Mean cognitive scores and 95% CIs for ε22, ε23, ε33, ε24, ε34, and ε44 were 45.0 (41.5 to 48.4); 43.1 (42.3 to 43.9); 44.1 (43.8 to 44.4); 41.0 (39.5 to 42.6); 43.8 (43.3 to 44.2); and 42.9 (41.5 to 44.3), respectively (Table 2). This outcome remained after adjusting for 18F-florbetapir SUVR ( $\beta = -2.94$ ;  $P = .005$ ) and also after adjusting for cardiovascular risk ( $\beta = -2.97$ ;  $P = .005$ ).

## Discussion

The main findings of this study were (1) APOE ε2 was associated with a reduction in both the overall and the age-dependent level of Aβ in the presence of ε4, (2) large differences in Aβ between APOE groups were already apparent at age 65 years, (3) the association between Aβ and decreasing PACC scores did not differ by APOE genotype, and (4) the associated reduction in performance of the PACC in APOE ε4 carriers compared with noncarriers was completely mediated by Aβ.

There was a large protective outcome of APOE ε2 in the presence of APOE ε4 (Table 1 and Figure 1). β-Amyloid levels in the APOE ε24 group increased at less than half the rate with respect

to increasing age compared with the APOE ε34 group. A 2015 meta-analysis did not find a protective effect of carrying the ε2 allele in the presence of ε4 with respect to Aβ positivity.<sup>7</sup> However, this study had one-third of the number of ε24 participants (n = 41) compared with the A4 Study, most of whom were younger than 70 years. In Figure 1, separation between the ε24 and ε34 groups becomes clear as the groups approach 70 years of age. The reduced levels of Aβ in ε24 compared with ε34 participants shown here may be one of the primary drivers behind the protective outcome of the ε2 allele against AD dementia, shown previously in a large case-control study.<sup>17</sup> The ε24 group demonstrated an associated reduced risk of AD dementia (odds ratio, 2.68 [95% CI, 1.65-4.36]) compared with the ε34 group (odds ratio, 6.13 [95% CI, 5.08-7.41]) when comparing both groups with ε33 participants. However, the presence of the ε2 allele does not completely protect against Aβ positivity, as 16% of ε2 homozygotes in the A4 Study had positive Aβ levels, nor does it completely protect against AD dementia, as 5 of 24 ε2 homozygotes had a neuropathologically confirmed AD dementia diagnosis.<sup>17</sup> Although the APOE genotype is one of the strongest risk factors for AD, it does not determine Aβ accumulation or cognitive decline.

One of the largest studies to date evaluating age and APOE (including 2914 participants without cognitive impairment) found Aβ positivity in 13.2% of APOE ε4-negative participants and 37.8% of APOE ε4-positive participants at 65 years and 27.7%

and 67.8%, respectively, at 80 years.<sup>7</sup> However, a limitation of previous studies is the focus on A $\beta$  positivity (using dichotomous data with conservative thresholds) to define preclinical AD. Using continuous 18F-florbetapir data allows for the estimation of the first increases in A $\beta$  at subthreshold levels. In *APOE*  $\epsilon 4$  carriers, the mean 18F-florbetapir levels were already greatly increased at the minimum age (65 years) compared with *APOE*  $\epsilon 4$  noncarriers. The *APOE*  $\epsilon 34$  and *APOE*  $\epsilon 44$  groups had mean SUVRs of approximately 1.10 and 1.25 at age 65, whereas the  $\epsilon 33$  and  $\epsilon 23$  groups had mean SUVRs near 1.0. *APOE*  $\epsilon 4$  carrier longitudinal rates of global 18F-florbetapir change have been estimated to be 0.0044 SUVR per year in A $\beta$ -negative individuals and 0.0126 SUVR per year in A $\beta$ -positive individuals,<sup>1</sup> suggesting that it would take decades for the *APOE*  $\epsilon 4$  carrier groups to reach the A $\beta$  levels observed at age 65 years in this study. This coincides with the estimated prevalence of A $\beta$  positivity in  $\epsilon 44$  individuals between 25% and 30% at age 45 years and 10% in  $\epsilon 34$  individuals at age 50 years.<sup>7</sup> With A $\beta$  positivity already observable in some individuals in their 40s, the gradual accumulation likely begins much earlier. Indeed, reductions of cerebrospinal fluid A $\beta$  have been observed in  $\epsilon 44$  carriers in their 20s.<sup>18</sup> A protein-modifying treatment mimicking the protective effect of the  $\epsilon 2$  allele against A $\beta$  accumulation may be most effective before significant A $\beta$  deposition. The age at which such a treatment should be initiated would vary greatly by *APOE* genotype and individual, but if done safely, it could be used to slow A $\beta$  accumulation in early middle age for those at highest risk.

The association between A $\beta$  and performance on the PACC did not differ by *APOE* genotype. In a recent meta-analysis of 3 large preclinical AD studies,<sup>19</sup> 2 of the 3 studies did not find an interaction between A $\beta$  and *APOE* genotype to predict cognitive decline.<sup>20,21</sup> The current study, with a sample size 4 times the size of the previous 3 studies combined, shows the same mean PACC score for a given level of A $\beta$  regardless of *APOE* genotype. When adjusting for A $\beta$  levels, the significant reduction of PACC scores by 0.08 points in  $\epsilon 4$  carriers without A $\beta$  adjustment was completely removed. This reduction is quite modest and refers to a reduction of 0.08 SDs within the A $\beta$ -negative group. However, considering that these participants lack cognitive impairment, this outcome may indicate a nonignorable initial level of cognitive dysfunction. This suggests that the negative association of *APOE*  $\epsilon 4$  positivity on cognition is likely mediated entirely by A $\beta$  accumulation at the preclinical stage of AD. Although many A $\beta$ -independent mechanisms of *APOE*  $\epsilon 4$  have been described,<sup>3,22</sup> these findings suggest that such A $\beta$ -independent associations of *APOE*  $\epsilon 4$  positivity do not markedly contribute to cognitive decline in the early stages of AD.

Reduced Digit Symbol Substitution test scores in *APOE*  $\epsilon 2$  carriers were unexpected. Although the *APOE*  $\epsilon 2$  allele shows clear protective outcomes against A $\beta$  accumulation, it is also associated with increased risk of atherosclerosis,<sup>23</sup> which in turn is linked to increased risk of cognitive decline and vascular dementia.<sup>24,25</sup> The associated reduction in executive function and processing speed in the *APOE*  $\epsilon 24$  group observed in this co-

hort may reflect a non-Alzheimer path to cognitive dysfunction, especially as the adjustment for A $\beta$  burden showed no mediating outcome. Additionally, increased cardiovascular risk scores were associated with decreased cognition in the A4 Study and were highest in the *APOE*  $\epsilon 24$  group, although adjusting for cardiovascular risk factors did not mediate the reduced Digit Symbol Substitution scores observed in the *APOE*  $\epsilon 24$  group. These analyses were exploratory and need to be replicated with longitudinal cognitive trajectories. Still, although the  $\epsilon 2$  allele appears to confer protection against A $\beta$  accumulation, safely developing a treatment that mimics its protective outcome will require care not to increase cardiovascular risk or another non-A $\beta$  path to cognitive dysfunction.

### Limitations

This study has several limitations. This study was limited to participants without cognitive impairment older than 65 years of age, thereby limiting analyses to the outcome of emerging A $\beta$  pathology in the absence of significant cognitive dysfunction. Importantly, this is a cross-sectional study, and these results do not apply to changes within individuals. Longitudinal follow-up of early middle-aged individuals, with low and intermediate levels of amyloid, will be required to further clarify when *APOE* groups initially diverge. Importantly, participation in an AD prevention trial is voluntary, which may introduce bias and reduce generalizability. A4 Study participants are highly educated relative to the general population. The vast majority of A4 Study participants are White and are not representative of the population at risk for AD. Exclusion criteria limited participation to those without health conditions that could interfere with the study, which may introduce bias. Although the sample size of our primary group of interest,  $\epsilon 24$  carriers, was relatively large compared with previous studies, further subdivision by factors known to be associated with *APOE* genotype, particularly race/ethnicity,<sup>26</sup> were precluded by small sample sizes. Finally, use of the PACC, a cognitive composite, may be limited in its sensitivity to specific cognitive differences depending on the distribution across cognitive domains.

### Conclusions

This study's findings suggest that the protective outcome of carrying an  $\epsilon 2$  allele in the presence of an  $\epsilon 4$  allele offers potential for a treatment that attempts to mimic this protective outcome in order to facilitate A $\beta$  clearance in  $\epsilon 4$  carriers. Such a treatment strategy is appealing, as  $\epsilon 4$  carriers make up 67% of patients with AD dementia, and it could represent an early treatment option, as many  $\epsilon 4$  carriers begin to accumulate A $\beta$  in early middle age. If the goal is to interfere early in the disease process before activation of downstream pathways, AD prevention trials may consider targeting much younger people before the accumulation of high or even intermediate levels of A $\beta$  develop.

#### ARTICLE INFORMATION

Accepted for Publication: July 28, 2020.

Published Online: October 12, 2020.  
doi:10.1001/jamaneurol.2020.3780

Author Contributions: Mr Insel had full access to all of the data in the study and takes responsibility

for the integrity of the data and the accuracy of the data analysis.

**Concept and design:** All authors.

**Acquisition, analysis, or interpretation of data:** Insel, Hansson.

**Drafting of the manuscript:** Insel.

**Critical revision of the manuscript for important intellectual content:** All authors.

**Statistical analysis:** Insel.

**Obtained funding:** Mattsson-Carlgen.

**Supervision:** Hansson, Mattsson-Carlgen.

**Conflict of Interest Disclosures:** Dr Hansson reported receiving research support (for the institution) from Roche, Pfizer, GE Healthcare, Biogen, Eli Lilly, and AVID Radiopharmaceuticals and consultancy or speaker fees (paid to the institution) from Biogen and Roche. No other disclosures were reported.

**Funding/Support:** This study was supported by the Wallenberg Center for Molecular Medicine, The Knut and Alice Wallenberg Foundation, The Medical Faculty at Lund University, Region Skåne, the European Research Council, the Swedish Research Council, the Marianne and Marcus Wallenberg Foundation, the Strategic Research Area MultiPark (Multidisciplinary Research in Parkinson's Disease) at Lund University, the Swedish Alzheimer Foundation, the Swedish Brain Foundation, the Parkinson Foundation of Sweden, the Parkinson Research Foundation, the Swedish Medical Association, the Konung Gustaf V:s och Drottning Victorias Frimurare Stiftelse, the Skåne University Hospital Foundation, and the Swedish federal government under the Agreement for Medical Education and Research.

**Role of the Funder/Sponsor:** The funders had no role in the design and conduct of the study; collection, management, analysis, and interpretation of the data; preparation, review, or approval of the manuscript; and decision to submit the manuscript for publication.

**Additional Information:** The Anti-Amyloid Treatment in Asymptomatic Alzheimer Disease Study (A4 Study) is a secondary prevention trial in preclinical Alzheimer disease, aiming to slow cognitive decline associated with brain amyloid accumulation in clinically normal older individuals. The A4 Study is funded by a public-private-philanthropic partnership, including funding from the National Institutes of Health-National Institute on Aging (U19AG010483; R01AG063689), Eli Lilly and Company, Alzheimer Association, Accelerating Medicines Partnership, GHR Foundation, an anonymous foundation, and additional private donors, with in-kind support from Avid, Cogstate, Albert Einstein College of Medicine, US Against Alzheimer Disease, and Foundation for Neurologic Diseases. The companion observational Longitudinal Evaluation of Amyloid Risk and Neurodegeneration Study is funded by the Alzheimer Association and GHR Foundation. The A4 and Longitudinal Evaluation of Amyloid Risk and Neurodegeneration Studies are led by Reisa Sperling, MD, at the Brigham and Women's Hospital, Harvard Medical School and Paul Aisen, MD, at the Alzheimer Therapeutic Research Institute, University of Southern California. The A4 and Longitudinal Evaluation of Amyloid Risk and Neurodegeneration Studies are coordinated by the Alzheimer Therapeutic Research Institute at the University of Southern California, and the data are made available through

the Laboratory for Neuro Imaging at the University of Southern California. The participants screening for the A4 Study provided permission to share their deidentified data in order to advance the quest to find a successful treatment for Alzheimer disease. The complete A4 Study Team list is available at [a4study.org/a4-study-team](http://a4study.org/a4-study-team).

**Additional Contributions:** We thank all the participants, the site personnel, and all of the partnership team members who continue to make the A4 Study and Longitudinal Evaluation of Amyloid Risk and Neurodegeneration Studies possible. There was no financial compensation for these contributions.

## REFERENCES

- Lim YY, Mormino EC; Alzheimer's Disease Neuroimaging Initiative. APOE genotype and early β-amyloid accumulation in older adults without dementia. *Neurology*. 2017;89(10):1028-1034. doi:10.1212/WNL.0000000000004336
- Suidan GL, Ramaswamy G. Targeting apolipoprotein E for Alzheimer's disease: an industry perspective. *Int J Mol Sci*. 2019;20(9):E2161. doi:10.3390/ijms20092161
- Liu CC, Kanekiyo T, Xu H, Bu G. Apolipoprotein E and Alzheimer disease: risk, mechanisms and therapy. *Nat Rev Neurol*. 2013;9(2):106-118. doi:10.1038/nrneurol.2012.263
- Mattsson N, Groot C, Jansen WJ, et al. Prevalence of the apolipoprotein E ε4 allele in amyloid β positive subjects across the spectrum of Alzheimer's disease. *Alzheimers Dement*. 2018;14(7):913-924. doi:10.1016/j.jalz.2018.02.009
- Kanekiyo T, Xu H, Bu G. ApoE and Aβ in Alzheimer's disease: accidental encounters or partners? *Neuron*. 2014;81(4):740-754. doi:10.1016/j.neuron.2014.01.045
- Mahley RW. Apolipoprotein E: cholesterol transport protein with expanding role in cell biology. *Science*. 1988;240(4852):622-630. doi:10.1126/science.3283935
- Jansen WJ, Ossenkoppelle R, Knol DL, et al; Amyloid Biomarker Study Group. Prevalence of cerebral amyloid pathology in persons without dementia: a meta-analysis. *JAMA*. 2015;313(19):1924-1938. doi:10.1001/jama.2015.4668
- Sperling RA, Rentz DM, Johnson KA, et al. The A4 study: stopping AD before symptoms begin? *Sci Transl Med*. 2014;6(228):228fs13. doi:10.1126/scitranslmed.3007941
- Sperling RA, Donohue MC, Raman R, et al; A4 Study Team. Association of factors with elevated amyloid burden in clinically normal older individuals. *JAMA Neurol*. 2020;77(6):735-745. doi:10.1001/jamaneurol.2020.0387
- Johnson KA, Schultz AP, Raman R, et al. Tau PET in A4: preliminary report. *Alzheimers Dement*. 2018;14(7):P1583-P1584. doi:10.1016/j.jalz.2018.07.144
- Joshi AD, Pontecorvo MJ, Clark CM, et al; Florbetapir F 18 Study Investigators. Performance characteristics of amyloid PET with florbetapir F 18 in patients with Alzheimer's disease and cognitively normal subjects. *J Nucl Med*. 2012;53(3):378-384. doi:10.2967/jnumed.111.030340
- Clark CM, Pontecorvo MJ, Beach TG, et al; AV-45-A16 Study Group. Cerebral PET with florbetapir compared with neuropathology at autopsy for detection of neuritic amyloid-β plaques: a prospective cohort study. *Lancet Neurol*. 2012;11(8):669-678. doi:10.1016/S1474-4422(12)70142-4

13. Donohue MC, Sperling RA, Salmon DP, et al; Australian Imaging, Biomarkers, and Lifestyle Flagship Study of Ageing; Alzheimer's Disease Neuroimaging Initiative; Alzheimer's Disease Cooperative Study. The Preclinical Alzheimer Cognitive Composite: measuring amyloid-related decline. *JAMA Neurol*. 2014;71(8):961-970. doi:10.1001/jamaneurol.2014.803

14. Donohue MC, Sperling RA, Petersen R, Sun C-K, Weiner MW, Aisen PS; Alzheimer's Disease Neuroimaging Initiative. Association between elevated brain amyloid and subsequent cognitive decline among cognitively normal persons. *JAMA*. 2017;317(22):2305-2316. doi:10.1001/jama.2017.6669

15. Ramsay JO. Monotone regression splines in action. *Statist Sci*. 1988;3(4):425-441. doi:10.1214/ss/1177012761

16. Holm S. A simple sequentially rejective multiple test procedure. *Scand J Statist*. 1979;6(2):65-70.

17. Reiman EM, Arboleda-Velasquez JF, Quiroz YT, et al; Alzheimer's Disease Genetics Consortium. Exceptionally low likelihood of Alzheimer's dementia in APOE2 homozygotes from a 5,000-person neuropathological study. *Nat Commun*. 2020;11(1):667. doi:10.1038/s41467-019-14279-8

18. Lautner R, Insel PS, Skilback T, et al. Preclinical effects of APOE ε4 on cerebrospinal fluid Aβ42 concentrations. *Alzheimers Res Ther*. 2017;9(1):87. doi:10.1186/s13195-017-0313-3

19. Insel PS, Weiner M, Mackin RS, et al. Determining clinically meaningful decline in preclinical Alzheimer disease. *Neurology*. 2019;93(4):e322-e333. doi:10.1212/WNL.0000000000007831

20. Lim YY, Villemagne VL, Pietrzak RH, et al; Australian Imaging, Biomarkers and Lifestyle (AIBL) Research Group. APOE ε4 moderates amyloid-related memory decline in preclinical Alzheimer's disease. *Neurobiol Aging*. 2015;36(3):1239-1244. doi:10.1016/j.neurobiolaging.2014.12.008

21. Mormino E, Betensky RA, Hedden T, et al; Alzheimer's Disease Neuroimaging Initiative; Australian Imaging Biomarkers and Lifestyle Flagship Study of Ageing; Harvard Aging Brain Study. Amyloid and APOE4 interact to influence short-term decline in preclinical Alzheimer disease. *Neurology*. 2014;82(20):1760-1767.

22. Yamazaki Y, Zhao N, Caulfield TR, Liu C-C, Bu G. Apolipoprotein E and Alzheimer disease: pathobiology and targeting strategies. *Nat Rev Neurol*. 2019;15(9):501-518. doi:10.1038/s41582-019-0228-7

23. Mahley RW. Apolipoprotein E: from cardiovascular disease to neurodegenerative disorders. *J Mol Med (Berl)*. 2016;94(7):739-746. doi:10.1007/s00109-016-1427-y

24. Vinkers DJ, Stek ML, van der Mast RC, et al. Generalized atherosclerosis, cognitive decline, and depressive symptoms in old age. *Neurology*. 2005;65(1):107-112. doi:10.1212/01.wnl.0000167544.54228.95

25. Hofman A, Ott A, Breteler MMB, et al. Atherosclerosis, apolipoprotein E, and prevalence of dementia and Alzheimer's disease in the Rotterdam Study. *Lancet*. 1997;349(9046):151-154. doi:10.1016/S0140-6736(96)09328-2

26. Evans DA, Bennett DA, Wilson RS, et al. Incidence of Alzheimer disease in a biracial urban community: relation to apolipoprotein E allele status. *Arch Neurol*. 2003;60(2):185-189. doi:10.1001/archneur.60.2.185









**FACULTY OF  
MEDICINE**

Department of Clinical Sciences, Malmö

Lund University, Faculty of Medicine  
Doctoral Dissertation Series 2021:50

ISBN 978-91-8021-056-0

ISSN 1652-8220

